



UNIVERSITÀ DEGLI STUDI DI MILANO

DEPARTMENT OF PHARMACEUTICAL SCIENCES

DOCTORAL SCHOOL IN PHARMACEUTICAL SCIENCES

PhD – Cycle the 35th

**SCREENING AND IDENTIFICATION OF NEW FOOD
DERIVED PEPTIDES WITH MULTI-TARGET
CHOLESTEROL-LOWERING ACTIVITY**

Sector CHIM/10 – Food chemistry

Dr. Li Jianqiang

R12715

Faculty advisor: Prof. Carmen Lammi

PhD coordinator: Prof. Vistoli Giulio

ACADEMIC YEAR

2021/2022

INDEX

Aim of the thesis

Motivations and outlines of the PhD thesis	10
---	-----------

Part I. State of the art

1. Introduction.....	15
-----------------------------	-----------

1.1 Food-derived bioactive peptides	15
---	----

1.2 Molecular mechanisms of hypocholesterolemic peptides	19
--	----

1.2.1 HMGCoAR-inhibiting effect of food-derived peptides	30
--	----

1.2.2 PCSK9-mediated effects of food-derived peptides	32
---	----

1.2.3 Regulation of transcription factors by peptides.....	36
--	----

1.3 Hypocholesterolemic peptides exhibiting multifunctional behavior	38
--	----

2. Production, absorption mechanisms and bioavailability of hypocholesterolemic peptides	41
---	-----------

2.1 Production of hypocholesterolemic peptides	41
--	----

2.2 Digestion, transportation, and absorption of hypocholesterolemic peptides	44
---	----

2.2.1 Gastrointestinal digestion.....	44
---------------------------------------	----

2.2.2 Intestinal transport and potential bioavailability of hypocholesterolemic peptides	46
--	----

Part II. Scientific contributions

TRANS-EPITHELIAL TRANSPORT, METABOLISM, AND BIOLOGICAL ACTIVITY ASSESSMENT OF THE MULTI-TARGET LUPIN PEPTIDE LILPKHSDAD (P5) AND ITS METABOLITE LPKHSDAD (P5-MET)

3. Abstract.....	69
-------------------------	-----------

3.1	Introduction.....	69
3.2	Material and methods.....	71
3.2.1	Chemicals	71
3.2.2	Caco-2 Cell Culture and Differentiation.....	72
3.2.3	Cell Monolayers Integrity Evaluation	73
3.2.4	Trans-Epithelial Transport Experiments.....	73
3.2.5	LC-MS/MS Operating Conditions.....	74
3.2.6	Calibration Curve for the Quantification of Absorbed P5-Met and Method Validation	75
3.2.7	HepG2 Cell Culture Conditions and Treatment	76
3.2.8	HMGCoAR Aactivity Assay	76
3.2.9	<i>In Vitro</i> PCSK9-LDLR Binding Assay	76
3.2.10	In-Cell Western (ICW) Assay	77
3.2.11	Fluorescent LDL Uptake	78
3.2.12	Western Blot Analysis.....	78
3.2.13	Quantification of PCSK9 Secreted by HepG2 Cells through ELISA	79
3.2.14	Molecular Modeling	80
3.2.15	Circular Dichroism (CD) Spectroscopy	81
3.2.16	Statistical Analysis.....	81
3.3	Results.....	81
3.3.1	Intestinal Transport of P5 Alone or in Combination with Other Peptides across Caco-2 Cells.....	81
3.3.2	Analysis of the Metabolites of P5 Produced by Caco-2 Cells.....	83
3.3.3	Characterization of the Transport of P5-Met Across the Caco-2 Cell Monolayer.....	84
3.3.4	P5-Met Modulates the Hepatic LDLR Pathway through the Inhibition of HMGCoAR Activity	86
3.3.5	P5-Met Modulates the Hepatic PCSK9 Pathway and Impairs the PPI between PCSK9 and the LDLR.....	88
3.4	Discussion.....	92

3.5 Supporting information.....	96
3.6 References.....	98

COMPUTATIONAL DESIGN AND BIOLOGICAL EVALUATION OF ANALOGS OF LUPIN PEPTIDE P5 ENDOWED WITH DUAL PCSK9/HMGCOAR INHIBITING ACTIVITY

4. Abstract.....	104
4.1 Introduction.....	104
4.2 Materials and Methods.....	108
4.2.1 System Setup and MD Simulations	108
4.2.2 Cluster Analysis	109
4.2.3 Alanine Scanning.....	109
4.2.4 Computational Design of New P5 Analogs.....	110
4.2.5 HMG-CoA Reductase Model Setup and Simulations Protocol.....	110
4.2.6 Peptide Synthesis	111
4.2.7 HepG2 Cell Culture Conditions and Treatment	111
4.2.8 HMG-CoAR Activity Assay	111
4.2.9 <i>In Vitro</i> PCSK9-LDLR Binding Assay	112
4.2.10 In-Cell Western (ICW) Assay	112
4.2.11 Fluorescent LDL Uptake	112
4.2.12 Western Blot Analysis.....	112
4.2.13 Quantification of PCSK9 Secreted by HepG2 Cells through ELISA	112
4.2.14 Statistical Analysis.....	113
4.3 Results.....	113
4.3.1 Identification of Hotspots and Designs of New P5 Analogs	113
4.3.2 Design of P5 Analogs with Improved PCSK9 Predicted Affinity	116
4.3.3 Experimental Validation of the Computational Predictions	120
4.3.4 Analogs Impair the PPI between PCSK9 and LDLR	121
4.3.5 P5 Analogs Modulate the Hepatic LDLR Pathway by Inhibiting HMG-	

CoAR Activity	124
4.3.6 P5 Analogs Modulate the Hepatic PCSK9 Pathway	127
4.3.7 P5 Analogs Increase the Expression of LDLR Localized in the Cellular Membranes and Modulate LDL Uptake in HepG2 Cells	128
4.3.8 Docking of P5-S7A and MD Simulations on HMG-CoAR	129
4.4 Conclusions.....	133
4.5 Supporting information.....	135
4.6 References.....	142

INVESTIGATION OF THE INTESTINAL TRANS-EPITHELIAL TRANSPORT AND ANTIOXIDANT ACTIVITY OF TWO HEMPSEED PEPTIDES WVSPLAGRT (H2) AND IGFLIIWV (H3)

5. Abstract.....	149
5.1 Introduction.....	149
5.2 Material and Methods	151
5.2.1 Chemicals	151
5.2.2 Preparation and analysis of the peptic hydrolysate from hempseed protein (HP).....	152
5.2.3 Intestinal trans-epithelial transport of hempseed hydrolysate assessment	153
5.2.4 Antioxidant activity of hempseed peptides.	155
5.2.5 Antioxidant activity of hempseed peptides on HepG2 cells.....	157
5.2.6 Statistical analysis.....	159
5.3 Results & discussion.....	159
5.3.1 Antioxidant activity of HP hydrolysate	159
5.3.2 Trans-epithelial transport of HP hydrolysate using differentiated Caco-2 cells	162
5.3.3 Screening of the antioxidant activity of transported hempseed peptides	166
5.3.4 H2 and H3 decrease the H ₂ O ₂ -induced ROS and lipid peroxidation levels	

in hepatic HepG2 cells	168
5.3.5 H2 and H3 mediate antioxidant activity through the Nrf-2 pathway modulation	170
5.3.6 H2 and H3 modulate the H ₂ O ₂ -induced NO level production via the iNOS protein modulation in HepG2 cells	172
5.4 Conclusions.....	174
5.5 Supporting information.....	176
5.6 Reference	180

HEMPSEED (*CANNABIS SATIVA*) PEPTIDES WVSPLAGRT AND IGFLIIWV EXERT ANTI-INFLAMMATORY ACTIVITY IN THE LPS-STIMULATED HUMAN HEPATIC CELL LINE

6. Abstract.....	186
6.1 Introduction.....	187
6.2 Material and methods.....	189
6.2.1 Chemicals and Reagents	189
6.2.2 Cell Culture and Western Blot	189
6.2.3 Cytokine Quantification.....	190
6.2.4 Nitric Oxide Quantification	190
6.2.5 Statistical Analysis.....	190
6.3 Results.....	191
6.3.1 H2 and H3 Modulate the LPS-Activated NF-κB Pathway in HepG2 Cells	191
6.3.2 H2 and H3 Decrease the LPS-Induced Cytokine Production in Hepatic HepG2 Cells.....	193
6.3.3 H2 and H3 Promote an Anti-inflammatory Microenvironment	195
6.3.4 H2 and H3 Modulate the LPS-Activated iNOS Pathway in HepG2 Cells	196
6.4 Discussion	197

6.5 Supporting information.....	202
6.6 References.....	205

HEMPSEED (*CANNABIS SATIVA*) PEPTIDE H3 (IGFLIIWV) EXERTS CHOLESTEROL-LOWERING EFFECTS IN HUMAN HEPATIC CELL LINE

7. Abstract.....	211
7.1 Introduction.....	212
7.2 Material and methods.....	214
7.2.1 Chemicals.....	214
7.2.2 HepG2 Cell Culture Conditions and Treatment.....	215
7.2.3 HMGCoAR Activity Assay	215
7.2.4 MTT Assay	216
7.2.5 In-Cell Western (ICW) Assay	216
7.2.6 Fluorescent LDL Uptake	217
7.2.7 Western Blot Analysis.....	217
7.2.8 Quantification through ELISA of PCSK9 Secreted by HepG2 Cells.....	218
7.2.9 Computational Methods	219
7.2.10 Statistical Analysis.....	219
7.3 Results.....	219
7.3.1 Peptide H3 Drops HMGCoAR Activity <i>In Vitro</i>	219
7.3.2 Peptide H3 Effects on the Cell Vitality of HepG2.....	221
7.3.3 Peptide H3 Modulates the LDLR Pathway	222
7.3.4 Peptide H3 Modulates Intracellular HMGCoAR Protein Levels	224
7.3.5 Peptide H3 Increases the Expression of LDLR Localized on Cellular Membranes and Modulates LDL-uptake in the HepG2 Cell Environment	226
7.3.6 Effect of Peptide H3 on the Modulation of PCSK9 Protein and Release Levels.....	227
7.4 Discussion.....	228
7.5 Conclusins.....	232

7.6 Supporting information.....	233
7.7 References.....	234

Part III. Concluding Remarks

GENERAL CONCLUSIONS AND PERSPECTIVES.....	240
--	------------

Appendix.....	244
----------------------	------------

INTEGRATED EVALUATION OF THE MULTIFUNCTIONAL DPP-IV AND ACE INHIBITORY EFFECT OF SOYBEAN AND PEA PROTEIN HYDROLYSATES

I. Abstract.....	246
-------------------------	------------

I-1 Introduction	246
------------------------	-----

I-2 Material and methods	249
--------------------------------	-----

I-2.1 Chemicals	249
-----------------------	-----

I-2.2 SH and PH Ultrafiltration.....	249
--------------------------------------	-----

I-2.3 Mass Spectrometry Analysis (HPLC Chip ESI-MS/MS)	249
--	-----

I-2.4 Biochemical Investigation of DPP-IV and ACE Inhibitory Activity of SH and PH Peptides	250
---	-----

I-2.5 Cellular Measurement of SH and PH Inhibitory Effect of DPP-IV and ACE Activities	251
--	-----

I-2.6 Statistical Analysis	252
----------------------------------	-----

I-3 Results	252
-------------------	-----

I-3.1 Peptidomic Characterization of SH and PH.....	252
---	-----

I-3.2 SH and PH Peptides: Biochemical Investigation of DPP-IV and ACE Inhibitory Activities	256
---	-----

I-3.3 Cellular Assessment of DPP-IV and ACE Inhibition by SH and PH Peptides	259
--	-----

I-4 Discussion	263
----------------------	-----

I-5 Conclusions	267
-----------------------	-----

I-6 Supporting information	268
I-7 References	274

EVALUATION OF THE MULTIFUNCTIONAL DIPEPTIDYL-PEPTIDASE IV AND ANGIOTENSIN CONVERTING ENZYME INHIBITORY PROPERTIES OF A CASEIN HYDROLYSATE USING CELL-FREE AND CELL-BASED ASSAYS

II. Abstract.....	279
II-1 Introduction.....	279
II-2 Material and methods.....	281
II-2.1 Chemicals.....	281
II-2.2 Ultrafiltration of CH	282
II-2.3 Analysis of mass spectrometry.....	282
II-2.4 Characterization of the inhibitory effects of CH on DPP-IV and ACE through biochemical assays	283
II-2.5 Assessment of the inhibitory effects of CH on DPP-IV and ACE activities using cellular assays.....	284
II-2.6 Statistical analysis.....	285
II-3 Results.....	285
II-3.1 Peptidomic characterization of CH.....	285
II-3.2 Biochemical study of the DPP-IV and ACE inhibitory activities of CH..	290
II-3.3 The examination of DPP-IV and ACE inhibition by CH and CH (F3) at the cellular level.....	292
II-4 Discussion.....	295
II-5 Conclusions.....	298
II-6 References.....	300
SCIENTIFIC PUBLICATIONS & COMMUNICATIONS	306

Aim of the thesis

Motivations and outlines of the PhD thesis

In recent years, there is a significant focus on the potential health benefits of food peptides. These short and medium-size peptides are produced by the hydrolysis of food proteins and may be absorbed by the body to modulate specific metabolic pathways by binding or inhibiting targeted receptors. This modulation can lead to positive effects on metabolic diseases, making it particularly noteworthy because it aligns with the trend of many individuals seeking healthier lifestyles through dietary management rather than relying on pharmaceuticals. Additionally, bioactive peptides are typically associated with very low or non-existent toxic or adverse effects. Thus, the identification and exploration of the mechanisms behind bioactive peptides present the opportunity to develop innovative functional foods and nutraceuticals.

To date, eggs, meat, fish, soybean, wheat, milk, and its derivatives have been the primary sources of bioactive peptides, as they are widely available and easily accessible. Notably, recent research has also focused on alternative sources such as lupin and hempseed, which are rich in protein and have shown promising health benefits. Lupin, a legume commonly found in Mediterranean countries, has been found to contain bioactive peptides that can lower blood pressure and improve cardiovascular health. Similarly, hempseed, derived from the industrial hemp, has been shown to have anti-inflammatory and antioxidant properties, making it a potential source of bioactive peptides that could have a range of health benefits.

Based on these considerations, the aim of my PhD thesis was to screen and identify new promising peptides from lupin and hempseed protein. The identified peptides were evaluated for their ability to target hypercholesterolemia, which is a medical condition characterized by high levels of cholesterol and is a major risk factor for the development of cardiovascular disease (CVD). To achieve this objective, multidisciplinary approaches were employed, involving peptidomic techniques to profile the peptide sequences, molecular modeling methods to predict potentially

bioactive peptides, and biochemical and cellular tools to evaluate the bioactivity of peptides and to explore their possible mechanism of action.

The thesis includes three parts:

Part I introduces the state of the art of hypocholesterolemic peptides. **Chapter 1** reports the health-promoting effect of bioactive peptides and their molecular mechanisms of cholesterol-lowering. Numerous works of literature highlight the importance of food-derived bioactive peptides in managing hypercholesterolemia and even preventing cardiovascular diseases. **Chapter 2** states the production, absorption mechanisms and bioavailability hypocholesterolemic peptides.

Part II presents my scientific contributions in the PhD period, which contains two cases, including the assessment of the multi-target lupin (*Lupinus albus*) peptides (**Case I**) and the investigation of hempseed (*Cannabis sativa*) peptides (**Case II**).

Case I: lupin peptides

Chapter 3 focus on the trans-epithelial transport, metabolism, and biological activity assessment of the multi-target lupin peptide LILPKHSDAD (P5) and its metabolite LPKHSDAD (P5-met). This work demonstrated: i) P5-met is produced from P5 by intestinal peptidases during the transport experiments; ii) P5 and P5-met are linearly absorbed by differentiated human intestinal Caco-2 cells; iii) both peptides have unique characteristics and share the same mechanisms of action, exerting an intrinsically multi-target behavior being able to regulate cholesterol metabolism by modulating different pathways. This work highlights the dynamic nature of bioactive peptides that may be modulated by the biological systems they get in contact with.

Chapter 4 is dedicated to design analogs of P5 by using a computational approach and then evaluate their biological activities. This study presented: i) *in silico* study, new analogs with improved affinity to PCSK9 were obtained by optimizing the primary structure of P5; ii) by *in vitro* and cellular experiments, potential analogs, including P5-Best (LYLPKHSDRD), P5-H6A (LILPKASDAD) and P5-S7A (LILPKHADAD), maintained the dual PCSK9/HMG-CoAR inhibitory activity and remarkably P5-Best exerted the strongest hypocholesterolemic effect. This study,

especially the atomistic details of the P5-Best/PCSK9 and P5-Best/HMG-CoAR interactions, represents a reliable starting point for the design of new promising molecular entities endowed with hypocholesterolemic activity.

Case II: hempseed peptides

Chapter 5 presents an investigation of the intestinal trans-epithelial transport and antioxidant activity of specific peptides from hempseed (*Cannabis sativa*) peptic hydrolysate that has been proven to display a cholesterol-lowering activity with a statin-like mechanism of action in HepG2 cells. Overall, this study achieved these results: i) five transported peptides was identified by using differentiated Caco-2 cells; ii) a screening of the antioxidant activity of transported hempseed peptides *in vitro*; iii) an evaluation of the antioxidant activity of selected peptides, including WVSPLAGRT (H2) and IGFLIIWV (H3), by cellular techniques.

Due to the close link between inflammation and oxidative stress and with the objective of fostering the multifunctional behavior of bioactive peptides, **Chapter 6** was focused on the the molecular characterization of the anti-inflammatory and immunomodulatory properties of H2 and H3. In this work, both peptides were shown to modulate the production of pro (IFN- γ , TNF and IL-6)- and anti (IL-10)-inflammatory cytokines and nitric oxide (NO) through regulation of the NF- κ B and iNOS pathways, respectively, in HepG2 cells stimulated by lipopolysaccharides.

Finally, the hypocholesterolemic effects of peptide H3 was investigated in HepG2 cells. **Chapter 7** elucidated the molecular mechanism of cholesterol-lowering peptide H3. In detail, peptide H3 is able to inhibit the 3-hydroxy-3-methylglutaryl co-enzyme A reductase (HMGCoAR) activity *in vitro* and regulate the intracellular HMGCoAR activity through the increase of its phosphorylation by the activation of adenosine monophosphate (AMP)-activated protein kinase (AMPK) pathways. Moreover, it can increase low-density lipoprotein (LDL) receptor (LDLR) protein levels by the activation of the sterol regulatory element binding proteins (SREBP)-2 transcription factor. Unlike the hempseed hydrolysate, peptide H3 can reduce the proprotein convertase subtilisin/kexin 9 (PCSK9) protein levels and its secretion in the extracellular environment via the decrease of hepatic nuclear factor 1 α (HNF-1 α).

Part III presents the concluding remarks and the impact of this thesis on the field of hypocholesterolemic peptides. In addition, the appendix contains my contributions to another project: integrated evaluation of the multifunctional DPP-IV and ACE inhibitory effect of hydrolysates digested from soybean protein, pea protein and casein.

Part I.
State of the art

CHAPTER 1

1. Introduction

1.1 Food-derived bioactive peptides

Food proteins, apart from the well-known energetic and nutritional functions, exert numerous biological activities. To do this, dietary proteins must be digested into amino acids and peptides, which are then absorbed in adequate concentrations into blood circulation (Yoshikawa, 2015). Amino acids are primarily essential for physical development, growth, maintenance, repair and proper functioning of body organs and cells (Ha & Zemel, 2003), whereas bioactive peptides, specific protein fragments (vary from 2 to 20 amino acid residues), encrypted in the primary sequences of proteins, exert positive impacts on biological functions and health conditions (Xu, Hong, Wu, & Yan, 2019). Bioactive peptides can be released from proteins by enzymatic hydrolysis (exogenous or endogenous proteolytic enzymes), microbial fermentation, or during food processing. Once the protein was hydrolyzed, it was possible to purify and characterize the peptides by empirical methods. Eventually, *in vitro*, *in vivo*, and human studies were performed to evaluate the peptides for the targeted bioactivities (Arnoldi, Lammi, & Aiello, 2019).

In order to reach their target organs, bioactive peptides must be absorbed. Especially, small peptides (di- and tri-peptides) are more efficiently absorbed than larger ones, which are susceptible to hydrolysis by enterocyte peptidases (Lundquist & Artursson, 2016). These small bioactive peptides possess low molecular weight, high bioavailability, and flexible molecular structure that allow them to interact easily with different receptors *in vitro* and within the human body (Rivero-Pino, 2023; Udenigwe, Abioye, Okagu, & Obeme-Nmom, 2021). Bioactive peptides contribute to promoting several activities, including antimicrobial, antioxidant, antihypertensive, immunomodulatory, hypocholesterolemic, anti-diabetes, anti-inflammatory and

antithrombotic (Korhonen & Pihlanto, 2006; Mohanty, Jena, Choudhury, Pattnaik, Mohapatra, & Saini, 2016; Nwachukwu & Aluko, 2019). During digestion, the bioactive peptides can be transported across the intestinal epithelial cells and absorbed into the blood circulation, thus exerting biological effects (Segura-Campos, Chel-Guerrero, Betancur-Ancona, & Hernandez-Escalante, 2011). In recent years, the isolation, identification and characterization of bioactive peptides have gained much attention and become an emerging field of research. Bioactive peptides are also of commercial interest as components of functional foods or nutraceuticals with specific health claims (Fan, Liu, Zhang, Zhang, Liu, & Wang, 2022; Mora & Toldrá, 2023).

The increasingly poor dietary habits in modern society have resulted in epidemics of lifestyle-related chronic diseases. With the exponential increase in the prevalence of lifestyle diseases, millions of people die globally every year due to lifestyle and its related complications, which has become a major concern of the twenty-first century (Guo, Sun, Wu, & Wu, 2022). Cardiovascular disease, a chronic condition of lifestyle disease, is one of the leading causes of mortality worldwide, resulting in more than 17.8 million deaths every year in the world (Gaidai, Cao, & Loginov, 2023; Mensah, Roth, & Fuster, 2019). Hypercholesterolemia is a metabolic condition characterized by elevated blood cholesterol levels, which is one of the most critical factors of cardiovascular disease. High levels of plasma cholesterol, particularly low-density lipoprotein (LDL) cholesterol, may cause arteriosclerosis by developing plaques in the arteries, with implication for cardiovascular disease outcome (Superko, 2000).

Despite a few drugs that have proved to be quite effective in hypercholesterolemia, the safety issues associated with these compounds, such as the toxic or adverse effects (Bove, Cicero, & Borghi, 2019; Laufs, Banach, Mancini, Gaudet, Bloedon, Sterling, et al., 2019), are their limitations that stimulate research on the natural alternatives for the prevention and treatment of these disorders. It is worth noting that not all natural compounds have favorable effects on human health, as a plethora of natural toxins and toxic proteins/peptides exist. For instance, lectins (Van Damme, 2014; Van Damme, Lannoo, & Peumans, 2008) and protease inhibitors (Murdock & Shade, 2002; Svensson, Fukuda, Nielsen, & Bønsager, 2004) found in plant-based foods, gluten-

derived peptides in wheat (Perez-Gregorio, Días, Mateus, & de Freitas, 2018), and histamine in specific fish species (Dalgaard & Emborg, 2009; Kovacova-Hanuszkova, Buday, Gavliakova, & Plevkova, 2015) have the potential to trigger adverse reactions and cause poisoning in individuals. However, amidst this complexity, there is also a growing interest in exploring the potential benefits of certain natural compounds. Food-derived peptides, for example, are a group of natural compounds currently being investigated for the prevention and treatment of hypercholesterolemia and related disorders (Noce, Di Lauro, Di Daniele, Pietroboni Zaitseva, Marrone, Borboni, et al., 2021). Inhibition of various enzymes, especially metabolic enzymes, may be an important function of bioactive peptides in the prevention and treatment of these diseases (Cicero, Fogacci, & Colletti, 2017).

Food-derived peptides emerged as a promising strategy for controlling endogenous cholesterol. Notably, the limitations of food-derived peptides in managing endogenous cholesterol exist. Firstly, as mentioned, potentially toxic and allergenic peptides, often showing biological activities, may be released during the hydrolysis of food proteins (Khan, Niaz, & Abdollahi, 2018; Santi, Maggioli, Mastroberto, Tufoni, Napoli, & Caraceni, 2012; Tordesillas, Berin, & Sampson, 2017). Additionally, processes such as amino acid racemization, peptide modification/derivatization (including the formation of iso-peptide bonds), and the Maillard reaction may occur during protein extraction, sample pretreatment, and peptide preparation, potentially leading to the formation of numerous hazardous compounds (Borad, Kumar, & Singh, 2017; Mohan & Udenigwe, 2015; Paulus, Henle, Haeßner, & Klostermeyer, 1997). Moreover, the safety and efficacy of bioactive peptides can also be affected by factors such as the dosage (including frequency) and duration of administration (Liu, Li, Zheng, Bu, He, & Wu, 2020). Furthermore, the relatively limited clinical studies are not sufficient to demonstrate the hypocholesterolemic effects of food-derived bioactive peptides (Nagaoka, Takeuchi, & Banno, 2021; Patil, Usman, Zhang, Mehmood, Zhou, Teng, et al., 2022; Yang, Chen, Huang, Yang, Cai, Chen, et al., 2021) compared to other natural strategies, such as berberine sourced from plants of the *Berberidaceae* family (Feng, Sureda, Jafari, Memariani, Tewari, Annunziata, et al.,

2019; Song, Hao, & Fan, 2020), curcumin extracted from *Curcuma longa* (Ashraf, Butt, Iahisham Ul, Nadeem, Aadil, Rusu, et al., 2022; Zeng, Yu, Hao, Yang, & Chen, 2021), and fermented red rice-based supplements (Chen, Chen, Xu, Ma, Hu, & Chen, 2023).

However, the significant advantages of food-derived peptides compared to these natural approaches are also noticeable. Food-derived peptides offer targeted and specific biological activities related to cholesterol regulation. For example, lupin protein peptides (Lammi, Zanoni, Calabresi, & Arnoldi, 2016; Lammi, Zanoni, Scigliuolo, D'Amato, & Arnoldi, 2014), soybean protein peptides (Lammi, Zanoni, & Arnoldi, 2015; Lammi, Zanoni, Arnoldi, & Vistoli, 2015), and milk derived peptides (Iwaniak & Mogut, 2020; Nagaoka, Futamura, Miwa, Awano, Yamauchi, Kanamaru, et al., 2001) have been shown to inhibit cholesterol synthesis enzymes, such as 3-hydroxy-3-methylglutaryl coenzyme A reductase (HMGCoAR), or increase cholesterol excretion, directly impacting cholesterol metabolism. In contrast, berberine-containing extracts, curcumin, and fermented red rice-based supplements may have broader effects on multiple pathways, which can be advantageous in some cases but may also introduce potential off-target effects or interfere with other physiological processes (Cicero, Fogacci, & Banach, 2019; Och, Podgórski, & Nowak, 2020; Yadollahi, Dastani, Zargarani, Ghasemi, & Rahimi, 2019). Moreover, food-derived peptides demonstrate excellent bioavailability and efficient absorption and utilization within the body (Patil, et al., 2022; Peng, Song, Chen, Li, & Guan, 2022). Conversely, berberine-containing extracts and curcumin exhibit relatively low bioavailability due to the factors such as poor solubility or hepatic metabolism (Behl, Singh, Sharma, Zahoor, Albarrati, Albratty, et al., 2022; Dei Cas & Ghidoni, 2019), which can hinder their effectiveness. In addition, peptide-based inhibitors, such as peptide-based proprotein convertase subtilisin/kexin type-9 (PCSK9) inhibitors (Tombling, Zhang, Huang, Craik, & Wang, 2021), can be designed for specific interactions with crucial enzymes, receptors, or transport proteins involved in cholesterol metabolism, thereby facilitating the modulation of cholesterol. The combination of peptide-based drugs with statins enables the targeting of both

cholesterol synthesis and clearance pathways, resulting in a more comprehensive and effective regulation of cholesterol levels (Nishikido & Ray, 2019).

In conclusion, despite limitations, food-derived peptides have shown promise in managing cholesterol levels by inhibiting cholesterol synthesis enzymes, increasing cholesterol excretion, and interacting with key proteins involved in cholesterol metabolism. Further research is needed to gain a comprehensive understanding of their mechanisms of action in cholesterol management. The knowledge of the relationship between the structure and physiological regulatory function of bioactive peptides is crucial in advancing the industrial application of metabolic regulatory peptides for human health and well-being.

1.2 Molecular mechanisms of hypocholesterolemic peptides

Numerous studies have established that peptides exert hypocholesterolemic effects by modulating endogenous cholesterol levels through cholesterol metabolism pathways (Singh, Aluko, Hati, & Solanki, 2022). Regarding endogenous cholesterol, it can be modulated if the peptides can be absorbed into the blood circulating system and are bioavailable in the targeted organ or tissues. Thus, it is necessary to establish the absorption, distribution, metabolism, excretion, and toxicity of the peptides and their derivatives, which are directly related to the effect of peptides on endogenous cholesterol metabolism in tissues (Segura-Campos, Chel-Guerrero, Betancur-Ancona, & Hernandez-Escalante, 2011). Several studies have reported particular hypocholesterolemic mechanisms of food-derived peptides, mainly focusing on the inhibition of HMGCoAR activity, whereas PCSK9 has also received more attention due to its association with low-density lipoprotein (LDL) receptor (LDLR) degradation (Lammi, Aiello, Boschini, & Arnoldi, 2019). Meanwhile, the effect of food-derived peptides on the expression of proteins involved in cholesterol metabolism was evaluated, including transcription factors sterol regulatory element binding protein 2 (SREBP-2) and hepatocyte nuclear factor 1 α (HNF-1 α). **Table 1** summarizes food-derived peptides that exhibit hypocholesterolemic effects by

different mechanisms. The cholesterol-lowering mechanisms of food-derived peptides were discussed below.

Table 1. Food-derived hypocholesterolemic peptides.

Peptide sequence	Protein source	Hydrolytic enzyme	<i>In vitro</i> or <i>in vivo</i>	Mechanism of action	Hypocholesterolemic effect	References
Peptide mixtures	Chia protein	Alcalase, Flavourzyme and sequential Alcalase-Flavourzyme	<i>In vitro</i>	Inhibition of HMGC _o AR activity	↓ <i>In vitro</i> HMGC _o AR activity (More effective at 3 mg/mL)	(Coelho, Soares-Freitas, Arêas, Gandra, & Salas-Mellado, 2018)
HPP and SGQR	Silkworm pupae protein	neutral proteinase	<i>In vitro</i>	Inhibition of HMGC _o AR activity	↓The mRNA and protein level of HMGC _o AR (1.2- to 1.7-fold decrease at 0.5 mg/mL)	(Sun, Wang, Wang, Zhang, Zhu, Li, et al., 2021)
DA, DD, EE, ES, and LL	Dry-cured ham	Generated during the manufacturing	<i>In vitro</i>	Inhibition of HMGC _o AR activity (statin-like interactions of the dipeptides with HMGC _o AR)	↓ <i>In vitro</i> HMGC _o AR activity (More than 40% at 1 mM)	(Heres, Mora, & Toldrá, 2021a)
RCD and SNV	Spirulina platensis	Gastrointestinal digestion	<i>In vitro</i>	Inhibition of HMGC _o AR activity	↓ <i>In vitro</i> HMGC _o AR activity (IC ₅₀ : 6.9 μM and 20.1 μM, respectively)	(Chen & Yang, 2021)

Lunasin	Soybean		<i>In vitro</i> (HepG2 cells)	Inhibition of HMGCoAR activity	↓HMGCoAR expression ↑LDLR expression	(Galvez, 2012)
Peptide mixtures	Olive seed	Alcalase	<i>In vitro</i> and <i>in vivo</i> (mice)	Inhibition of HMGCoAR activity	↓HMGCoAR expression ↑LDLR expression (At dose of 200 or 400 mg/kg/day)	(Prados, Orellana, Marina, & García, 2020)
Peptide mixtures	Cowpea (raw and cooked beans)	Gastrointestinal digestion	<i>In vitro</i>	Inhibition of HMGCoAR activity and micellar cholesterol solubility	↓ <i>In vitro</i> HMGCoAR activity ↓The micellar solubility of cholesterol (The peptides from the protein isolate of raw cowpeas inhibit HMGCoAR activity, while the peptides from cooked cowpeas are more effective in inhibiting the micellar solubility of cholesterol)	(Marques, Soares Freitas, Corrêa Carlos, Siguemoto, Fontanari, & Arêas, 2015)
GCTLN	Cowpea bean	Gastrointestinal digestion	<i>In vitro</i>	Inhibition of HMGCoAR activity and micellar cholesterol solubility	↓ <i>In vitro</i> HMGCoAR activity ↓The micellar solubility of cholesterol	(Marques, Fontanari, Pimenta, Soares-Freitas, & Arêas, 2015)
IAF, QGF, and QDF	Cowpea bean β-vignin protein	Gastrointestinal digestion	<i>In vitro</i>	Inhibition of HMGCoAR activity (Lower cholesterol	↓ <i>In vitro</i> HMGCoAR activity (At 500 μM concentration, IAF, QGF, and QDF reduced the	(Silva, Philadelpho, Santos, Souza,

				synthesis through a statin-like regulation mechanism)	HMGCoAR activity by 69%, 77% and 78%)	Souza, Santiago, et al., 2021; Silva, Souza, Philadelpho, Cunha, Batista, Silva, et al., 2018)
GGV, IVG, and VGVL	Amaranth (<i>amaranthus cruentus</i>)	Multi-enzyme system	<i>In vitro</i>	Inhibition of HMGCoAR activity	↓ <i>In vitro</i> HMGCoAR activity (IC ₅₀ of VGVL: 50 μM)	(Soares, Mendonça, De Castro, Menezes, & Arêas, 2015)
GEQQQQPGM	Rice protein α-globulin	Pepsin and trypsin sequential <i>in vitro</i> digestion	<i>In vivo</i> (hamsters)	Lower plasma LDL cholesterol	↓LDL cholesterol (a dose of 100 mg/kg bodyweight)	(Tong, Ju, Qiu, Wang, Liu, Zhou, et al., 2017)
Peptide mixtures	Chickpea	Alcalase	<i>In vivo</i> (high-fat diet-induced obese rats)	Inhibition of HMGCoAR activity and micellar cholesterol solubility	↓HMGCoAR ↑LDLR	(Shi, Hou, Guo, & He, 2019)
VFVRN	Chickpea	Identified from chickpea peptides by using pharmacophore model	<i>In vitro</i> (HepG2 cells)	Inhibition of HMGCoAR activity	↓ <i>In vitro</i> HMGCoAR activity (0.4 mM inhibited the activity of HMGCoAR by 64.38%) ↓HMGCoAR expression in HepG2 cells	(Shi, Hou, Guo, & He, 2019)

Peptide mixtures Peptide mixtures	Lupin (<i>Lupinus albus</i>) Lupin (<i>Lupinus albus</i>)	Pepsin Trypsin	<i>In vitro</i> (HepG2 cells)	Inhibition of HMGCoAR activity and PCSK9-LDLR binding, <i>in vitro</i> Increasing SREBP-2 and LDLR protein levels and decreasing PCSK9 production via effect on HNF-1 α protein	<i>In vitro</i> HMGCoAR activity (Decrease 17% by peptic peptides and 57% by tryptic peptides at 2.5 mg/mL) ↓PCSK9-LDLR binding ↓PCSK9 ↓HNF-1 α ↑SREBP-2 ↑LDLR ↑LDL uptake ↑activation of PI3K/Akt/GSK3 β kinases	(Lammi, Aiello, Vistoli, Zanoni, Arnoldi, Sambuy, et al., 2016; Lammi, Zanoni, Aiello, Arnoldi, & Grazioso, 2016; Lammi, Zanoni, Calabresi, & Arnoldi, 2016; Lammi, Zanoni, Scigliuolo, D'Amato, & Arnoldi, 2014)
YDFYPSSTKDQQS	Lupin (<i>Lupinus albus</i>) β -conglutin	Pepsin	<i>In vitro</i> (HepG2 cells)	Inhibition of HMGCoAR activity (Modulates cholesterol metabolism in HepG2 cells via SREBP-1 activation)	<i>In vitro</i> HMGCoAR activity ↑LDLR ↑LDL uptake ↑SREBP-1	(Lammi, Zanoni, Arnoldi, & Aiello, 2018)

GQEQSHQDEGVIVR	Lupin (<i>Lupinus albus</i>) β-conglutin	Trypsin	<i>In vitro</i> (HepG2 cells)	Modulates the mutant PCSK9 ^{D374Y} Pathway, a dual mechanism of action involving either the modulation of the PCSK9 ^{D374Y} or LDLR pathways	↓PCSK9 ^{D374Y} -LDLR binding (IC ₅₀ : 285.6 ± 2.46 μM) ↓PCSK9 ^{D374Y} -FLAG protein ↓HNF-1α ↓ <i>In vitro</i> HMGC _o AR activity (IC ₅₀ : 99.5 ± 0.56 μM) ↓HMGC _o AR ↑LDLR ↑LDL uptake ↑SREBP-2	(Grazioso, Bollati, Sgrignani, Arnoldi, & Lammi, 2018; Lammi, Bollati, Lecca, Abbracchio, & Arnoldi, 2019)
GQRQWKQAEGVMVR	Analogues of GQEQSHQDEGVIVR (Computational design)	Computational design	<i>In vitro</i>	Inhibit the mutant PCSK9 ^{D374Y} Activity	↓PCSK9 ^{D374Y} -LDLR binding (IC ₅₀ : 147.8 ± 3.23 μM)	(Lammi, Sgrignani, Roda, Arnoldi, & Grazioso, 2019)
LILPKHSDAD	Lupin (<i>Lupinus albus</i>) β-conglutin	Pepsin	<i>In vitro</i> (HepG2 cells)	Inhibition of HMGC _o AR activity and PCSK9-LDLR binding, <i>in vitro</i> Increasing SREBP-2 and LDLR protein levels and decreasing PCSK9 production via effect on HNF-1α protein	↓ <i>In vitro</i> HMGC _o AR activity (IC ₅₀ : 147 μM) ↓PCSK9 ↓HNF-1α ↓PCSK9-LDLR binding ↑p-HMGC _o AR (Ser 872) ↑p-AMPK (Thr 172) ↑LDLR ↑LDL uptake ↑SREBP-2	(Zanoni, Aiello, Arnoldi, & Lammi, 2017b)

LPKHS DAD	Metabolite of Pepsin and intestinal peptidases during epithelial transport experiments	and <i>In vitro</i> (HepG2 cells)	Inhibition of HMGCoAR activity and PCSK9-LDLR binding, <i>in vitro</i> Increasing SREBP-2 and LDLR protein levels and decreasing PCSK9 production via effect on HNF-1 α protein	<p>↓<i>In vitro</i> HMGCoAR activity (IC₅₀: 175.3 μM)</p> <p>↓PCSK9</p> <p>↓HNF-1α</p> <p>↓PCSK9-LDLR binding (IC₅₀: 1.7 μM)</p> <p>↑p-HMGCoAR (Ser 872)</p> <p>↑p-AMPK (Thr 172)</p> <p>↑LDLR</p> <p>↑LDL uptake</p> <p>↑SREBP-2</p>	(Lammi, Aiello, Bollati, Li, Bartolomei, Ranaldi, et al., 2021)	
LYLPKHS DRD, LILPKAS DAD, and LILPKHADAD	Analogues of LILPKHS DAD	of Computational design	<i>In vitro</i>	Inhibition of HMGCoAR activity and PCSK9-LDLR binding, <i>in vitro</i> Increasing SREBP-2 and LDLR protein levels and decreasing PCSK9 production via effect on HNF-1 α protein	<p>Showed the same/similar effects of LILPKHS DAD.</p> <p>↓<i>In vitro</i> HMGCoAR activity (IC₅₀: 88.9 μM, 74.4 μM, and 73.8 μM)</p> <p>↓PCSK9-LDLR binding (IC₅₀: 0.7 μM, 9.0 μM, and 1.45 μM)</p>	(Lammi, Fassi, Li, Bartolomei, Benigno, Roda, et al., 2022)

LTFPGSAED	Lupin (<i>Lupinus albus</i>) β-conglutin	Pepsin	<i>In vitro</i> (HepG2 cells)	Inhibition of HMGCoAR activity Increasing SREBP-2 and LDLR protein levels	↓ <i>In vitro</i> HMGCoAR activity (IC ₅₀ : 68 μM) ↑p-HMGCoAR (Ser 872) ↑p-AMPK (Thr 172) ↑LDLR ↑LDL uptake ↑SREBP-2	(Zanoni, Aiello, Arnoldi, & Lammi, 2017b)
LTFPG	Metabolite of LTFPGSAED, during epithelial transport experiments	Pepsin and intestinal peptidases	<i>In vitro</i>	Inhibition of HMGCoAR activity	↓ <i>In vitro</i> HMGCoAR activity (Inhibit the enzyme by 4.7 ± 0.3 and 10.3 ± 0.8% at 100 and 250 μM)	(Lammi, Aiello, Dellafiora, Bollati, Boschin, Ranaldi, et al., 2020)
Peptide mixtures	Lupin (<i>Lupinus angustifolius</i>)	Alcalase	<i>In vivo</i> (Western diet-fed ApoE ^{-/-} mice)	Exerts hypocholesterolemic effects in Western diet-fed ApoE ^{-/-} mice through the modulation of LDLR and PCSK9 pathways	↓ <i>In vitro</i> HMGCoAR activity (Decreased by 51.5 ± 0.6% at 2.5 mg/mL) ↓PCSK9 ↓HNF-1α ↓HMGCoAR ↑p-HMGCoAR (Ser 872) ↑p-AMPK (Thr 172) ↓LDLR ↑LDL uptake ↓SREBP-2	(Santos-Sánchez, Cruz-Chamorro, Bollati, Bartolomei, Pedroche, Millán, et al., 2022)

IAVPGEVA, IAVPTGVA, and LPYP	Soy glycinin	Pepsin trypsin	or	<i>In vitro</i> (HepG2 cells)	Inhibition of HMGCoAR activity Increasing SREBP2 and LDLR protein levels via the activation of AMPK and ERK 1/2	↓ <i>In vitro</i> HMGCoAR activity (IC ₅₀ : 222 ± 90, 274 ± 95, and 300 ± 150 μM) ↑LDLR ↑LDL uptake ↑SREBP-2 ↑p-AMPK (Thr 172) ↑p-HMGCoAR (Ser 872) ↑p-ERK 1/2 (Thr 202/Tyr 204)	(Lammi, Zanoni, & Arnoldi, 2015)
YVVNPDNDEN and YVVNPDNNEN	Soy β-conglycinin	Pepsin trypsin	or	<i>In vitro</i> (HepG2 cells)	Inhibition of HMGCoAR activity Increasing SREBP2 and LDLR protein levels	↓ <i>In vitro</i> HMGCoAR activity (IC ₅₀ : 150 and 200 μM) ↑LDLR ↑LDL uptake ↑SREBP-2	(Lammi, Zanoni, Arnoldi, & Vistoli, 2015)
Peptide mixtures (Including 90 identified peptides belonging to 33 proteins)	Hempseed (<i>Canabis sativa</i>)	Pepsin		<i>In vitro</i> (HepG2 cells)	Inhibition of HMGCoAR activity (Exert hypocholesterolemic effects with a statin-Like mechanism)	↓ <i>In vitro</i> HMGCoAR activity ↑p-HMGCoAR (Ser 872) ↑p-AMPK (Thr 172) ↑LDLR ↑LDL uptake ↑SREBP-2 ↑PCSK9	(Zanoni, Aiello, Arnoldi, & Lammi, 2017a)

Short-chain peptide mixture, medium-chain peptide mixture, and total hydrolysate	Hempseed	Alcalase	<i>In vitro</i> (HepG2 cells)	Inhibition of HMGCoAR activity Increasing SREBP-2 and LDLR protein levels and decreasing PCSK9 production via effect on HNF-1 α protein	↓ <i>In vitro</i> HMGCoAR activity ↓PCSK9 ↓HNF-1 α ↑LDLR ↑SREBP-2	(Cerrato, Lammi, Laura Capriotti, Bollati, Cavaliere, Maria Montone, et al., 2023)
IGFLIIWV	Hempseed (<i>Cannabis sativa</i>)	Pepsin	<i>In vitro</i> (HepG2 cells)	Inhibition of HMGCoAR activity Increasing SREBP-2 and LDLR protein levels and decreasing PCSK9 production via effect on HNF-1 α protein	↓ <i>In vitro</i> HMGCoAR activity ↓PCSK9 ↓HNF-1 α ↑p-HMGCoAR (Ser 872) ↑p-AMPK (Thr 172) ↑LDLR ↑LDL uptake ↑SREBP-2	(Li, Bollati, Bartolomei, Mazzolari, Arnoldi, Vistoli, et al., 2022)
Lunasin (a 43-amino acid polypeptide)	soybean		<i>In vitro</i> (HepG2 cells) and <i>in vivo</i> (ApoE ^{-/-} mice)	Inhibits PCSK9 expression by down-regulating HNF-1 α and enhances LDLR expression via PI3K/Akt-mediated activation of SREBP-2 pathway.	↓PCSK9 at mRNA and protein levels ↓HNF-1 α ↑LDLR ↑LDL uptake	(Fernández-Tomé & Hernández-Ledesma, 2019; Gu, Wang, Xu, Tian, Lei, Zhao, et al., 2017)

Hypocholesterolemic effects observed in food-derived peptides in the different *in vitro* and *in vivo* models. ↑, increase; ↓, decrease.

1.2.1 HMGCoAR-inhibiting effect of food-derived peptides

Apart from obtaining cholesterol through diet, the majority of cholesterol is synthesized endogenously in the body. The most common pharmacological strategy for hypercholesterolemia treatment is based on the inhibition of HMGCoAR, which is the rate-controlling enzyme in the mevalonate pathway and is a key factor in endogenous cholesterol biosynthesis, thereby elevating the LDLR expression to increase the LDL particle uptake from the circulation (Friesen & Rodwell, 2004). The most representative oral agents targeted to HMGCoAR for the prevention and treatment of cardiovascular diseases associated to hypercholesterolemia are the statins, such as lovastatin, simvastatin, pravastatin, fluvastatin, atorvastatin, pitavastatin, and rosuvastatin, which are reversible competitive inhibitors of HMGCoAR (Brautbar & Ballantyne, 2011; Chauvin, Drouot, Barrail-Tran, & Taburet, 2013). Although statins are effective medications for primary or secondary prevention of CVD and are consumed by approximately 25% of the world population (> 65 years old), patients treated with statins may complain due to their undesirable side effects, such as muscle complaints, including muscle weakness, myalgia, stiffness, cramps, and arthralgia (Bellosta & Corsini, 2012; Reiner, 2014). Moreover, other limitations of statins, for instance, the considerable variability of individual LDL-C reduction in the response to statin therapy (varying from 5 to 70%) and the inability to reduce LDL-C to desirable and safe levels for ~ 50% of patients, are also observed (Taylor & Thompson, 2016). The limitations of statins have stimulated research towards discovering new compounds and drugs for cholesterol management, and food-derived peptides stand out due to their very low or nonexistent toxic or adverse effects.

Over the years, some food-derived peptides were found to inhibit HMGCoAR activity *in vitro*, and/or lower endogenous cholesterol levels *in vivo* through combining their statin-like effects with other mechanisms. For instance, lupin (*Lupinus albus*) protein hydrolysates digested by pepsin or trypsin were proved to reduce HMGCoAR activity *in vitro* (17% of peptic peptides and 57% of tryptic peptides at 2.5 mg/mL) and improved the capacity of hepatic HepG2 cells to uptake LDL-C from extracellular

environment by evaluating the LDLR (Lammi, Zanoni, Scigliuolo, D'Amato, & Arnoldi, 2014). Furthermore, the lupin protein-derived peptides LILPKHSDAD and LTFPGSAED have been shown more active than protein hydrolysates to inhibit HMGCoA activity *in vitro* with an IC₅₀ values of 147 μM and 68 μM, respectively, and an in-silico investigation has predicted the potential binding mode to the catalytic site of this enzyme (Zanoni, Aiello, Arnoldi, & Lammi, 2017b). Peptides LPKHSDAD and LTFPG are the metabolite of LILPKHSDAD and LTFPGSAED, respectively, during the epithelial transport experiments, which also shown the inhibitor activity of HMGCoAR *in vitro* (Lammi, et al., 2021; Lammi, et al., 2020). In addition, this feature was demonstrated *in vitro* with these computational design analogs of LILPKHSDAD, including LYLPKHSRD (IC₅₀ ~ 88.9 μM), LILPKASDAD (IC₅₀ ~ 74.4 μM), and LILPKHADAD (IC₅₀ ~ 73.8 μM) (Lammi, et al., 2022). Similarly, HMGCoAR-inhibitory peptides were also found in hempseed protein. A study on a culture of hepatic HepG2 cells has demonstrated that the cholesterol-lowering effect of hempseed protein hydrolysate digested by pepsin, is due to the inhibition of HMGCoAR activity with a statin-like mechanism (Zanoni, Aiello, Arnoldi, & Lammi, 2017a). Moreover, the HMGCoAR inhibitory activities were observed for hempseed protein derived short-chain peptide mixture (IC₅₀ ~ 0.18 mg/mL), medium-chain peptide mixture (IC₅₀ ~ 0.25 mg/mL), and total hydrolysate (IC₅₀ ~ 0.38 mg/mL), which are generated by Alcalase. Especially, a short-chain peptide mixture is more active on the cholesterol metabolism pathway through the modulation of low-density lipoprotein receptor (Cerrato, et al., 2023). Another study identified IGFLIIWV from hempseed protein that is a multifunctional octapeptide, except for antioxidant and anti-inflammatory activities, inhibiting HMGCoAR activity *in vitro* with dose-dependent manner (IC₅₀ ~ 59 μM) (Cerrato, et al., 2023). One of the major sources of peptides in research on the cholesterol-lowering effect targeted to HMGCoAR is soybean protein. Three kinds of peptides (IAVPGEVA, IAVPTGVA, and LPYP) produced from soy glycinin are capable of inhibiting HMGCoAR activity with IC₅₀ of 222, 274 and 300 μM *in vitro*, respectively (Lammi, Zanoni, & Arnoldi, 2015). And two soy β-conglycinin-derived peptides

YVVNPDNDEN and YVVNPDNNEN exhibited higher HMGCoAR inhibitory activity with IC₅₀ of 150 and 175 μM, respectively (Lammi, Zanoni, Arnoldi, & Vistoli, 2015). Moreover, Lunasin, a 43-amino acid polypeptide initially isolated from soybean, has been shown to significantly reduce HMGCoAR expression in HepG2 cells grown in cholesterol-free media (Galvez, 2012).

In addition, peptides released from raw or cooked cowpea bean, chickpea, and olive seed, respectively, are capable of decreasing HMGCoAR activity besides the ability to reduce micellar cholesterol solubility, inhibiting cholesterol metabolism from two routes (Marques, Soares Freitas, Corrêa Carlos, Siguemoto, Fontanari, & Arêas, 2015; Prados, Marina, & García, 2018; Prados, Orellana, Marina, & García, 2020; Shi, Hou, Guo, & He, 2019). Moreover, smaller peptides, such as GCTLN (Marques, Fontanari, Pimenta, Soares-Freitas, & Arêas, 2015), IAF, QGF, and QDF (Silva, et al., 2021; Silva, et al., 2018) derived from cowpea bean protein, GGV, IVG and VGVL isolated from amaranth (*Amaranthus cruentus*) protein (Soares, Mendonça, De Castro, Menezes, & Arêas, 2015), VFVRN derived from chickpea protein (Shi, Hou, Guo, & He, 2019), and DA, DD, EE, ES, and LL derived from dry-cured ham (Heres, Mora, & Toldrá, 2021a), were also observed to inhibit HMGCoAR activity *in vitro* and some showed statin-like interactions with HMGCoAR. Small peptides, especially di- and tri- peptides, are generally considered to be transported across the intestine epithelium by pepT1 transporter or together with other transport routes in an intact form, and be bioavailable where activity is needed (Daniel, 2004), exerting a hypocholesterolemic effect. Based on these reported cases, despite food-derived peptides are promising for use in managing hypercholesterolemia by targeting cholesterol biosynthetic pathway, there is a limited knowledge on their structure–activity relationship, bioavailability, and related research *in vivo*, which makes it necessary to conduct further investigations.

1.2.2 PCSK9-mediated effects of food-derived peptides

As a promising therapeutic target for endogenous cholesterol regulation, PCSK9 has gained increased attention, and its biological mechanism for cholesterol modulation is

also now well-established. PCSK9 is a major regulator of hepatocyte LDLR concentrations by inhibiting the receptor recycling pathway, causing excessive accumulation of the plasma levels of LDL-cholesterols (LDL-C), which subsequently accelerate atherosclerosis (Momtazi, Banach, Pirro, Katsiki, & Sahebkar, 2017). Specifically, LDLR is responsible for the cellular uptake and subsequent degradation of LDL, playing a crucial role in cholesterol homeostasis. Extracellular LDL can bind to the N-terminal domain of LDLR to form LDL: LDLR complex that is internalized by receptor-mediated endocytosis and then migrated to the endosome, where low pH condition drives LDLR to release LDL and recycle back to the cell surface. Subsequently, separated LDL is shifted to the lysosome where it is degraded to provide cholesterol or amino acid to the cell (Goldstein & Brown, 2009). PCSK9 can facilitate the catabolism of LDLR within lysosomes and block its normal recycling to the hepatocyte surface, via binding to LDLR on the hepatocyte surfaces (Lambert, Charlton, Rye, & Piper, 2009). Therefore, the inhibition of PCSK9 would diminish LDLR degradation, thereby lowering LDL-C concentrations in the blood, offering an additional therapeutic option for patients with primary and secondary cardiovascular events (Norata, Tibolla, & Catapano, 2014; Rosenson Robert, Hegele Robert, Fazio, & Cannon Christopher, 2018).

Although approved monoclonal antibodies, including alirocumab and evolocumab (McDonagh, Peterson, Holzhammer, & Fazio, 2016), are very effective in lowering LDL-C by inhibiting PCSK9, the high costs of treatment have prevented them from being widely used so far (Sible, Nawarskas, & Anderson, 2016). The limitation of these antibodies has eventually facilitated the development of alternative drug modalities. For instance, small molecules, monoclonal-antibody mimetics, small interfering RNA inhibitors (siRNA), gene-silencing CRISPR-Cas9 technology and nucleic acid polymers are all at different stages of clinical development (Ahamad, Mathew, Khan, & Mohanan, 2022; Sible, Nawarskas, & Anderson, 2016). In addition to these therapeutic interventions, peptides have simulated considerable interest as more accessible PCSK9 antagonists for cholesterol-lowering therapy due to their advantageous properties, such as relatively predictable safety profiles, lower

manufacturing costs than antibodies, and the ability to engineer peptides to enhance oral bioavailability (Tombling, Zhang, Huang, Craik, & Wang, 2021). Over the years, considerable research has been devoted to discovering peptides for PCSK9 regulation, and plant-derived peptides have been also taken into account, as highlighted in **Table 1**.

As the lupin protein hydrolysate mentioned above, except for HMGCoAR inhibitory property, the ability of impairing the protein-protein interaction (PPI) between PCSK9 and LDLR *in vitro* and reducing the PCSK9 protein level in HepG2 cells was detected (Lammi, Zanoni, Aiello, Arnoldi, & Grazioso, 2016). Meanwhile, another protein hydrolysate generated from the species narrow-leaf lupin (*Lupinus angustifolius*) by Alcalase shown hypocholesterolemic effects in western diet-fed ApoE^{-/-} mice through the modulation of PCSK9 and LDLR pathways (Santos-Sánchez, et al., 2022). Surprisingly, the identified peptide from this hydrolysate evidenced the result. Two peptides LILPKHSDAD and GQEQSHQDEGVIVR, isolated from *Lupinus albus* protein hydrolysate, competitively bound to PCSK9 with moderate micromolar activity and were capable of restoring LDL uptake (Lammi, Zanoni, Aiello, Arnoldi, & Grazioso, 2016). LILPKHSDAD shown the higher inhibitory activity of PPI between PCSK9 and LDLR with an IC₅₀ of 1.6 µM and decrease the PCSK9 protein level and its secretion in HepG2 cell. Moreover, the inhibitory activities of PPI between LDLR and PCSK9 for metabolite LPKHSDAD (IC₅₀ ~ 1.7 µM) of LILPKHSDAD, even its analogs LYLPKHSDRD (IC₅₀ ~ 0.7 µM), LILPKASDAD (IC₅₀ ~ 9.0 µM), and LILPKHADAD (IC₅₀ ~ 1.45 µM), were observed (Lammi, et al., 2021; Lammi, et al., 2022). In addition, GQEQSHQDEGVIVR not only intervened with the PPI between PCSK9 and LDLR with an IC₅₀ of 320 µM, but also inhibited the PCSK9^{D374Y}:LDLR interaction with an IC₅₀ of 285.6 µM (Lammi, Sgrignani, Roda, Arnoldi, & Grazioso, 2019). Whereas, the most active compound against wild-type PCSK9, LILPKHSDAD, was inactive against PCSK9^{D374Y} that is the familial hypercholesterolemia (FH) associated gain-of-function PCSK9 mutant (Grazioso, Bollati, Sgrignani, Arnoldi, & Lammi, 2018; Lammi, Bollati, Lecca, Abbracchio, & Arnoldi, 2019). Optimization of GQEQSHQDEGVIVR by computational design

(GQRQWKQAEGVMVR) gained an around twice improvement in PCSK9^{D374Y}:LDLR antagonistic ($IC_{50} \sim 147.8 \mu M$) activity and restored cellular LDLR function more efficiently (Lammi, Sgrignani, Roda, Arnoldi, & Grazioso, 2019). This inhibitory behavior of lupin protein hydrolysate and its derived peptides determined an improved ability of treated HepG2 cells to uptake extracellular LDL with a final hypocholesterolemic effect.

Although hempseed protein hydrolysate isolated with pepsin exerts hypocholesterolemic effects with a statin-like mechanism which led to an increase of PCSK9 levels, the identified peptide IGFLIIWV from this hydrolysate is capable of reducing PCSK9 protein levels and subsequent secretion of mature PCSK9 in HepG2 cells (Li, et al., 2022). Moreover, short-chain peptide mixture, medium-chain peptide mixture, and total hydrolysate digested by Alcalase from hempseed protein were tested in HepG2 cells, resulting in the decrease expression levels of PCSK9 protein (Cerrato, et al., 2023). Soybean-derived peptide lunasin has been previously reported the inhibitory ability of HMGCoAR, and the capability of down-regulation of PCSK9 expression as a new mechanism that increased cell-surface LDLR level and enhanced LDL uptake was also confirmed *in vitro* and *in vivo* (Fernández-Tomé & Hernández-Ledesma, 2019; Gu, et al., 2017). Lunasin was found to dose-and-time dependently inhibit PCSK9 expression at mRNA and protein levels in HepG2 cells, thereby contributing to increasing LDLR level and functionally enhancing LDL uptake. ApoE^{-/-} mice receiving lunasin administration by intraperitoneal injection at doses of 0.125~0.5 $\mu mol/kg/day$ for 4 weeks had significantly lower PCSK9 and higher LDLR levels in hepatic tissue, as well as remarkably reduced LDL in blood versus control group mice (Gu, et al., 2017). Interestingly, HMGCoAR-inhibiting peptides also inhibited or modulated the expression of PCSK9, showing a unique synergistic and dual HMGCoAR/PCSK9 inhibitory ability. The activity of these peptides also suggest they are promising starting points for further optimization to develop new hypocholesterolemic compounds. Although these studies suggest potential hypocholesterolemia effects of food-derived peptides by inhibiting expression of PCSK9, only a few peptides have been investigated in this area. Thus, more efforts

are necessary to exploit these dual inhibitory peptides as effective cholesterol-regulating agents.

1.2.3 Regulation of transcription factors by peptides

In cholesterol biosynthetic pathway, SREBP-2 is a crucial player, which functions as a master transcriptional regulator of cholesterol biosynthesis (Sato, 2010). SREBP-2 is synthesized as an endoplasmic reticulum (ER) anchored precursor consisting of an N-terminal transcription factor domain, two transmembrane segments, and a C-terminal regulatory domain that interacts with the domain of SREBP-cleavage activating protein (SCAP). To become active, the complex of SREBP-2 and SCAP membrane experienced a successive two-step cleavage process in Golgi to liberate the N-terminal fragment from the membrane. Subsequently, the processed SREBP-2 enters the nucleus as a homodimer, binds to the sterol regulatory element (SRE) sequence in the promoters of target genes, including HMGCoAR, LDLR and PCSK9, and upregulates their transcription (Horton, Goldstein, & Brown, 2002; Sato, 2010). Thus, SREBP-2 activation is important for cholesterol homeostasis, since its target genes are crucial in cholesterol synthesis and uptake. Food derived peptides have been found to influence SREBP-2-mediated processes with hypocholesterolemic activity. For instance, peptides isolated from lupin (*Lupinus albus*) can increase the expression of LDLR at protein level by the activation of SREBP-2 pathway, resulting in an improved capability of HepG2 cells to uptake LDL from extracellular environment (Lammi, Zanoni, Scigliuolo, D'Amato, & Arnoldi, 2014). The up-regulation of SREBP-2 was associated with activation of the PI3K/Akt/GSK3b pathway in cultured hepatocytes. This feature has been also proved in the identified peptides GQEQSHQDEGVIVR (Lammi, Bollati, Lecca, Abbracchio, & Arnoldi, 2019) and LILPKHSDAD (Zanoni, Aiello, Arnoldi, & Lammi, 2017b), which effectively increased SREBP-2 and LDLR protein levels followed by improvement of HepG2 cells LDL-uptake. Soy glycinin-derived peptides, IAVPGEVA, IAVPTGVA and LPYP, also modulated cholesterol metabolism in HepG2 cells through the activation of the LDLR/SREBP-2 pathway (Lammi, Zanoni, & Arnoldi, 2015). Moreover, two

peptides YVVNPDNDEN and YVVNPDNNEN generated from soy β -conglycinin also showed the ability to increase SREBP-2 protein level, leading to elevated LDLR and LDL uptake in HepG2 cells (Lammi, Zanoni, Arnoldi, & Vistoli, 2015). Meanwhile, LDLR expression was up-regulated by lunasin via PI3K/Akt-mediated activation of SREBP-2 in HepG2 cells (Gu, et al., 2017). Similarly, total protein hydrolysates, medium-chain peptide mixture and short-chain peptide mixture derived from hempseed increased the protein level of SREBP-2 with concomitant augmentation in the protein levels of LDLR and HMGCoAR (Cerrato, et al., 2023). This cholesterol-lowering mechanism has also been observed for a specific peptide IGFLIIWV identified from hempseed protein (Li, et al., 2022).

Unlike SREBP-2 transcription factor, HNF-1 α transcriptionally upregulated PCSK9 by binding to the HNF1 site on the PCSK9 promoter without direct effect on LDLR and HMGCoAR expression (Liu, Zhu, Jiang, Li, & Lv, 2022), which are regulated by only SREBP-2 transcription factor, in HepG2 cells. HNF-1 α knockdown resulted in reduction of circulating PCSK9 protein levels and accumulation of intracellular cholesterol in HepG2 hepatocytes and in primary hepatocytes of normolipidemic mice (Shende, Wu, Singh, Dong, Kan, & Liu, 2015). Moreover, the absence of HNF-1 α function caused a higher accumulation of lipid droplets and increased intracellular cholesterol accumulation in HepG2 cells transfected with HNF-1 α siRNA (Hu, Huang, Han, & Ji, 2020). Furthermore, HNF-1 α can directly upregulate the transcription of microRNA (miR)-122 to enhance miR-122-inhibited SCAP expression and to interfere with the maturation of SREBP-2, leading to a decrease in lipid biosynthesis and lipid uptake by HepG2 cells (Liu, Zhu, Jiang, Li, & Lv, 2022). These findings demonstrated that HNF-1 α plays an important role in the regulation of intracellular cholesterol metabolism. Hempseed derived peptide IGFLIIWV has been found to decrease circulating protein levels of PCSK9 by down-regulated the expression of HNF-1 α (Li, et al., 2022), independent of SREBP2 transcription factor, showing a different and distinct hypocholesterolemic mechanism in HepG2 cells. This mechanism of action to affect PCSK9 protein levels by decreasing HNF-1 α was evidenced in treated HepG2 cell by hempseed peptide mixture (Cerrato, et al., 2023),

including short-chain peptide mixture, medium-chain peptide mixture, and total hydrolysate, respectively. Lupin peptide LILPKHSDAD, its metabolite LPKHSDAD and its analogs (LYLPKHSDRD, LILPKASDAD, and LILPKHADAD) reduced PCSK9 protein levels by decreasing HNF-1 α , thereby improving the functional ability of HepG2 to uptake extracellular LDL (Lammi, et al., 2021; Lammi, et al., 2022). HepG2 cells treated with lunasin inhibited the expression of PCSK9 at mRNA and protein levels in a dose-and-time dependent manner via down-regulating HNF-1 α , thereby contributing to increasing LDLR level and functionally enhancing LDL uptake (Gu, et al., 2017).

It is anticipated that a strategic combination of food-sourced peptides that focuses on various metabolic and signaling pathways will result in significant hypocholesterolemic effects in living organisms, and may eradicate the side effects associated with long-term usage of a single approach, particularly HMGCoA reductase inhibition.

1.3 Hypocholesterolemic peptides exhibiting multifunctional behavior

Peptides with antioxidant and anti-inflammatory features were identified in hempseed. Octapeptide IGFLIIWV obtained from the hydrolysis of hempseed proteins using pepsin could be transported intact by differentiated Caco-2 cells and exert cholesterol-lowering effects in HepG2 cell line. Briefly, peptide IGFLIIWV inhibited the HMGCoAR activity *in vitro* in a dose-dependent manner with an IC₅₀ value of 59 μ M. Furthermore, the activation of the SREBP-2 transcription factor, followed by the increase of low-density lipoprotein LDLR protein levels, was observed in HepG2 cells treated with peptide IGFLIIWV at 25 μ M. Similar to statins, peptide IGFLIIWV increased the phosphorylation level of adenosine monophosphate-activated protein kinase (AMPK) at the Thr172 residue of the catalytic subunit, which in turn produces an inhibition of intracellular HMGCoAR activity through its phosphorylation on the Ser872 residue (the inactive form of HMGCoAR), which is the phosphorylation site

of AMPK. Consequently, the augmentation of the LDLR localized on the cellular membranes led to the improved ability of HepG2 cells to uptake extracellular LDL with a positive effect on cholesterol levels. In addition, peptide IGFLIIWV can reduce the PCSK9 protein levels and its secretion in the extracellular environment via the decrease of transcription factor HNF-1 α (Li, et al., 2022).

The antioxidant property of peptide IGFLIIWV has been confirmed *in vitro* and at cellular level (Bollati, Cruz-Chamorro, Aiello, Li, Bartolomei, Santos-Sánchez, et al., 2022). *In vitro* assessment, at the concentration 25 μ M, IGFLIIWV (1) scavenged the 2,2-azino-bis-(3-ethylbenzo-thiazoline-6-sulfonic) acid (ABTS) radical by 146.1%, (2) had 2,2-diphenyl-1-picryl-hydrazyl-hydrate (DPPH) radical scavenging activity equal to 29.8%, (3) scavenged the peroxy radicals generated by 2,2'-azobis (2-methylpropionamidine) dihydrochloride up to 181.8% in oxygen radical absorbance capacity (ORAC) test, and (4) increased the ferric reducing antioxidant power (FRAP) by 299.3%, displaying a significant antioxidant behavior. Regarding cellular assays, peptide IGFLIIWV was able to reduce the H₂O₂-induced reactive oxygen species (ROS) and lipid peroxidation by 23.2% and 44% at 25 μ M versus HepG2 cells treated with H₂O₂ alone, respectively. The reduction of H₂O₂-induced nitric oxide (NO) production levels was observed after treatment of HepG2 cells with peptide IGFLIIWV, which was associated with the regulation of inducible nitric oxide synthase (iNOS). Moreover, peptide IGFLIIWV suppressed H₂O₂-induced oxidant stress by modulating the nuclear factor erythroid 2-related factor 2 (Nrf-2) pathway that plays a crucial role in the protection against oxidative stress and is responsible for the maintenance of homeostasis and redox balance in cells and tissue.

Inflammation can be triggered by a wide variety of stimuli, including pathogens, damaged cells, toxins, and allergens. The release of these inflammatory mediators, such as cytokines, tumor necrosis factor α (TNF- α), prostaglandins (PGs), nitric oxide (NO), and leukotrienes (LTs), is a key aspect of the inflammatory response. These mediators play a central role in coordinating the immune response and orchestrating the various cellular and physiological processes that are involved in the healing and repair of damaged tissue (Chakrabarti, Jahandideh, & Wu, 2014). It is also worth

mentioning that the balance between pro-inflammatory and anti-inflammatory mediators is critical for the proper resolution of inflammation. As far as anti-inflammatory activity is concerned, the regulation of inflammation by the peptide IGFLIIWV is due to its capacity to modulate the production and release of cytokines through the regulation of the nuclear factor- κ B (NF- κ B) and iNOS pathways (Cruz-Chamorro, Santos-Sánchez, Bollati, Bartolomei, Li, Arnoldi, et al., 2022). Since the NF- κ B pathway plays a major role in the pro-inflammatory response, peptide IGFLIIWV (25 μ M) has the ability to reduce both NF- κ B and its more active phosphorylated form (p(Ser276)NF- κ B) protein levels in lipopolysaccharide (LPS)-stimulated HepG2 cells, thus mitigating the inflammatory effect. In fact, peptide IGFLIIWV has been shown to effectively suppress the production of pro-inflammatory cytokines (IFN- γ : $-13.1 \pm 2.0\%$, TNF: $-20.3 \pm 1.7\%$, and IL-6: $-15.1 \pm 6.5\%$), while promoting the expression of anti-inflammatory cytokine IL-10 ($+26.0 \pm 2.3\%$), and the reduction of the iNOS protein level and NO production was observed as well.

A recent review summarizes the major biological activity of lunasin (Lammi, Aiello, Boschin, & Arnoldi, 2019), evidence suggest that this polypeptide is also antioxidant, hypocholesterolemic, and anti-inflammatory.

CHAPTER 2

2. Production, absorption mechanisms and bioavailability of hypocholesterolemic peptides

2.1 Production of hypocholesterolemic peptides

The generation of hypocholesterolemic peptides from food can be accomplished by a number of strategies, whereas all the strategies are based on enzymatic hydrolysis, microbial fermentation or chemical hydrolysis (Korhonen & Pihlanto, 2006; Ulug, Jahandideh, & Wu, 2021). Enzymatic hydrolysis is the most common method to obtain hypocholesterolemic peptides from their original protein source and may involve one or multiple enzymes. Enzymatic hydrolysis has more advantages than the other methods due to the use of mild temperature and pH conditions, the selectivity of commercial enzymes compared with chemical hydrolysis, the absence of secondary products that often appears during microbial fermentations and the absence of chemical compounds that makes this type of hydrolysis more friendly to the environment (Aluko, 2012; Xue, Yin, Howell, & Zhang, 2021). The process of enzymatic hydrolysis is simple and easy to inactivate and, once optimized, it can yield high amounts of bioactive peptides with good quality.

Many natural peptides are produced from food proteins during normal human digestion process, hydrolyzed by gastrointestinal enzymes, such as pepsin, pancreatin, trypsin, α -chymotrypsin, and peptidases. Enzymes from plants, food, bacteria and fungi, and commercial enzymes are also commonly used to produce peptides from various proteins (da Silva, 2017). For instance, food-grade enzyme (i.e., Alcalase) can release hypocholesterolemic peptides from different plant proteins such as lupin, soy, hempseed, and olive seed (Cerrato, et al., 2023; Prados, Marina, & García, 2018; Santos-Sánchez, et al., 2022). The type of hypocholesterolemic peptide produced after protein hydrolysis depends on the type of protease selected, as different enzymes have different cleavage sites and could produce different peptides even from the same

substrate. For instance, when white lupin protein is hydrolyzed by pepsin or trypsin, peptides with different amino acid sequences and HMGCoAR-inhibitory activity are produced. In fact, the hydrolysate produced by pepsin showed lower HMGCoAR-inhibitory activity *in vitro* (−17%) at the maximum tested dose (2.5 mg/mL), whereas the hydrolysate produced by trypsin significantly inhibited the HMGCoAR activity *in vitro* by 57% at the same concentration (Lammi, Zanoni, Scigliuolo, D’Amato, & Arnoldi, 2014). Moreover, the hydrolysate produced by Alcalase from narrow-leaf lupin caused a reduction of HMGCoAR activity *in vitro* by 51.5% at the concentration of 2.5 mg/mL (Santos-Sánchez, et al., 2022). Interestingly, hempseed was digested with Alcalase and pepsin, respectively, and both hydrolysates showed HMGCoAR-inhibitory activity, whereas the hydrolysate produced from Alcalase was able to decrease the PCSK9 protein level in HepG2 cells (Cerrato, et al., 2023), while the hydrolysate generated from pepsin showed an opposite activity which facilitated the expression of PCSK9 (Zanoni, Aiello, Arnoldi, & Lammi, 2017a). Furthermore, the combination of different enzymes would influence the peptides produced further and some known hypocholesterolemic peptides deriving from plant proteins have been generated by a multi-enzyme system that simulates gastrointestinal digestion, as reported for the investigation of rice protein hydrolysates (Tong, et al., 2017). Thus, the selection of the enzyme exerting suitable endo- and exopeptidase activities is crucial steps in the production of hypocholesterolemic peptides.

In addition, numerous processing methods, including microwave, pulsed electric field, high hydrostatic pressure, and ultrasound, may be combined with enzymatic hydrolysis to increase protein digestibility and peptide release (Marciniak, Suwal, Naderi, Pouliot, & Doyen, 2018; Ulug, Jahandideh, & Wu, 2021). It is believed that the processing techniques may cause the protein to unfold and increase the accessibility of the enzyme to break the peptide bonds. A study reported that the rate of β -lactoglobulin hydrolysis was increased 5–10 times under the treatment of high hydrostatic pressure (300 or 450 MPa) together with specific enzymes (trypsin, chymotrypsin and a protease from *Bacillus licheniformis*) (Knudsen, Otte, Olsen, & Skibsted, 2002). The reason is that pressure can affect the conformation of β -

lactoglobulin, causing it to unfold and expose some hydrophobic areas, thereby increasing the enzyme-substrate collision rate. This in turn strengthens enzymatic activity, increasing the rate of protein hydrolysis and promoting the release of active peptides. In another study, high-pressure-assisted hydrolysis with commercial enzymes was employed to increase the levels of active peptides in *Spirulina platensis* hydrolysates, and two HMGCoAR-inhibiting peptides (RCD and SNV) were identified (Chen & Yang, 2021). Likewise, cholesterol micelle formation inhibitory peptides were released from fermented seabass byproduct through high hydrostatic pressure-assisted protease hydrolysis (Chen, Lin, Huang, Lin, & Lin, 2021). Eovalbumin (Quirós, Chichón, Recio, & López-Fandiño, 2007), chickpea protein (Zhang, Jiang, Miao, Mu, & Li, 2012) and pinto bean protein (Garcia-Mora, Peñas, Frias, Zieliński, Wiczkowski, Zielińska, et al., 2016), have been explored in this context. Besides high hydrostatic pressure, ultrasonic-assisted technology has also been used in the production of hypocholesterolemic peptides because of its ability to unfold protein structure and strengthen the affinity between enzymes and proteins (Umego, He, Ren, Xu, & Ma, 2021). For example, mung bean hydrolysate exhibited higher inhibition of cholesterol solubilization after the pre-treatment of thermosonication (Ashraf, Liu, Awais, Xiao, Wang, Zhou, et al., 2020). Ultrasound-assisted sodium bisulfite pre-treatment improved the cholesterol-lowering activity of soybean protein hydrolysates after simulated gastrointestinal digestion by loosening soybean protein structure and exposing more hydrophobic groups (Huang, Li, Li, Ruan, Roknul Azam, Ou Yang, et al., 2021). Moreover, peptides with different hypocholesterolemic activities may also result from these various procedures. For example, the peptides from the protein isolate of raw cowpeas inhibit HMGCoAR activity, while the peptides from cooked cowpeas are more effective in inhibiting the micellar solubility of cholesterol (Marques, Soares Freitas, Corrêa Carlos, Siguemoto, Fontanari, & Arêas, 2015). This may be due to the treatment temperature of cowpeas, which causes greater protein denaturation and release of various bioactive peptides. Overall, processing technologies are being applied in the production of

hypocholesterolemic peptides and have been found to reduce the time and costs of processing and improve the yield of bioactive peptides.

On the other hand, modern *in silico* strategies based on simulation using bioinformatics tools are also supplying large amounts of data in comparison to the empirical approaches traditionally used. For higher hydrolysis rates and larger production, continuous reactors are being developed by using membranes or immobilized enzymes (Alavi & Ciftci, 2023; Regnier & Kim, 2014; Sitanggang, Sumitra, & Budijanto, 2021). Although much research has been performed at laboratory scale, further research is needed to overcome the challenges related to large-scale production of hypocholesterolemic peptides.

2.2 Digestion, transportation, and absorption of hypocholesterolemic peptides

The hypocholesterolemic effect of peptides *in vitro* does not determine their cholesterol-lowering effects *in vivo*, because there are several physical and biological barriers that must be overcome before they can reach blood circulation system (Amigo & Hernández-Ledesma, 2020). The hypocholesterolemic peptides *in vivo* can be stimulated only if these peptides are transported across the intestinal barrier into blood circulation system in an intact or active form with adequate concentrations and must reach their target organs and tissues. Thus, the hypocholesterolemic effect of peptides is subject to their resistance to hydrolysis by gastrointestinal tract proteases and brush border peptidases, and their permeability into blood circulation system in an intact or active form (Rutherford-Markwick, 2012; Shen & Matsui, 2017).

2.2.1 Gastrointestinal digestion

The digestive enzymes in the gastrointestinal tract may act upon the hypocholesterolemic peptides, and the resistance of a peptide to digestive enzymes depends on whether there are cleavage sites for digestive enzymes in its sequence and whether these cleavage sites are exposed (Ahmed, Sun, & Udenigwe, 2022). Most of peptides generated from proteins enter the intestine, which plays a key role in

absorption of peptides. The intestinal brush-border membrane, which is highly folded, provides a large surface area for metabolic activities, such as enzyme secretion and transporter presentation (Picariello, Miralles, Mamone, Sánchez-Rivera, Recio, Addeo, et al., 2015). Some hypocholesterolemic peptides can be produced in the gastrointestinal tract during protein digestion by multiple microbial or digestive enzymes in the brush-border membrane. Generally, *in vitro* digestion systems can be used to produce hypocholesterolemic peptides and study their resistance to gastrointestinal degradation. Enzymes, including pepsin, trypsin, pancreatic protease, elastase, α -chymotrypsin, and carboxypeptidases A and B are commonly used to mimic the process of human gastrointestinal digestion (Guerra, Etienne-Mesmin, Livrelli, Denis, Blanquet-Diot, & Alric, 2012). For instance, two hypocholesterolemic peptides VKP and VKK have been identified from freshwater clam hydrolysate with *in vitro* gastrointestinal digestion, display the bile-acid-binding capacity and inhibitory activity of cholesterol micelle formation (Lin, Tsai, & Chen, 2017). Cowpea bean, *S. platensis* protein, and rice protein have been investigated in this context (Chen & Yang, 2021; Marques, Fontanari, Pimenta, Soares-Freitas, & Arêas, 2015; Tong, et al., 2017).

The stability of peptides in gastrointestinal digestion depends on the length and molecular size of the peptides and their structural characteristics (Picariello, Siano, Di Stasio, Mamone, Addeo, & Ferranti, 2023). Numerous studies have shown that peptides with a molecular weight above 3 kDa are more likely to be hydrolyzed by gastrointestinal enzymes than those below 3 kDa (Dupont & Mackie, 2015). Another study suggested that small peptides (2 ~ 6 amino acids) are less susceptible to hydrolysis by digestive enzymes, probably due to a reduced number of enzyme-susceptible peptide bonds and less structural flexibility (Xu, Hong, Wu, & Yan, 2019). Structural properties, including hydrophobicity, net charge, acid-base properties, C- and N-terminal amino acid residues, amino acid sequence, and amino acid composition, all have an impact on the digestive stability of peptides (Pei, Gao, Pan, Hua, He, Liu, et al., 2022). Generally, peptides containing high content of proline residues, especially at the C-terminal, are more resistant to degradation by digestive

enzymes (Dupont & Mackie, 2015; Segura-Campos, Chel-Guerrero, Betancur-Ancona, & Hernandez-Escalante, 2011). This behavior is in agreement with experimental evidence that many tripeptides with proline residues were detected in human blood plasma after oral ingestion of corn and wheat hydrolysates, demonstrating marked stability to *in vivo* digestive conditions (Akika, Megumi, Yasushi, & Kenji, 2018). Peptides containing acidic amino acids were reported to display higher resistance to gastrointestinal enzymes in comparison with peptides containing neutral and basic amino acids, such as Arg, His and Lys (Agudelo, Gauthier, Pouliot, Marin, & Savoie, 2004; Wang, Wang, & Li, 2016). Moreover, net negatively charged peptide fractions with higher acidic amino acid contents were reported to easily escape from *in vitro* gastrointestinal digestion than positively charged fractions containing a higher amount of basic and aromatic residues (Ao & Li, 2013). Regarding hydrophobicity, high numbers of hydrophobic amino acids, such as Val and Leu, would cause the lower stability of peptides, which are susceptible to enzymatic digestions. As a recent review has reported that Leu was completely absent at the C-terminal of stable peptides but accounted for a large proportion of C-terminal cleavages in unstable peptides (Ahmed, Sun, & Udenigwe, 2022). This finding is consistent with the specificity of carboxypeptidase A1, which preferentially cleaves at C-terminal hydrophobic residues such as Leu. In addition, the cyclization induced by disulfide bond linkage would potentially prevent susceptible peptide bonds from enzymatic cleavage during gastrointestinal digestion (Góngora-Benítez, Tulla-Puche, & Albericio, 2014; Wang, Yadav, Smart, Tajiri, & Basit, 2015).

2.2.2 Intestinal transport and potential bioavailability of hypocholesterolemic peptides

It is important to note that there is not any specific mechanism of transport for hypocholesterolemic peptides, which are transported using the same mechanisms as other bioactive peptides (Xu, Hong, Wu, & Yan, 2019). Caco-2 cells derived from a human intestinal adenocarcinoma can be employed to investigate peptide transport and resistance of peptide to hydrolysis by brush border peptidases on the intestinal

cell membrane. The peptides can be transported across the intestinal epithelial cells through one or more routes, including peptide transport 1 (PepT1)-mediated routes, the paracellular route via tight junctions, transcytosis via vesicles and passive transcellular diffusion (Miner-Williams, Stevens, & Moughan, 2014; Xu, Hong, Wu, & Yan, 2019). Trans-epithelial transport and routes of transport of peptides vary based on physicochemical properties, including net charge, hydrophobicity, chain length and sequence of the peptide (Segura-Campos, Chel-Guerrero, Betancur-Ancona, & Hernandez-Escalante, 2011).

Commonly, di- and tripeptides can be actively transported intact across the brush border membrane of the epithelial cells into enterocytes via PepT1, which is responsible for the transportation of small peptides (< 500 Da). PepT1 is mainly distributed in the intestinal brush border membrane and is a high-capacity and low-affinity transporter that takes advantage of the proton's gradient between the intestinal lumen (pH 5.5–6.0) and epithelial cells (pH 7.0) (Wang, Xie, & Li, 2019). For example, antihypertensive peptides IPP and LKP isolated from bonito fish muscle and bovine milk β -casein, respectively, have been evidenced to be transported in part via the PepT1 using *in vitro*, *ex vivo*, and *in vivo* intestinal models (Gleeson, Brayden, & Ryan, 2017). Two peptides IW and IWH generated from spent hen also could pass through the intestinal epithelium via PepT1 in human intestinal Caco-2 cell monolayers (Fan, Xu, Hong, & Wu, 2018). Other food-derived peptides, like YPY, IV, AP (Wang & Li, 2017), IQW (Xu, Fan, Yu, Hong, & Wu, 2017), GP and IRW (Bejjani & Wu, 2013), can be transported by PepT1 transporter. However, thousands of transported di- and tripeptides are reported as anti-hypertensive, antioxidant, antidiabetic, and anti-inflammatory peptides (Xu, Hong, Wu, & Yan, 2019), and few kinds of literature have reported the mechanism of transport of di- or tripeptides with cholesterol-lowering activity. For instance, dry-cured ham derived dipeptides DA, DD, EE, ES, and LL (Heres, Mora, & Toldrá, 2021b), amaranth (*amaranthus cruentus*) derived tripeptides GGV and IVG (Tovar-Pérez, Lugo-Radillo, & Aguilera-Aguirre, 2019), and cowpea bean β -vignin protein derived tripeptides IAF, QGF, and QDF (Silva, et al., 2021), are identified as HMGCoAR inhibitors *in vitro* without

information about the mechanism of their transport. As mentioned in a recent review, 400 dipeptides and 8,000 tripeptides can be recognized and transported by the PepT1 (Xue, Yin, Howell, & Zhang, 2021), without selecting for specific amino acid sequence. Therefore, the mechanism of transport of these HMGCoAR inhibitory di- and tripeptides may involve PepT1-mediated route, which needs to be verified.

The passive paracellular route is influenced by peptide properties and tends to transport low molecular weight peptides (500 ~ 1600 Da) that are water-soluble (hydrophilic), whereas peptides with high hydrophobicity are more easily transported by simple passive transcellular diffusion or by transcytosis (Xu, Hong, Wu, & Yan, 2019; Xue, Yin, Howell, & Zhang, 2021). In a recent study (Lammi, et al., 2021), lupin peptide LILPKHSDAD with a dual HMGCoAR/PCSK9 inhibitory activity was examined the intestinal transport ability in the differentiated Caco-2 cell model. Since LILPKHSDAD is a decapeptide with a net charge (-1) and a hydrophobicity (+17.79 kcal/mol), it might be preferentially transported by passive transcellular diffusion or by transcytosis. It is difficult to assess the transport through the passive diffusion route due to the lack of regulators of this route, whereas wortmannin can be used as a transcytosis inhibitor to investigate the transcytosis route (Vij, Reddi, Kapila, & Kapila, 2016). In the presence of wortmannin, the transport of LILPKHSDAD was significantly impaired, which suggested that LILPKHSDAD is mainly transported by the transcytotic route. Another study investigated the intestinal trans-epithelial transport of hempseed peptides IGFLIIWV with hypocholesterolemic activity, and results suggested that this peptide may be preferentially transported by paracellular route and/or by transcytosis due to its hydrophobic property (Bollati, et al., 2022). Generally, intestinal transport and the route of transport of hypocholesterolemic peptides, especially via transcytosis, have been shown to depend on molecular weight, net charge, and hydrophobicity of peptides, with small-sized, positively charged and hydrophobic peptides being generally more permeable than others (Shimizu & Ok Son, 2007). Nevertheless, the structural requirements of peptides for transepithelial transport in general are currently not well understood. This highlights the need for

comprehensive structure-transport relationship investigations by employing known bioavailable peptides and physiologically relevant intestinal models.

Furthermore, the *in vivo* bioactivities of some peptides may be also directly associated with their fragments generated by the action of peptidases during intestinal transport (Daroit & Brandelli, 2021; Karaś, 2019). For example, the peptide LPKHSDAD was produced by hydrolysis of LILPKHSDAD by Caco-2 cell peptidases and transported across the cell monolayer via a passive diffusion mechanism or the paracellular route, and not by intracellular transcytosis due to unaffected by wortmannin. LPKHSDAD was also proved to exert a hypocholesterolemic behavior and shared the same mechanism of action with its native peptide (Lammi, et al., 2021). However, in some cases, metabolism under the action of peptidases may generate a fragment whose activity is enhanced and/or shifted to different targets. The HMGCoAR inhibitory peptide LTFPGSAED from white lupin protein hydrolysates was reported to be hydrolyzed to LTFPG by Caco-2 cell peptidases, and both the native peptide and its fragment were transported across the cell monolayer (Lammi, et al., 2020). Especially, LTFPGSAED was transported across the cell monolayer by transcellular route, whereas the mechanism of transport of LTFPG may involve the paracellular route. Although LTFPG maintains a modest ability to reduce the *in vitro* HMGCoAR activity, it is an effective hypotensive peptide whose activity has been demonstrated either *in vitro* or *in vivo* whereas its native peptide LTFPGSAED is a poor inhibitor of the ACE activity. This phenomenon may be invoked to explain the multifunctional activities of peptides *in vivo* and the difference observed between *in vitro* assays and *in vivo* results. Based on *in vitro* bioactivity, the transported peptides are strong candidates for further evaluation of hypocholesterolemic properties and/or other health-promoting activities at the tissue levels *in vivo*.

In addition, despite their permeability across the intestinal epithelium, many bioactive peptides are not bioavailable in substantial amounts *in vivo*. An 8.5% decrease in plasma PCSK9 level followed by a cholesterol-lowering effect was observed in mildly hypercholesterolemic humans who consumed 30 g of lupin protein/day for 4 weeks (Lammi, Zanoni, Calabresi, & Arnoldi, 2016). Although this may suggest that

the hypocholesterolemic peptides were absorbed, detection and quantification of the parent peptides in the serum and tissues are crucial to validating their biostability and bioavailability. Based on the limited literatures in this area, short chain hydrophobic peptides are hypothesized to be more resistant to hydrolysis by intestinal brush border proteases and to permeate the intestinal epithelium in their intact form (Daniel, 2004). Some hypocholesterolemic peptides that are not absorbed through the intestine can also offer health benefits by binding bile acid and inhibiting cholesterol micellar solubility to modulate dietary cholesterol metabolism in the gut (Nagaoka, Nakamura, Shibata, & Kanamaru, 2010). Unabsorbed bioactive peptides may also influence the gut microbiota population and metabolism in a special way to exert a positive cholesterol-lowering state (Ashaolu, 2020). Given that gut microbiota has been reported to mediate other health-promoting effects of bioactive peptides, future studies should consider defining the role of gut microbiota in the hypocholesterolemic properties of unabsorbed peptides (Guo, Yi, Hu, Shi, Xin, Gu, et al., 2021; Wu, Bekhit, Wu, Chen, Liao, Wang, et al., 2021; Yu, Amorim, Marques, Calhau, & Pintado, 2016).

References

- Agudelo, R. A., Gauthier, S. F., Pouliot, Y., Marin, J., & Savoie, L. (2004). Kinetics of peptide fraction release during in vitro digestion of casein. *Journal of the Science of Food and Agriculture*, 84(4), 325-332.
- Ahamad, S., Mathew, S., Khan, W. A., & Mohanan, K. (2022). Development of small-molecule PCSK9 inhibitors for the treatment of hypercholesterolemia. *Drug Discovery Today*, 27(5), 1332-1349.
- Ahmed, T., Sun, X., & Udenigwe, C. C. (2022). Role of structural properties of bioactive peptides in their stability during simulated gastrointestinal digestion: A systematic review. *Trends in Food Science & Technology*, 120, 265-273.
- Akika, E., Megumi, N., Yasushi, A. S., & Kenji, S. (2018). Identification of food-derived peptides in human blood after ingestion of corn and wheat gluten hydrolysates. *Journal of Food Bioactives*, 2(2).
- Alavi, F., & Ciftci, O. N. (2023). Purification and fractionation of bioactive peptides through membrane filtration: A critical and application review. *Trends in Food Science & Technology*, 131, 118-128.
- Aluko, R. (2012). Bioactive Peptides. In R. E. Aluko (Ed.), *Functional Foods and Nutraceuticals*, (pp. 37-61). New York, NY: Springer New York.
- Amigo, L., & Hernández-Ledesma, B. (2020). Current Evidence on the Bioavailability of Food Bioactive Peptides. In *Molecules*, vol. 25).
- Ao, J., & Li, B. (2013). Stability and antioxidative activities of casein peptide fractions during simulated gastrointestinal digestion in vitro: Charge properties of peptides affect digestive stability. *Food Research International*, 52(1), 334-341.
- Arnoldi, A., Lammi, C., & Aiello, G. (2019). Cholesterol-Reducing Foods: Proteins and Peptides. In L. Melton, F. Shahidi & P. Varelis (Eds.), *Encyclopedia of Food Chemistry*, (pp. 323-329). Oxford: Academic Press.
- Ashaolu, T. J. (2020). Soy bioactive peptides and the gut microbiota modulation. *Applied Microbiology and Biotechnology*, 104(21), 9009-9017.

- Ashraf, H., Butt, M. S., Iahtisham Ul, H., Nadeem, M., Aadil, R. M., Rusu, A. V., & Trif, M. (2022). Microencapsulated curcumin from *Curcuma longa* modulates diet-induced hypercholesterolemia in Sprague Dawley rats. *Front Nutr*, *9*, 1026890.
- Ashraf, J., Liu, L., Awais, M., Xiao, T., Wang, L., Zhou, X., Tong, L.-T., & Zhou, S. (2020). Effect of thermosonication pre-treatment on mung bean (*Vigna radiata*) and white kidney bean (*Phaseolus vulgaris*) proteins: Enzymatic hydrolysis, cholesterol lowering activity and structural characterization. *Ultrasonics Sonochemistry*, *66*, 105121.
- Behl, T., Singh, S., Sharma, N., Zahoor, I., Albarrati, A., Albratty, M., Meraya, A. M., Najmi, A., & Bungau, S. (2022). Expatiating the Pharmacological and Nanotechnological Aspects of the Alkaloidal Drug Berberine: Current and Future Trends. In *Molecules*, vol. 27).
- Bejjani, S., & Wu, J. (2013). Transport of IRW, an Ovotransferrin-Derived Antihypertensive Peptide, in Human Intestinal Epithelial Caco-2 Cells. *Journal of Agricultural and Food Chemistry*, *61*(7), 1487-1492.
- Bellosta, S., & Corsini, A. (2012). Statin drug interactions and related adverse reactions. *Expert Opinion on Drug Safety*, *11*(6), 933-946.
- Bollati, C., Cruz-Chamorro, I., Aiello, G., Li, J., Bartolomei, M., Santos-Sánchez, G., Ranaldi, G., Ferruzza, S., Sambuy, Y., Arnoldi, A., & Lammi, C. (2022). Investigation of the intestinal trans-epithelial transport and antioxidant activity of two hempseed peptides WVSPLAGRT (H2) and IGFLIIWV (H3). *Food Research International*, *152*, 110720.
- Borad, S. G., Kumar, A., & Singh, A. K. (2017). Effect of processing on nutritive values of milk protein. *Critical Reviews in Food Science and Nutrition*, *57*(17), 3690-3702.
- Bove, M., Cicero, A. F. G., & Borghi, C. (2019). Emerging drugs for the treatment of hypercholesterolemia. *Expert Opinion on Emerging Drugs*, *24*(1), 63-69.
- Brautbar, A., & Ballantyne, C. M. (2011). Pharmacological strategies for lowering LDL cholesterol: statins and beyond. *Nature Reviews Cardiology*, *8*(5), 253-265.
- Cerrato, A., Lammi, C., Laura Capriotti, A., Bollati, C., Cavaliere, C., Maria Montone, C., Bartolomei, M., Boschini, G., Li, J., Piovesana, S., Arnoldi, A., & Laganà, A. (2023). Isolation and functional characterization of hemp seed protein-derived short- and medium-chain peptide mixtures with multifunctional properties for metabolic syndrome prevention. *Food Research International*, *163*, 112219.

- Chakrabarti, S., Jahandideh, F., & Wu, J. (2014). Food-Derived Bioactive Peptides on Inflammation and Oxidative Stress. *BioMed Research International*, 2014, 608979.
- Chauvin, B., Drouot, S., Barrail-Tran, A., & Taburet, A.-M. (2013). Drug–Drug Interactions Between HMG-CoA Reductase Inhibitors (Statins) and Antiviral Protease Inhibitors. *Clinical Pharmacokinetics*, 52(10), 815-831.
- Chen, G.-W., Lin, H.-T. V., Huang, L.-W., Lin, C.-H., & Lin, Y.-H. (2021). Purification and Identification of Cholesterol Micelle Formation Inhibitory Peptides of Hydrolysate from High Hydrostatic Pressure-Assisted Protease Hydrolysis of Fermented Seabass Byproduct. In *International Journal of Molecular Sciences*, vol. 22).
- Chen, G.-W., & Yang, M.-H. (2021). Production and Purification of Novel Hypocholesterolemic Peptides from Lactic Fermented *Spirulina platensis* through High Hydrostatic Pressure-Assisted Protease Hydrolysis. In *Catalysts*, vol. 11).
- Chen, G., Chen, W., Xu, J., Ma, G., Hu, X., & Chen, G. (2023). The current trend and challenges of developing red yeast rice-based food supplements for hypercholesterolemia. *Journal of Future Foods*, 3(4), 312-329.
- Cicero, A. F. G., Fogacci, F., & Banach, M. (2019). Red Yeast Rice for Hypercholesterolemia. *Methodist Debakey Cardiovasc J*, 15(3), 192-199.
- Cicero, A. F. G., Fogacci, F., & Colletti, A. (2017). Potential role of bioactive peptides in prevention and treatment of chronic diseases: a narrative review. *British Journal of Pharmacology*, 174(11), 1378-1394.
- Coelho, M. S., Soares-Freitas, R. A. M., Arêas, J. A. G., Gandra, E. A., & Salas-Mellado, M. d. I. M. (2018). Peptides from Chia Present Antibacterial Activity and Inhibit Cholesterol Synthesis. *Plant Foods for Human Nutrition*, 73(2), 101-107.
- Cruz-Chamorro, I., Santos-Sánchez, G., Bollati, C., Bartolomei, M., Li, J., Arnoldi, A., & Lammi, C. (2022). Hempseed (*Cannabis sativa*) Peptides WVSPLAGRT and IGFLIIWV Exert Anti-inflammatory Activity in the LPS-Stimulated Human Hepatic Cell Line. *Journal of Agricultural and Food Chemistry*, 70(2), 577-583.
- da Silva, R. R. (2017). Bacterial and Fungal Proteolytic Enzymes: Production, Catalysis and Potential Applications. *Applied Biochemistry and Biotechnology*, 183(1), 1-19.

- Dalgaard, P., & Emborg, J. (2009). 31 - Histamine fish poisoning – new information to control a common seafood safety issue. In C. d. W. Blackburn & P. J. McClure (Eds.), *Foodborne Pathogens (Second Edition)*, (pp. 1140-1160): Woodhead Publishing.
- Daniel, H. (2004). Molecular and Integrative Physiology of Intestinal Peptide Transport. *Annual Review of Physiology*, 66(1), 361-384.
- Daroit, D. J., & Brandelli, A. (2021). In vivo bioactivities of food protein-derived peptides – a current review. *Current Opinion in Food Science*, 39, 120-129.
- Dei Cas, M., & Ghidoni, R. (2019). Dietary Curcumin: Correlation between Bioavailability and Health Potential. In *Nutrients*, vol. 11).
- Dupont, D., & Mackie, A. R. (2015). Static and dynamic in vitro digestion models to study protein stability in the gastrointestinal tract. *Drug Discovery Today: Disease Models*, 17-18, 23-27.
- Fan, H., Liu, H., Zhang, Y., Zhang, S., Liu, T., & Wang, D. (2022). Review on plant-derived bioactive peptides: biological activities, mechanism of action and utilizations in food development. *Journal of Future Foods*, 2(2), 143-159.
- Fan, H., Xu, Q., Hong, H., & Wu, J. (2018). Stability and Transport of Spent Hen-Derived ACE-Inhibitory Peptides IWHHT, IWH, and IW in Human Intestinal Caco-2 Cell Monolayers. *Journal of Agricultural and Food Chemistry*, 66(43), 11347-11354.
- Feng, X., Sureda, A., Jafari, S., Memariani, Z., Tewari, D., Annunziata, G., Barrea, L., Hassan, S. T. S., Šmejkal, K., Malaník, M., Sychrová, A., Barreca, D., Ziberna, L., Mahomoodally, M. F., Zengin, G., Xu, S., Nabavi, S. M., & Shen, A. Z. (2019). Berberine in Cardiovascular and Metabolic Diseases: From Mechanisms to Therapeutics. *Theranostics*, 9(7), 1923-1951.
- Fernández-Tomé, S., & Hernández-Ledesma, B. (2019). Current state of art after twenty years of the discovery of bioactive peptide lunasin. *Food Research International*, 116, 71-78.
- Friesen, J. A., & Rodwell, V. W. (2004). The 3-hydroxy-3-methylglutaryl coenzyme-A (HMG-CoA) reductases. *Genome Biology*, 5(11), 248.
- Gaidai, O., Cao, Y., & Loginov, S. (2023). Global cardiovascular diseases death rate prediction. *Current Problems in Cardiology*, 101622.
- Galvez, A. F. (2012). Abstract 10693: Identification of Lunasin as the Active Component in Soy Protein Responsible for Reducing LDL Cholesterol and Risk of Cardiovascular Disease. *Circulation*, 126(suppl_21), A10693-A10693.

- Garcia-Mora, P., Peñas, E., Frias, J., Zieliński, H., Wiczowski, W., Zielińska, D., & Martínez-Villaluenga, C. (2016). High-Pressure-Assisted Enzymatic Release of Peptides and Phenolics Increases Angiotensin Converting Enzyme I Inhibitory and Antioxidant Activities of Pinto Bean Hydrolysates. *Journal of Agricultural and Food Chemistry*, *64*(8), 1730-1740.
- Gleeson, J. P., Brayden, D. J., & Ryan, S. M. (2017). Evaluation of PepT1 transport of food-derived antihypertensive peptides, Ile-Pro-Pro and Leu-Lys-Pro using in vitro, ex vivo and in vivo transport models. *European Journal of Pharmaceutics and Biopharmaceutics*, *115*, 276-284.
- Goldstein, J. L., & Brown, M. S. (2009). The LDL Receptor. *Arteriosclerosis, Thrombosis, and Vascular Biology*, *29*(4), 431-438.
- Góngora-Benítez, M., Tulla-Puche, J., & Albericio, F. (2014). Multifaceted Roles of Disulfide Bonds. Peptides as Therapeutics. *Chemical Reviews*, *114*(2), 901-926.
- Grazioso, G., Bollati, C., Sgrignani, J., Arnoldi, A., & Lammi, C. (2018). First Food-Derived Peptide Inhibitor of the Protein–Protein Interaction between Gain-of-Function PCSK9D374Y and the Low-Density Lipoprotein Receptor. *Journal of Agricultural and Food Chemistry*, *66*(40), 10552-10557.
- Gu, L., Wang, Y., Xu, Y., Tian, Q., Lei, G., Zhao, C., Gao, Z., Pan, Q., Zhao, W., Nong, L., & Tan, S. (2017). Lunasin functionally enhances LDL uptake via inhibiting PCSK9 and enhancing LDLR expression in vitro and in vivo. *Oncotarget*, *8*(46), 80826-80840.
- Guerra, A., Etienne-Mesmin, L., Livrelli, V., Denis, S., Blanquet-Diot, S., & Alric, M. (2012). Relevance and challenges in modeling human gastric and small intestinal digestion. *Trends in Biotechnology*, *30*(11), 591-600.
- Guo, J., Sun, Q., Wu, C., & Wu, J. (2022). Adherence to lifestyle advice and its related cardiovascular disease risk among US adults with high cholesterol. *Clinical Nutrition ESPEN*, *51*, 267-273.
- Guo, Z., Yi, D., Hu, B., Shi, Y., Xin, Y., Gu, Z., Liu, H., & Zhang, L. (2021). The alteration of gut microbiota by bioactive peptides: a review. *Systems Microbiology and Biomanufacturing*, *1*(4), 363-377.
- Ha, E., & Zemel, M. B. (2003). Functional properties of whey, whey components, and essential amino acids: mechanisms underlying health benefits for active people (review). *The Journal of Nutritional Biochemistry*, *14*(5), 251-258.

- Heres, A., Mora, L., & Toldrá, F. (2021a). Correction to: Inhibition of 3-hydroxy-3-methylglutarylcoenzyme A reductase enzyme by dipeptides identified in dry-cured ham. *Food Production, Processing and Nutrition*, 3(1), 24.
- Heres, A., Mora, L., & Toldrá, F. (2021b). Inhibition of 3-hydroxy-3-methyl-glutaryl-coenzyme A reductase enzyme by dipeptides identified in dry-cured ham. *Food Production, Processing and Nutrition*, 3(1), 18.
- Horton, J. D., Goldstein, J. L., & Brown, M. S. (2002). SREBPs: activators of the complete program of cholesterol and fatty acid synthesis in the liver. *The Journal of Clinical Investigation*, 109(9), 1125-1131.
- Hu, M., Huang, X., Han, X., & Ji, L. (2020). Loss of HNF1 α Function Contributes to Hepatocyte Proliferation and Abnormal Cholesterol Metabolism via Downregulating miR-122: A Novel Mechanism of MODY3. *Diabetes Metab Syndr Obes*, 13, 627-639.
- Huang, S., Li, Y., Li, C., Ruan, S., Roknul Azam, S. M., Ou Yang, N., Ye, X., Wang, Y., & Ma, H. (2021). Effects of ultrasound-assisted sodium bisulfite pretreatment on the preparation of cholesterol-lowering peptide precursors from soybean protein. *International Journal of Biological Macromolecules*, 183, 295-304.
- Iwaniak, A., & Mogut, D. (2020). Metabolic Syndrome-Preventive Peptides Derived from Milk Proteins and Their Presence in Cheeses: A Review. In *Applied Sciences*, vol. 10).
- Karaš, M. (2019). Influence of physiological and chemical factors on the absorption of bioactive peptides. *International Journal of Food Science & Technology*, 54(5), 1486-1496.
- Khan, F., Niaz, K., & Abdollahi, M. (2018). Toxicity of Biologically Active Peptides and Future Safety Aspects: An Update. *Current Drug Discovery Technologies*, 15(3), 236-242.
- Knudsen, J. C., Otte, J., Olsen, K., & Skibsted, L. H. (2002). Effect of high hydrostatic pressure on the conformation of β -lactoglobulin A as assessed by proteolytic peptide profiling. *International Dairy Journal*, 12(10), 791-803.
- Korhonen, H., & Pihlanto, A. (2006). Bioactive peptides: Production and functionality. *International Dairy Journal*, 16(9), 945-960.
- Kovacova-Hanusikova, E., Buday, T., Gavliakova, S., & Plevkova, J. (2015). Histamine, histamine intoxication and intolerance. *Allergologia et Immunopathologia*, 43(5), 498-506.

- Lambert, G., Charlton, F., Rye, K.-A., & Piper, D. E. (2009). Molecular basis of PCSK9 function. *Atherosclerosis*, *203*(1), 1-7.
- Lammi, C., Aiello, G., Bollati, C., Li, J., Bartolomei, M., Ranaldi, G., Ferruzza, S., Fassi, E. M., Grazioso, G., Sambuy, Y., & Arnoldi, A. (2021). Trans-Epithelial Transport, Metabolism, and Biological Activity Assessment of the Multi-Target Lupin Peptide LILPKHSDAD (P5) and Its Metabolite LPKHSDAD (P5-Met). In *Nutrients*, vol. 13).
- Lammi, C., Aiello, G., Boschini, G., & Arnoldi, A. (2019). Multifunctional peptides for the prevention of cardiovascular disease: A new concept in the area of bioactive food-derived peptides. *Journal of Functional Foods*, *55*, 135-145.
- Lammi, C., Aiello, G., Dellafiora, L., Bollati, C., Boschini, G., Ranaldi, G., Ferruzza, S., Sambuy, Y., Galaverna, G., & Arnoldi, A. (2020). Assessment of the Multifunctional Behavior of Lupin Peptide P7 and Its Metabolite Using an Integrated Strategy. *Journal of Agricultural and Food Chemistry*, *68*(46), 13179-13188.
- Lammi, C., Aiello, G., Vistoli, G., Zanoni, C., Arnoldi, A., Sambuy, Y., Ferruzza, S., & Ranaldi, G. (2016). A multidisciplinary investigation on the bioavailability and activity of peptides from lupin protein. *Journal of Functional Foods*, *24*, 297-306.
- Lammi, C., Bollati, C., Lecca, D., Abbracchio, M. P., & Arnoldi, A. (2019). Lupin Peptide T9 (GQEQSHQDEGVIVR) Modulates the Mutant PCSK9D374Y Pathway: in vitro Characterization of its Dual Hypocholesterolemic Behavior. In *Nutrients*, vol. 11).
- Lammi, C., Fassi, E. M. A., Li, J., Bartolomei, M., Benigno, G., Roda, G., Arnoldi, A., & Grazioso, G. (2022). Computational Design and Biological Evaluation of Analogs of Lupin Peptide P5 Endowed with Dual PCSK9/HMG-CoAR Inhibiting Activity. In *Pharmaceutics*, vol. 14).
- Lammi, C., Sgrignani, J., Roda, G., Arnoldi, A., & Grazioso, G. (2019). Inhibition of PCSK9D374Y/LDLR Protein-Protein Interaction by Computationally Designed T9 Lupin Peptide. *ACS Medicinal Chemistry Letters*, *10*(4), 425-430.
- Lammi, C., Zanoni, C., Aiello, G., Arnoldi, A., & Grazioso, G. (2016). Lupin Peptides Modulate the Protein-Protein Interaction of PCSK9 with the Low Density Lipoprotein Receptor in HepG2 Cells. *Scientific Reports*, *6*(1), 29931.

- Lammi, C., Zanoni, C., & Arnoldi, A. (2015). IAVPGEVA, IAVPTGVA, and LPYP, three peptides from soy glycinin, modulate cholesterol metabolism in HepG2 cells through the activation of the LDLR-SREBP2 pathway. *Journal of Functional Foods*, *14*, 469-478.
- Lammi, C., Zanoni, C., Arnoldi, A., & Aiello, G. (2018). YDFYPSSTKDQQS (P3), a peptide from lupin protein, absorbed by Caco-2 cells, modulates cholesterol metabolism in HepG2 cells via SREBP-1 activation. *Journal of Food Biochemistry*, *42*(3), e12524.
- Lammi, C., Zanoni, C., Arnoldi, A., & Vistoli, G. (2015). Two Peptides from Soy β -Conglycinin Induce a Hypocholesterolemic Effect in HepG2 Cells by a Statin-Like Mechanism: Comparative in Vitro and in Silico Modeling Studies. *Journal of Agricultural and Food Chemistry*, *63*(36), 7945-7951.
- Lammi, C., Zanoni, C., Calabresi, L., & Arnoldi, A. (2016). Lupin protein exerts cholesterol-lowering effects targeting PCSK9: From clinical evidences to elucidation of the in vitro molecular mechanism using HepG2 cells. *Journal of Functional Foods*, *23*, 230-240.
- Lammi, C., Zanoni, C., Scigliuolo, G. M., D'Amato, A., & Arnoldi, A. (2014). Lupin Peptides Lower Low-Density Lipoprotein (LDL) Cholesterol through an Up-regulation of the LDL Receptor/Sterol Regulatory Element Binding Protein 2 (SREBP2) Pathway at HepG2 Cell Line. *Journal of Agricultural and Food Chemistry*, *62*(29), 7151-7159.
- Laufs, U., Banach, M., Mancini, G. B. J., Gaudet, D., Bloedon, L. T., Sterling, L. R., Kelly, S., & Stroes, E. S. G. (2019). Efficacy and Safety of Bempedoic Acid in Patients With Hypercholesterolemia and Statin Intolerance. *Journal of the American Heart Association*, *8*(7), e011662.
- Li, J., Bollati, C., Bartolomei, M., Mazzolari, A., Arnoldi, A., Vistoli, G., & Lammi, C. (2022). Hempseed (*Cannabis sativa*) Peptide H3 (IGFLIIWV) Exerts Cholesterol-Lowering Effects in Human Hepatic Cell Line. In *Nutrients*, vol. 14).
- Lin, Y.-H., Tsai, J.-S., & Chen, G.-W. (2017). Purification and identification of hypocholesterolemic peptides from freshwater clam hydrolysate with in vitro gastrointestinal digestion. *Journal of Food Biochemistry*, *41*(4), e12385.
- Liu, F., Zhu, X., Jiang, X., Li, S., & Lv, Y. (2022). Transcriptional control by HNF-1: Emerging evidence showing its role in lipid metabolism and lipid metabolism disorders. *Genes & Diseases*, *9*(5), 1248-1257.

- Liu, L., Li, S., Zheng, J., Bu, T., He, G., & Wu, J. (2020). Safety considerations on food protein-derived bioactive peptides. *Trends in Food Science & Technology*, *96*, 199-207.
- Lundquist, P., & Artursson, P. (2016). Oral absorption of peptides and nanoparticles across the human intestine: Opportunities, limitations and studies in human tissues. *Advanced Drug Delivery Reviews*, *106*, 256-276.
- Marciniak, A., Suwal, S., Naderi, N., Pouliot, Y., & Doyen, A. (2018). Enhancing enzymatic hydrolysis of food proteins and production of bioactive peptides using high hydrostatic pressure technology. *Trends in Food Science & Technology*, *80*, 187-198.
- Marques, M. R., Fontanari, G. G., Pimenta, D. C., Soares-Freitas, R. M., & Arêas, J. A. G. (2015). Proteolytic hydrolysis of cowpea proteins is able to release peptides with hypocholesterolemic activity. *Food Research International*, *77*, 43-48.
- Marques, M. R., Soares Freitas, R. A. M., Corrêa Carlos, A. C., Siguemoto, É. S., Fontanari, G. G., & Arêas, J. A. G. (2015). Peptides from cowpea present antioxidant activity, inhibit cholesterol synthesis and its solubilisation into micelles. *Food Chemistry*, *168*, 288-293.
- McDonagh, M., Peterson, K., Holzhammer, B., & Fazio, S. (2016). A Systematic Review of PCSK9 Inhibitors Alirocumab and Evolocumab. *Journal of Managed Care & Specialty Pharmacy*, *22*(6), 641-653q.
- Mensah, G. A., Roth, G. A., & Fuster, V. (2019). The Global Burden of Cardiovascular Diseases and Risk Factors. *74*(20), 2529-2532.
- Miner-Williams, W. M., Stevens, B. R., & Moughan, P. J. (2014). Are intact peptides absorbed from the healthy gut in the adult human? *Nutrition Research Reviews*, *27*(2), 308-329.
- Mohan, A., & Udenigwe, C. C. (2015). Towards the design of hypolipidaemic peptides: Deoxycholate binding affinity of hydrophobic peptide aggregates of casein plastein. *Journal of Functional Foods*, *18*, 129-136.
- Mohanty, D., Jena, R., Choudhury, P. K., Pattnaik, R., Mohapatra, S., & Saini, M. R. (2016). Milk Derived Antimicrobial Bioactive Peptides: A Review. *International Journal of Food Properties*, *19*(4), 837-846.
- Momtazi, A. A., Banach, M., Pirro, M., Katsiki, N., & Sahebkar, A. (2017). Regulation of PCSK9 by nutraceuticals. *Pharmacological Research*, *120*, 157-169.

- Mora, L., & Toldrá, F. (2023). Advanced enzymatic hydrolysis of food proteins for the production of bioactive peptides. *Current Opinion in Food Science*, *49*, 100973.
- Murdock, L. L., & Shade, R. E. (2002). Lectins and Protease Inhibitors as Plant Defenses against Insects. *Journal of Agricultural and Food Chemistry*, *50*(22), 6605-6611.
- Nagaoka, S., Futamura, Y., Miwa, K., Awano, T., Yamauchi, K., Kanamaru, Y., Tadashi, K., & Kuwata, T. (2001). Identification of Novel Hypocholesterolemic Peptides Derived from Bovine Milk β -Lactoglobulin. *Biochemical and Biophysical Research Communications*, *281*(1), 11-17.
- Nagaoka, S., Nakamura, A., Shibata, H., & Kanamaru, Y. (2010). Soystatin (VAWWMY), a Novel Bile Acid-Binding Peptide, Decreased Micellar Solubility and Inhibited Cholesterol Absorption in Rats. *Bioscience, Biotechnology, and Biochemistry*, *74*(8), 1738-1741.
- Nagaoka, S., Takeuchi, A., & Banno, A. (2021). Plant-derived peptides improving lipid and glucose metabolism. *Peptides*, *142*, 170577.
- Nishikido, T., & Ray, K. K. (2019). Non-antibody Approaches to Proprotein Convertase Subtilisin Kexin 9 Inhibition: siRNA, Antisense Oligonucleotides, Adnectins, Vaccination, and New Attempts at Small-Molecule Inhibitors Based on New Discoveries. *5*.
- Noce, A., Di Lauro, M., Di Daniele, F., Pietroboni Zaitseva, A., Marrone, G., Borboni, P., & Di Daniele, N. (2021). Natural Bioactive Compounds Useful in Clinical Management of Metabolic Syndrome. In *Nutrients*, vol. 13).
- Norata, G. D., Tibolla, G., & Catapano, A. L. (2014). PCSK9 inhibition for the treatment of hypercholesterolemia: Promises and emerging challenges. *Vascular Pharmacology*, *62*(2), 103-111.
- Nwachukwu, I. D., & Aluko, R. E. (2019). Structural and functional properties of food protein-derived antioxidant peptides. *Journal of Food Biochemistry*, *43*(1), e12761.
- Och, A., Podgórski, R., & Nowak, R. (2020). Biological Activity of Berberine—A Summary Update. In *Toxins*, vol. 12).
- Patil, P. J., Usman, M., Zhang, C., Mehmood, A., Zhou, M., Teng, C., & Li, X. (2022). An updated review on food-derived bioactive peptides: Focus on the regulatory requirements, safety, and bioavailability. *Comprehensive Reviews in Food Science and Food Safety*, *21*(2), 1732-1776.

- Paulus, T., Henle, T., Haeßner, R., & Klostermeyer, H. (1997). Formation of thiazolines within the peptide chain during heating of proteins. *Zeitschrift für Lebensmitteluntersuchung und -Forschung A*, 204(4), 247-251.
- Pei, J., Gao, X., Pan, D., Hua, Y., He, J., Liu, Z., & Dang, Y. (2022). Advances in the stability challenges of bioactive peptides and improvement strategies. *Current Research in Food Science*, 5, 2162-2170.
- Peng, S., Song, H., Chen, Y., Li, S., & Guan, X. (2022). Oral Delivery of Food-derived Bioactive Peptides: Challenges and Strategies. *Food Reviews International*, 1-29.
- Perez-Gregorio, M. R., Días, R., Mateus, N., & de Freitas, V. (2018). Identification and characterization of proteolytically resistant gluten-derived peptides. *Food & Function*, 9(3), 1726-1735.
- Picariello, G., Miralles, B., Mamone, G., Sánchez-Rivera, L., Recio, I., Addeo, F., & Ferranti, P. (2015). Role of intestinal brush border peptidases in the simulated digestion of milk proteins. *Molecular Nutrition & Food Research*, 59(5), 948-956.
- Picariello, G., Siano, F., Di Stasio, L., Mamone, G., Addeo, F., & Ferranti, P. (2023). Structural properties of food proteins underlying stability or susceptibility to human gastrointestinal digestion. *Current Opinion in Food Science*, 50, 100992.
- Prados, I. M., Marina, M. L., & García, M. C. (2018). Isolation and identification by high resolution liquid chromatography tandem mass spectrometry of novel peptides with multifunctional lipid-lowering capacity. *Food Research International*, 111, 77-86.
- Prados, I. M., Orellana, J. M., Marina, M. L., & García, M. C. (2020). Identification of Peptides Potentially Responsible for In Vivo Hypolipidemic Activity of a Hydrolysate from Olive Seeds. *Journal of Agricultural and Food Chemistry*, 68(14), 4237-4244.
- Quirós, A., Chichón, R., Recio, I., & López-Fandiño, R. (2007). The use of high hydrostatic pressure to promote the proteolysis and release of bioactive peptides from ovalbumin. *Food Chemistry*, 104(4), 1734-1739.
- Regnier, F. E., & Kim, J. (2014). Accelerating trypsin digestion: the immobilized enzyme reactor. *Bioanalysis*, 6(19), 2685-2698.
- Reiner, Ž. (2014). Primary Prevention of Cardiovascular Disease with Statins in the Elderly. *Current Atherosclerosis Reports*, 16(7), 420.

- Rivero-Pino, F. (2023). Bioactive food-derived peptides for functional nutrition: Effect of fortification, processing and storage on peptide stability and bioactivity within food matrices. *Food Chemistry*, 406, 135046.
- Rosenson Robert, S., Hegele Robert, A., Fazio, S., & Cannon Christopher, P. (2018). The Evolving Future of PCSK9 Inhibitors. *Journal of the American College of Cardiology*, 72(3), 314-329.
- Rutherford-Markwick, K. J. (2012). Food proteins as a source of bioactive peptides with diverse functions. *British Journal of Nutrition*, 108(S2), S149-S157.
- Santi, L., Maggioli, C., Mastroroberto, M., Tufoni, M., Napoli, L., & Caraceni, P. (2012). Acute Liver Failure Caused by *Amanita phalloides* Poisoning. *International Journal of Hepatology*, 2012, 487480.
- Santos-Sánchez, G., Cruz-Chamorro, I., Bollati, C., Bartolomei, M., Pedroche, J., Millán, F., Millán-Linares, M. d. C., Capriotti, A. L., Cerrato, A., Laganà, A., Arnoldi, A., Carrillo-Vico, A., & Lammi, C. (2022). A *Lupinus angustifolius* protein hydrolysate exerts hypocholesterolemic effects in Western diet-fed ApoE^{-/-} mice through the modulation of LDLR and PCSK9 pathways. *Food & Function*, 13(7), 4158-4170.
- Sato, R. (2010). Sterol metabolism and SREBP activation. *Archives of Biochemistry and Biophysics*, 501(2), 177-181.
- Segura-Campos, M., Chel-Guerrero, L., Betancur-Ancona, D., & Hernandez-Escalante, V. M. (2011). Bioavailability of Bioactive Peptides. *Food Reviews International*, 27(3), 213-226.
- Shen, W., & Matsui, T. (2017). Current knowledge of intestinal absorption of bioactive peptides. *Food & Function*, 8(12), 4306-4314.
- Shende, V. R., Wu, M., Singh, A. B., Dong, B., Kan, C. F. K., & Liu, J. (2015). Reduction of circulating PCSK9 and LDL-C levels by liver-specific knockdown of HNF1 α in normolipidemic mice[S]. *J Lipid Res*, 56(4), 801-809.
- Shi, W., Hou, T., Guo, D., & He, H. (2019). Evaluation of hypolipidemic peptide (Val-Phe-Val-Arg-Asn) virtual screened from chickpea peptides by pharmacophore model in high-fat diet-induced obese rat. *Journal of Functional Foods*, 54, 136-145.
- Shimizu, M., & Ok Son, D. (2007). Food-Derived Peptides and Intestinal Functions. *Current Pharmaceutical Design*, 13(9), 885-895.

- Sible, A. M., Nawarskas, J. J., & Anderson, J. R. (2016). PCSK9 Inhibitors: An Innovative Approach to Treating Hyperlipidemia. *Cardiology in Review*, 24(3).
- Silva, M., Philadelpho, B., Santos, J., Souza, V., Souza, C., Santiago, V., Silva, J., Souza, C., Azeredo, F., Castilho, M., Cilli, E., & Ferreira, E. (2021). IAF, QGF, and QDF Peptides Exhibit Cholesterol-Lowering Activity through a Statin-like HMG-CoA Reductase Regulation Mechanism: In Silico and In Vitro Approach. In *International Journal of Molecular Sciences*, vol. 22).
- Silva, M. B. d. C. e., Souza, C. A. d. C., Philadelpho, B. O., Cunha, M. M. N. d., Batista, F. P. R., Silva, J. R. d., Druzian, J. I., Castilho, M. S., Cilli, E. M., & Ferreira, E. S. (2018). In vitro and in silico studies of 3-hydroxy-3-methyl-glutaryl coenzyme A reductase inhibitory activity of the cowpea Gln-Asp-Phe peptide. *Food Chemistry*, 259, 270-277.
- Singh, B. P., Aluko, R. E., Hati, S., & Solanki, D. (2022). Bioactive peptides in the management of lifestyle-related diseases: Current trends and future perspectives. *Critical Reviews in Food Science and Nutrition*, 62(17), 4593-4606.
- Sitanggang, A. B., Sumitra, J., & Budijanto, S. (2021). Continuous production of tempe-based bioactive peptides using an automated enzymatic membrane reactor. *Innovative Food Science & Emerging Technologies*, 68, 102639.
- Soares, R. A., Mendonça, S., De Castro, L. Í. A., Menezes, A. C., & Arêas, J. A. (2015). Major Peptides from Amaranth (*Amaranthus cruentus*) Protein Inhibit HMG-CoA Reductase Activity. In *International Journal of Molecular Sciences*, vol. 16 (pp. 4150-4160).
- Song, D., Hao, J., & Fan, D. (2020). Biological properties and clinical applications of berberine. *Frontiers of Medicine*, 14(5), 564-582.
- Sun, S., Wang, W., Wang, N., Zhang, Y., Zhu, Z., Li, X., Wang, J., Chen, Q., Ahmed Sadiq, F., Yang, H., Qi, Q., & Zhang, G. (2021). HPP and SGQR peptides from silkworm pupae protein hydrolysates regulated biosynthesis of cholesterol in HepG2 cell line. *Journal of Functional Foods*, 77, 104328.
- Superko, H. R. (2000). Hypercholesterolemia and dyslipidemia. *Current Treatment Options in Cardiovascular Medicine*, 2(2), 173-187.
- Svensson, B., Fukuda, K., Nielsen, P. K., & Bønsager, B. C. (2004). Proteinaceous α -amylase inhibitors. *Biochimica et Biophysica Acta (BBA) - Proteins and Proteomics*, 1696(2), 145-156.

- Taylor, B. A., & Thompson, P. D. (2016). Statins and Their Effect on PCSK9—Impact and Clinical Relevance. *Current Atherosclerosis Reports*, 18(8), 46.
- Tombling, B. J., Zhang, Y., Huang, Y.-H., Craik, D. J., & Wang, C. K. (2021). The emerging landscape of peptide-based inhibitors of PCSK9. *Atherosclerosis*, 330, 52-60.
- Tong, L.-T., Ju, Z., Qiu, J., Wang, L., Liu, L., Zhou, X., & Zhou, S. (2017). Peptide GEQQQQPGM derived from rice α -globulin reduces the risk of atherosclerosis in hamsters by improving vascular endothelial cells injury. *RSC Advances*, 7(78), 49194-49203.
- Tordesillas, L., Berin, M. C., & Sampson, H. A. (2017). Immunology of Food Allergy. *Immunity*, 47(1), 32-50.
- Tovar-Pérez, E. G., Lugo-Radillo, A., & Aguilera-Aguirre, S. (2019). Amaranth grain as a potential source of biologically active peptides: a review of their identification, production, bioactivity, and characterization. *Food Reviews International*, 35(3), 221-245.
- Udenigwe, C. C., Abioye, R. O., Okagu, I. U., & Obeme-Nmom, J. I. (2021). Bioaccessibility of bioactive peptides: recent advances and perspectives. *Current Opinion in Food Science*, 39, 182-189.
- Ulug, S. K., Jahandideh, F., & Wu, J. (2021). Novel technologies for the production of bioactive peptides. *Trends in Food Science & Technology*, 108, 27-39.
- Umego, E. C., He, R., Ren, W., Xu, H., & Ma, H. (2021). Ultrasonic-assisted enzymolysis: Principle and applications. *Process Biochemistry*, 100, 59-68.
- Van Damme, E. J. M. (2014). History of Plant Lectin Research. In J. Hirabayashi (Ed.), *Lectins: Methods and Protocols*, (pp. 3-13). New York, NY: Springer New York.
- Van Damme, E. J. M., Lannoo, N., & Peumans, W. J. (2008). Plant Lectins. In J.-C. Kader & M. Delseny (Eds.), *Advances in Botanical Research*, vol. 48 (pp. 107-209): Academic Press.
- Vij, R., Reddi, S., Kapila, S., & Kapila, R. (2016). Transepithelial transport of milk derived bioactive peptide VLPVPQK. *Food Chemistry*, 190, 681-688.
- Wang, B., & Li, B. (2017). Effect of molecular weight on the transepithelial transport and peptidase degradation of casein-derived peptides by using Caco-2 cell model. *Food Chemistry*, 218, 1-8.
- Wang, B., Xie, N., & Li, B. (2019). Influence of peptide characteristics on their stability, intestinal transport, and in vitro bioavailability: A review. *Journal of Food Biochemistry*, 43(1), e12571.

- Wang, C., Wang, B., & Li, B. (2016). Bioavailability of peptides from casein hydrolysate in vitro: Amino acid compositions of peptides affect the antioxidant efficacy and resistance to intestinal peptidases. *Food Research International*, *81*, 188-196.
- Wang, J., Yadav, V., Smart, A. L., Tajiri, S., & Basit, A. W. (2015). Stability of peptide drugs in the colon. *European Journal of Pharmaceutical Sciences*, *78*, 31-36.
- Wu, S., Bekhit, A. E.-D. A., Wu, Q., Chen, M., Liao, X., Wang, J., & Ding, Y. (2021). Bioactive peptides and gut microbiota: Candidates for a novel strategy for reduction and control of neurodegenerative diseases. *Trends in Food Science & Technology*, *108*, 164-176.
- Xu, Q., Fan, H., Yu, W., Hong, H., & Wu, J. (2017). Transport Study of Egg-Derived Antihypertensive Peptides (LKP and IQW) Using Caco-2 and HT29 Coculture Monolayers. *Journal of Agricultural and Food Chemistry*, *65*(34), 7406-7414.
- Xu, Q., Hong, H., Wu, J., & Yan, X. (2019). Bioavailability of bioactive peptides derived from food proteins across the intestinal epithelial membrane: A review. *Trends in Food Science & Technology*, *86*, 399-411.
- Xue, L., Yin, R., Howell, K., & Zhang, P. (2021). Activity and bioavailability of food protein-derived angiotensin-I-converting enzyme-inhibitory peptides. *Comprehensive Reviews in Food Science and Food Safety*, *20*(2), 1150-1187.
- Yadollahi, A., Dastani, M., Zargarani, B., Ghasemi, A. H., & Rahimi, H. R. J. R. i. C. M. (2019). The Beneficial Effects of Curcumin on Cardiovascular Diseases and Their Risk Factors. *6*(1).
- Yang, F.-j., Chen, X., Huang, M.-c., Yang, Q., Cai, X.-x., Chen, X., Du, M., Huang, J.-l., & Wang, S.-y. (2021). Molecular characteristics and structure-activity relationships of food-derived bioactive peptides. *Journal of Integrative Agriculture*, *20*(9), 2313-2332.
- Yoshikawa, M. (2015). Bioactive peptides derived from natural proteins with respect to diversity of their receptors and physiological effects. *Peptides*, *72*, 208-225.
- Yu, Y.-J., Amorim, M., Marques, C., Calhau, C., & Pintado, M. (2016). Effects of whey peptide extract on the growth of probiotics and gut microbiota. *Journal of Functional Foods*, *21*, 507-516.
- Zanoni, C., Aiello, G., Arnoldi, A., & Lammi, C. (2017a). Hempseed Peptides Exert Hypocholesterolemic Effects with a Statin-Like Mechanism. *Journal of Agricultural and Food Chemistry*, *65*(40), 8829-8838.

- Zanoni, C., Aiello, G., Arnoldi, A., & Lammi, C. (2017b). Investigations on the hypocholesterolaemic activity of LILPKHSDAD and LTFPGSAED, two peptides from lupin β -conglutin: Focus on LDLR and PCSK9 pathways. *Journal of Functional Foods*, 32, 1-8.
- Zeng, L., Yu, G., Hao, W., Yang, K., & Chen, H. (2021). The efficacy and safety of *Curcuma longa* extract and curcumin supplements on osteoarthritis: a systematic review and meta-analysis. *Bioscience Reports*, 41(6), BSR20210817.
- Zhang, T., Jiang, B., Miao, M., Mu, W., & Li, Y. (2012). Combined effects of high-pressure and enzymatic treatments on the hydrolysis of chickpea protein isolates and antioxidant activity of the hydrolysates. *Food Chemistry*, 135(3), 904-912.

Part II.
Scientific contributions

CHAPTER 3

MANUSCRIPT 1

TRANS-EPITHELIAL TRANSPORT, METABOLISM, AND BIOLOGICAL ACTIVITY ASSESSMENT OF THE MULTI- TARGET LUPIN PEPTIDE LILPKHSDAD (P5) AND ITS METABOLITE LPKHSDAD (P5-MET)

Carmen Lammi^{1*}, Gilda Aiello^{1,2}, Carlotta Bollati¹, **Jianqiang Li¹**,
Martina Bartolomei¹, Giulia Ranaldi³, Simonetta Ferruzza³, Enrico Mario
Alessandro Fassi¹, Giovanni Grazioso¹, Yula Sambuy³ and Anna Arnoldi¹

¹**Department of Pharmaceutical Sciences, University of Milan, 20122 Milan, Italy**

²**Department of Human Science and Quality of Life Promotion, Telematic
University San Raffaele, 00166 Rome, Italy**

³**Food and Nutrition Research Centre, CREA, 00178 Rome, Italy**

Author Contributions: Experiment ideation C.L.; biological experiments, C.L., S.F.,
G.R., C.B., J.L. and M.B.; analytical experiments: G.A.; molecular modeling study:
E.M.A.F. and G.G.; writing—original draft, C.L.; writing – review & editing, C.L.,
Y.S. and A.A.

3. Abstract

P5 (LILPKHSDAD) is a hypocholesterolemic peptide from lupin protein with a multi-target activity, since it inhibits both 3-hydroxy-3-methylglutaryl coenzyme A reductase (HMGCoAR) and proprotein convertase subtilisin/kexin type-9 (PCSK9). This work shows that, during epithelial transport experiments, the metabolic transformation mediated by intestinal peptidases produces two main detected peptides, ILPKHSDAD (P5-frag) and LPKHSDAD (P5-met), and that both P5 and P5-met are linearly absorbed by differentiated human intestinal Caco-2 cells. Extensive comparative structural, biochemical, and cellular characterizations of P5-met and the parent peptide P5 demonstrate that both peptides have unique characteristics and share the same mechanisms of action. In fact, they exert an intrinsically multi-target behavior being able to regulate cholesterol metabolism by modulating different pathways. The results of this study also highlight the dynamic nature of bioactive peptides that may be modulated by the biological systems they get in contact with.

3.1 Introduction

In addition to their nutritional values, proteins provide numerous health benefits through their ability to modulate one or more targets involved in specific physiological pathways (Lammi, Aiello, Boschini, & Arnoldi, 2019; Udenigwe & Aluko, 2012). This generally depends on the formation of bioactive peptides that are processed by digestion from the protein sequences and subsequently absorbed at the intestinal level (Aiello, Ferruzza, Ranaldi, Sambuy, Arnoldi, Vistoli, et al., 2018; Amigo-Benavent, Clemente, Caira, Stiuso, Ferranti, & del Castillo, 2014; Fan, Yu, Liao, & Wu, 2020). These peptides eventually reach the organs where they modulate the target of interest, exerting their biological activity. Indeed, food bioactive peptides are increasingly recognized for their great potential of improving human health and preventing chronic diseases (Chakrabarti, Guha, & Majumder, 2018).

In this framework, lupin protein hydrolysates, obtained by treating the proteins with pepsin and trypsin, show synergistic hypocholesterolemic effects through the

modulation of both 3-hydroxy-3-methylglutaryl coenzyme A reductase (HMGCoAR) and proprotein convertase subtilisin/kexin type-9 (PCSK9) targets (Lammi, Aiello, Vistoli, Zanoni, Arnoldi, Sambuy, et al., 2016; Lammi, Zanoni, Aiello, Arnoldi, & Grazioso, 2016; Lammi, Zanoni, Calabresi, & Arnoldi, 2016; Lammi, Zanoni, Ferruzza, Ranaldi, Sambuy, & Arnoldi, 2016; Lammi, Zanoni, Scigliuolo, D'Amato, & Arnoldi, 2014). In fact, both the peptic and tryptic hydrolysates decrease HMGCoAR activity *in vitro*, inducing the intracellular low-density lipoprotein receptor (LDLR) pathway, reducing the PCSK9 one, and improving the ability of human hepatic HepG2 cells to uptake low-density lipoproteins (LDL) from the extracellular environment (Lammi, Zanoni, Calabresi, & Arnoldi, 2016; Lammi, Zanoni, Scigliuolo, D'Amato, & Arnoldi, 2014). In addition, these lupin hydrolysates impair the protein–protein interaction (PPI) between PCSK9 and LDLR (Lammi, Zanoni, Aiello, Arnoldi, & Grazioso, 2016). Although it seems possible that these complementary activities might be due to the synergistic effects of different peptides in the hydrolysates, it cannot be excluded that single peptides endowed of a multi-target inhibitory behavior may be present inside these hydrolysates, which have a very complex composition.

Recently, it has been possible to identify from the peptic hydrolysate peptide P5 (LILPKHSDAD), one of the most potent food peptides capable of inhibiting the PPI between PCSK9 and LDLR (Lammi, Zanoni, Aiello, Arnoldi, & Grazioso, 2016; Zanoni, Aiello, Arnoldi, & Lammi, 2017). A molecular docking analysis has allowed to simulate the effects induced by P5 on this PPI. In fact, the superimposition of P5 on the EGF-A domain of LDLR co-crystallized with PCSK9 (PDB code 4NE9) shows a good overlapping, justifying the P5 inhibitory property (Lammi, Zanoni, Aiello, Arnoldi, & Grazioso, 2016). In parallel, an experiment has demonstrated that P5 is able to reduce the catalytic activity of HMGCoAR with an IC₅₀ value of 147.2 μ M and an *in silico* investigation has predicted the potential binding mode to the catalytic site of this enzyme (Zanoni, Aiello, Arnoldi, & Lammi, 2017). Through the inhibition of the HMGCoAR activity, P5 increases the LDLR protein level on HepG2 cells through the activation of the SREBP-2 transcription factor and, through a down-

regulation of HNF-1 α , it reduces the PCSK9 protein levels and its secretion in the extracellular environment (Zanoni, Aiello, Arnoldi, & Lammi, 2017). This unique synergistic multi-target inhibitory behavior of P5 determines an improved ability of HepG2 cells to uptake extracellular LDL with a final hypocholesterolemic effect. In the peptic protein hydrolysate, P5 stands out also for its favorable transport across the *in vitro* model of the intestinal barrier provided by differentiated human Caco-2 cells (Lammi, et al., 2016).

Considering the very peculiar features of P5, it appeared necessary to get a deeper insight of its bioavailability. Therefore, the first objective of this study was an investigation of the behavior of P5 in the differentiated Caco-2 cell model, focusing the attention either on the transport or the possible concomitant degradation by active peptidases expressed on the apical (AP) membrane, and consequent production of metabolites. For a better understanding of the transport phenomenon, two different conditions were examined, i.e., P5 alone and in mixture with two other lupin peptides, YDFYPSSTKDQQS (P3) and LTFPGSAED (P7), which had already been shown to be transported in the same model system (Lammi, Aiello, Dellafiora, Bollati, Boschin, Ranaldi, et al., 2020). Interestingly, an abundantly transported metabolite, LPHKSDAD (P5-met), was identified in these experiments. According to the hypothesis that this breakdown peptide may retain a multi-target activity, the second objective of the work was an extensive structural, biochemical, and cellular characterization of P5-met in comparison with P5 as the reference compound.

3.2 Material and methods

3.2.1 Chemicals

Dulbecco's modified Eagle's medium (DMEM), stable L-glutamine, fetal bovine serum (FBS), phosphate buffered saline (PBS), penicillin/streptomycin, chemiluminescent reagent, and 96-well plates were purchased from Euroclone (Milan, Italy). The HMGC α AR assay kit, bovine serum albumin (BSA), Janus Green B, formaldehyde, HCl and H₂SO₄ were from Sigma-Aldrich (St. Louis, MO, USA). The

antibody against LDLR and the 3,3', 5,5' -tetramethylbenzidine (TMB) substrate were bought from Thermo Fisher Scientific (Waltham, MA, USA). The Quantikine ELISA kit was bought from R&D Systems (Minneapolis, MN, USA). The LDL-DyLight™ 550 was from Cayman Chemical (Ann Arbor, MI, USA). The CircuLex PCSK9 *in vitro* binding Assay Kit was from CircuLex (CycLex Co., Nagano, Japan). The peptides (P5, P5-met, P3, and P7) were synthesized by the company GeneScript (Piscataway, NJ, USA) at > 95% purity. The antibody against HMGCoAR was bought from Abcam (Cambridge, UK). Phenylmethanesulfonyl fluoride (PMSF), Na-orthovanadate inhibitors, and the antibodies against rabbit Ig-horseradish peroxidase (HRP), mouse Ig-HRP, and SREBP-2 (which recognizes epitope located in a region between 833–1141 and bands at about 132 kDa) were purchased from Santa Cruz Biotechnology Inc. (Santa Cruz, CA, USA). The antibodies against hepatocyte nuclear factor 1-alpha (HNF1-alpha) and PCSK9 were bought from GeneTex (Irvine, CA, USA). The inhibitor cocktail Complete Midi was from Roche (Basel, Switzerland). Mini protean TGX pre-cast gel 7.5% and Mini nitrocellulose Transfer Packs were purchased from BioRad (Hercules, CA, USA).

3.2.2 Caco-2 Cell Culture and Differentiation

Human intestinal Caco-2 cells, obtained from INSERM (Paris, France), were cultured according to a published protocol (Natoli, Leoni, D'Agnano, Zucco, & Felsani, 2012). For differentiation, they were seeded on polycarbonate filters, 12 mm diameter, 0.4 μ m pore diameter (Transwell, Corning Inc., Lowell, MA, US) at a 3.5×10^5 cells/cm² density in complete medium supplemented with 10% FBS in both AP and BL compartments for 2 d to allow the formation of a confluent cell monolayer. Starting from day three after seeding, cells were transferred to FBS-free medium in both compartments, supplemented with ITS (final concentration 10 mg/L insulin (I), 5.5 mg/L transferrin (T), 6.7 μ g/L sodium selenite (S); GIBCO-Invitrogen, San Giuliano Milanese, Italy) only in the basolateral (BL) compartment, and allowed to differentiate for 18–21 days with regular medium changes three times weekly (Ferruzza, Rossi, Sambuy, & Scarino, 2013).

3.2.3 Cell Monolayers Integrity Evaluation

The transepithelial electrical resistance (TEER) of differentiated Caco-2 cells was measured at 37 °C using the voltmeter apparatus Millicell (Millipore Co., Billerica, MA, USA), immediately before and at the end of the transport experiments. In addition, at the end of transport experiments, cells were incubated from the AP side with 1 mM phenol-red in PBS containing Ca ++ (0.9 mM) and Mg ++ (0.5 mM) for 1 h at 37 °C, to monitor the paracellular permeability of the cell monolayer. The BL solutions were then collected and NaOH (70 µL, 0.1 N) was added before reading the absorbance at 560 nm by a microplate reader Synergy H1 from Biotek (Winooski, VT, USA). Phenol-red passage was quantified using a standard phenol-red curve. Only filters showing TEER values and phenol-red passages similar to untreated control cells were considered for peptide transport analysis.

3.2.4 Trans-Epithelial Transport Experiments

Prior to experiments, the cell monolayer integrity and differentiation were checked by TEER measurement as described in detail above. Peptide trans-epithelial passage was assayed in differentiated Caco-2 cells in transport buffer solution (137 mM NaCl, 5.36 mM KCl, 1.26 mM CaCl₂, and 1.1 mM MgCl₂, 5.5 mM glucose) according to previously described conditions. In order to reproduce the pH conditions existing *in vivo* in the small intestinal mucosa, the apical (AP) solutions were maintained at pH 6.0 (buffered with 10 mM morpholinoethane sulfonic acid), and the basolateral (BL) solutions were maintained at pH 7.4 (buffered with 10 mM N-2-hydroxyethylpiperazine-N-4-butanesulfonic acid). Prior to transport experiments, cells were washed twice with 500 µL PBS containing Ca ++ and Mg ++. Peptide transportation by mature Caco-2 cells was assayed by loading the AP compartment with P5 alone, in mixture with YDFYPSSTKDQQS (P3) and LTFPGSDAD (P7), and/or P5-met (500 µM) in the AP transport solution (500 µL) and the BL compartment with the BL transport solution (700 µL). The plates were incubated at 37 °C and the BL solutions were collected at different time points (i.e., 15, 30, 60, 90, and 120 min) and replaced with fresh solutions pre-warmed at 37 °C. All BL and AP solutions

collected at the end of the transport experiment were stored at $-80\text{ }^{\circ}\text{C}$ prior to analysis. Three independent transport experiments were performed, each in duplicate. In order to assess the involvement of transcytotic process in peptides passage, parallel transport experiments were performed in the presence of 500 nM wortmannin in both the AP and BL compartment, over 60 min incubation time.

3.2.5 LC-MS/MS Operating Conditions

The medium collected at the end of transport experiments from AP and BL chambers (500 μL and 700 μL , respectively) were freeze-dried and residues were solubilized in HPLC water (100 μL). Samples were desalted with C18 resin ZipTip by using 80% ACN, 0.1% FA as eluent (Millipore Corporation, Bedford, MA, USA). Each sample was lyophilized under speed-vacuum for 5 h at $30\text{ }^{\circ}\text{C}$ and re-dissolved in 50 μL (0.1% formic acid), before MS analysis. Purified BL samples were analyzed on a SL IT mass spectrometer interfaced with a HPLC- Chip Cube source (Agilent Technologies, Palo Alto, CA, USA). Data were processed with MSD Trap control 4.2, and Data analysis 4.2 version (Agilent Technologies, Palo Alto, CA, USA). The chromatographic separation was performed using a 1200 HPLC system equipped with a binary pump. The peptide enrichment was performed on a 160 nL enrichment column (Zorbax 300SB-C18, 5 μm pore size, Agilent Technologies Italia SpA, Milan, Italy), followed by separation on a 150 mm \times 75 μm analytical column packed (Zorbax300SB-C18, 5 μm pore size, Agilent Technologies Italia SpA, Milan, Italy). The samples (1 μL), acidified with formic acid, were loaded onto the enrichment column at a flow rate 4 $\mu\text{L}/\text{min}$ using isocratic 100% C solvent phase (99% water, 1% ACN and 0.1% formic acid). After clean-up, P5-met was injected into the mass spectrometer at the constant flow rate of 300 nL/min. The LC solvent A was 95% water, 5% ACN, 0.1% formic acid; solvent B was 5% water, 95% ACN, 0.1% formic acid. The nano-pump gradient program was as follows: 5% solvent B (0 min), 70% solvent B (0–8 min), and back to 5% in 2 min. The drying gas temperature was $300\text{ }^{\circ}\text{C}$, flow rate 3 L/min (nitrogen). Data acquisition occurred in positive ionization mode. Capillary voltage was -1900 V , with endplate offset -500 V . Mass spectra

were acquired with ICC target 30,000, and maximum accumulation time 150 ms. The LC/MS analysis were performed in multiple reaction monitoring (MRM) mode. Specifically, the monitored MRM transitions of P5-met were from the mono-charged precursor ion $[M + H]^+$ (m/z 882.43) to product-ions m/z 678.3 and 407.1, respectively.

3.2.6 Calibration Curve for the Quantification of Absorbed P5-Met and Method Validation

The quantitative analysis of P5-met in the BL samples was carried out by the Ion Trap MS in MRM mode, monitoring two of the most intense diagnostic transitions (882.43 \rightarrow 678.3 and 882.43 \rightarrow 407.1), after optimization of the acquisition parameters, such as retention time, MS profile, and MS/MS fragmentation spectrum (Supplementary Materials, Figure S1). A blank was analyzed between samples to ensure the absence of any carryover effect. Seven different concentrations of standard peptide P5-met ranging from 0.1, 0.4, 0.8, 1.5, 3, 5, and 10 μ M were analyzed in three technical replicates. To determine the relation between the peak area under the curves and the concentration of peptide, the calibration curve was built by plotting the mean response factor (peak area) against the respective concentrations of P5-met. Then, BL samples were analyzed using the same optimized parameters. Data were processed by Data analysis v.4.2 (Agilent Technologies, Palo Alto, CA, USA). The peak areas of all monitored transitions from P5-met were integrated and used for the quantification. The analytical method was validated in terms of selectivity, linearity, limit of detection (LOD), limit of quantification (LOQ), accuracy and precision, according to the guidelines for bioanalytical method validation of the Center for Drug Evaluation and Research of the U.S. Food and Drug Administration (Food and Drug Administration 2001). Quality control samples were obtained by spiking peptide P5-met (0.5 μ M) in a BL sample from control Caco-2 cells.

3.2.7 HepG2 Cell Culture Conditions and Treatment

The HepG2 cell line was bought from ATCC (HB-8065, ATCC from LGC Standards, Milan, Italy) and was cultured in DMEM high glucose with stable L-glutamine, supplemented with 10% FBS, 100 U/mL penicillin, 100 µg/mL streptomycin (complete growth medium) with incubation at 37 °C under 5% CO₂ atmosphere.

3.2.8 HMGC_oAR Aactivity Assay

The experiments were carried out following the manufacturer instructions and optimized protocol (Aiello, Lammi, Boschin, Zanoni, & Arnoldi, 2017). The assay buffer, NADPH, substrate solution, and HMGC_oAR were provided in the HMGC_oAR Assay Kit (Sigma Aldrich SRL, Milan, Italy). The experiments were carried out following the manufacturer instructions at 37 °C. In particular, each reaction (200 µL) was prepared adding the reagents in the following order: 1 × assay buffer, a 10–500 µM doses of P5 and P5-met or vehicle (C), the NADPH (4 µL), the substrate solution (12 µL), and finally the HMGC_oAR (catalytic domain) (2 µL). Subsequently, the samples were mixed and the absorbance at 340 nm read by the microplate reader Synergy H1 (Winooski, VT, USA) at time 0 and 10 min. The HMGC_oAR-dependent oxidation of NADPH and the inhibition properties of peptides were measured by absorbance reduction, which is directly proportional to enzyme activity.

3.2.9 *In Vitro* PCSK9-LDLR Binding Assay

Peptides P5 and P5-met (0.1–100 µM) were tested using the *in vitro* PCSK9-LDLR binding assay (CycLex Co., Nagano, Japan) following the manufacture instructions and conditions already optimized (Lammi, Zanoni, Aiello, Arnoldi, & Grazioso, 2016). Briefly, plates are pre-coated with a recombinant LDLR-AB domain containing the binding site of PCSK9. Before starting the assay, tested peptides and/or the vehicle were diluted in the reaction buffer and added in microcentrifuge tubes. Afterwards, the reaction mixtures were added in each well of the microplate and the reaction was started by adding His-tagged PCSK9 solution (3 µL). The microplate

was allowed to incubate for 2 h at room temperature (RT) shaking at 300 rpm on an orbital microplate shaker. Subsequently, wells were washed 4 times with the wash buffer. After the last wash, the biotinylated anti-His-tag monoclonal antibody (100 μ L) was added and incubated at RT for 1h shaking at 300 rpm. After incubation, wells were washed for 4 times with wash buffer. After the last wash, 100 μ L of HRP-conjugated streptavidin were added and the plate was incubated for 20 min at RT. After incubation, wells were washed 4 times with wash buffer. Finally, the substrate reagent (tetra-methylbenzidine) was added, and the plate was incubated for 10 min at RT shaking at ca. 300 rpm. The reaction was stopped with 2.0 M sulfuric acid and the absorbance at 450 nm was measured using the Synergy H1 fluorescent plate reader (Winooski, VT, USA).

3.2.10 In-Cell Western (ICW) Assay

For the experiments, a total of 3×10^4 HepG2 cells/well were seeded in 96-well plates. The following day, cells were washed with PBS and then starved overnight (O/N) in DMEM without FBS and antibiotics. After starvation, HepG2 cells were treated with 4.0 μ g/mL PCSK9-WT and 4.0 μ g/mL PCSK9 + peptides P5 and/or P5-met (50 μ M) and vehicle (H_2O) for 2 h at 37 $^{\circ}C$ under 5% CO_2 atmosphere. Subsequently, they were fixed in 4% paraformaldehyde for 20 min at room temperature (RT). Cells were washed 5 times with 100 μ L of PBS/well (each wash was for 5 min at RT) and the endogenous peroxides activity quenched adding 3% H_2O_2 for 20 min at RT. Non-specific sites were blocked with 100 μ L/well of 5% bovine serum albumin (BSA, Sigma) in PBS for 1.5 h at RT. LDLR primary antibody solution (1:3000 in 5% BSA in PBS, 25 μ L/well) was incubated O/N at + 4 $^{\circ}C$. Subsequently, the primary antibody solution was discarded and each sample was washed 5 times with 100 μ L/well of PBS (each wash was for 5 min at RT). Goat anti-rabbit Ig-HRP secondary antibody solution (Santa Cruz) (1:6000 in 5% BSA in PBS, 50 μ L/well), was added and incubated 1 h at RT. The secondary antibody solution was washed 5 times with 100 μ L/well of PBS (each wash for 5 min at RT). Freshly prepared TMB substrate (Pierce, 100 μ L/well) was added and the plate was incubated at RT until desired color

was developed. The reaction was stopped with 2 M H₂SO₄ and then the absorbance at 450 nm was measured using the microplate reader Synergy H1 (Winooski, VT, USA). After the read, cells were stained by adding 1 × Janus Green stain, incubating for 5 min at RT. The dye was removed and the sample washed 5 times with water. Afterward 100 µL 0.5 M HCl for well were added and incubated for 10 min. After 10 seconds shaking, the OD at 595 nm was measured using the microplate reader Synergy H1 (Winooski, VT, USA).

3.2.11 Fluorescent LDL Uptake

HepG2 cells (3×10^4 /well) were seeded in 96-well plates and kept in complete growth medium for 2 days before treatment. The third day, cells were washed with PBS and then starved overnight (O/N) in DMEM without FBS and antibiotics. After starvation, they were treated with 4.0 µg/mL PCSK9 and 4.0 µg/mL PCSK9 + P5 and P5-met peptides (50.0 µM), and vehicle (H₂O) for 2 h with at 37 °C under 5% CO₂ atmosphere. At the end of the treatment, the culture medium was replaced with 50 µL/well LDL-DyLight™ 550 working solution (Cayman Chemical Company, Ann Arbor, MI, USA) prepared in DMEM without FBS and antibiotics. The cells were additionally incubated for 2 h at 37 °C and then the culture medium was aspirated and replaced with PBS (100 µL/well). The degree of LDL uptake was measured using the Synergy H1 fluorescent plate reader (Winooski, VT, USA) (excitation and emission wavelengths 540 and 570 nm, respectively). Fluorescent LDL-uptake was finally assessed following optimized protocol (Zanoni, Aiello, Arnoldi, & Lammi, 2017).

3.2.12 Western Blot Analysis

Immunoblotting experiments were performed using optimized protocol (Zanoni, Aiello, Arnoldi, & Lammi, 2017). A total of 1.5×10^5 HepG2 cells/well (24-well plate) were treated with 50 µM of P5 and P5-met for 24 h. After each treatment, the supernatants were collected and stored at -80 °C; cells were scraped in 40 µL ice-cold lysis buffer (RIPA buffer+ inhibitor cocktail + 1:100 PMSF + 1:100 Na-orthovanadate + 1:1000 β-mercaptoethanol) and transferred in ice-cold

microcentrifuge tubes. After centrifugation at 13,300 g for 15 min at 4 °C, the supernatants were recovered and transferred into new ice-cold tubes. Total proteins were quantified by the Bradford's method and 50 µg of total proteins loaded on a precast 7.5% Sodium Dodecyl Sulfate-Polyacrylamide (SDS-PAGE) gel at 130 V for 45 min. Subsequently, the gel was pre-equilibrated in H₂O for 5 min at room temperature (RT) and transferred to a nitrocellulose membrane (Mini nitrocellulose Transfer Packs,) using a Trans-Blot Turbo at 1.3 A, 25 V for 7 min. Target proteins, on milk or BSA blocked membrane, were detected by primary antibodies as follows: anti-SREBP-2, anti-LDLR, anti-HMGCoAR, anti-PCSK9, anti HNF-1 α and anti- β -actin. Secondary antibodies conjugated with HRP and a chemiluminescent reagent were used to visualize target proteins and their signal was quantified using the Image Lab Software (Biorad, Hercules, CA, USA). The internal control β -actin was used to normalize loading variations.

3.2.13 Quantification of PCSK9 Secreted by HepG2 Cells through ELISA

The supernatants collected from treated HepG2 cells (50.0 µM of P5 and/or P5-met) were centrifuged at 600 × g for 10 min at 4 °C and ELISA assay performed using protocol already optimized (Zanoni, Aiello, Arnoldi, & Lammi, 2017). They were recovered and diluted to the ratio 1:10 with DMEM in a new ice-cold tube. PCSK9 was quantified by ELISA (R&D System, Minneapolis, MN, USA). Briefly, the experiments were carried out at 37 °C, following the manufacturer's instructions. Before starting the assay, human PCSK9 standard curve (20.0, 10.0, 5.0, 2.5, 1.25, and 0.625 ng/mL) was prepared by serial dilutions from a 40 ng/mL stock. 100 µL of the Assay Diluent RD1-9 (provided into the kit) were placed in each well, before adding the standards and the samples (50 µL) and incubating the ELISA plate for 2 h at RT. Subsequently, wells were washed 4 times with the wash buffer, and 200 µL of human PCSK9-conjugate (HRP-labelled anti-PCSK9) was added to each well for 2 h at RT. Following aspiration, wells was washed 4 times with the kit wash buffer. After the last wash, 200 µL of substrate solution were added to the wells and allowed to incubate for 30 min at RT. The reaction was stopped with 50 µL of the stop solution

(2 M sulfuric acid) and the absorbance at 450 nm was measured using Synergy H1 microplate (Winooski, VT, USA).

3.2.14 Molecular Modeling

The PCSK9/P5-met model was built starting from the coordinates of the PCSK9/P5 complex model reported by us (Lammi, Zanoni, Aiello, Arnoldi, & Grazioso, 2016). Here, the first two residues (residues LI) of peptide P5 were manually removed from the PCSK9/P5 complex model, by means of the molecular modeling tools available in Maestro software (Schrödinger Inc, Mannheim, Germany.). Then, the resulting complex model was energy minimized and equilibrated through three MD simulations replicas (each lasting more than 300 ns) utilizing the pmemd.cuda module of AMBER 2017 package (Case, Cerutti, Cheatham, Darden, Duke, Giese, et al., 2017). In the production runs, the computational protocol applied in our previous studies (Lammi, Sgrignani, Arnoldi, & Grazioso, 2019; Lammi, Sgrignani, Arnoldi, Lesma, Spatti, Silvani, et al., 2019) was applied. In particular, the ff14SB AMBER force field (Maier, Martinez, Kasavajhala, Wickstrom, Hauser, & Simmerling, 2015) was used for the protein, while the TIP3P model (Mao & Zhang, 2012) was used to explicitly represent water molecules (about 25,000). Then, after the addition of the sodium ions needed to neutralize the overall charge of the simulation system, the MD trajectories acquired in the production runs were examined by visual inspection with VMD (Humphrey, Dalke, & Schulten, 1996), ensuring that the thermalization did not cause any structural distortion. Finally, the three MD replicas' trajectory frames were collected in order to cluster the conformations assumed by the small peptide backbone atoms bound on the PCSK9 surface. The cluster analysis was performed using the cpptraj module of AMBER17 (Case, et al., 2017). By this, the MD frames were divided into clusters by the complete average linkage algorithm, and the PCSK9/P5-met complex conformations with the lowest root mean square deviation (RMSD) to the cluster centers (the structures representative of the cluster, SRC), were acquired and visually inspected. MM-GBSA calculations were performed on the most populated cluster of P5-met conformations, the MMPBSA.py module of AMBER17 (Case, et al., 2017)

package was used to this aim. The computational details and applied parameters of these calculations were the ones reported on our previous paper (Lammi, Sgrignani, Arnoldi, & Grazioso, 2019).

3.2.15 Circular Dichroism (CD) Spectroscopy

Circular dichroism (CD) spectra were recorded in continuous scanning mode (190–300 nm) at 25 °C using a Jasco J-810 (Jasco Corp., Tokyo, Japan) spectropolarimeter. All spectra were collected using a 1 mm path-length quartz cell and averaged over three accumulations (speed: 10 nm min⁻¹). A reference spectrum of distilled water was recorded and subtracted from each spectrum.

3.2.16 Statistical Analysis

All the data sets were checked for normal distribution by D'Agostino and Pearson test. Since they are all normally disturbed with p -values < 0.05 , we proceeded with statistical analyses by One-Way ANOVA followed by Dunnett's and Tukey's post-hoc tests and using Graphpad Prism 9 (San Diego, CA, USA). Values were reported as means \pm S.D.; p -values < 0.05 were considered to be significant.

3.3 Results

3.3.1 Intestinal Transport of P5 Alone or in Combination with Other Peptides across Caco-2 Cells

Recently, we have demonstrated that the intestinal transport of a peptide is highly influenced by the presence of other peptides (Lammi, et al., 2020). For this reason, the kinetics of the transport of P5 was investigated in two different conditions, i.e., either when it was alone or in a mixture with P3 (YDFYPSSTKDQQS) and P7 (LTFPGSAED), two lupin peptides that had already been shown to be transported in the same model system (Lammi, et al., 2020; Lammi, et al., 2016). Each peptide was added in the AP compartment at the final concentration of 500 μ M. As shown in **Figure 3.1A**, in both conditions, P5 was linearly transported across the Caco-2 cells

monolayer as a function of time. When it was alone, the rate of absorption was 16.3 ± 0.3 nmoles / (mL \times min) (R^2 0.999), whereas in the mixture the rate was 80.3 ± 0.4 nmoles / (mL \times min) (R^2 0.988) (**Figure 3.1A**). Moreover, at the end of the incubation (2 h), the amount of P5 in the BL compartment was about 3.5-fold higher when it was tested in mixture (1.1 ± 0.2 μ g, equal to 0.99 nmoles) than when it was tested alone (0.3 ± 0.02 μ g, equal to 0.271 nmoles). Both evidences suggest that the presence of other peptides favored the transport possibly by increasing the stability of P5 and impairing its degradation. Food derived peptides may be transported across the intestinal brush-border membrane into the bloodstream via one or more of the following routes: (i) peptide transport 1 (PepT1)-mediated route, (ii) paracellular route via tight junctions (TJs), (iii) transcytosis route, and (iv) passive transcellular diffusion (Xu, Hong, Wu, & Yan, 2019). Peptide size, charge, hydrophobicity, and degradation due to the action of peptidases are among the main factors influencing the absorption through one or more of these routes. In general, short peptides, such as dipeptides and tripeptides, are preferentially transported by PepT1, due to its high-capacity, low-affinity, and high expression in intestinal epithelium (Daniel, 2004), whereas highly hydrophobic peptides are transported by simple passive transcellular diffusion or by transcytosis (Miguel, Dávalos, Manso, de la Peña, Lasunción, & López-Fandiño, 2008). Since P5 is a decapeptide with a net charge equal to -1 and a hydrophobicity of $+17.79$ kcal/mol, it may be hypothesized that it might be preferentially transported by passive transcellular diffusion or by transcytosis. Whereas it is difficult to assess the transport via the former route, due to the lack of passive diffusion regulators, wortmannin can be used as transcytosis inhibitor to investigate the latter route. Therefore, specific experiments in the presence of wortmannin were performed in order to assess the mechanism of transport of peptide P5 across the Caco-2 cell layer. As shown in **Figure 3.1B, C**, wortmannin significantly impairs the transport of P5, strongly suggesting that P5 is mainly transported by the transcytotic route.

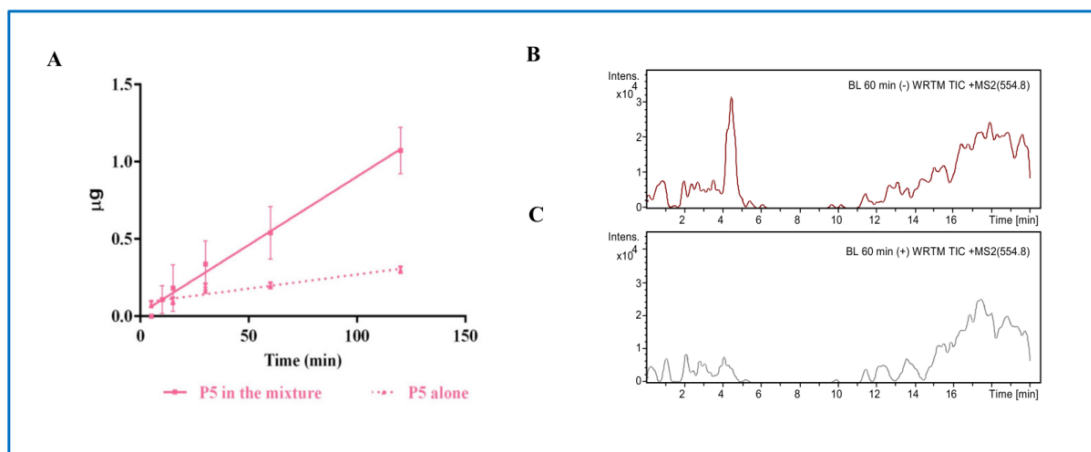


Figure 3.1 Transport of P5 across differentiated Caco-2 cells. (A) Quantification of P5 in the basolateral (BL) compartment as a function of time; pink dashed line: P5 alone; pink line: in mixture. Data represent the mean \pm SD of three independent experiments performed in triplicate. (B) HPLC-Chip MS of BL compartment at time 60 min: total ion current (TIC) of $[M + 2H]^{2+}$ m/z 554.8 without wortmannin, and (C) with wortmannin.

3.3.2 Analysis of the Metabolites of P5 Produced by Caco-2 Cells

Mature enterocytes develop microvilli that function as the primary surface of nutrient absorption in the gastrointestinal tract. Their membrane is packed with enzymes that favor the breakdown of complex nutrients into simpler compounds that are more easily absorbed. The dynamic equilibrium between bioactive peptide degradation and transport is crucially important from a physiological point of view. Possessing a wide range of membrane peptidases naturally expressed by the AP side of enterocytes, including DPP-IV and ACE (Aiello, Li, Boschin, Bollati, Arnoldi, & Lammi, 2019; Caron, Domenger, Dhulster, Ravallec, & Cudennec, 2017; Lammi, Bollati, Ferruzza, Ranaldi, Sambuy, & Arnoldi, 2018), the differentiated Caco-2 model is also a reliable tool for investigating the proteolytic activity of the brush border barrier.

Under the hypothesis that during the transport experiments P5 may also be metabolized by the enzymes expressed on the AP surface of the Caco-2 cells, it was decided to look for possible metabolites through mass spectrometry analysis of the AP solutions. Indeed, P5 was dynamically metabolized in two main breakdown fragments (**Table 3.1**): ILPKHSDAD (P5-frag, m/z 995.51), deriving from the cleavage of a

leucine from the N-terminal of the parent peptide, and LPHKSDAD (P5-met, m/z 882.43), formally deriving from the cleavage of a leucine-isoleucine fragment from the N-terminal of P5. An aminopeptidase, such as leucine aminopeptidase (LAP), may catalyze the hydrolysis of the leucine residue at the N-terminus of the parent peptide generating P5-frag and then the N-terminal isoleucine may be further cleaved to generate P5-met. However, P5-met may also derive from the direct cleavage of a leucine-isoleucine fragment from P5. Instead, P5 does not seem to be susceptible to the action of endopeptidases, such DPP-IV.

Table 3.1 Metabolites of P5 identified in the AP compartment of the Caco-2 cell model system at the end of incubation (120 min).

Metabolite Sequence	ID	[M + H] ⁺ (Da)	m/z (Da)	Spectral Intensity	Rt (min)	Mixture	Alone
ILPKHSDAD	P5-frag	995.51	332.42	3.88×10^6	2.2	x	n.d.
LPKHSDAD	P5-met	882.43	441.51	1.21×10^7	2.2	x	x

x, detected; n.d., not detected.

Interestingly, whereas P5-met was abundant and was produced in both conditions, P5-frag was detected only when P5 was tested in combination with P3 and P7 and, based on the spectral intensity, was a minor metabolite. This suggests that the transformation of P5-frag into P5-met may be such a fast process that only the concomitant presence of very easily cleavable peptides (like P7) permitted its detection, by protecting it from degradation. However, we cannot exclude those other smaller fragments, such as tripeptides and dipeptides, were also generated in these conditions, since they are intrinsically difficult to detect.

3.3.3 Characterization of the Transport of P5-Met Across the Caco-2 Cell Monolayer

Since the octapeptide P5-met was the most abundant and the smallest metabolite, it was decided to synthesize it in order to obtain structural, functional, and biological

characterization. To compare the secondary structure of P5-met and the parent compound P5, the CD spectra in the far-UV region of 190–240 nm were recorded. One negative peak was observed at 200 nm, suggesting that both peptides have a random coil conformation (**Figure 3.2**) and confirming the three-dimensional structure of P5 at the end of MD simulations and subsequent energy minimization (Lammi, Zanoni, Aiello, Arnoldi, & Grazioso, 2016).

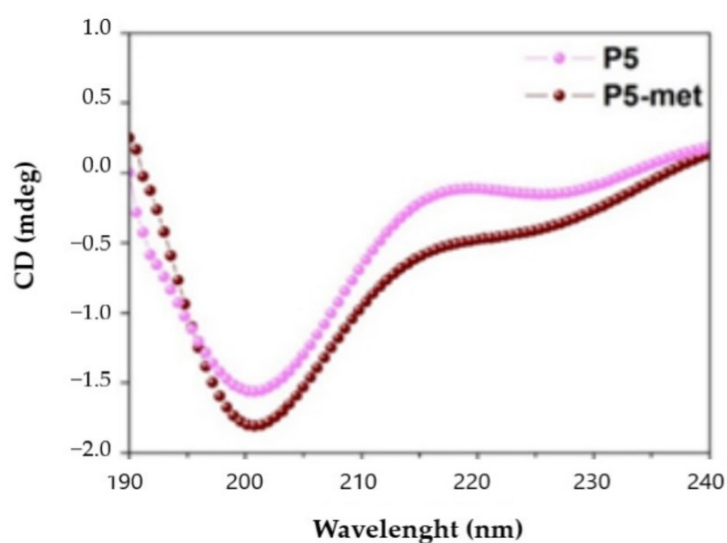


Figure 3.2 Circular dichroism (CD) spectra of P5 and P5-met registered in the range of 190–240 nm.

Afterward, trans-epithelial transport experiments were performed using differentiated Caco-2 cells (**Figure 3.3**): the rate of transport of P5-met (incubated alone in the AP compartment at the concentration of 500 μ M) up to 30 min was 81.7 nmoles \pm 0.3 ng / (mL \times min) (R^2 0.99). A decline in transport rate was observed after 60 min (data not shown) probably due to a decline of P5-met concentration in the donor AP compartment, caused by metabolism. The concentration of P5-met in the BL compartment after 30 min (0.54 ± 0.02 μ g, equal to 0.613 nmoles) (**Figure 3.3**) was much higher than that of the parent peptide tested alone after 60 min (0.20 ± 0.02 μ g, equal to 0.227 nmoles) (**Figure 3.1**), suggesting that P5-met is either efficiently transported or poorly metabolized by Caco-2 cells or both. Additional experiments showed that P5-met is transported also in the presence of wortmannin (**Figure 3.3B**),

indicating that the mechanism of transport may involve a passive diffusion mechanism or passage through the paracellular route. It is important to underline, however, that dedicated experiments would be required for a complete characterization of the transport mechanism of P5-met. Interestingly, similar results have been obtained in transport experiments performed with LTFPG, a metabolite of peptide P7 (Lammi, et al., 2020).

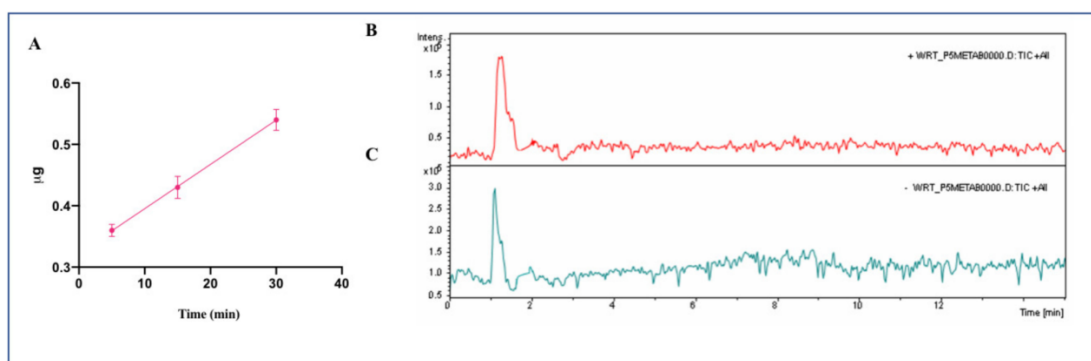


Figure 3.3 Transport of P5-met across differentiated Caco-2 cells. (A) Quantification of P5-met in the BL compartment as a function of time. Data represent the mean \pm S.D. of three independent experiments performed in triplicate. The accuracy of analytical was higher than 95%. LOQ was 0.10 μg whereas LOD was detected equal to 0.09 μg . (B) HPLC-Chip MS of BL compartment at time 60 min: TIC of P5-met without wortmannin, and (C) with wortmannin.

3.3.4 P5-Met Modulates the Hepatic LDLR Pathway through the Inhibition of HMGCoAR Activity

A biochemical investigation was carried out for assessing the ability of P5-met to modulate *in vitro* HMGCoAR activity. P5-met was active as HMGCoAR inhibitor with an IC_{50} of 175.3 μM (**Figure 3.4A**), similarly to the parent peptide, which displayed an IC_{50} of 147.2 μM , whereas the positive control pravastatin reduced the enzyme activity by 82.0% at 1.0 μM , as indicated in the Supplementary Materials (**Figure 3-S2**). Based on these results, further experiments aimed at comparing the ability of P5-met and P5 to modulate the LDLR and PCSK9 pathways on HepG2 cells were carried out at the fixed concentration of 50 μM , which was the same concentration already used for testing peptide P5 on the same cellular system (Zanoni,

Aiello, Arnoldi, & Lammi, 2017), although different from that absorbed by Caco-2 cells after the incubation of 500 μM in the AP side. P5-met and P5 induced an up-regulation of the protein level of the SREBP-2 transcription factor to $130.4 \pm 16.4\%$ and $125.7 \pm 16\%$ ($p < 0.05$), respectively, versus the control (**Figure 3.4B**). As a consequence, the LDLR protein levels were increased up to $150.4 \pm 29.2\%$ and $133.4 \pm 15.5\%$ ($p < 0.001$), respectively (**Figure 3.4C**), and the HMGCoAR protein levels up to $117.9 \pm 12.1\%$ and $117.3 \pm 9.1\%$ ($p < 0.05$), respectively (**Figure 3.4D**). In agreement with these results, P5-met and P5 induced an increased expression of the LDLR localized on the cellular membranes of HepG2 cells by $145.2 \pm 15.2\%$ and $153.6 \pm 16.4\%$ ($p < 0.0001$), respectively, versus the control (**Figure 3.4E**). The overall up-regulation of the LDLR protein levels, led to an increased functional ability of HepG2 cells to absorb extracellular LDL up to $181.2 \pm 40.1\%$ versus the control after treatment with P5-met and by $174.3 \pm 32.3\%$ after treatment with P5 (**Figure 3.4F**).

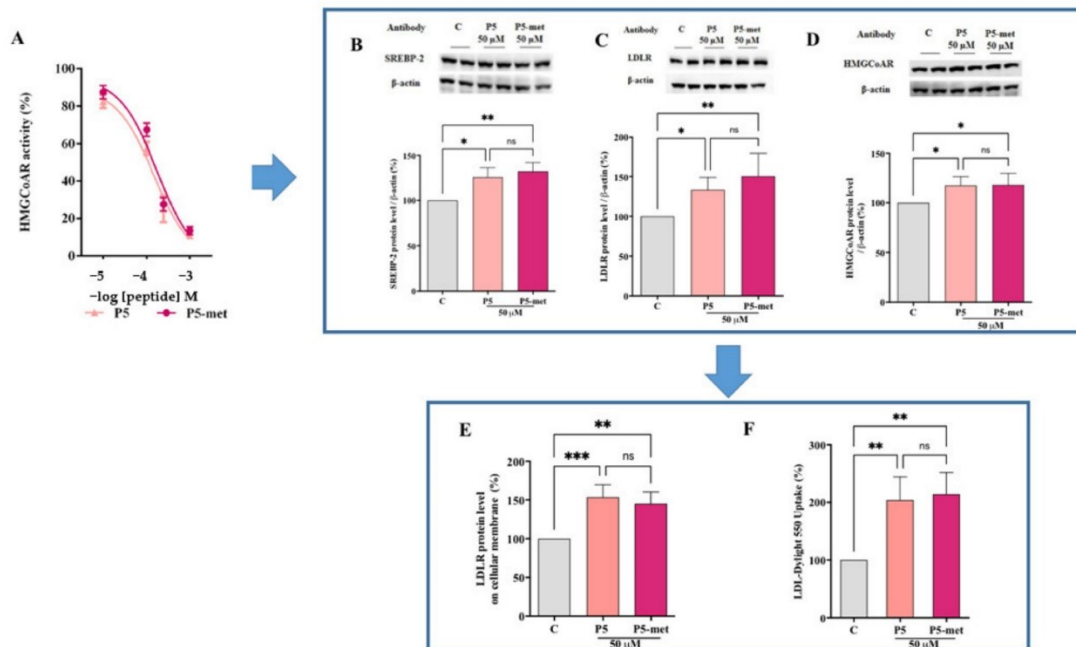


Figure 3.4 Modulation of low-density lipoprotein receptor (LDLR) pathway in HepG2 cells treated with P5 and P5-met. (A) *In vitro* inhibition of the HMGCoAR activity with IC_{50} values equal to 147.2 and 175.3 μM , respectively. (B) After the treatment of HepG2 cells with P5 and

P5-met, the SREBP-2 protein level was increased, as well as (C) the LDLR and (D) the HMGCoAR protein levels, and (E) the LDLR localized on the surface of hepatic cell. (F) Enhancement of functional ability of hepatic cells to uptake LDL from the extracellular environment. Data points represent the averages \pm SD of four independent experiments performed in duplicate. C vs. P5 and P5-met samples were analyzed by One-Way ANOVA followed by Dunnett's test; (*) $p < 0.05$; (**) $p < 0.01$ (***) $p < 0.0001$. C: control sample; ns: not significant.

3.3.5 P5-Met Modulates the Hepatic PCSK9 Pathway and Impairs the PPI between PCSK9 and the LDLR

PCSK9 is a secreted protein expressed in many organs, such as liver, kidney, and intestine, which is able to bind the LDLR expressed on the surface of the hepatocytes (J. D. Horton, Cohen, & Hobbs, 2007). PCSK9-LDLR binding activates the receptor catabolism leading to degradation of the hepatic LDLR. Thus, PCSK9 inhibition and/or modulation are considered promising strategies for the development of new hypocholesterolemic drugs (Seidah & Prat, 2007). Interestingly, PCSK9 and LDLR are co-regulated by SREBP-2, since both proteins contain functional sterol regulatory elements (SREs) in their promoters that respond to changes in intracellular cholesterol levels through the activation of the SREBP pathway (Dubuc, Chamberland, Wassef, Davignon, Seidah, Bernier, et al., 2004; Maxwell, Fisher, & Breslow, 2005). However, since the HNF-1 α binding site is unique to the PCSK9 promoter and is not present in the LDLR promoter, the modulation of the PCSK9 transcription through HNF-1 α does not affect the LDLR gene expression. Thus, the co-regulation of PCSK9 from LDLR and other SREBP target genes is disconnected by the HNF-1 α binding site (Dong, Li, Singh, Cao, & Liu, 2015). Similarly to P5, P5-met decreases the hepatic PCSK9 production and extra cellular secretion through the downregulation of the HNF-1 α protein content in HepG2 cells (**Figure 3.5A–C**). More in detail, P5-met decreases the HNF-1 α protein by $10.8 \pm 3.5\%$ and P5 by $7.7 \pm 1.5\%$ ($p < 0.01$; **Figure 3.5A**). This slight, but significant reduction leads to a decrease of PCSK9 by $29 \pm 8.1\%$ and $31 \pm 4.6\%$ for P5-met and P5, respectively ($p < 0.05$; **Figure 3.5B**). In agreement, both P5-met and P5 are also able to decrease the secretion of mature PCSK9 by 22.2

$\pm 4.9\%$ and $12.3 \pm 1.6\%$, respectively ($p < 0.05$; **Figure 3.5C**).

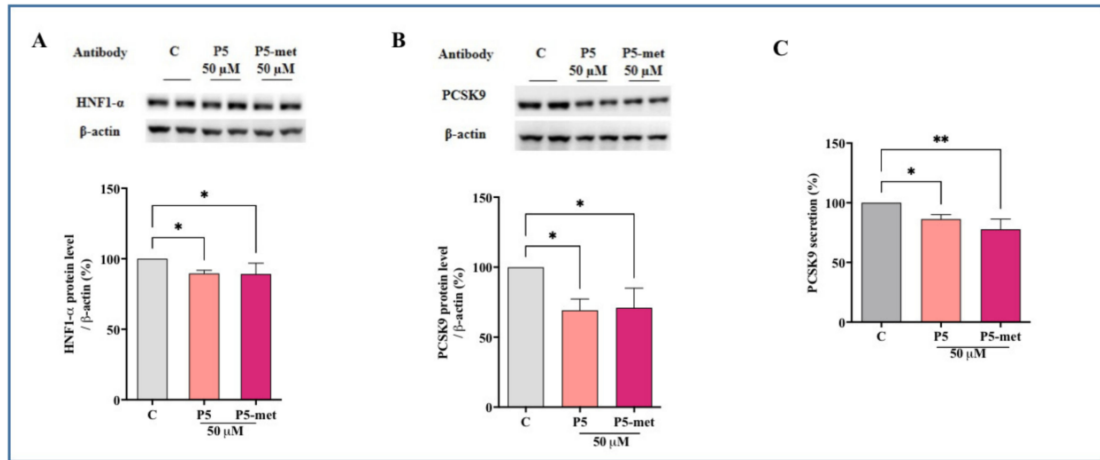


Figure 3.5 Modulation of PCSK9 pathway in HepG2 cells treated with P5 and P5-met. (A) Effects on the HNF-1 α protein level; (B) effects on the PCSK9 protein levels; (C) effects on mature PCSK9 secretion. Data points represent the averages \pm SD of six independent experiments performed in duplicate. C versus P5 and P5-met samples were analyzed by One-Way ANOVA followed by Dunnett’s test; (*) $p < 0.05$, (**) $p < 0.01$. C: control sample.

Aiming at the evaluation of the multi-target inhibitory ability of P5-met, experiments were performed in order to assess its ability to directly impair the PCSK9-LDLR PPI. Results indicate that P5-met reduces PCSK9-LDLR binding with a dose-response trend and an IC_{50} of $1.7 \mu\text{M}$ (**Figure 3.6A**), which is similar to the IC_{50} of P5 ($1.3 \mu\text{M}$) tested in parallel. This last result confirms P5 activity as an inhibitor of the PCSK9-LDLR PPI observed in a previous paper (Lammi, Zanoni, Aiello, Arnoldi, & Grazioso, 2016). The effects on the modulation of the LDLR localized on the HepG2 cell surface were investigated using an ICW assay in the presence of PCSK9 (Lammi, Zanoni, & Arnoldi, 2015b). Findings indicate that the LDLR protein levels decrease in the presence of PCSK9 alone by $24.7 \pm 1.9\%$ ($p < 0.001$) versus the control cells, and that P5 and P5-met ($50 \mu\text{M}$) are able to significantly increase the LDLR protein levels when co-incubated with PCK9 ($p < 0.0001$). In particular, peptide P5 restored the LDLR level up to $99.3 \pm 1.8\%$, whereas peptide P5-met up to $90.1 \pm 0.1\%$ (**Figure 3.6B**). Finally, functional experiments were carried out for assessing the

ability of each peptide to modulate the capacity of HepG2 cells to uptake extracellular LDL, treating HepG2 cells with PCSK9 alone or in the presence of each peptide (50 μ M). After treatment with PCSK9 alone, the ability of HepG2 cells to uptake fluorescent LDL was reduced by $43.5 \pm 9.7\%$ ($p < 0.05$) versus untreated cells (**Figure 3.6C**), and the treatment with P5 and P5-met reversed this effect up to $100.4 \pm 7.5\%$ and $104.1 \pm 8.5\%$ ($p < 0.05$), respectively (**Figure 3.6D**). To get a deeper inside on these phenomena, it was decided to investigate the interaction of P5-met with PCSK9 through a dedicated computational study. Notably, the 3D structure of the PCSK9/P5-met complex was modeled and refined following the procedure described in the Section 3.2.14. Essentially, the simulations system (enzyme, small peptide, ions, and water) was equilibrated and optimized by means of three 300 ns-long MD simulations replicas. The attained trajectories showed that the small peptide displayed diverse binding modes over the simulation time, although it remained firmly anchored on the PCSK9 surface. Then, a cluster analysis of the trajectory frames was accomplished in order to establish which was the most preferred conformation of the small peptide and to acquire major details on the PCSK9 area involved in the interaction with P5-met.

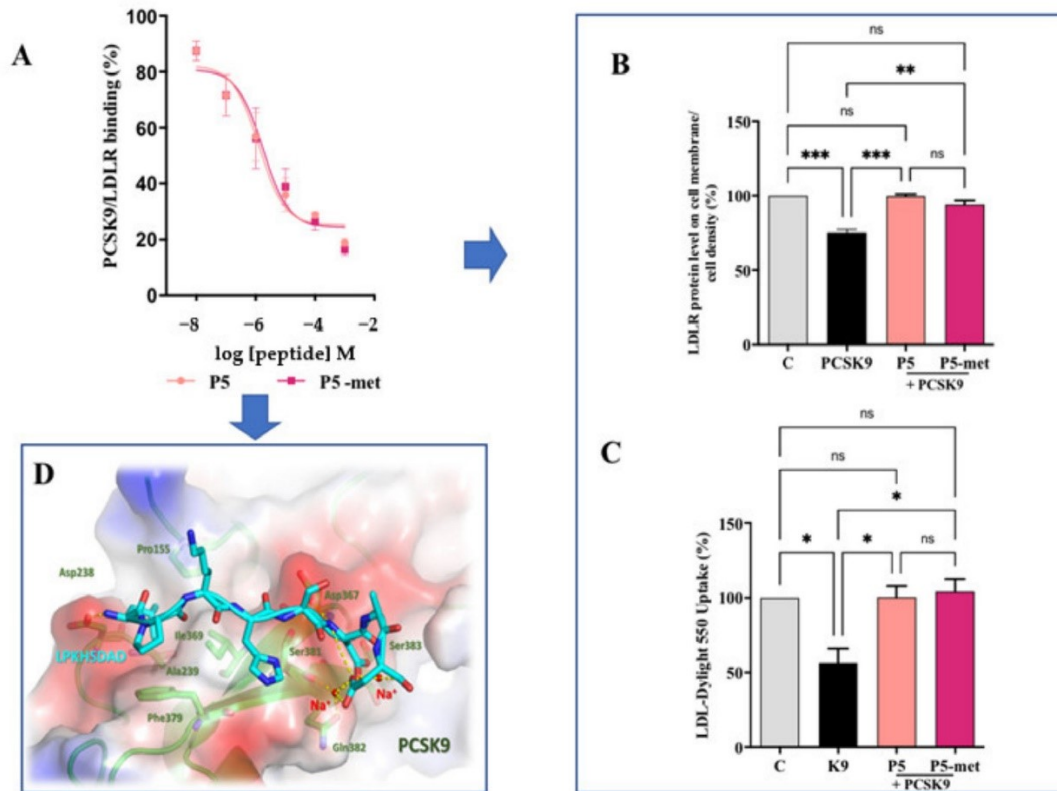


Figure 3.6 Inhibition of the PPI between PCSK9 and LDLR. (A) Impairment of the protein–protein interaction between PCSK9 and LDLR. (B) The treatment of HepG2 cells with PCSK9 (4 $\mu\text{g}/\text{mL}$) reduced active LDLR protein levels localized on the surface of cells, which were restored by P5 or P5-met (50 μM). (C) The decreased functional ability of HepG2 cells to absorb LDL from the extracellular space observed after incubation with PCSK9 (4 $\mu\text{g}/\text{mL}$) is improved after treatment with both peptides. (D) Hypothetical binding mode of P5-met in the LDLR binding site located on the surface of PCSK9. The data points represent the averages \pm SD of four independent experiments performed in duplicate. Data were analyzed by One-Way ANOVA followed by Tukey’s post-hoc test; (*) $p < 0.05$, (**) $p < 0.01$, and (***) $p < 0.0001$. C: control sample; ns: not significant.

The results of these calculations showed that the small peptide backbone atoms, in the 84% of frames, was bound on PCSK9 area responsible for the interaction with the EGFA domain of LDLR, confirming that P5-met is a PCSK9-LDLR PPI inhibitor. Moreover, the visual inspection of the P5-met conformation displaying the lowest binding free energy (calculated by MM-GBSA approach) permitted to acquire details

on the small peptide hypothetical binding mode (**Figure 3.6D**). In our hypotheses, the side chain of the Leu1 was inserted in the hydrophobic pocket shaped by the PCSK9 residues Pro155, Ile369, Ala239, and Phe379. Additionally, an H-bond network stabilized P5-met on the PCSK9 surface, these interactions were shaped by: 1) the side chain of the small peptide His4 and the backbone of PCSK9-Ser381, 2) the peptide charged N-term and the PCSK9-Asp238 side chain (this bond additionally enforced by a salt bridge), 3) the backbone NH of Asp6 with the side chain of PCSK9-Asp367, 4) the side chain Asp6 with the one of PCSK9-Ser383. Finally, it is useful to note that two sodium ions (needed to neutralize the total charge of the simulation system) were greatly involved in the stabilization of the binding mode of P5-met. In fact, the negatively charged peptide C-term and the side chains of the P5-met-Asp6 and -Asp8 interacted with the side chain of PCSK9-Gln382 and the backbone atoms of PCSK9-Ser381 and -Ser383. Both electrostatic interactions were bridged by the presence of two positively charged sodium ions (**Figure 3.6D**).

3.4 Discussion

In the field of food bioactive peptides, some activities have been investigated much more extensively than others, i.e., the angiotensin converting enzyme (ACE) and DPP-IV inhibitory activity (Murray & FitzGerald, 2007; Nongonierma & FitzGerald, 2019). Hence, many hypotensive and antidiabetic peptides have been identified from several different food matrices. On the contrary, only scarce and incomplete information are available about hypocholesterolemic peptides. In this panorama, lupin peptide P5 represents a unique case of multi-target biological activity. In fact, P5 is able to inhibit both HMGCoAR and PCSK9 activities, showing a multi-target behavior. Both enzymes are among the main targets for the treatment of the hypercholesterolemia and the prevention of cardiovascular disease (J. Horton, Goldstein, & Brown, 2002). Some peptides able to inhibit HMGCoAR have been identified from amaranth (Soares, Mendonça, De Castro, Menezes, & Arêas, 2015), soybean (Lammi, Zanoni, & Arnoldi, 2015a; Lammi, Zanoni, Arnoldi, & Vistoli, 2015), lupin (Zanoni, Aiello, Arnoldi, & Lammi, 2017), and cowpea (Marques,

Fontanari, Pimenta, Soares-Freitas, & Arêas, 2015) proteins.

On the contrary, PCSK9 is a new target for the prevention and treatment of hypercholesterolemia (Lagace, Curtis, Garuti, McNutt, Park, Prather, et al., 2006; Levy, Ouadda, Spahis, Sane, Garofalo, Grenier, et al., 2013), which has been only rarely investigated in the area of food bioactive peptides. In fact, P5 is the unique peptide described so far that is able to inhibit PCSK9. This gap of knowledge on the one hand suggests the need to increase the efforts for identifying new active peptides from different food sources, and on the other indicates that it is crucial to promote the exploitation of the few known active species through in-depth studies regarding, in particular, their bioavailability. Indeed, intestinal metabolism and transport of bioactive peptides still remain relevant issues that need to be addressed in order to overcome the discrepancy observed between *in vitro* assays and *in vivo* results and to select good candidates to be translated into practice.

From a physiological point of view, the dynamic equilibrium between the transport and degradation of bioactive peptides is crucially important. In this context, a relevant outcome of this study is the demonstration that the transport across the Caco-2 monolayer is highly affected by the concomitant presence of other peptides. Indeed, the transport is more efficient and its degradation less extensive when P5 is incubated in the presence of peptides P3 and P7. It is important to note, however, that P5 and P7 have completely different behaviors, since the transport rate of P5 tested alone is 1.8 ± 0.3 ng/(mL \times min) and in mixture becomes 8.9 ± 0.4 ng/(mL \times min), whereas the transport rate of P7 alone is 4.2 ± 0.6 ng/(mL \times min) and in mixture becomes 1.98 ± 0.21 ng/(mL \times min) (Lammi, et al., 2020). The outcomes on P5 and P7 are therefore divergent, being the transport of P5 favored by the presence of the other peptides, while that of P7 impaired. P5 appears to be less sensitive to the activity of endopeptidases, such as DPP-IV, but more sensitive to the activity of aminopeptidases, which generate two main breakdown fragments, i.e., P5-frag and P5-met. Instead, when tested in mixture, P7 is sensitive not only to the action of aminopeptidases, such as LAP, but also to endopeptidases, such as DPP-IV, leading to the formation of metabolites TFPGSAED and LTFPG, respectively (Lammi, et al., 2020).

Another relevant outcome of this study is the information acquired on the mechanism of transport of P5 and P5-met. In fact, although both species are efficiently transported, P5 is mainly transported by transcytosis, whereas P5-met mainly by the paracellular or other passive mechanism.

The biological characterization of P5-met indicates that it retains the multi-target inhibitory activity of the parent peptide on HMGCoAR and PCSK9. In addition, P5-met is also capable to modulate the PCSK9 signaling pathway at the intracellular level, leading to a decrease of mature PCSK9 secretion through the reduction of HNF-1 α . More in detail, after the inhibition of HMGCoAR, P5-met leads to the up-regulation of the LDLR pathway, with an increase of LDLR protein levels due to the augmentation of SREBP-2 transcription factor. The molecular modulation of the LDLR-pathway has the consequence of the improvement of the functional ability of HepG2 cells to uptake LDL from the extracellular environment. Notwithstanding the SREBP-2 activation, the HNF-1 α protein level reduction leads to a significant decrease of PCSK9 protein level and a subsequent reduction of mature PCSK9 secretion. Indeed, these results highlight the very original hypocholesterolemic mechanism of action of P5 and P5-met that differs from the mechanism of statin. In fact, statins increase PCSK9 expression, which dampens an effective LDL clearing by promoting LDLR degradation (Dubuc, et al., 2004), thereby counteracting their therapeutic effects. Instead, literature suggests that curcumin (Tai, Chen, Chen, Wu, Ho, & Yen, 2014), from *Curcuma longa*, and berberine (Kong, Wei, Abidi, Lin, Inaba, Li, et al., 2004; Lau, Yao, Chen, Ko, & Huang, 2001), from plants of the *Berberidaceae* family, display a hypocholesterolemic activity through the reduction of PCSK9 protein levels.

P5 and P5-met are also able to impair the PPI between PCSK9 and the LDLR. The experimental results were confirmed *in silico*, through the prediction of the binding mode of P5-met in the LDLR binding site located on the PCSK9 target. The inhibition of PCSK9- LDLR by P5-met leads to an efficient restoration of active LDLR protein levels localized on the cellular membrane of hepatocytes co-incubated with PCSK9 and P5 or P5-met versus HepG2 cells incubated with PCSK9 alone. Accordingly, a

recovery of the functional capacity of HepG2 cells to uptake extracellular LDL is also observed. In light of these results, we propose a new concept of hypocholesterolemic peptide, based on the modulation of peripheral cholesterol homeostasis rather than simple cholesterol inhibition. In this context, P5 and P5-met are unique and interesting examples of food-derived intrinsically multi-target peptides able to exert complementary effects on the regulation of cholesterol metabolism, which undoubtably opens the route toward a new area of active molecules with cholesterol-lowering properties. Finally, our results suggest that P5 may be a good candidate for further *in vivo* study.

3.5 Supporting information

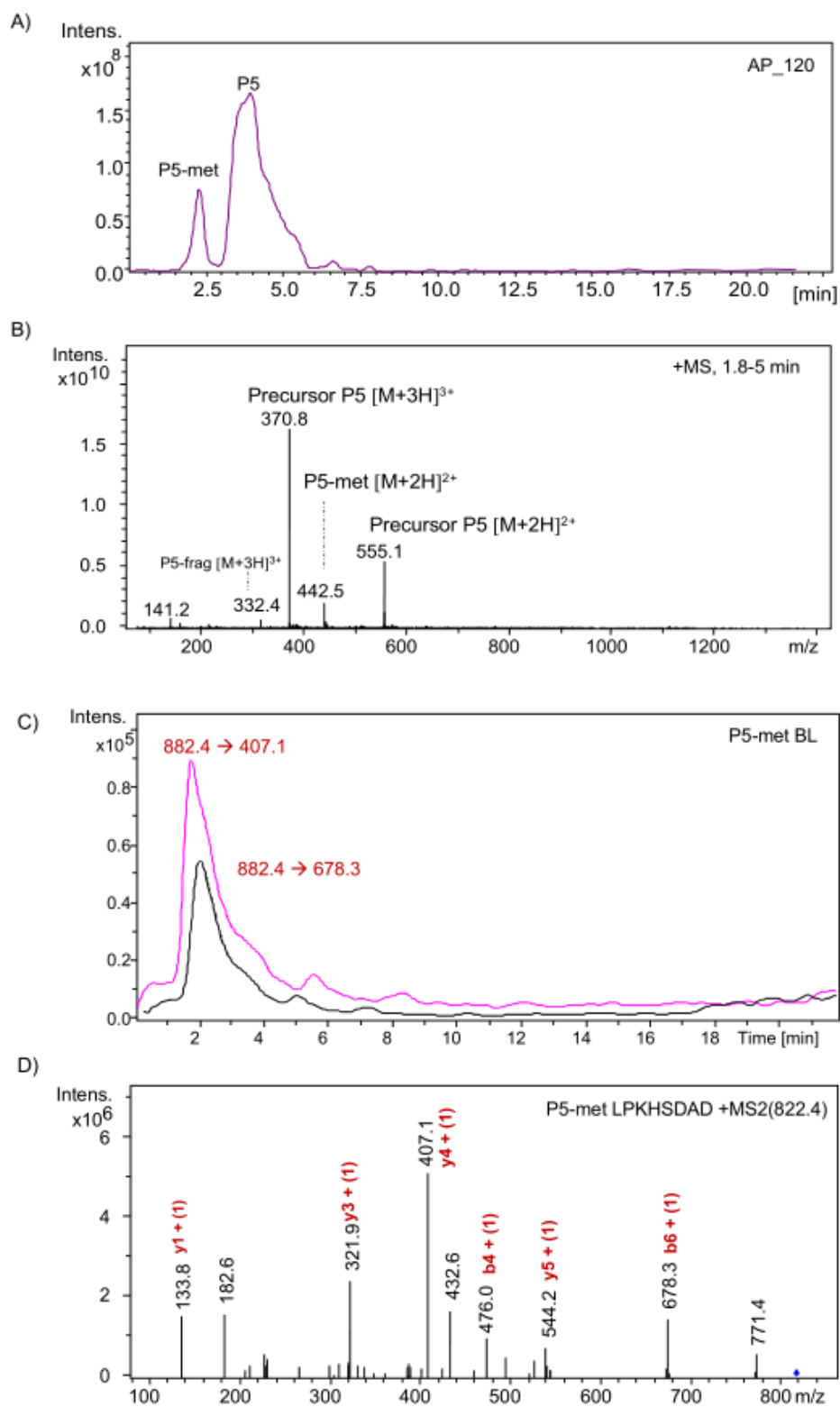


Figure 3-S1 Transport of P5 across differentiated Caco-2 cells. (A) TIC spectrum of AP

compartment at time 60 min. (B) MS spectrum. (C) HPLC-MRM of 882.4→407.1; 882.4→678.3. (D) MS/MS spectrum of P5-met LPKHSDAD m/z 882.4 with peptide sequence coverage.

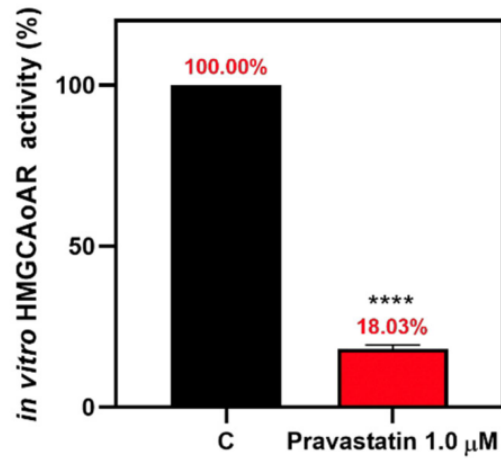


Figure 3-S2 Effect of pravastatin (1.0 μM) on the HMGCaoAR activity. **** $p < 0.0001$.

3.6 References

- Aiello, G., Ferruzza, S., Ranaldi, G., Sambuy, Y., Arnoldi, A., Vistoli, G., & Lammi, C. (2018). Behavior of three hypocholesterolemic peptides from soy protein in an intestinal model based on differentiated Caco-2 cell. *Journal of Functional Foods*, *45*, 363-370.
- Aiello, G., Lammi, C., Boschini, G., Zanoni, C., & Arnoldi, A. (2017). Exploration of Potentially Bioactive Peptides Generated from the Enzymatic Hydrolysis of Hempseed Proteins. *Journal of Agricultural and Food Chemistry*, *65*(47), 10174-10184.
- Aiello, G., Li, Y., Boschini, G., Bollati, C., Arnoldi, A., & Lammi, C. (2019). Chemical and biological characterization of spirulina protein hydrolysates: Focus on ACE and DPP-IV activities modulation. *Journal of Functional Foods*, *63*, 103592.
- Amigo-Benavent, M., Clemente, A., Caira, S., Stiuso, P., Ferranti, P., & del Castillo, M. D. (2014). Use of phytochemicals to evaluate the bioavailability and bioactivity of antioxidant peptides of soybean β -conglycinin. *Food Research International*, *35*(11), 1582-1589.
- Caron, J., Domenger, D., Dhulster, P., Ravallec, R., & Cudennec, B. (2017). Using Caco-2 cells as novel identification tool for food-derived DPP-IV inhibitors. *Food Research International*, *92*, 113-118.
- Case, D. A., Cerutti, D. S., Cheatham, T. E., III, Darden, T. A., Duke, R. E., Giese, T. J., Gohlke, H., Goetz, A. W., Greene, D., & Homeyer, N. (2017). AMBER 2017 Reference Manual (Covers Amber16 and AmberTolls17). *University of California: San Francisco, CA, USA*.
- Chakrabarti, S., Guha, S., & Majumder, K. (2018). Food-Derived Bioactive Peptides in Human Health: Challenges and Opportunities. *Food Research International*, *10*(11), 1738.
- Daniel, H. (2004). Molecular and Integrative Physiology of Intestinal Peptide Transport. *Annual Review of Physiology*, *66*(1), 361-384.
- Dong, B., Li, H., Singh, A. B., Cao, A., & Liu, J. (2015). Inhibition of PCSK9 Transcription by Berberine Involves Down-regulation of Hepatic HNF1 α Protein Expression through the Ubiquitin-Proteasome Degradation Pathway*. *Journal of Biological Chemistry*, *290*(7), 4047-4058.
- Dubuc, G., Chamberland, A., Wassef, H., Davignon, J., Seidah, N. G., Bernier, L., & Prat, A. (2004). Statins Upregulate PCSK9, the Gene Encoding the Proprotein Convertase Neural Apoptosis-

- Regulated Convertase-1 Implicated in Familial Hypercholesterolemia. *Arteriosclerosis, Thrombosis, and Vascular Biology*, 24(8), 1454-1459.
- Fan, H., Yu, W., Liao, W., & Wu, J. (2020). Spent Hen Protein Hydrolysate with Good Gastrointestinal Stability and Permeability in Caco-2 Cells Shows Antihypertensive Activity in SHR. 9(10), 1384.
- Ferruzza, S., Rossi, C., Sambuy, Y., & Scarino, M. L. (2013). Serum-reduced and serum-free media for differentiation of Caco-2 cells. *ALTEX - Alternatives to animal experimentation*, 30(2), 159-168.
- Horton, J., Goldstein, J., & Brown, M. (2002). SREBPs: transcriptional mediators of lipid homeostasis. In *Cold Spring Harbor symposia on quantitative biology*, vol. 67 (pp. 491-498): Cold Spring Harbor Laboratory Press.
- Horton, J. D., Cohen, J. C., & Hobbs, H. H. (2007). Molecular biology of PCSK9: its role in LDL metabolism. *Trends in Biochemical Sciences*, 32(2), 71-77.
- Humphrey, W., Dalke, A., & Schulten, K. (1996). VMD: Visual molecular dynamics. *Journal of Molecular Graphics*, 14(1), 33-38.
- Kong, W., Wei, J., Abidi, P., Lin, M., Inaba, S., Li, C., Wang, Y., Wang, Z., Si, S., Pan, H., Wang, S., Wu, J., Wang, Y., Li, Z., Liu, J., & Jiang, J.-D. (2004). Berberine is a novel cholesterol-lowering drug working through a unique mechanism distinct from statins. *Nature Medicine*, 10(12), 1344-1351.
- Lagace, T. A., Curtis, D. E., Garuti, R., McNutt, M. C., Park, S. W., Prather, H. B., Anderson, N. N., Ho, Y. K., Hammer, R. E., & Horton, J. D. (2006). Secreted PCSK9 decreases the number of LDL receptors in hepatocytes and in livers of parabiotic mice. *The Journal of Clinical Investigation*, 116(11), 2995-3005.
- Lammi, C., Aiello, G., Boschin, G., & Arnoldi, A. (2019). Multifunctional peptides for the prevention of cardiovascular disease: A new concept in the area of bioactive food-derived peptides. *Journal of Functional Foods*, 55, 135-145.
- Lammi, C., Aiello, G., Dellafiora, L., Bollati, C., Boschin, G., Ranaldi, G., Ferruzza, S., Sambuy, Y., Galaverna, G., & Arnoldi, A. (2020). Assessment of the Multifunctional Behavior of Lupin Peptide P7 and Its Metabolite Using an Integrated Strategy. *Journal of Agricultural and Food Chemistry*, 68(46), 13179-13188.

- Lammi, C., Aiello, G., Vistoli, G., Zanoni, C., Arnoldi, A., Sambuy, Y., Ferruzza, S., & Ranaldi, G. (2016). A multidisciplinary investigation on the bioavailability and activity of peptides from lupin protein. *Journal of Functional Foods*, *24*, 297-306.
- Lammi, C., Bollati, C., Ferruzza, S., Ranaldi, G., Sambuy, Y., & Arnoldi, A. (2018). Soybean- and Lupin-Derived Peptides Inhibit DPP-IV Activity on In Situ Human Intestinal Caco-2 Cells and Ex Vivo Human Serum. *10*(8), 1082.
- Lammi, C., Sgrignani, J., Arnoldi, A., & Grazioso, G. (2019). Biological Characterization of Computationally Designed Analogs of peptide TVFTSWEELYLDWV (Pep2-8) with Increased PCSK9 Antagonistic Activity. *Scientific Reports*, *9*(1), 2343.
- Lammi, C., Sgrignani, J., Arnoldi, A., Lesma, G., Spatti, C., Silvani, A., & Grazioso, G. (2019). Computationally Driven Structure Optimization, Synthesis, and Biological Evaluation of Imidazole-Based Proprotein Convertase Subtilisin/Kexin 9 (PCSK9) Inhibitors. *Journal of Medicinal Chemistry*, *62*(13), 6163-6174.
- Lammi, C., Zanoni, C., Aiello, G., Arnoldi, A., & Grazioso, G. (2016). Lupin Peptides Modulate the Protein-Protein Interaction of PCSK9 with the Low Density Lipoprotein Receptor in HepG2 Cells. *Scientific Reports*, *6*(1), 29931.
- Lammi, C., Zanoni, C., & Arnoldi, A. (2015a). IAVPGEVA, IAVPTGVA, and LPYP, three peptides from soy glycinin, modulate cholesterol metabolism in HepG2 cells through the activation of the LDLR-SREBP2 pathway. *Journal of Functional Foods*, *14*, 469-478.
- Lammi, C., Zanoni, C., & Arnoldi, A. (2015b). A simple and high-throughput in-cell Western assay using HepG2 cell line for investigating the potential hypocholesterolemic effects of food components and nutraceuticals. *Food Chemistry*, *169*, 59-64.
- Lammi, C., Zanoni, C., Arnoldi, A., & Vistoli, G. (2015). Two Peptides from Soy β -Conglycinin Induce a Hypocholesterolemic Effect in HepG2 Cells by a Statin-Like Mechanism: Comparative *in Vitro* and *in Silico* Modeling Studies. *Journal of Agricultural and Food Chemistry*, *63*(36), 7945-7951.
- Lammi, C., Zanoni, C., Calabresi, L., & Arnoldi, A. (2016). Lupin protein exerts cholesterol-lowering effects targeting PCSK9: From clinical evidences to elucidation of the *in vitro* molecular mechanism using HepG2 cells. *Journal of Functional Foods*, *23*, 230-240.

- Lammi, C., Zanoni, C., Ferruzza, S., Ranaldi, G., Sambuy, Y., & Arnoldi, A. (2016). Hypocholesterolaemic Activity of Lupin Peptides: Investigation on the Crosstalk between Human Enterocytes and Hepatocytes Using a Co-Culture System Including Caco-2 and HepG2 Cells. *8*(7), 437.
- Lammi, C., Zanoni, C., Scigliuolo, G. M., D'Amato, A., & Arnoldi, A. (2014). Lupin Peptides Lower Low-Density Lipoprotein (LDL) Cholesterol through an Up-regulation of the LDL Receptor/Sterol Regulatory Element Binding Protein 2 (SREBP2) Pathway at HepG2 Cell Line. *Journal of Agricultural and Food Chemistry*, *62*(29), 7151-7159.
- Lau, C.-W., Yao, X.-Q., Chen, Z.-Y., Ko, W.-H., & Huang, Y. (2001). Cardiovascular Actions of Berberine. *Cardiovascular Drug Reviews*, *19*(3), 234-244.
- Levy, E., Ouadda, A. B. D., Spahis, S., Sane, A. T., Garofalo, C., Grenier, É., Emonnot, L., Yara, S., Couture, P., Beaulieu, J.-F., Ménard, D., Seidah, N. G., & Elchebly, M. (2013). PCSK9 plays a significant role in cholesterol homeostasis and lipid transport in intestinal epithelial cells. *Atherosclerosis*, *227*(2), 297-306.
- Maier, J. A., Martinez, C., Kasavajhala, K., Wickstrom, L., Hauser, K. E., & Simmerling, C. (2015). ff14SB: Improving the Accuracy of Protein Side Chain and Backbone Parameters from ff99SB. *Journal of Chemical Theory and Computation*, *11*(8), 3696-3713.
- Mao, Y., & Zhang, Y. (2012). Thermal conductivity, shear viscosity and specific heat of rigid water models. *Chemical Physics Letters*, *542*, 37-41.
- Marques, M. R., Fontanari, G. G., Pimenta, D. C., Soares-Freitas, R. M., & Arêas, J. A. G. (2015). Proteolytic hydrolysis of cowpea proteins is able to release peptides with hypocholesterolemic activity. *Food Research International*, *77*, 43-48.
- Maxwell, K. N., Fisher, E. A., & Breslow, J. L. (2005). Overexpression of PCSK9 accelerates the degradation of the LDLR in a post-endoplasmic reticulum compartment. *Proceedings of the National Academy of Sciences*, *102*(6), 2069-2074.
- Míguez, M., Dávalos, A., Manso, M. A., de la Peña, G., Lasunción, M. A., & López-Fandiño, R. (2008). Transepithelial transport across Caco-2 cell monolayers of antihypertensive egg-derived peptides. PepT1-mediated flux of Tyr-Pro-Ile. *52*(12), 1507-1513.

- Murray, A. B., & FitzGerald, J. R. (2007). Angiotensin Converting Enzyme Inhibitory Peptides Derived from Food Proteins: Biochemistry, Bioactivity and Production. *Current Pharmaceutical Design*, 13(8), 773-791.
- Natoli, M., Leoni, B. D., D'Agnano, I., Zucco, F., & Felsani, A. (2012). Good Caco-2 cell culture practices. *Toxicology in Vitro*, 26(8), 1243-1246.
- Nongonierma, A. B., & FitzGerald, R. J. (2019). Features of dipeptidyl peptidase IV (DPP-IV) inhibitory peptides from dietary proteins. *Journal of Food Biochemistry*, 43(1), e12451.
- Seidah, N. G., & Prat, A. (2007). The proprotein convertases are potential targets in the treatment of dyslipidemia. *Journal of Molecular Medicine*, 85(7), 685-696.
- Soares, R. A. M., Mendonça, S., De Castro, L. Í. A., Menezes, A. C. C. C. C., & Arêas, J. A. G. (2015). Major Peptides from Amaranth (*Amaranthus cruentus*) Protein Inhibit HMG-CoA Reductase Activity. *16*(2), 4150-4160.
- Tai, M.-H., Chen, P.-K., Chen, P.-Y., Wu, M.-J., Ho, C.-T., & Yen, J.-H. (2014). Curcumin enhances cell-surface LDLR level and promotes LDL uptake through downregulation of PCSK9 gene expression in HepG2 cells. *Molecular Nutrition & Food Research*, 58(11), 2133-2145.
- Udenigwe, C. C., & Aluko, R. E. (2012). Food Protein-Derived Bioactive Peptides: Production, Processing, and Potential Health Benefits. 77(1), R11-R24.
- Xu, Q., Hong, H., Wu, J., & Yan, X. (2019). Bioavailability of bioactive peptides derived from food proteins across the intestinal epithelial membrane: A review. *Trends in Food Science & Technology*, 86, 399-411.
- Zanoni, C., Aiello, G., Arnoldi, A., & Lammi, C. (2017). Investigations on the hypocholesterolaemic activity of LILPKHSDAD and LTFPGSAED, two peptides from lupin β -conglutin: Focus on LDLR and PCSK9 pathways. *Journal of Functional Foods*, 32, 1-8.

CHAPTER 4

MANUSCRIPT 2

COMPUTATIONAL DESIGN AND BIOLOGICAL EVALUATION OF ANALOGS OF LUPIN PEPTIDE P5 ENDOWED WITH DUAL PCSK9/HMGCOAR INHIBITING ACTIVITY

Carmen Lammi^{*}, Enrico M. A. Fassi, **Jianqiang Li**, Martina Bartolomei,
Giulia Benigno, Gabriella Roda, Anna Arnoldi and Giovanni Grazioso^{*}

**Department of Pharmaceutical Sciences, University of Milan, Via L. Mangiagalli
25, 20133 Milan, Italy.**

Author Contributions: Conceptualization, G.G. (computational design) and C.L. (biological design); methodology, validation, investigation, G.B., E.M.A.F., J.L. and M.B.; resources, A.A., G.R., G.G. and C.L.; data curation, writing—original draft, G.G. and C.L.; writing – review & editing, A.A., G.R., C.L. and G.G.

4. Abstract

(1) Background: Proprotein convertase subtilisin/kexin 9 (PCSK9) is responsible for the degradation of the hepatic low-density lipoprotein receptor (LDLR), which regulates the circulating cholesterol level. In this field, we discovered natural peptides derived from lupin that showed PCSK9 inhibitory activity. Among these, the most active peptide, known as P5 (LILPHKSDAD), reduced the protein-protein interaction between PCSK9 and LDLR with an IC_{50} equals to 1.6 μ M and showed a dual hypocholesterolemic activity, since it shows complementary inhibition of the 3-hydroxy-3-methylglutaryl coenzyme A reductase (HMGCoAR). (2) Methods: In this study, by a computational approach, the P5 primary structure was optimized to obtain new analogs with improved affinity to PCSK9. Then, biological assays were carried out for fully characterizing the dual cholesterol-lowering activity of the P5 analogs by using both biochemical and cellular techniques. (3) Results: A new peptide, P5-Best (LYLPKHSDRD) displayed improved PCSK9 (IC_{50} 0.7 μ M) and HMGCoAR (IC_{50} 88.9 μ M) inhibitory activities. Moreover, *in vitro* biological assays on cells demonstrated that, not only P5-Best, but all tested peptides maintained the dual PCSK9/HMG-CoAR inhibitory activity and remarkably P5-Best exerted the strongest hypocholesterolemic effect. In fact, in the presence of this peptide, the ability of HepG2 cells to absorb extracellular LDL was improved by up to 254%. (4) Conclusions: the atomistic details of the P5-Best/PCSK9 and P5-Best/HMGCoAR interactions represent a reliable starting point for the design of new promising molecular entities endowed with hypocholesterolemic activity.

4.1 Introduction

Hyperlipidemia is a well-known risk factor for developing cardiovascular disease (Nelson, 2013). The most common drugs for hypercholesterolemia treatment are statins, which inhibit 3-hydroxy-3-methylglutaryl coenzyme A reductase (HMGCoAR), the rate-limiting enzyme in cholesterol biosynthesis. This enzyme lowers intracellular cholesterol levels, leading to an increased expression of LDL

receptors (LDLR) on cell surfaces and a reduction of serum LDL-cholesterol (LDL-C) via the activation of the sterol-regulatory element-binding protein (SREBP)-2 transcription factor pathway (Goldstein & Brown, 1990). Although this approach is considered an efficient way to reduce circulating LDL-C, cardiovascular events still occur in some patients. Moreover, statins induce known and serious side effects, such as headache, muscle and joint pain, and a higher risk of developing diabetes.

Another key player in the cholesterol homeostasis is the proprotein convertase subtilisin/kexin 9 (PCSK9) which was discovered in the 2003 and it has been recognized as one of the most promising targets for counteracting hypercholesterolemia and atherosclerotic cardiovascular diseases (Poirier, Mayer, & therapy, 2013). Under physiological conditions, the blood circulating PCSK9 interacts with the low-density lipoprotein receptor (LDLR) on the liver cell membrane, triggering the internalization of the LDLR/PCSK9 complex in a digestive vacuole (Seidah, Awan, Chrétien, & Mbikay, 2014). Consequently, the main biological activity of PCSK9 is the regulation of the LDLR population on the liver cell surface, resulting in the tuning of the cellular capacity to capture circulating LDL cholesterol (LDL-C). Accordingly, the inhibition of the PCSK9/LDLR interaction leads to an increased LDLR population on the cell membrane, resulting in an enhanced capacity to capture the blood-circulating LDL-C by liver cells (Kwon, Lagace, McNutt, Horton, & Deisenhofer, 2008).

The expression of PCSK9 is also controlled by the activity of SREBP-2 as well as a specific transcriptional activator hepatocyte nuclear factor-1 α (HNF-1 α) (Alvi, Ansari, Ahmad, Iqbal, & Khan, 2017), which is a liver-enriched transcription factor regulating many target (Odom, Zizlsperger, Gordon, Bell, Rinaldi, Murray, et al., 2004) genes in the liver and intestine. In contrast, the ability of SREBP-2 to co-stimulate the PCSK9 and LDLR expression limits the therapeutic efficacy of statins which are known to produce their effects via SREBP-2 activation. Indeed, it is well documented that statins improve the PCSK9 protein level production through the augmentation of the intracellular HNF-1 α levels (Dong, Singh, Shende, & Liu, 2017). Hence, in the last two decades, academia and pharmaceutical companies have

financed considerable research on the development of compounds capable of target PCSK9 developing different strategies including siRNA, anti-sense oligonucleotides (ASOs), peptide inhibitors, and monoclonal antibodies (mAbs) (Burdick, Skelton, Ultsch, Beresini, Eigenbrot, Li, et al., 2020; Dyrbuś, Gąsior, Penson, Ray, & Banach, 2020; Kirchhofer, Burdick, Skelton, Zhang, & Ultsch, 2020; Kwon, Lagace, McNutt, Horton, & Deisenhofer, 2008; Lammi, Sgrignani, Arnoldi, Lesma, Spatti, Silvani, et al., 2019; Londregan, Wei, Xiao, Lintner, Petersen, Dullea, et al., 2018; Salaheldin, Godugu, Bharali, Fujioka, Elshourbagy, & Mousa, 2022; Stucchi, Cairati, Cetin-Atalay, Christodoulou, Grazioso, Pescitelli, et al., 2015; Xia, Peng, Gu, Wang, Wang, & Zhang, 2021; Xie, Yang, Winston-McPherson, Stapleton, Keller, Attie, et al., 2020; Xu, Luo, Zhu, & Xu, 2019). In this field, we have recently sorted out the most potent natural peptide (LILPKHSDAD, P5) derived from a peptic lupin (*Lupinus A.*) protein hydrolysate (Lammi, Zanoni, Scigliuolo, D'Amato, & Arnoldi, 2014) with hypocholesterolemic activity (Lammi, Zanoni, Ferruzza, Ranaldi, Sambuy, & Arnoldi, 2016), which impairs the PCSK9-LDLR interaction with an IC₅₀ value of 1.6 μM (Lammi, Zanoni, Aiello, Arnoldi, & Grazioso, 2016). In parallel, P5 reduces the catalytic activity of HMG-CoAR with an IC₅₀ value of 147.2 μM (Zanoni, Aiello, Arnoldi, & Lammi, 2017); through the inhibition of the enzyme activity, P5 increases the LDLR protein level in HepG2 cells through the activation of SREBP-2, and through a downregulation of HNF-1α, it reduces the PCSK9 protein levels and its secretion in the extracellular environment (Zanoni, Aiello, Arnoldi, & Lammi, 2017). This unique synergistic multi-target inhibitory behavior of P5 determines the improved ability of HepG2 cells to uptake extracellular LDL with a final hypocholesterolemic effect. P5 was successfully transported by differentiated human intestinal Caco-2 cells (Lammi, Aiello, Vistoli, Zanoni, Arnoldi, Sambuy, et al., 2016) through transcytosis (Lammi, Aiello, Bollati, Li, Bartolomei, Ranaldi, et al., 2021), and, during transport, it was partially metabolized in a breakdown fragment (LPKHSDAD, P5-met), which retained the biological activity of the parent peptide (Lammi, et al., 2021). In facts, we have demonstrated that P5-met reduces PCSK9-LDLR binding with a dose-response trend and an IC₅₀ of 1.7 μM and inhibits the

HMGC_oAR with an IC₅₀ of 175.3 μM (Lammi, et al., 2021). At a cellular level, such as P5, P5-met improves the LDLR and reduces PCSK9 levels, through the modulation of both SREBP-2 and HNF-1α, respectively (Lammi, et al., 2021). Therefore, since P5-met displayed the same activity and behavior of the parent peptide, P5, our results indicated that the first two amino acid residues (LI) do not play a key role in the interaction with both PCSK9 and HMGC_oAR target.

These evidences clearly indicate that P5, with its dual-inhibitory activity, represents a new alternative strategy to the use of single classical PCSK9 and HMGC_oAR inhibitors. Notably, the strategy in which dual-inhibitors are employed may be more effective in overcoming the deficits attributed to the classical use of statins (adverse effects and co-stimulation of PCSK-9 and LDLR via a common transcriptional activator, i.e., SREBP-2, in statin-treated patients limited the efficacy of these classical HMGC_oAR inhibitors) or PCSK9 inhibitors (including expensiveness, low compliance of the patients, repeated administrations, and injection site irritations) on health and to meet the desired health goals and public priorities in terms of safety and cost-related issues.

Considering these observations, the overall aim of the present study is the development of new P5 analogs able to target both PCSK9 and HMGC_oAR, therefore displaying an improved and dual hypocholesterolemic activity. To achieve this objective, new P5 analogs with improved PCSK9 and HMGC_oAR inhibitory activity were computationally designed (Lammi, Sgrignani, Roda, Arnoldi, & Grazioso, 2019). Hence, the theoretical study was validated and confirmed by performing a detailed biological investigation on the most promising P5 analogs. Firstly, their ability to inhibit the protein–protein interaction (PPI) between PCSK9 and LDLR and the HMGC_oAR activity were evaluated using biochemical assays, respectively. Then, their effects on the cholesterol pathway modulation on HepG2 cells were deep characterized, fostering their dual inhibitory cholesterol-lowering activity. More in details, the effect of PCSK9 inhibition by P5 analogs on the LDLR protein levels on the surface of hepatocytes and their effect to improve the functional ability of hepatocytes to uptake LDL from the extracellular environment were assessed by

performing in cell-western (ICW) (Lammi, Zanoni, & Arnoldi, 2015) and LDL-uptake assay (Lammi, Bellumori, Cecchi, Bartolomei, Bollati, Clodoveo, et al., 2020), respectively, in the presence of PCSK9. In parallel, to assess the effects of P5 analogs on the cholesterol pathway upon HMGCoAR inhibition, western blotting was performed, monitoring the LDLR, SREBP-2, HMGCoAR, PCSK9, and HNF-1 α protein levels, respectively. In addition, by performing ELISA experiments, the effects of P5 analogs on the hepatic secretion of PCSK9 levels were assessed. Finally, LDL-uptake and ICW assays were carried out to investigate the functional ability of hepatic cells to absorb extracellular LDL upon treatment with P5 derived peptides.

4.2 Materials and Methods

4.2.1 System Setup and MD Simulations

The computational models utilized in this study were built starting from the coordinates of the PCSK9/P5 complex model previously reported by us (Lammi, Zanoni, Aiello, Arnoldi, & Grazioso, 2016). Here, the starting PCSK9/P5 complex model was additionally equilibrated through 1 μ s-long MD simulations, utilizing the pmemd.cuda module of the AMBER20 package (Case, Aktulga, Belfon, Ben-Shalom, Brozell, Cerutti, et al., 2021). In particular, the ff14SB AMBER force field (Maier, Martinez, Kasavajhala, Wickstrom, Hauser, & Simmerling, 2015) was used for simulating the protein atoms, while the TIP3P model (Mao & Zhang, 2012) was used to explicitly represent the water molecules (about 25,000). The sodium ions were added to neutralize the overall charge of the simulation system and the MD trajectories acquired during the production runs were examined by visual inspection by means of VMD (Humphrey, Dalke, & Schulten, 1996), ensuring that the thermalization did not cause any structural distortion. This protocol was also utilized to perform MD simulations on the PCSK9 complexes resulting from the mutations of the P5 sequence.

4.2.2 Cluster Analysis

The MD trajectory frames were analyzed by clustering the conformations adopted by the small peptide backbone atoms in complex with PCSK9. The cluster analysis was performed using the cptraj module (Roe & Cheatham, 2013) of AMBER20 (Case, et al., 2021). By this algorithm, the MD frames were divided into clusters by the complete average linkage algorithm, and the PCSK9/peptide complex conformations with the lowest root mean square deviation (RMSD) to the cluster centers (the structures representative of the cluster, SRC) were acquired and visually inspected. Molecular mechanics-generalized born surface area (MM-GBSA) calculations were performed on 100 frames belonging to the most populated cluster of PCSK9/peptide conformations, and the MMPBSA.py module (Miller, McGee, Swails, Homeyer, Gohlke, & Roitberg, 2012) of AMBER20 was used to this aim, keeping parameters in the default values. In these calculations, the single trajectory approach was applied and the entropy contributions to the binding free energy was neglected (Grazioso, Bollati, Sgrignani, Arnoldi, & Lammi, 2018; Lammi, Sgrignani, Roda, Arnoldi, & Grazioso, 2019). For this reason, the estimated binding free energy values are termed by us ΔG^* .

4.2.3 Alanine Scanning

The nine P5 alanine mutants were built systematically altering the peptide sequence on the PCSK9/P5 complex, by the tleap module of AMBER20 (Case, et al., 2021). The resulting complexes were energy minimized and equilibrated by accomplishing 250 ns of MD simulations, adopting the procedure and the parameters previously described for the PCSK9/P5 complex. A hundred of snapshots were regularly extracted from the trajectory frames in which the peptide under investigation displayed the smallest root mean square deviation (RMSD) value fluctuation, to ensure the lowest standard error in the binding free energy calculation. MM-GBSA calculations by MMPBSA.py module (Miller, McGee, Swails, Homeyer, Gohlke, & Roitberg, 2012) were finally performed to estimate the binding free energy values of the mutant peptides.

4.2.4 Computational Design of New P5 Analogs

The “protein preparation wizard” module implemented in the Maestro release 2019-4 (Schrödinger, LLC, New York, NY, USA, 2017) for molecular modeling ensured the accuracy of the PCSK9/P5 complex conformation previously equilibrated by MD simulations. In particular, this module permitted: (1) to check the residue protonation state at pH 7.4, (2) to check the residue completeness, (3) to eliminate atomic clashes, and (4) to assign the OPLS3e force field (Roos, Wu, Damm, Reboul, Stevenson, Lu, et al., 2019). Then, the 400 possible peptides were generated by the replacement of the P5 positions 2 and 9 with the twenty natural amino acids. The resulting PCSK9/peptide complexes were minimized by Prime MM-GBSA module of Maestro, which uses OPLS3e (Roos, et al., 2019) as force field and a continuum solvent models to include the solvent effect into the calculations. Then, affinity maturation functionality implemented in Bioluminate module (Schrödinger, LLC, New York, NY, USA, 2017) estimated the change in affinity (Δ Affinity) between PCSK9 and the mutant peptides, with respect to P5. Finally, the mutant peptides acquiring the highest gain in Δ Affinity were additionally refined by MD simulations and MM-GBSA calculations by AMBER20 package (Case, et al., 2021), as it was conducted previously for the alanine-mutant peptides (see the previous section for details).

4.2.5 HMGCoA Reductase Model Setup and Simulations Protocol

The HMGCoAR structure solved by X-ray crystallography (PDB accession code 3CCZ) (Sarver, Bills, Bolton, Bratton, Caspers, Dunbar, et al., 2008) used in this study was deposited as a homotetramer in which the (3R,5R)-7-[2-(4-fluorophenyl)-4-[(1S)-2-hydroxy-1-phenylethyl] carbamoyl -5-(1methylethyl) -1H-imidazol-1-yl] - 3,5-dihydroxyheptanoic acids are bound in the catalytic sites. For simplicity, we have performed simulations on the functionally active homodimer, choosing as peptide binding site the one identified by the presence of a statin in the X-ray complex. Since the homodimer contained two statin molecules, one of them was removed to allow the docking calculations, while the statin present in the second site was kept in its original position, to avoid any protein conformational distortion inducted by the absence of the

ligand. The system was prepared and minimized through the “protein preparation wizard” tool available in the Maestro software (release 2019-4). Peptide docking calculations of [S7A]P5 were performed by using the Glide docking tool (Friesner, Murphy, Repasky, Frye, Greenwood, Halgren, et al., 2006) of Maestro software, setting as center of the grid the centroid of the statin (residue code 5HI), co-crystallized in the catalytic site of the HMGCoAR. The “standard precision” mode was applied in these calculations, and the Glide gscore was applied as scoring algorithm. Ten peptides’ docking poses were generated, while the number of post-docking minimization poses was set to 50. The formation of cis amide bonds was not allowed. The [S7A]P5 pose with the best-predicted gscore (−9.881 kcal/mol) was selected for the following MD simulations and cluster analysis calculations (**Table 4-S1**, Supporting Material), adopting the AMBER20 protocol (Case, et al., 2021) previously described for the studies of the peptides in complex with PCSK9.

4.2.6 Peptide Synthesis

The Genscript (Piscataway, NJ, USA) synthesized for us the P5 analogs selected for biological assays. All compounds are >95% pure by HPLC analysis (see Supporting Information for details).

4.2.7 HepG2 Cell Culture Conditions and Treatment

The HepG2 cell line was bought from ATCC (HB-8065, ATCC from LGC Standards, Milan, Italy) and was cultured in DMEM high glucose with stable L-glutamine, supplemented with 10% FBS, 100 U/mL penicillin, 100 µg/mL streptomycin (complete growth medium) with incubation at 37 °C under 5% CO₂ atmosphere.

4.2.8 HMG-CoAR Activity Assay

The experiments were carried out following the manufacturer instructions and optimized protocol (Aiello, Lammi, Boschini, Zanoni, & Arnoldi, 2017). See Supplementary Materials for further details.

4.2.9 *In Vitro* PCSK9-LDLR Binding Assay

Peptides P5 and P5 analogs (0.1–100 μM) were tested using the *in vitro* PCSK9-LDLR binding assay (CycLex Co., Nagano, Japan) following the manufacture instructions and conditions already optimized (Lammi, Zanoni, Aiello, Arnoldi, & Grazioso, 2016). Further details are provided in Supplementary Materials.

4.2.10 In-Cell Western (ICW) Assay

For the experiments, a total of 3×10^4 HepG2 cells/well were seeded in 96-well plates and treated with 4.0 $\mu\text{g}/\text{mL}$ PCSK9-WT and 4.0 $\mu\text{g}/\text{mL}$ PCSK9 + peptides P5 and/or P5 analogs (50 μM) and vehicle (H_2O) for 2 h at 37 °C under 5% CO_2 atmosphere. Thus, cells underwent to ICW assay following conditions already optimized (Lammi, Zanoni, & Arnoldi, 2015). See Supplementary Materials for detailed information.

4.2.11 Fluorescent LDL Uptake

HepG2 cells (3×10^4 /well) were seeded in 96-well plates and kept in complete growth medium for 2 days before treatment. The third day, cells were washed with PBS and then starved overnight (O/N) in DMEM without FBS and antibiotics. After starvation, they were treated with 4.0 $\mu\text{g}/\text{mL}$ PCSK9 and 4.0 $\mu\text{g}/\text{mL}$ PCSK9 + P5 and P5 analogs peptides (50 μM), and vehicle (H_2O) for 2 h at 37 °C under 5% CO_2 atmosphere. Fluorescent LDL-uptake was finally assessed following optimized protocol (Zanoni, Aiello, Arnoldi, & Lammi, 2017). See Supplementary Materials for further details.

4.2.12 Western Blot Analysis

A total of 1.5×10^5 HepG2 cells/well (24-well plate) were treated with 50 μM of P5 and P5 analogs for 24 h. Immunoblotting experiments were performed using optimized protocol (Lammi, Aiello, Dellafiora, Bollati, Boschini, Ranaldi, et al., 2020). See Supplementary Materials for further details.

4.2.13 Quantification of PCSK9 Secreted by HepG2 Cells through ELISA

The supernatants collected from treated HepG2 cells (50 μM of P5 and/or P5 analogs) were centrifuged at $600 \times g$ for 10 min at 4 °C and ELISA assay performed using

protocol already optimized (Moreira, Fernandes, & Ramos, 2007). Detailed data are provided in Supplementary Materials.

4.2.14 Statistical Analysis

All the data set were checked for normal distribution by D'Agostino and Pearson test. Since they are all normally disturbed with p -values < 0.05 , we proceeded with statistical analyses by one-way ANOVA followed by Tukey's post-hoc tests and using Graphpad Prism 9. Values were reported as means \pm S.D.; p -values < 0.05 were considered significant.

4.3 Results

4.3.1 Identification of Hotspots and Designs of New P5 Analogs

To obtain a robust hypothesis on the peptide P5 binding mode, the PCSK9/P5 complex model we had previously developed (Lammi, Zanoni, Aiello, Arnoldi, & Grazioso, 2016) was optimized once more by extending the molecular dynamics (MD) simulations to 1 μ s (see **Figure 4-S1** in the Supporting Information for the RMSD plots). At the end of these simulations, the MD trajectory frames were grouped using a cluster analysis algorithm (see the Materials and Methods Section) to determine which was the most favored P5 conformation in complex with PCSK9. The PCSK9/P5 complex conformation representative of the most populated cluster (78%) suggested that peptide P5 could bind to PCSK9, as illustrated in **Figure 4.1**. In particular, P5 could bind to PCSK9 through (1) a salt bridge between the charged NH term of P5-Leu1 and the side chain of Asp238, (2) an H-bond between the imidazole ring of the P5-His6 and the NH group of Ser381, (3) an H-bond network between the side chain of P5-Ser7, the NH of P5-Asp8, and the side chain of Asp367, and (4) an H-bond shaped by the side chain of P5-Asp8 and the side chain of Ser383. The side chain of P5-Leu3 was deeply inserted into a hydrophobic basin sized by the PCSK9 residues Phe379, Pro155, and Ile369, creating vander Waals interactions.

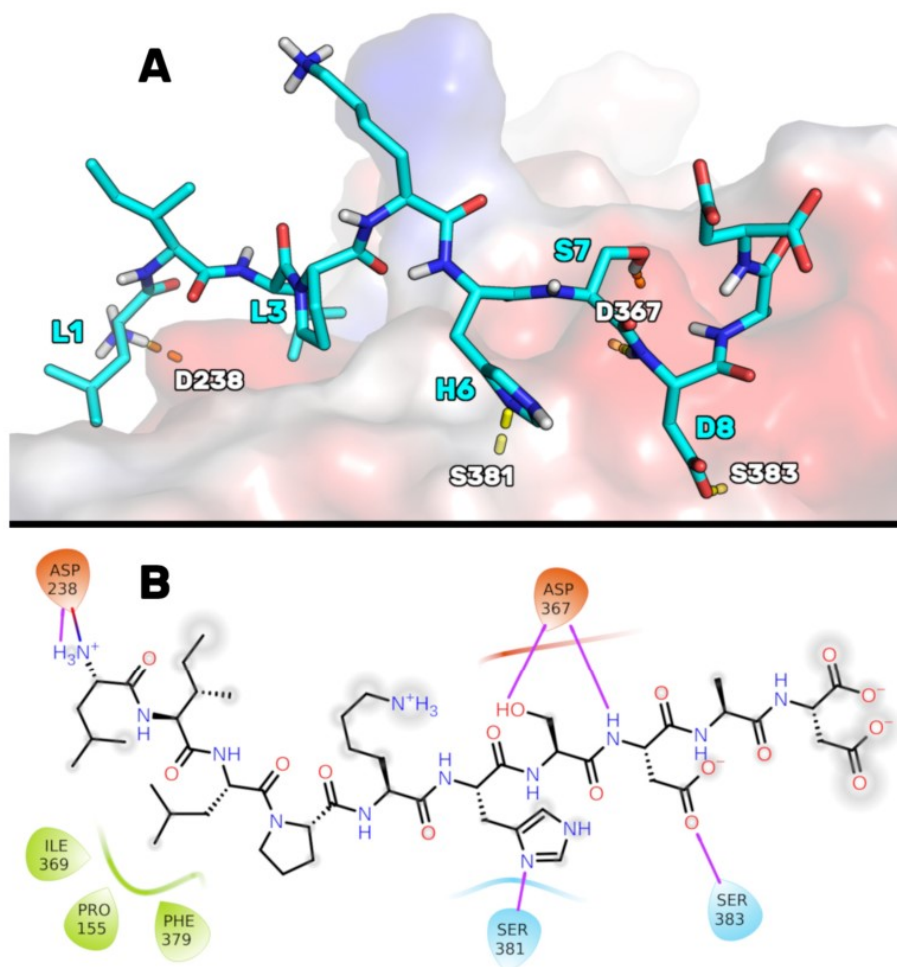


Figure 4.1 (A) The expected P5 binding mode on the PCSK9 surface after additional MD simulations. Yellow dotted lines highlight the H-bond network. The enzyme solvent-accessible surface is depicted accordingly by the partial charge of the residues: blue for positive areas and red for negative areas. Peptide P5 is represented as cyan sticks. (B) 2D representation of the predicted P5 binding mode in complex with PCSK9. H-bonds and salt bridges are highlighted in purple and blue/red lines, respectively. Hydrophobic residues interacting with P5 are colored in green.

Then, to identify new P5 analogs endowed with improved PCSK9 affinity, we designed new peptides by substituting the P5 residues not considerably involved in the PCSK9 contact (non-hotspot) with new amino acids showing an improved complementarity with the PCSK9 surface (Lammi, Sgrignani, Roda, Arnoldi, & Grazioso, 2019). In the first step, the hotspots and non-hotspots of P5 were discovered by performing a computational alanine-scanning mutagenesis analysis, in which all

the peptide residues in the PCSK9/P5 complex were systematically mutated into alanine. Specifically, nine 3D models, in which PCSK9 was in complex with each alanine-mutated peptide P5, were simulated by 200 ns-long MD simulations, and the subsequent molecular mechanics-generalized born surface area (MM-GBSA) calculations estimated the mutant peptides' binding free energy values (ΔG^* , **Table 4.1**). Then, by comparing the ΔG^* values calculated for the mutant peptides with those calculated for P5, identifying the hotspots and non-hotspots of P5 was possible (Homeyer, Stoll, Hillisch, & Gohlke, 2014; Moreira, Fernandes, & Ramos, 2007).

Table 4.1 Estimated binding free energy values of the peptides under investigation, as calculated using the MM-GBSA approach (ΔG^* , column 3).

Peptide/Mutation	Sequence	ΔG^* Value ¹	$\Delta\Delta G^*$ Value ²
P5	LILPKHSDAD	-18.9 ± 0.5	0
L1A	AILPKHSDAD	-13.5 ± 0.5	+5.4
I2A	LALPKHSDAD	-20.9 ± 0.5	-1.0
L3A	LIAPKHSDAD	-6.6 ± 0.7	+12.3
P4A	LILAKHSDAD	-23.0 ± 0.7	-4.1
K5A	LILPAHSDAD	-14.1 ± 0.6	+4.8
H6A (P5-H6A)	LILPKASDAD	-1.2 ± 0.5	+17.7
S7A (P5-S7A)	LILPKHADAD	-19.3 ± 0.3	-0.4
D8A	LILPKHSAAD	-21.9 ± 0.3	-3.0
D10A	LILPKHSDAA	-19.6 ± 0.5	-0.7

¹(kcal/mol \pm (Std. Err. of Mean)); ²(kcal/mol).

The attained results suggest that positions 3 and 6 can be considered hotspots, as their mutation into alanine led to P5 analogs endowed with a considerable reduction of the predicted binding affinity ($\Delta\Delta G^*$ higher than 10 kcal/mol). Specifically, P5-His6 seemed crucial for peptide binding because its substitution led to a dramatic drop in the peptide binding interaction energy. MD simulations suggest that the substitution of the basic side chain of His6 with a methyl group led to a change in the peptide binding mode due to a lack of an H-bond between the PCSK9-Ser282 amide group

and the imidazole ring of P5-His6. For this reason, the [H6A] peptide P5 was unbound from the PCSK9 surface after the initial steps of the MD simulations (see **Figure 4-S2** in the Supporting Information for the RMSD plots). Similarly, the removal of the side chain of P5-Leu3 led to a peptide incapable of maintaining the P5 initial binding mode, as the hydrophobic contacts engaged by the Leu3 isobutyl group with the hydrophobic crevice sized by the PCSK9 residues Leu159, Pro156, Ala240, and Ile370 were missing.

The alanine mutation of Leu1 and Lys5 led to peptides with a calculated binding affinity that was slightly lower than that of P5 ($\Delta\Delta G^*$ close +5 kcal/mol). However, given the inaccuracy of the MM-GBSA calculations and the observation that the side chains of Leu1 and Lys5 fluctuating in a solvent environment do not stably bind to PCSK9 during the MD simulations, positions 1 and 5 cannot be considered strong hotspots similar to positions 3 and 6. Conversely, the substitution with alanine of Ile2, Ser7, and Asp10 of P5 led to peptides with a predicted binding affinity close to that predicted for the template peptide. Therefore, they can be considered non-hotspots and can potentially be substituted with different amino acids. However, the predicted data on Leu1 and Ile2 are in accordance with our recent experimental data, which show that a metabolite of peptide P5 that does not contain the first two residues (P5-met, LPKHSDAD) displays an IC_{50} value close to the parent peptide P5 (Lammi, et al., 2021).

Conversely, the P4A and D8A mutant peptides showed a higher affinity to PCSK9 than P5. However, as the gain in the ΔG^* value was not extremely high, the synthesis and biological evaluation of these peptides was not considered suitable.

4.3.2 Design of P5 Analogs with Improved PCSK9 Predicted Affinity

The alanine-scanning study showed that the positions 1, 2, 7, and 10 on the P5 sequence could be considered non-hotspots. Moreover, the alanine in position 9 should be considered a non-hotspot, as alanine is already present in the natural P5 sequence. Nevertheless, the P5-Ser7 OH group could create an H-bond with PCSK9-Asp367, and the P5-Asp10 side chain could be involved in the fold of the peptide, as

an internal H-bond could be shaped with the side chain of P5-Ser7. Thus, we decided to mutate the residues in positions 2 and 9 to develop novel P5 analogs with improved PCSK9 binding affinity.

Accordingly, with this assumption, 20² peptide P5 analogs were computationally designed through the systematic substitution of positions 2 and 9 with all natural amino acids. Their theoretical affinity for PCSK9 was preliminary evaluated by the Prime algorithm (Maestro, release 2019-4), which can estimate the peptide binding free energy using the MM-GBSA approach. PCSK9 in complex with the 10 top-ranking P5 analogs (i.e., those with the lowest Δ Affinity values, **Table 4.2**) again underwent MD simulations by applying the previously described AMBER20 MD protocol. The ΔG^* values were estimated using the MM-GBSA protocol (**Table 4.2**), which allowed for the acquisition of ΔG^* values comparable with those previously attained for P5 and other P5 alanine mutants.

Table 4.2 Estimated binding affinity values of newly designed P5 analogs (columns 1–2), calculated by Prime software (Δ Affinity, column 3) and standard MD/MM-GBSA calculations (ΔG^* values, column 4).

Peptide/Mutation	Sequence	Δ Affinity ¹	ΔG^* Value ²
P5	LILPKHSDAD		-18.9 ± 0.5
[I2P-A9R] P5	LPLPKHSDRD	-23.9	-26.3 ± 0.6
[I2M-A9R] P5	LMLPKHSDRD	-23.5	-26.3 ± 0.6
[I2R-A9R] P5	LRLPKHSDRD	-21.5	-30.3 ± 0.7
[I2Q-A9R] P5	LQLPKHSDRD	-21.0	-24.8 ± 0.8
[I2L-A9R] P5	LLLPKHSDRD	-20.7	-25.4 ± 0.6
[I2Y-A9R] P5 (P5-Best)	LYLPKHSDRD	-20.4	-41.7 ± 0.7
[I2H-A9R] P5	LHLPKHSDRD	-20.4	-24.6 ± 0.8
[I2T-A9R] P5	LTLPKHSDRD	-19.5	-28.0 ± 0.5
[I2F-A9R] P5	LFLPKHSDRD	-19.4	-19.2 ± 0.3
[I2E-A9R] P5	LELPKHSDRD	-19.1	-24.5 ± 0.6

¹(kcal/mol); ²(kcal/mol ± (Std. Err. of Mean)).

The Prime calculations (third column of **Table 4.2**) suggested that the peptides acquiring an improved predicted binding energy were the ones containing arginine in position 9. At variance, the substitutions in position 2 did not considerably affect the affinity of the resulting peptides (differences in the Δ Affinity values followed in the range of 5 kcal/mol). Subsequently, using the AMBER20/MM-GBSA calculations, the resulting ΔG^* values spanned from -19 to -42 kcal/mol. This allowed us to assess that the peptide [I2Y-A9R]P5 (i.e., P5-Best) was endowed with the highest predicted PCSK9 binding affinity (see **Figure 4-S3** in the Supporting Information for the RMSD plots). In fact, the ΔG^* value of P5-Best was two times the value predicted for the template peptide P5, suggesting that P5-Best could show an affinity to PCSK9 appreciably lower than P5. Our simulations showed that, as indicated in the conformation representative of the most populated cluster (**Figure 4.2**), P5-Best could acquire an ameliorated PCSK9 complementarity because of the possibility of creating two salt bridges: the first between the new arginine in position 9 and the side chains of Glu366 and Asp367, and the second between the side chain of P5-Best-Asp10 and the side chain of Lys222. These interactions were also enforced by the presence of an H-bond between the P5-Best-Asp10 and the OH group of Ser225. Moreover, the P5-Best-Ile3 side chain was in contact with the hydrophobic pocket sized by Phe379, while the phenol ring of the new residue P5-Best-Tyr2 was located close to Arg194. The NH groups of P5-Best-Tyr2 and -Ile3 created two H-bonds with the side chain of Asp238.

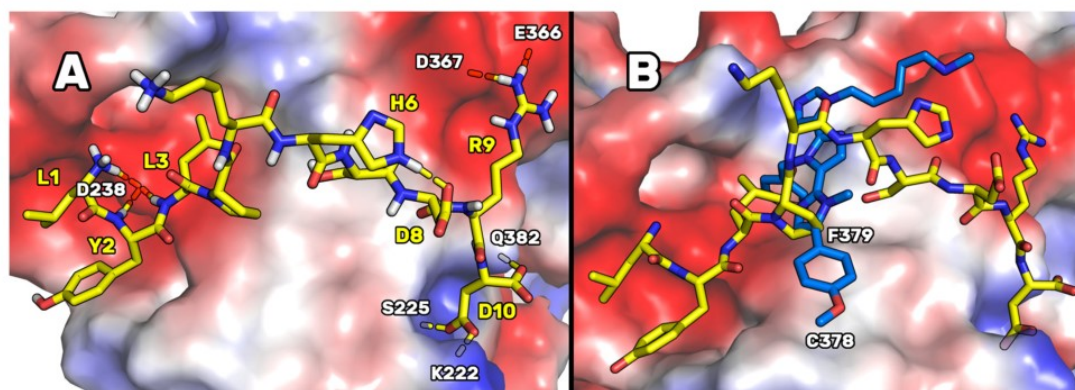


Figure 4.2 (A) Expected binding mode of [I2Y-A9R]P5 (i.e., P5-Best) on the PCSK9 surface resulting from the MD simulations and cluster analysis. Yellow dotted lines depict the H-bond network. The enzyme solvent-accessible surface is colored according to the partial charge of the residues: blue for positive areas and red for negative areas. P5-Best is represented as yellow sticks. (B) Superimposition of P5-Best and Rim13, both bound on the PCSK9 surface.

These results were also compared to the computational data attained designing the poly-imidazole derivatives capable of inhibiting PCSK9 (Lammi, et al., 2019). In fact, in our previous paper, by applying a computational approach such as the one here applied, we designed and biologically evaluated two poly-imidazole derivatives endowed with PCSK9 inhibiting activity. The biological evaluation of the most interesting poly-imidazoles, named Rim13 and Rim14, allowed us to report on their ability to modulate the LDLR expression on the human hepatic HepG2 cell surface, and their capacity to increase the extracellular uptake of LDL by the same cells. Here, structurally aligning the P5-Best and the Rim13 hypothetical binding modes, we noted that the backbone atoms of the peptide residues Pro4 and Lys5 were mimicked by the first two imidazole rings of Rim13 (**Figure 4.2B**). Moreover, the benzyl chain of the second imidazole ring of Rim13 was projected in the same hydrophobic cleft shaped by Phe379 and occupied by the side chain of P5-Best-Leu3, creating van der Waals interactions. Furthermore, the negatively charged area created by the PCSK9 residues Asp367 and Glu366 were in contact with the side chain of the P5-Best-Arg9 and the amino-methyl chain of Rim13. Since they bind similarly, creating contacts with the same PCSK9 residues, this alignment could help in the design of new poly-imidazole

derivatives. In fact, aiming at designing more potent poly-imidazoles derivatives, the benzyl moiety of Rim13 could be substituted by alkyl chains (linear or not), to reproduce the interactions played by the P5-Best-Leu3 residue. Conversely, regarding the design of new P5 analogs, the Pro4 of P5-Best could be replaced by aromatic residues such as Phe, Tyr or Trp, in order to reproduce the interactions played by the p-methoxyphenyl ring of Rim13. However, the oral PK properties of peptides remains strongly limited by the presence of degrading enzymes in the gastrointestinal tract. Nevertheless, the research efforts are still devoted to solve this limitation. In fact, active peptides could be orally administered together with penetration enhancers, within hydrogels or in combination with digestive enzyme inhibitors. As alternative, they can be suitably coated by acid-stable polymers or administered through intestinal patches (Drucker, 2020). By means of one of these innovative delivery strategies, even peptides active in the high micromolar range could be successfully employed for the treatment of several pathologies. Actually, numerous peptides are in phase III of clinical trials but, until now, only desmopressin is available in the market, and used in the clinic (Drucker, 2020).

4.3.3 Experimental Validation of the Computational Predictions

In light of these theoretical studies, empirical assays were performed on the [H6A] peptide P5 (i.e., P5-H6A) because position 6 was recognized as a hotspot (**Table 4.1**), on P5-Best because of its lowest predicted binding free energy value, and on [S7A]P5 (i.e., P5-S7A) because it represents one of the peptides for which the alanine mutation did not remarkably alter the predicted binding free energy value. Conversely, the mutation of P5-Asp10 into alanine affected peptide folding (as shown by MD simulations) and the water solubility of the peptide, as the negatively charged side chain of Asp10 should be substituted with the aliphatic methyl group of alanine. Thus, the peptides P5-H6A, P5-S7A, and P5-Best were purchased by GenScript and biochemically evaluated by *in vitro* experiments.

4.3.4 Analogs Impair the PPI between PCSK9 and LDLR

To verify whether the P5 derivatives could impair the PPI between PCSK9 and LDLR, dedicated biochemical experiments were assessed. The results showed that P5-Best, P5-H6A and P5-S7A reduced the PCSK9-LDLR binding with a dose-response trend and IC_{50} values of 0.7, 9.0, and 1.45 μ M, respectively (**Figure 4.3A**). The results confirmed that two of the new P5 derivatives were more active than P5 (1.6 μ M). These data are in line with the computational predictions. In fact, the peptides ΔG^* value calculations indicated that the most active peptide could be the double mutant peptide P5-Best ($\Delta G = -41.7$ kcal/mol) while, among other ones, P5-S7A should display binding affinity in the range of P5 (ΔG^* values of -19.3 and -18.9 kcal/mol, respectively), and P5-H6A should be do not active, since by our predictions, the side chain of H6 plays a crucial role in the stabilization of the peptide on the PCSK9 surface. Nevertheless, it has to be stated that a higher affinity should be expected for P5-Best, since the calculated ΔG^* value calculated for this peptide was double than that of P5. In our opinion, the lack of linearly between the binding affinity experimental data (IC_{50} values) and the computational predictions, could be due to the omitted calculation of the entropic contribution to binding free energy value. In fact, the calculation of this contribution is highly computationally demanding, and the error associated with the estimation is very often greater than the value itself. Moreover, the data attained by the further biological investigations on these peptides cannot be compared with the computational predictions, since it is very difficult to discuss the *in silico* results in comparison with the biological data obtained from the HepG2 cells. In fact, the molecular modeling studies have been performed on a PCSK9 model immersed in a box of water molecules and the biological experiment capable of reproducing these conditions is only the one in which the recombinant PCSK9 is in contact with the LDLR, i.e., the binding assays displayed in **Figure 4.3**. Conversely, when the biological properties of peptides are assessed in complex experimental conditions, such as the one in which cells are involved, the molecular modeling results cannot be linearly compared with the experimental data. In fact, the effects of

membranes, extracellular or intracellular enzymes cannot be considered by our calculations.

Furthermore, the ability of these P5 analogs to modulate the levels of LDLR localized on HepG2 surfaces was investigated in the presence of PCSK9 (4 $\mu\text{g/mL}$) using an in-cell western (ICW) assay. The results showed that the LDLR levels decreased in the presence of PCSK9 alone by $25.4 \pm 1.6\%$ ($p < 0.001$) compared with the untreated control cells, and that P5-Best, P5-H6A, and P5-S7A could significantly restore the LDLR levels to $96.9 \pm 10.4\%$, $93.4 \pm 5.2\%$, and $104.4 \pm 0.4\%$ ($p < 0.001$), respectively, when co-incubated with PCSK9 (**Figure 4.3B**). Finally, functional cell-based assays were performed to investigate the ability of HepG2 cells to uptake extracellular LDL in the presence of PCSK9. HepG2 cells incubated with PCSK9 alone showed a $43.6 \pm 9.6\%$ ($p < 0.05$) reduction in the uptake of fluorescent LDL compared with the untreated control cells. This result is in agreement with the reduction of active LDLR population on the cell surface, which was observed by ICW. After co-incubation with PCSK9, P5-Best, P5-H6A, and P5-S7A completely restored the LDLR function, increasing the LDL uptake to $129.2 \pm 21.9\%$ ($p < 0.001$), $107.4 \pm 23.0\%$ ($p < 0.05$), and $125.4 \pm 19.0\%$ ($p < 0.01$) (**Figure 4.3C**), respectively.

P5 analogs demonstrated to be more active than peptide Pep2-8 (TVFTSWEEYLDWV) (Zhang, Eigenbrot, Zhou, Shia, Li, Quan, et al., 2014) and its analogs [Y9A]Pep2-8 and [T4R,W12Y]Pep2-8 (Lammi, Sgrignani, Arnoldi, & Grazioso, 2019) as PPI inhibitors of PCSK9. More in details, at the fixed concentration of 100 μM , Pep2-8 impaired the PCSK9-LDLR binding by -36.5% vs. the control, whereas [Y9A]Pep2-8 and [T4R,W12Y]Pep2-8 by -69.8% and -93.0% , respectively (Lammi, Sgrignani, Arnoldi, & Grazioso, 2019). Indeed, the IC_{50} value of [Y9A]Pep2-8 was equal to $27.12 \pm 1.2 \mu\text{M}$ and that of [T4R,W12Y]Pep2-8 equal to $14.50 \pm 1.3 \mu\text{M}$ (Lammi, Sgrignani, Arnoldi, & Grazioso, 2019), clearly indicating that P5-Best is about 30- and 20-fold more potent than the Pep2-8 mutant peptides. In addition, at cellular levels, Pep2-8 and both Pep2-8 analogs were less efficient than P5 analogs to restore the LDLR protein levels and the functional ability of hepatocytes to absorb LDL from the extracellular environment (Lammi, Sgrignani, Arnoldi, &

Grazioso, 2019). On the contrary, P9-38, a cyclized Pep2-8 analogue, demonstrated to be 35-fold more potent than P5-Best in impairing the PPI between PCSK9/LDLR displaying and IC₅₀ equals to 20 nM and it was 1000-fold more potent to restore the LDLR level and functionality in HepG2 cells (Tombling, Lammi, Lawrence, Gilding, Grazioso, Craik, et al., 2021).

Finally, P5-Best is slightly more potent than the poly-imidazole Rim13 which inhibit the interaction between PCSK9 and LDLR by an IC₅₀ equals to 1.4 μM, a value similar to the reference peptide P5. In the same range of concentration of Rim13, P5 analogs successes in the restoring the functional activity of LDLRs on the surface of hepatocytes preventing their degradation (Tombling, et al., 2021).

Although all P5 analogs successfully restored the level of LDLR protein similar to peptide P5, statistical analysis revealed that from a functional point of view, both P5-Best and P5-S7A not only restored the ability of hepatic cells to uptake LDL from the extracellular environment but also improved this capability against untreated cells. These results suggest that the hypocholesterolemic effect occurs with a dual mechanism of action involving the modulation of HMGCoAR activity and protein levels. To assess this aspect and deepen this behavior, further HMGCoAR activity assay and western blot experiments were performed.

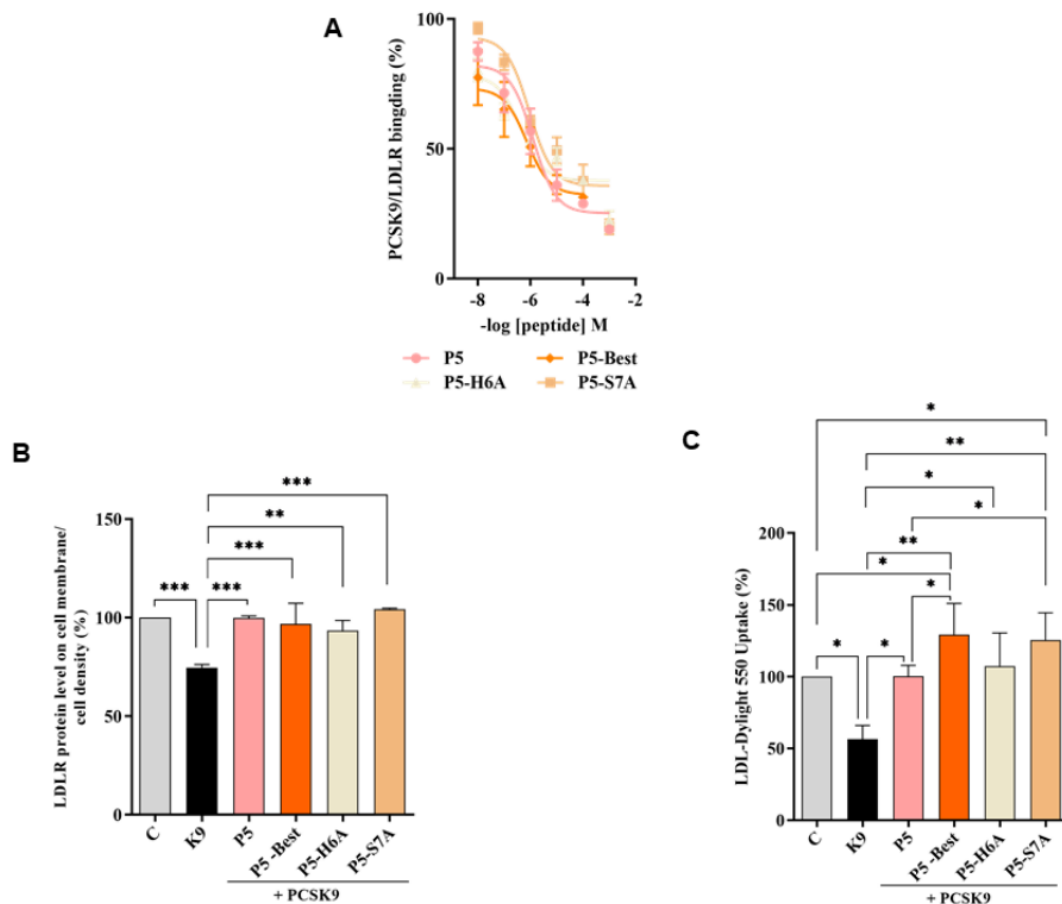


Figure 4.3 Inhibition of the PPI between PCSK9 and LDLR. (A) Impairment of the protein-protein interaction between PCSK9 and LDLR. (B) The treatment of HepG2 cells with PCSK9 (K9 in the graphs, 4 $\mu\text{g}/\text{mL}$) reduced the active LDLR protein levels localized on the surface of the cells, which were restored by P5 and P5 analogs (50 μM). (C) The decreased functional ability of HepG2 cells to absorb LDL from the extracellular space observed after incubation with PCSK9 (4 $\mu\text{g}/\text{mL}$) improved after treatment with P5 and P5 analogs (50 μM). The data points represent the average \pm SD of four independent experiments performed in duplicate. Data were analyzed using one-way ANOVA, followed by Tukey's post-hoc test; (*) $p < 0.05$, (**) $p < 0.01$, and (***) $p < 0.001$. C: control sample.

4.3.5 P5 Analogs Modulate the Hepatic LDLR Pathway by Inhibiting HMGCoAR Activity

To better characterize the dual inhibitory activity of all P5 analogs, a biochemical investigation was conducted to assess their effect on the modulation of HMGCoAR

activity. The results suggested that P5-Best, P5-H6A, and P5-S7A inhibited enzyme activity with an IC_{50} of 88.9, 74.4, and 73.8 μ M, respectively, showing more effective inhibitory activity than P5 (147.2 μ M) (**Figure 4.4A**), but they are still less active than statins. In fact, the IC_{50} values for the inhibition of HMG-CoAR activity for pravastatin simvastatin, atorvastatin, and rosuvastatin are equals to 44.1, 11.2, 8.2, and 5.4 nM, respectively (McTaggart, Buckett, Davidson, Holdgate, McCormick, Schneck, et al., 2001; Olsson, McTaggart, & Raza, 2002).

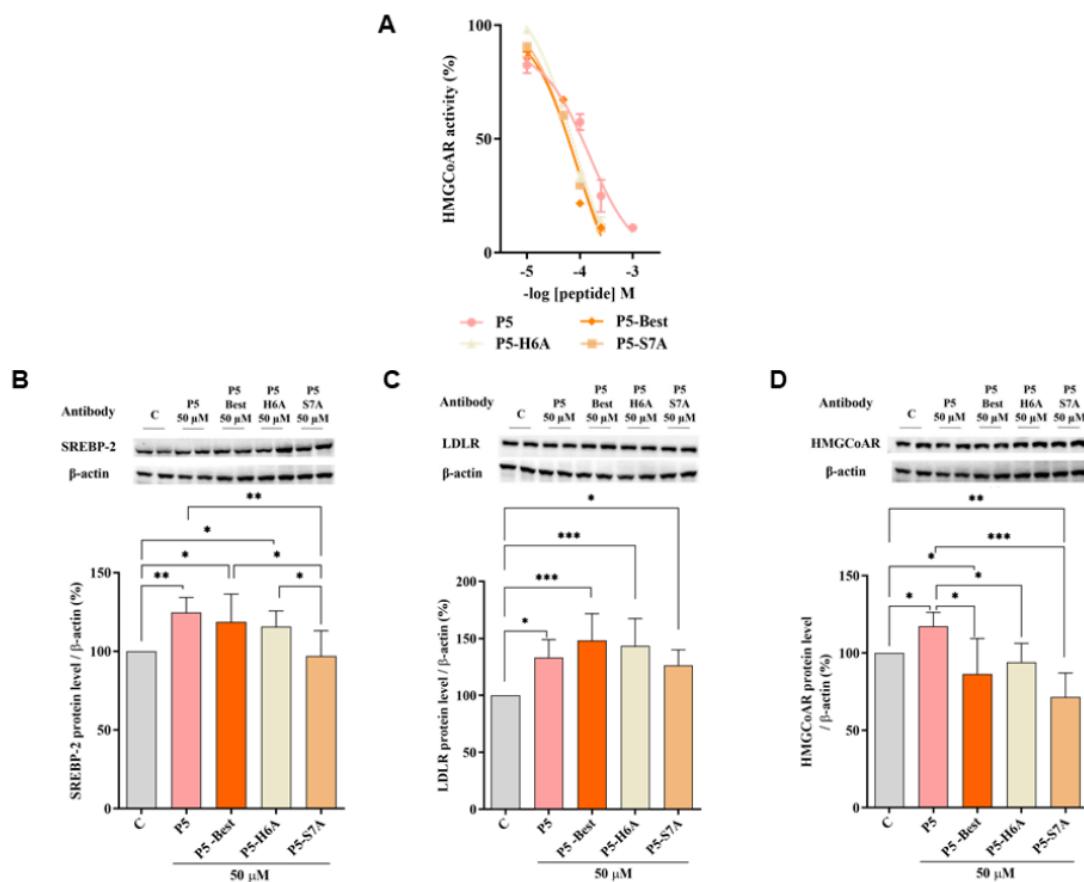


Figure 4.4 Modulation of the LDLR pathway in HepG2 cells treated with P5 and P5 analogs. (A) *In vitro* inhibition of HMGCoAR activity. (B) The effect on SREBP-2 protein levels, (C) LDLR protein levels, and (D) HMGCoAR protein levels after the treatment of HepG2 cells with P5 and P5 analogs, respectively. Data points represent the average \pm SD of four independent experiments performed in duplicate. C vs. P5 and P5 analog samples were analyzed using a one-way ANOVA, followed by by Tukey's test; (*) $p < 0.05$, (**) $p < 0.01$, and (***) $p < 0.001$. C: control sample.

Even though, P5 and P5 analogs are less active than statins as HMGCoAR inhibitors and their clinical implication is still too far, they display the unique feature to inhibit both HMGCoAR and PCSK9 targets, making them lead compounds for developing new peptidomimetic and/or small molecules endorsed by improved activity on both targets involved in the control of the circulating cholesterol level.

Further experiments were performed to verify the ability of these P5 analogs to modulate the LDLR pathway in HepG2 cells. Similar to P5, P5-Best and P5-H6A induced an up-regulation of the SREBP-2 transcription factor level up to $118.6 \pm 17.7\%$ and $115.6 \pm 10.1\%$ ($p < 0.05$) (**Figure 4.4B**), respectively, resulting in an augmentation of the LDLR protein levels up to $148.4 \pm 23.4\%$ and $143.5 \pm 24.0\%$ ($p < 0.001$), respectively (**Figure 4.4C**). Interestingly, although P5-S7A caused a slight reduction of the SREBP-2 protein level to $96.9 \pm 16.1\%$ (**Figure 4.4B**), it led to an increase in the LDLR protein level up to $126.5 \pm 13.6\%$ ($p < 0.05$) (**Figure 4.4C**). Thus, in contrast to P5, P5-Best, and P5-H6A, the upregulation of the LDLR protein level and activity induced by P5-S7A was not through SREBP-2 pathway activation. Notably, P3 (YDFYPSSTKDQQS), a peptide from lupin protein that inhibits HMGCoAR activity, leads to an increase in the LDLR protein levels without SREBP-2 activation but through the compensatory upregulation of the SREBP-1 (Lammi, Zanoni, Arnoldi, & Aiello, 2019). Therefore, it was hypothesized that P5-S7A could possess the same effect as P3 on LDLR protein production through the regulation of the SREBP-1 pathway. However, unlike P5, P5-Best, P5-H6A, and P5-S7A decreased the HMGCoAR levels up to $86.5 \pm 22.8\%$ ($p < 0.05$), $94.1 \pm 12.2\%$, and $71.6 \pm 15.5\%$ ($p < 0.01$), respectively (**Figure 4.4D**), indicating that the P5 analogs were more active as HMGCoAR inhibitors than P5. Interestingly, P5-Best, P5-H6A, and P5-S7A which are about two-fold more potent than P5 as both HMGCoAR and PCSK9/LDLR PPI inhibitors, respectively, are also more efficient in the reduction of the HMGCoAR protein levels with a direct effect in the intracellular cholesterol homeostasis. Indeed, overall P5-Best and P5-S7A can improve the functional ability of hepatic cells to absorb extracellular LDL (**Figure 4.4D**).

4.3.6 P5 Analogs Modulate the Hepatic PCSK9 Pathway

Figure 4.5 shows that P5-Best, P5-H6A, and P5-S7A decreased the PCSK9 protein levels by $21.8 \pm 11.8\%$, $28.2 \pm 17.5\%$, and $25.8 \pm 17.9\%$, respectively ($p < 0.05$) (**Figure 4.5A**). Moreover, also the HNF-1 α protein levels were decreased by $1.2 \pm 15.4\%$, $10.3 \pm 2.4\%$ ($p < 0.05$), and $18.7 \pm 7.6\%$ ($p < 0.01$) (**Figure 4.5B**), respectively.

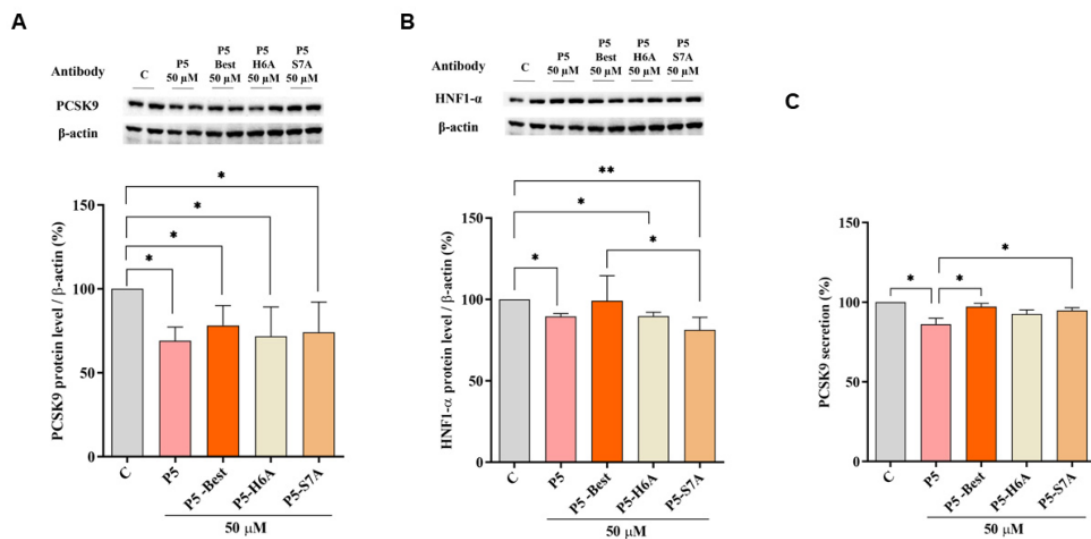


Figure 4.5 Modulation of the PCSK9 pathway in HepG2 cells. (A) Effects on the PCSK9 protein levels, (B) effects on the HNF1- α protein level, and (C) effects on mature PCSK9 secretion. Data points represent the average \pm SD of six independent experiments performed in duplicate. C vs. P5 and P5 analog samples were analyzed using a one-way ANOVA, followed by Tukey's test; (*) $p < 0.05$ and (**) $p < 0.001$. C: control sample.

Although the ability to reduce the secretion of mature PCSK9 was weaker than that of P5, P5-Best, P5-H6A, and P5-S7A could also induce a slight reduction by $2.7 \pm 1.9\%$, $7.4 \pm 2.6\%$, and $5.1 \pm 1.7\%$, respectively (**Figure 4.5C**). These results agree with the behavior of another naturally peptide from soybean β -Conglycinin (Macchi, Greco, Ferri, Magni, Arnoldi, Corsini, et al., 2022). In particular, YVVNPDNNEN peptide (at 250 μ M) reduces the PCSK9 protein level and its secretion via the modulation of HNF-1 α (Macchi, et al., 2022). Our results suggest that lupin P5 and its new analogs, being active at 50 μ M in the hepatic cells, are 5-fold more potent than

YVVNPDNNEN. In addition, it was also demonstrated that YVVNPDNNEN it is not a dual inhibitor peptide since being able to inhibit the HMG-CoAR activity (Lammi, Zanoni, Arnoldi, & Vistoli, 2015) but not the PPI between PCSK9 and the LDLR (Macchi, et al., 2022).

4.3.7 P5 Analogs Increase the Expression of LDLR Localized in the Cellular Membranes and Modulate LDL Uptake in HepG2 Cells

In accordance with the above results, P5-Best, P5-H6A, and P5-S7A increased the LDLR levels localized in the cellular membranes of HepG2 cells by $156.3 \pm 12.1\%$, $158.9 \pm 12.0\%$ ($p < 0.001$), and $140.2 \pm 15.1\%$ ($p < 0.01$) at $50 \mu\text{M}$, respectively (**Figure 4.6A**). Experiments were also performed in parallel, with P5 as the reference compound, which increased the membrane LDLR protein levels by $153.6 \pm 16.4\%$ ($p < 0.001$) at the same concentration of $50 \mu\text{M}$. Consequently, the functional capability of HepG2 cells to uptake extracellular LDL after treatments with P5, P5-Best, P5-H6A, and P5-S7A was observed, leading to an increased ability of $203.8 \pm 40.67\%$ ($p < 0.01$), $254.3 \pm 16.4\%$ ($p < 0.0001$), $229.8 \pm 27.9\%$ ($p < 0.001$), and $211.1 \pm 40.1\%$ ($p < 0.01$), respectively (**Figur 4.6B**).

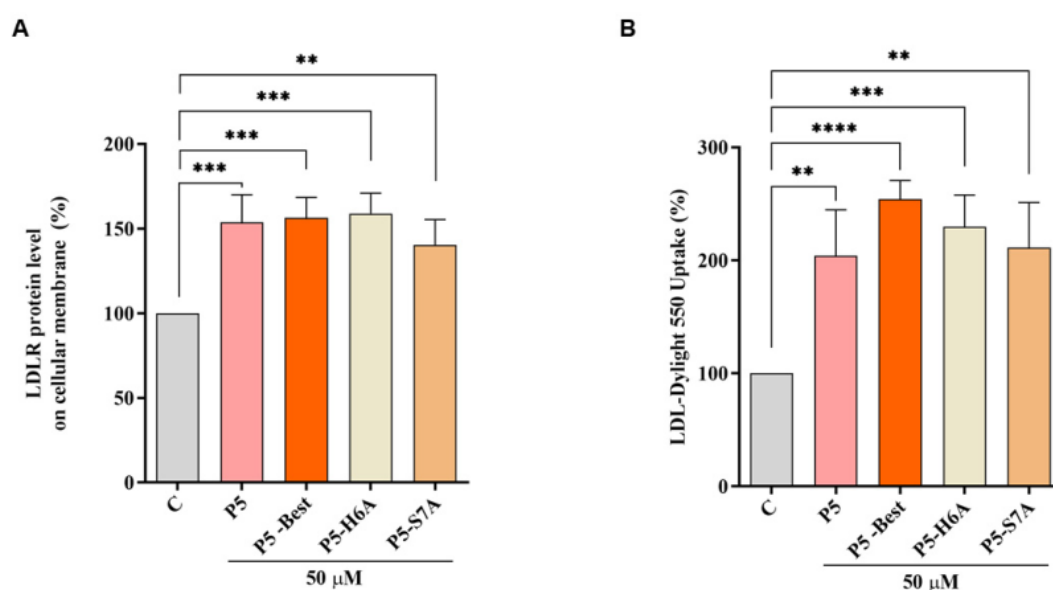


Figure 4.6 Modulation of the LDLR pathway in HepG2 cells. (A) The effect on the LDLR

localized on the surface of HepG2 cells after the treatment of HepG2 cells with P5 and P5 analogs, respectively. (B) Enhancement of the functional ability of HepG2 cells to uptake LDL from the extracellular environment. Data points represent the average \pm SD of four independent experiments performed in duplicate. C vs. P5, and P5 analog samples were analyzed using one-way ANOVA, followed by Tukey's test; (**) $p < 0.01$, (***) $p < 0.001$, and (****) $p < 0.0001$. C: control sample.

4.3.8 Docking of P5-S7A and MD Simulations on HMG-CoAR

The experimental assays on the purchased peptides highlighted the improvement in the dual inhibitory activity of the P5 mutant peptides. Specifically, P5-S7A showed the lowest IC_{50} value for HMG-CoAR. Thus, docking and MD simulations were conducted to acquire atomistic details on the putative binding mode of P5-S7A in complex with HMG-CoAR. This study can pave the way for the design of more dual-active peptides. P5-S7A was docked to the statin binding site of HMG-CoAR using Glide (see the Experimental Section for details), and the best docking pose (gscore = -9.881 kcal/mol) was selected for further 500 ns-long MD simulations in explicit water solvent (see **Figure 4-S4** in the Supporting Information for the RMSD plots). As the enzyme was in the dimeric state, the statin present in the other binding sites was not deleted (see the Experimental Section for details) to preserve the overall folding of the simulating system. At the end of the MD simulations, the root mean square deviation (RMSD) of the peptide was analyzed, and the peptide conformations sampled during the MD production run were clustered using the average-linkage method, which was previously prescribed for the PCSK9/peptide complexes. The results showed that only one cluster was mainly populated, representing 73.1% of the peptide conformations. The structure representative of this cluster is depicted in **Figure 4.7**.

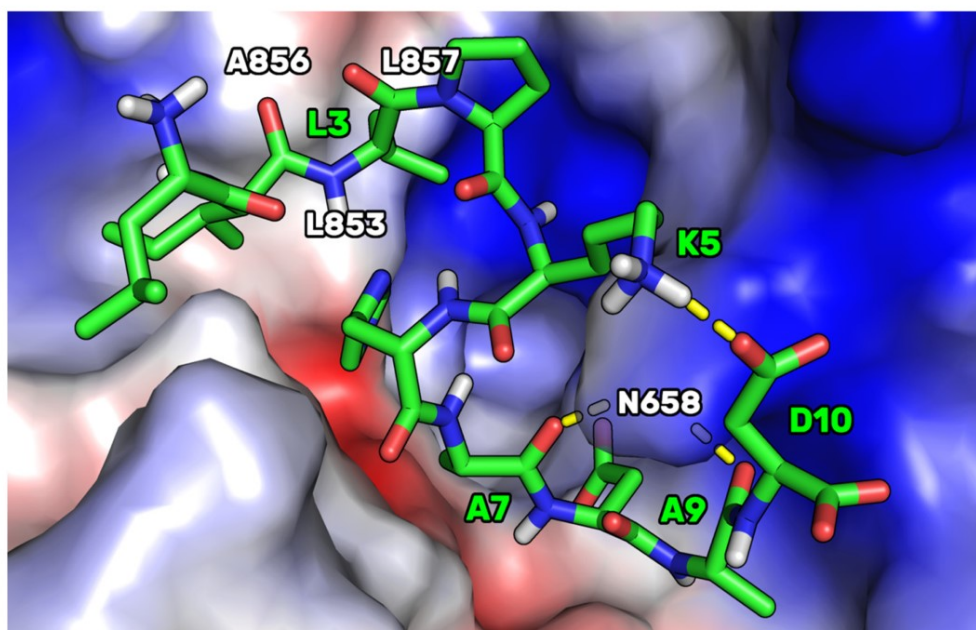


Figure 4.7 The representative structure of the most populated cluster of P5-S7A (green sticks) bound to HMG-CoAR (electrostatic surface). The small hydrophobic pocket (Leu853, Ala856, and Leu857) interacting with P5-S7A-Leu3 is highlighted. The H-bonds are represented by yellow dashed lines. Only polar hydrogens are shown in the figure.

This HMGC_oAR/P5-S7A complex showed the presence of a H-bond network between the P5-S7A-Ala7 and -Ala9 backbone atoms, with a side chain of HMGC_oAR-Asn658. P5-S7A-Leu3 projected its side chain in a small hydrophobic pocket sized by HMGC_oAR-Leu853, -Ala856, and -Leu857. Interestingly, the presence of an intramolecular H-bond between the side chains of P5-S7A-Lys5 and -Asp10 improved the overall peptide conformational stability. Moreover, the supposed binding mode of P5-S7A was consistent with the binding affinity data, indicating that the IC₅₀ of P5-H6A on HMGC_oAR was close to that of P5-S7A. Both residues could point their side chains to an effectively empty pocket sized by HMGC_oAR-Leu853, -Ala856, and -Leu857, which did not create any interactions with the HMGC_oAR counterpart. Thus, the substitution of positions 6 and 7 with alanine did not elicit any strong variation in the experimental binding affinity. This hypothesis paves the way for the design of new P5 analogs in which positions 6 and 7 can be mutated by unnatural amino acids capable of creating stronger interactions with HMGC_oAR.

The binding mode supposed for P5-S7A was then compared to the one of P5 in complex with HMGCoAR, to understand the possible reasons on the base of the improved binding affinity displayed by the mutant peptide. In our previous article (Lammi, Zanoni, Aiello, Arnoldi, & Grazioso, 2016) we have reported on the results of docking calculations of P5. Here, performing MD simulations starting from the P5 docking pose (see **Figure 4-S5** in the Supporting Information for the RMSD plots), we noted that, in the complex conformation representative of the most populated cluster (70%), P5 adopted a binding mode in which the side chain of P5-S7 created two intramolecular H-bonds with the NH groups of P5-A9 and P5-D10 (**Figure 4.8**). In the mutant peptide P5-S7A, these internal bonds cannot be created for the absence of the OH group in position 7. This, in our opinion, led to a peptide endowed with an increased conformational freedom, leaving the C-terminal residues to adopt a cyclic conformation in which an internal salt bridge can be shaped between the side chains of P5-K5 and P5-D10. This conformation could be more prone to create remodeled and ameliorated interactions with the enzyme.

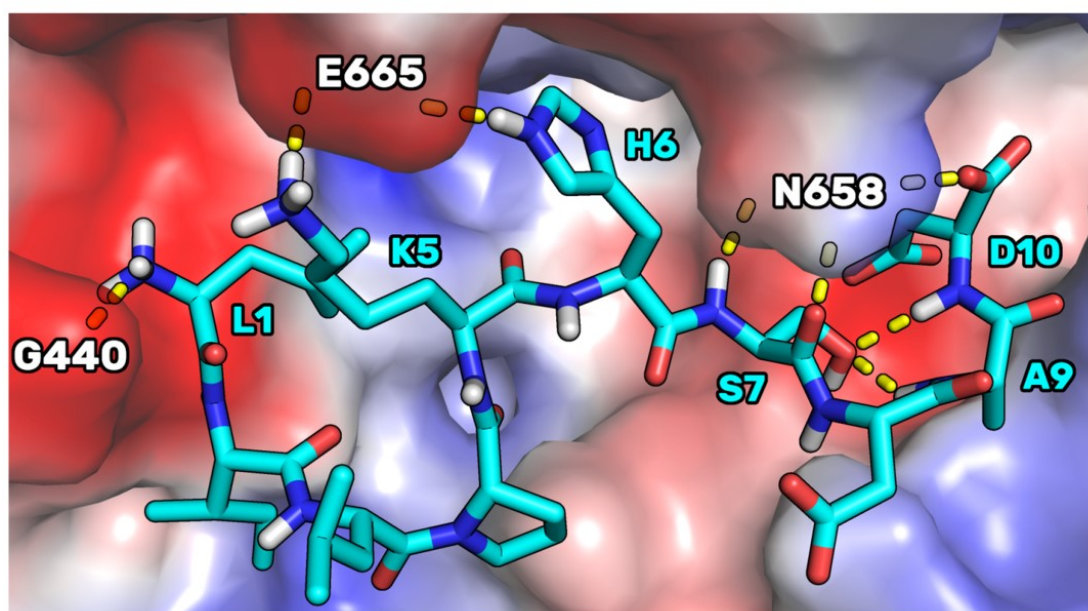


Figure 4.8 The representative structure of the most populated cluster of P5 (cyan sticks) bound to HMG-CoAR (electrostatic surface). H-bonds are represented by yellow dashed lines. Only polar hydrogens are shown in the figure.

ly, the binding mode supposed for P5-S7A was also compared to that of atorvastatin in complex with HMGCoAR (as reported in the PDB, accession code 1HWK (Istvan & Deisenhofer, 2001)). The structural alignment of both complexes (**Figure 4.9**) permitted to us suppose that the first four residues of P5-S7A essentially reproduce the contact played by the three aromatic substituents of the atorvastatin pyrrole ring. In particular, the aniline is mimicked by the P5-S7A-Ile2 side chain, the P5-S7A-Leu3 was overlapped to the phenyl ring of the statin, and the p-F-phenyl ring of atorvastatin was spatially close to the P5-S7A-Pro4 (**Figure 4.9**). Unfortunately, the remaining moiety of the peptide pointed to an enzyme area different from the one in which the 3,5-dihydroxyl-heptanoic acid moiety was bound in the HMGCoAR/atorvastatin complex. This portion is considered essential for the biological activity of the statins and could explain the reason on the base of the low affinity displayed by the mutant peptide. More efforts should be made to design peptides capable of mimicking such interactions and occupying the HMGCoAR pocket sized by Lys735, Ser684, Arg590, Lys 691, Asn755, and Glu559 residues (**Figure 4.9B**)

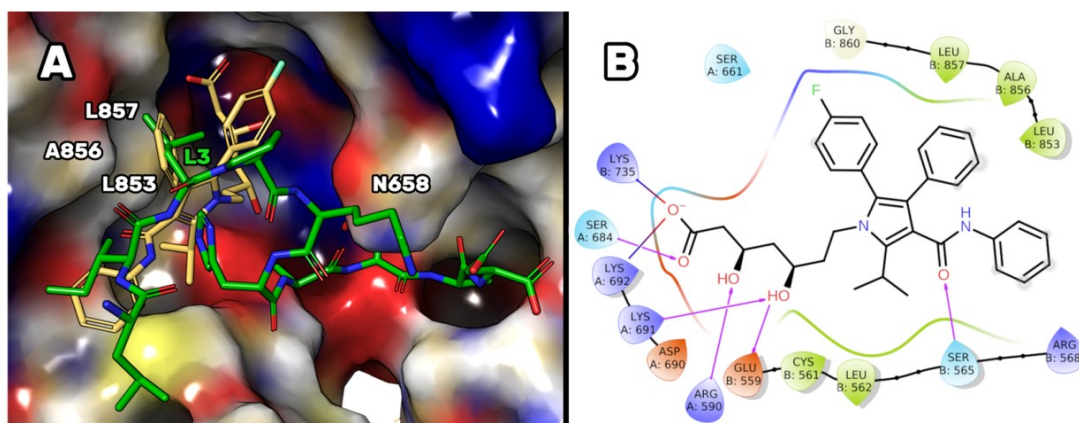


Figure 4.9 (A) Crystallographic pose of atorvastatin (yellow sticks), as was found in the X-ray structure available in the PDB (accession code 1HWK (Istvan & Deisenhofer, 2001)), superimposed on the representative structure of the most populated cluster of P5-S7A (green sticks) in complex with HMG-CoAR. (B) 2D representation of the protein-ligand contacts displayed by atorvastatin (cutoff = 3.00 Å) in complex with HMGCoA, as in the X-ray structure. H-bonds are highlighted by purple arrows and the hydrophobic residues involved in the protein-

ligand interactions are colored in green.

4.4 Conclusions

In this study, using promising data on the dual hypocholesterolemic activity of the lupin peptide P5, we computationally designed new analogs endowed with improved PCSK9 and HMGCoAR inhibitory activities. After the computational alanine-scanning mutational analysis, the non-hotspot residue of P5 was suitably substituted with other amino acids capable of improving the complementarity between PCSK9 and the peptide. Therefore, using our “affinity maturation protocol”, we selected P5-Best, P5-H6A, and P5-S7A peptides for the experimental assays. The attained experimental data confirmed the theoretical studies, revealing that the affinity of the mutant P5-H6A peptide on PCSK9 was reduced almost seven times ($IC_{50} = 9.0 \mu\text{M}$), whereas the affinity of P5-S7A was slightly higher than that of P5 ($IC_{50} = 1.45 \mu\text{M}$). Remarkably, the mutant peptide P5-Best showed the lowest PCSK9 IC_{50} value of $0.7 \mu\text{M}$. Further biological assays demonstrated that all mutant peptides that maintained the dual PCSK9/HMGCoAR inhibitory activity improved the ability of HepG2 cells to absorb extracellular LDL by up to 254% (P5-Best data). Doubtless, peptide P5 and its analogs display activity in the micromolar range suggesting that still their exploitation in the clinical application is challenging. Therefore, more efforts have to be pursued in order to improve their dual-inhibitory activity. However, evidences support the fact that P5 and its analogs can be considered as promising lead compounds for the development of a new class of hypocholesterolemic drugs endowed with dual-inhibitory activity of both PCSK9 and HMGCoAR targets. Indeed, the dual and synergistic activity may be useful for better achieving the biological effect than compound actives on one of those targets.

Further experiments will be performed to evaluate the intestinal stability and propensity of P5 analogs to be trans-epithelial transported by mature Caco-2 cells. Experiments will be performed using the parent peptide P5 and the natural intestinal metabolite P5-met as positive controls. This study confirms that a multidisciplinary

approach in the design of new peptides is successful in identifying peptides endowed with hypocholesterolemic effects, offering a promising starting point for the design of peptidomimetics that lack the bioavailability problems of peptides.

4.5 Supporting information

Table 4-S1 Percentage of population of P5-S7A clusters identified by means of average-linkage method implemented in AmberTools20.

P5-S7A Peptide population	
Cluster number	%
1	73.1
2	11.7
3	5.7
4	3.4
5	2.2
6	1.6
7	1.1
8	0.9
9	0.1
10	0.1

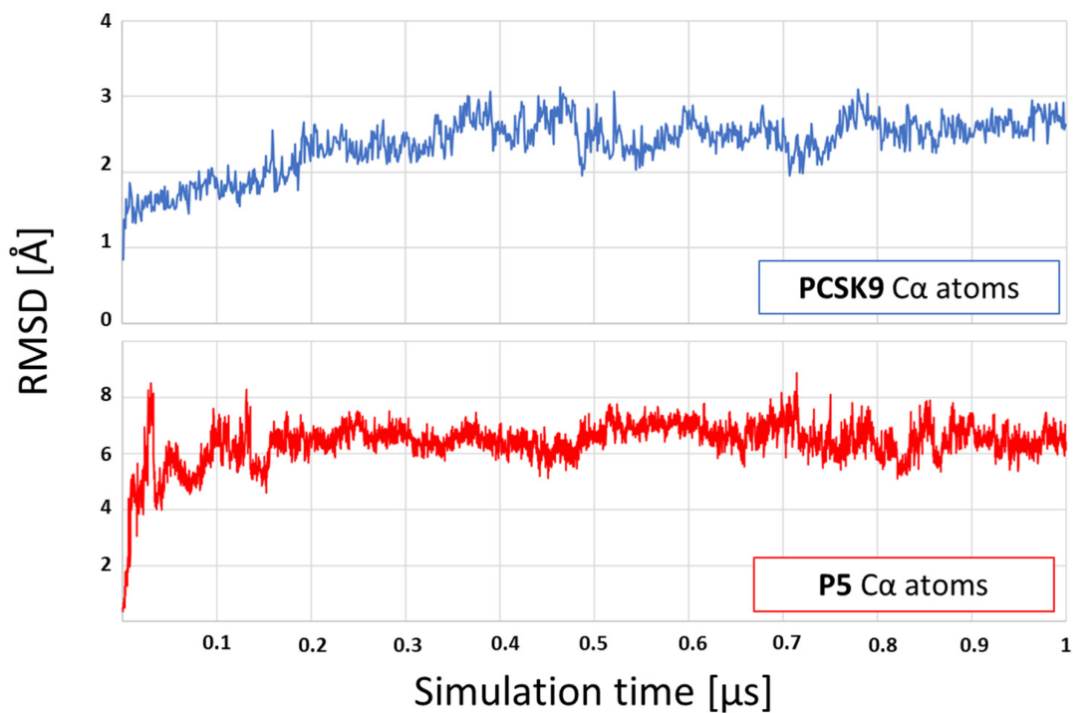


Figure 4-S1 RMSD (Å) over simulation time of the complex PCSK9/P5 Cα atoms aligned on the

equilibrated structure of PCSK9.

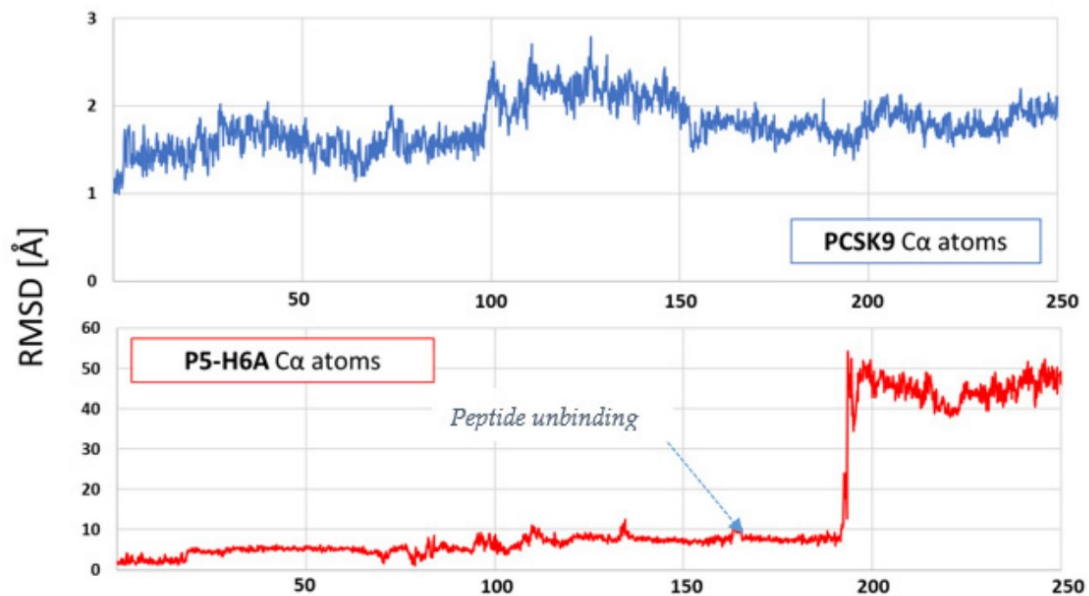


Figure 4-S2 RMSD (Å) over simulation time of the complex PCSK9/P5-H6A Cα atoms aligned on the equilibrated structure of PCSK9.

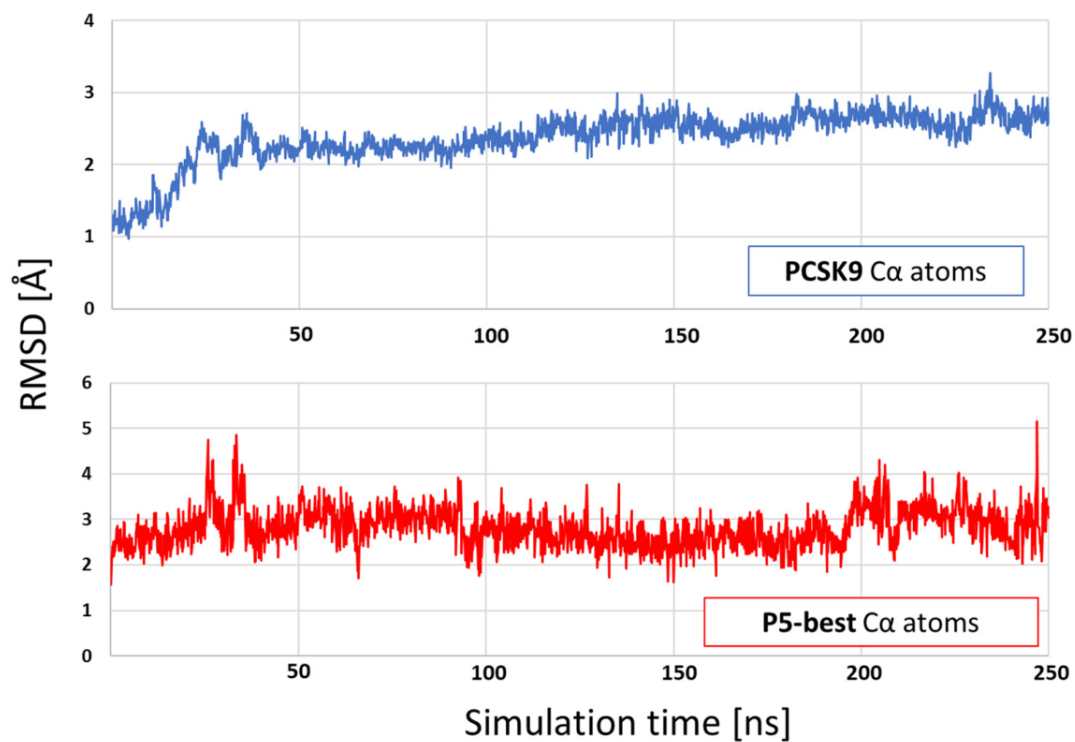


Figure 4-S3 RMSD (Å) over simulation time of the complex PCSK9/P5-best C α atoms aligned on the equilibrated structure of PCSK9.

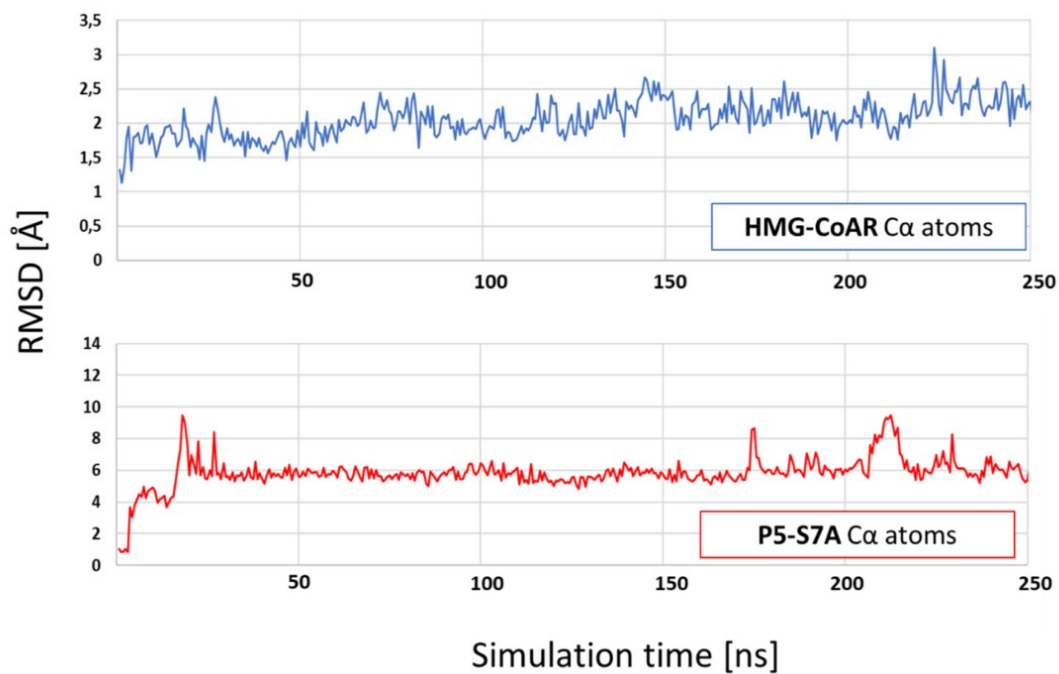


Figure 4-S4 RMSD (Å) over simulation time of the complex HMG-CoAR/P5-S7A C α atoms aligned on the equilibrated structure of HMG-CoAR.

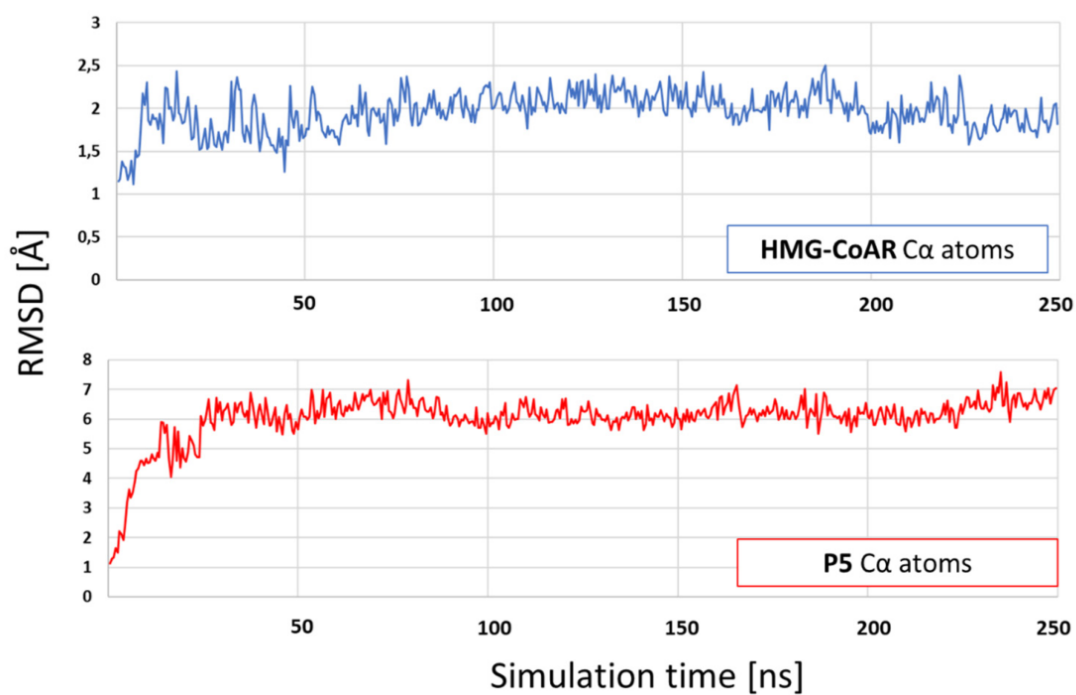


Figure 4-S5 RMSD (Å) over simulation time of the complex HMG-CoAR/P5 C α atoms aligned on the equilibrated structure of HMG-CoAR.

Materials and Methods

Chemicals. Dulbecco's modified Eagle's medium (DMEM), stable L-glutamine, fetal bovine serum (FBS), phosphate buffered saline (PBS), penicillin/streptomycin, chemiluminescent reagent, and 96-well plates were purchased from Euroclone (Milan, Italy). The HMGCoAR assay kit, bovine serum albumin (BSA), Janus Green B, formaldehyde, HCl and H₂SO₄ were from Sigma-Aldrich (St. Louis, MO, USA). The antibody against LDLR and the 3, 3',5, 5'-tetramethylbenzidine (TMB) substrate were bought from Thermo Fisher Scientific (Waltham, MA, USA). The Quantikine ELISA kit was bought from R&D Systems (Minneapolis, MN, USA). The LDL-DyLight TM 550 was from Cayman Chemical (Ann Arbor, MI, USA). The CircuLex PCSK9 *in vitro* binding Assay Kit was from CircuLex (Cy-cLex Co., Nagano, Japan). The peptides (P5, P5-Best, P-H6A, and P5-S7A) were synthesized by the company GeneScript (Piscataway, NJ, USA) at >95% purity. The antibody against HMG-CoAR was bought from Abcam (Cambridge, UK). Phenylmethanesulfonyl fluoride (PMSF), Na-orthovanadate inhibitors, and the antibodies against rabbit Ig-horse-radish peroxidase (HRP), mouse Ig-HRP, and SREBP-2 (which recognizes epitope located in a region between 833–1141 and bands at about 132 kDa) were purchased from Santa Cruz Biotechnology Inc. (Santa Cruz, CA, USA). The antibodies against hepatocyte nuclear factor 1-alpha (HNF1-alpha) and PCSK9 were bought from GeneTex (Irvine, CA, USA). The inhibitor cocktail Complete Midi was from Roche (Basel, Switzerland). Mini protean TGX pre-cast gel 7.5% and Mini nitrocellulose Transfer Packs were purchased from BioRad (Hercules, CA, USA).

HepG2 Cell Culture Conditions and Treatment. The HepG2 cell line was bought from ATCC (HB-8065, ATCC from LGC Standards, Milan, Italy) and was cultured in DMEM high glucose with stable L-glutamine, supplemented with 10% FBS, 100 U/ml penicillin, 100 µg/ml streptomycin (complete growth medium) with incubation at 37 °C under 5% CO₂ atmosphere.

HMGCoAR Aactivity Assay. The experiments were carried out following the manufacturer instructions and optimized protocol (Aiello, Lammi, Boschin, Zanoni, & Arnoldi, 2017). The assay buffer, NADPH, substrate solution, and HMG-CoAR were provided in the HMG-CoAR Assay Kit (Sigma Aldrich SRL, Milan, Italy). The experiments were carried out following the manufacturer instructions at 37 °C. In particular, each reaction (200 µL) was prepared adding the reagents in the following order: 1 X assay buffer, a 10–500 µM doses of P5 and P5 analogs or vehicle (C), the NADPH (4 µL), the substrate solution (12 µL), and finally the HMGCoAR (catalytic domain) (2 µL). Subsequently, the samples were mixed and the absorbance at 340 nm read by the microplate reader Synergy H1 (Winooski, VT, USA) at time 0 and 10 min. The HMG-CoAR-dependent oxidation of NADPH and the inhibition properties of peptides were measured by absorbance reduction, which is directly proportional to enzyme activity.

***In Vitro* PCSK9-LDLR Binding Assay.** Peptides P5 and P5 analogs (0.1–100 µM) were tested using the *in vitro* PCSK9-LDLR binding assay (CycLex Co., Nagano, Japan) following the manufacture instructions and conditions already optimized (Lammi, Zanoni, Aiello, Arnoldi, & Grazioso, 2016). Briefly, plates are pre-coated with a recombinant LDLR-AB domain containing the binding site of PCSK9. Before starting the assay, tested peptides and/or the vehicle were diluted in the reaction buffer and added in microcentrifuge tubes. Afterwards, the reaction mixtures were added in each well of the microplate and the reaction was started by adding His-tagged PCSK9 solution (3 µL). The microplate was allowed to incubate for 2 h at room temperature (RT) shaking at 300 rpm on an orbital microplate shaker. Subsequently, wells were washed 4 times with the wash buffer. After the last wash, the biotinylated anti-His-tag monoclonal antibody (100 µL) was added and incubated at RT for 1 h shaking at 300 rpm. After incubation, wells were washed for 4 times with wash buffer. After the last wash, 100 µL of HRP-conjugated streptavidin were added and the plate was incubated for 20 min at RT. After incubation, wells were washed 4 times with wash buffer. Finally, the substrate reagent (tetra-methylbenzidine) was added, and the plate was incubated for 10 min at RT shaking at ca. 300 rpm. The reaction was stopped with 2.0

M sulfuric acid and the absorbance at 450nm was measured using the Synergy H1 fluorescent plate reader (Winooski, VT, USA).

In-Cell Western (ICW) Assay. For the experiments, a total of 3×10^4 HepG2 cells/well were seeded in 96-well plates. The following day, cells were washed with PBS and then starved overnight (O/N) in DMEM without FBS and antibiotics. After starvation, HepG2 cells were treated with 4.0 $\mu\text{g/mL}$ PCSK9-WT and 4.0 $\mu\text{g/mL}$ PCSK9 + peptides P5 and/or P5 analogs (50.0 μM) and vehicle (H_2O) for 2 h at 37 °C under 5% CO_2 atmosphere. Subsequently, they were fixed in 4% paraformaldehyde for 20 min at room temperature (RT). Cells were washed 5 times with 100 μL of PBS/well (each wash was for 5 min at RT) and the endogenous peroxides activity quenched adding 3% H_2O_2 for 20 min at RT. Non-specific sites were blocked with 100 μL /well of 5% bovine serum albumin (BSA, Sigma) in PBS for 1.5 h at RT. LDLR primary antibody solution (1:3000 in 5% BSA in PBS, 25 μL /well) was incubated O/N at +4 °C. Subsequently, the primary antibody solution was discarded and each sample was washed 5 times with 100 μL /well of PBS (each wash was for 5 min at RT). Goat anti-rabbit Ig-HRP secondary antibody solution (Santa Cruz) (1:6000 in 5% BSA in PBS, 50 μL /well), was added and incubated 1 h at RT. The secondary antibody solution was washed 5 times with 100 μL /well of PBS (each wash for 5 min at RT). Freshly prepared TMB substrate (Pierce, 100 μL /well) was added and the plate was incubated at RT until desired color was developed. The reaction was stopped with 2 M H_2SO_4 and then the absorbance at 450 nm was measured using the microplate reader Synergy H1 (Winooski, VT, USA). After the read, cells were stained by adding 1 \times Janus Green stain, incubating for 5 min at RT. The dye was removed, and the sample washed 5 times with water. Afterward 100 μL 0.5 M HCl for well were added and incubated for 10 min. After 10 seconds shaking, the OD at 595 nm was measured using the microplate reader Synergy H1 (Winooski, VT, USA).

Fluorescent LDL Uptake. HepG2 cells (3×10^4 /well) were seeded in 96-well plates and kept in complete growth medium for 2 days before treatment. The third day, cells were washed with PBS and then starved overnight (O/N) in DMEM without FBS and antibiotics. After starvation, they were treated with 4.0 $\mu\text{g/mL}$ PCSK9 and 4.0 $\mu\text{g/mL}$

PCSK9 + P5 and/or P5 analogs (50.0 μ M), and vehicle (H₂O) for 2 h with at 37 °C under 5% CO₂ atmosphere. At the end of the treatment, the culture medium was replaced with 50 μ L/well LDL-DyLight™ 550 working solution (Cayman Chemical Company, Ann Arbor, MI, USA) prepared in DMEM without FBS and antibiotics. The cells were additionally incubated for 2 h at 37 °C and then the culture medium was aspirated and replaced with PBS (100 μ L/well). The degree of LDL uptake was measured using the Synergy H1 fluorescent plate reader (Winooski, VT, USA) (excitation and emission wavelengths 540 and 570 nm, respectively). Fluorescent LDL-uptake was finally assessed following optimized protocol (Zanoni, Aiello, Arnoldi, & Lammi, 2017).

Western Blot Analysis. Immunoblotting experiments were performed using optimized protocol (Zanoni, Aiello, Arnoldi, & Lammi, 2017). A total of 1.5×10^5 HepG2 cells/well (24-well plate) were treated with 50.0 μ M of P5 and P5 analogs for 24 h. After each treatment, the supernatants were collected and stored at -20 °C; cells were scraped in 40 μ L ice-cold lysis buffer (RIPA buffer + inhibitor cocktail + 1:100 PMSF + 1:100 Na-orthovanadate + 1:1000 β -mercaptoethanol) and transferred in ice-cold microcentrifuge tubes. After centrifugation at 13,300 g for 15 min at 4 °C, the supernatants were recovered and transferred into new ice-cold tubes. Total proteins were quantified by the Bradford's method and 50 μ g of total proteins loaded on a pre-cast 7.5% Sodium Dodecyl Sulfate-Polyacrylamide (SDS-PAGE) gel at 130 V for 45 min. Subsequently, the gel was pre-equilibrated in H₂O for 5 min at room temperature (RT) and transferred to a nitrocellulose membrane (Mini nitrocellulose Transfer Packs,) using a Trans-Blot Turbo at 1.3 A, 25 V for 7 min. Target proteins, on milk or BSA blocked membrane, were detected by primary antibodies as follows: anti-SREBP-2, anti-LDLR, anti-HMG-CoAR, anti-PCSK9, anti HNF-1 α and anti- β -actin. Secondary antibodies conjugated with HRP and a chemiluminescent reagent were used to visualize target proteins and their signal was quantified using the Image Lab Software (Biorad, Hercules, CA, USA). The internal control β -actin was used to normalize loading variations.

4.6 References

- Aiello, G., Lammi, C., Boschin, G., Zanoni, C., & Arnoldi, A. (2017). Exploration of Potentially Bioactive Peptides Generated from the Enzymatic Hydrolysis of Hempseed Proteins. *Journal of Agricultural and Food Chemistry*, 65(47), 10174-10184.
- Alvi, S. S., Ansari, I. A., Ahmad, M. K., Iqbal, J., & Khan, M. S. (2017). Lycopene amends LPS induced oxidative stress and hypertriglyceridemia via modulating PCSK-9 expression and Apo-CIII mediated lipoprotein lipase activity. *Biomedicine & Pharmacotherapy*, 96, 1082-1093.
- Burdick, D. J., Skelton, N. J., Ultsch, M., Beresini, M. H., Eigenbrot, C., Li, W., Zhang, Y., Nguyen, H., Kong-Beltran, M., Quinn, J. G., & Kirchhofer, D. (2020). Design of Organo-Peptides As Bipartite PCSK9 Antagonists. *ACS Chemical Biology*, 15(2), 425-436.
- Case, D. A., Aktulga, H. M., Belfon, K., Ben-Shalom, I., Brozell, S. R., Cerutti, D. S., Cheatham III, T. E., Cruzeiro, V. W. D., Darden, T. A., & Duke, R. E. (2021). *Amber 2021*: University of California, San Francisco.
- Dong, B., Singh, A. B., Shende, V. R., & Liu, J. (2017). Hepatic HNF1 transcription factors control the induction of PCSK9 mediated by rosuvastatin in normolipidemic hamsters. *Int J Mol Med*, 39(3), 749-756.
- Drucker, D. J. (2020). Advances in oral peptide therapeutics. *Nature Reviews Drug Discovery*, 19(4), 277-289.
- Dyrbuś, K., Gaśior, M., Penson, P., Ray, K. K., & Banach, M. J. J. o. C. L. (2020). Inclisiran—new hope in the management of lipid disorders? , 14(1), 16-27.
- Friesner, R. A., Murphy, R. B., Repasky, M. P., Frye, L. L., Greenwood, J. R., Halgren, T. A., Sanschagrin, P. C., & Mainz, D. T. (2006). Extra Precision Glide: Docking and Scoring Incorporating a Model of Hydrophobic Enclosure for Protein–Ligand Complexes. *Journal of Medicinal Chemistry*, 49(21), 6177-6196.
- Goldstein, J. L., & Brown, M. S. (1990). Regulation of the mevalonate pathway. *Nature*, 343(6257), 425-430.
- Grazioso, G., Bollati, C., Sgrignani, J., Arnoldi, A., & Lammi, C. (2018). First Food-Derived Peptide Inhibitor of the Protein–Protein Interaction between Gain-of-Function PCSK9D374Y and the

- Low-Density Lipoprotein Receptor. *Journal of Agricultural and Food Chemistry*, 66(40), 10552-10557.
- Homeyer, N., Stoll, F., Hillisch, A., & Gohlke, H. (2014). Binding Free Energy Calculations for Lead Optimization: Assessment of Their Accuracy in an Industrial Drug Design Context. *Journal of Chemical Theory and Computation*, 10(8), 3331-3344.
- Humphrey, W., Dalke, A., & Schulten, K. (1996). VMD: Visual molecular dynamics. *Journal of Molecular Graphics*, 14(1), 33-38.
- Istvan, E. S., & Deisenhofer, J. (2001). Structural Mechanism for Statin Inhibition of HMG-CoA Reductase. *Science*, 292(5519), 1160-1164.
- Kirchhofer, D., Burdick, D. J., Skelton, N. J., Zhang, Y., & Ultsch, M. (2020). Regions of conformational flexibility in the proprotein convertase PCSK9 and design of antagonists for LDL cholesterol lowering. *Biochemical Society Transactions*, 48(4), 1323-1336.
- Kwon, H. J., Lagace, T. A., McNutt, M. C., Horton, J. D., & Deisenhofer, J. (2008). Molecular basis for LDL receptor recognition by PCSK9. *Proceedings of the National Academy of Sciences*, 105(6), 1820-1825.
- Lammi, C., Aiello, G., Bollati, C., Li, J., Bartolomei, M., Ranaldi, G., Ferruzza, S., Fassi, E. M., Grazioso, G., Sambuy, Y., & Arnoldi, A. (2021). Trans-Epithelial Transport, Metabolism, and Biological Activity Assessment of the Multi-Target Lupin Peptide LILPKHSDAD (P5) and Its Metabolite LPKHSDAD (P5-Met). In *Nutrients*, vol. 13).
- Lammi, C., Aiello, G., Dellaflora, L., Bollati, C., Boschini, G., Ranaldi, G., Ferruzza, S., Sambuy, Y., Galaverna, G., & Arnoldi, A. (2020). Assessment of the Multifunctional Behavior of Lupin Peptide P7 and Its Metabolite Using an Integrated Strategy. *Journal of Agricultural and Food Chemistry*, 68(46), 13179-13188.
- Lammi, C., Aiello, G., Vistoli, G., Zannoni, C., Arnoldi, A., Sambuy, Y., Ferruzza, S., & Ranaldi, G. (2016). A multidisciplinary investigation on the bioavailability and activity of peptides from lupin protein. *Journal of Functional Foods*, 24, 297-306.
- Lammi, C., Bellumori, M., Cecchi, L., Bartolomei, M., Bollati, C., Clodoveo, M. L., Corbo, F., Arnoldi, A., & Mulinacci, N. (2020). Extra Virgin Olive Oil Phenol Extracts Exert Hypocholesterolemic Effects through the Modulation of the LDLR Pathway: *In Vitro* and Cellular Mechanism of Action Elucidation. In *Nutrients*, vol. 12).

- Lammi, C., Sgrignani, J., Arnoldi, A., & Grazioso, G. (2019). Biological Characterization of Computationally Designed Analogs of peptide TVFTSWEEYLDWV (Pep2-8) with Increased PCSK9 Antagonistic Activity. *Scientific Reports*, 9(1), 2343.
- Lammi, C., Sgrignani, J., Arnoldi, A., Lesma, G., Spatti, C., Silvani, A., & Grazioso, G. (2019). Computationally Driven Structure Optimization, Synthesis, and Biological Evaluation of Imidazole-Based Proprotein Convertase Subtilisin/Kexin 9 (PCSK9) Inhibitors. *Journal of Medicinal Chemistry*, 62(13), 6163-6174.
- Lammi, C., Sgrignani, J., Roda, G., Arnoldi, A., & Grazioso, G. (2019). Inhibition of PCSK9D374Y/LDLR Protein-Protein Interaction by Computationally Designed T9 Lupin Peptide. *ACS Medicinal Chemistry Letters*, 10(4), 425-430.
- Lammi, C., Zanoni, C., Aiello, G., Arnoldi, A., & Grazioso, G. (2016). Lupin Peptides Modulate the Protein-Protein Interaction of PCSK9 with the Low Density Lipoprotein Receptor in HepG2 Cells. *Scientific Reports*, 6(1), 29931.
- Lammi, C., Zanoni, C., & Arnoldi, A. (2015). A simple and high-throughput in-cell Western assay using HepG2 cell line for investigating the potential hypocholesterolemic effects of food components and nutraceuticals. *Food Chemistry*, 169, 59-64.
- Lammi, C., Zanoni, C., Arnoldi, A., & Aiello, G. (2019). YDFYPSSTKDQQS (P3), a peptide from lupin protein, absorbed by Caco-2 cells, modulates cholesterol metabolism in HepG2 cells via SREBP-1 activation. *Journal of Food Biochemistry*, 43(1), e12757.
- Lammi, C., Zanoni, C., Arnoldi, A., & Vistoli, G. (2015). Two Peptides from Soy β -Conglycinin Induce a Hypocholesterolemic Effect in HepG2 Cells by a Statin-Like Mechanism: Comparative *in Vitro* and *in Silico* Modeling Studies. *Journal of Agricultural and Food Chemistry*, 63(36), 7945-7951.
- Lammi, C., Zanoni, C., Ferruzza, S., Ranaldi, G., Sambuy, Y., & Arnoldi, A. (2016). Hypocholesterolaemic Activity of Lupin Peptides: Investigation on the Crosstalk between Human Enterocytes and Hepatocytes Using a Co-Culture System Including Caco-2 and HepG2 Cells. In *Nutrients*, vol. 8).
- Lammi, C., Zanoni, C., Scigliuolo, G. M., D'Amato, A., & Arnoldi, A. (2014). Lupin Peptides Lower Low-Density Lipoprotein (LDL) Cholesterol through an Up-regulation of the LDL

- Receptor/Sterol Regulatory Element Binding Protein 2 (SREBP2) Pathway at HepG2 Cell Line. *Journal of Agricultural and Food Chemistry*, 62(29), 7151-7159.
- Londregan, A. T., Wei, L., Xiao, J., Lintner, N. G., Petersen, D., Dullea, R. G., McClure, K. F., Bolt, M. W., Warmus, J. S., Coffey, S. B., Limberakis, C., Genovino, J., Thuma, B. A., Hesp, K. D., Aspnes, G. E., Reidich, B., Salatto, C. T., Chabot, J. R., Cate, J. H. D., Liras, S., & Piotrowski, D. W. (2018). Small Molecule Proprotein Convertase Subtilisin/Kexin Type 9 (PCSK9) Inhibitors: Hit to Lead Optimization of Systemic Agents. *Journal of Medicinal Chemistry*, 61(13), 5704-5718.
- Macchi, C., Greco, M. F., Ferri, N., Magni, P., Arnoldi, A., Corsini, A., Sirtori, C. R., Ruscica, M., & Lammi, C. (2022). Impact of Soy β -Conglycinin Peptides on PCSK9 Protein Expression in HepG2 Cells. In *Nutrients*, vol. 14).
- Maier, J. A., Martinez, C., Kasavajhala, K., Wickstrom, L., Hauser, K. E., & Simmerling, C. (2015). ff14SB: Improving the Accuracy of Protein Side Chain and Backbone Parameters from ff99SB. *Journal of Chemical Theory and Computation*, 11(8), 3696-3713.
- Mao, Y., & Zhang, Y. (2012). Thermal conductivity, shear viscosity and specific heat of rigid water models. *Chemical Physics Letters*, 542, 37-41.
- McTaggart, F., Buckett, L., Davidson, R., Holdgate, G., McCormick, A., Schneck, D., Smith, G., & Warwick, M. J. T. A. J. O. C. (2001). Preclinical and clinical pharmacology of Rosuvastatin, a new 3-hydroxy-3-methylglutaryl coenzyme A reductase inhibitor. *87(5)*, 28-32.
- Miller, B. R., III, McGee, T. D., Jr., Swails, J. M., Homeyer, N., Gohlke, H., & Roitberg, A. E. (2012). MMPBSA.py: An Efficient Program for End-State Free Energy Calculations. *Journal of Chemical Theory and Computation*, 8(9), 3314-3321.
- Moreira, I. S., Fernandes, P. A., & Ramos, M. J. (2007). Computational alanine scanning mutagenesis—An improved methodological approach. *Journal of Computational Chemistry*, 28(3), 644-654.
- Nelson, R. H. (2013). Hyperlipidemia as a Risk Factor for Cardiovascular Disease. *Primary Care: Clinics in Office Practice*, 40(1), 195-211.
- Odom, D. T., Zizlsperger, N., Gordon, D. B., Bell, G. W., Rinaldi, N. J., Murray, H. L., Volkert, T. L., Schreiber, J., Rolfe, P. A., Gifford, D. K., Fraenkel, E., Bell, G. I., & Young, R. A. (2004).

- Control of pancreas and liver gene expression by HNF transcription factors. *Science*, 303(5662), 1378-1381.
- Olsson, A. G., McTaggart, F., & Raza, A. (2002). Rosuvastatin: A Highly Effective New HMG-CoA Reductase Inhibitor. *Cardiovascular Drug Reviews*, 20(4), 303-328.
- Poirier, S., Mayer, G. J. D. d., development, & therapy. (2013). The biology of PCSK9 from the endoplasmic reticulum to lysosomes: new and emerging therapeutics to control low-density lipoprotein cholesterol. 1135-1148.
- Roe, D. R., & Cheatham, T. E., III. (2013). PTRAJ and CPPTRAJ: Software for Processing and Analysis of Molecular Dynamics Trajectory Data. *Journal of Chemical Theory and Computation*, 9(7), 3084-3095.
- Roos, K., Wu, C., Damm, W., Reboul, M., Stevenson, J. M., Lu, C., Dahlgren, M. K., Mondal, S., Chen, W., Wang, L., Abel, R., Friesner, R. A., & Harder, E. D. (2019). OPLS3e: Extending Force Field Coverage for Drug-Like Small Molecules. *Journal of Chemical Theory and Computation*, 15(3), 1863-1874.
- Salaheldin, T. A., Godugu, K., Bharali, D. J., Fujioka, K., Elshourbagy, N., & Mousa, S. A. (2022). Novel oral nano-hepatic targeted anti-PCSK9 in hypercholesterolemia. *Nanomedicine: Nanotechnology, Biology and Medicine*, 40, 102480.
- Sarver, R. W., Bills, E., Bolton, G., Bratton, L. D., Caspers, N. L., Dunbar, J. B., Harris, M. S., Hutchings, R. H., Kennedy, R. M., Larsen, S. D., Pavlovsky, A., Pfefferkorn, J. A., & Bainbridge, G. (2008). Thermodynamic and Structure Guided Design of Statin Based Inhibitors of 3-Hydroxy-3-Methylglutaryl Coenzyme A Reductase. *Journal of Medicinal Chemistry*, 51(13), 3804-3813.
- Seidah, N. G., Awan, Z., Chrétien, M., & Mbikay, M. (2014). PCSK9. *Circulation Research*, 114(6), 1022-1036.
- Stucchi, M., Cairati, S., Cetin-Atalay, R., Christodoulou, M. S., Grazioso, G., Pescitelli, G., Silvani, A., Yildirim, D. C., & Lesma, G. (2015). Application of the Ugi reaction with multiple amino acid-derived components: synthesis and conformational evaluation of piperazine-based minimalist peptidomimetics. *Organic & Biomolecular Chemistry*, 13(17), 4993-5005.
- Tombling, B. J., Lammi, C., Lawrence, N., Gilding, E. K., Grazioso, G., Craik, D. J., & Wang, C. K. (2021). Bioactive Cyclization Optimizes the Affinity of a Proprotein Convertase

- Subtilisin/Kexin Type 9 (PCSK9) Peptide Inhibitor. *Journal of Medicinal Chemistry*, 64(5), 2523-2533.
- Xia, X.-d., Peng, Z.-s., Gu, H.-m., Wang, M., Wang, G.-q., & Zhang, D.-w. (2021). Regulation of PCSK9 Expression and Function: Mechanisms and Therapeutic Implications. 8.
- Xie, H., Yang, K., Winston-McPherson, G. N., Stapleton, D. S., Keller, M. P., Attie, A. D., Smith, K. A., & Tang, W. (2020). From methylene bridged diindole to carbonyl linked benzimidazoleindole: Development of potent and metabolically stable PCSK9 modulators. *European Journal of Medicinal Chemistry*, 206, 112678.
- Xu, S., Luo, S., Zhu, Z., & Xu, J. (2019). Small molecules as inhibitors of PCSK9: Current status and future challenges. *European Journal of Medicinal Chemistry*, 162, 212-233.
- Zanoni, C., Aiello, G., Arnoldi, A., & Lammi, C. (2017). Investigations on the hypocholesterolaemic activity of LILPKHSDAD and LTFPGSAED, two peptides from lupin β -conglutin: Focus on LDLR and PCSK9 pathways. *Journal of Functional Foods*, 32, 1-8.
- Zhang, Y., Eigenbrot, C., Zhou, L., Shia, S., Li, W., Quan, C., Tom, J., Moran, P., Di Lello, P., & Skelton, N. J. J. J. o. B. C. (2014). Identification of a small peptide that inhibits PCSK9 protein binding to the low density lipoprotein receptor. 289(2), 942-955.

CHAPTER 5

MANUSCRIPT 3

INVESTIGATION OF THE INTESTINAL TRANS- EPITHELIAL TRANSPORT AND ANTIOXIDANT ACTIVITY OF TWO HEMPSEED PEPTIDES WVSPLAGRT (H2) AND IGFLIIWV (H3)

Carlotta Bollati^a, Ivan Cruz-Chamorro^{a,b}, Gilda Aiello^c, **Jianqiang Li^a**,
Martina Bartolomei^a, Guillermo Santos-Sánchez^{a,b}, Giulia Ranaldi^d,
Simonetta Ferruzza^d, Yula Sambuy^d, Anna Arnoldi^a, Carmen Lammi^{a,*}

^aDepartment of Pharmaceutical Sciences, University of Milan, 20122 Milan, Italy

^bDepartamento de Bioquímica Médica y Biología Molecular e Inmunología,
Universidad de Sevilla, 41009 Seville, Spain

^cDepartment of Human Science and Quality of Life Promotion, Telematic
University San Raffaele, 00166 Rome, Italy

^dCREA, Food and Nutrition Research Centre, Via Ardeatina, 546, 00178 Roma
RM, Italy

Author Contributions: Conceptualization, C.L.; formal analysis, C.B.; investigation, C.B., I.C.-C., G. A., J.L., M.B., G.S.-S. and S.F.; writing—original draft, C.L.; writing—review & editing, Y.S., A.A. and C.L.; supervision, C.L.; data curation, C.L.; funding acquisition, A.A.

5. Abstract

A preceding paper has shown that a hempseed peptic hydrolysate displays a cholesterol-lowering activity with a statin-like mechanism of action in HepG2 cells and a potential hypoglycemic activity by the inhibition of dipeptidyl peptidase-IV in Caco-2 cells. In the framework of a research aimed at fostering the multifunctional behavior of hempseed peptides, we present here the identification and evaluation of some antioxidant peptides from the same hydrolysate. After evaluation of its diphenyl-2-picrylhydrazyl (DPPH) radical scavenging activity, a trans-epithelial transport experiment was performed using differentiated Caco-2 cells that permitted the identification of five transported peptides that were synthesized and evaluated by measuring the oxygen radical absorbance capacity (ORAC), the ferric reducing antioxidant power (FRAP), and the 2,2-azino-bis-(3-ethylbenzo-thiazoline-6-sulfonic) acid (ABTS), and diphenyl-2-picrylhydrazyl radical DPPH assays. The most active peptides, i.e. WVSPLAGRT (H2) and IGFLIIWV (H3), were then tested in cell assays. Both peptides were able to reduce the H₂O₂-induced reactive oxygen species (ROS), lipid peroxidation, and nitric oxide (NO) production levels in HepG2 cells, via the modulation of Nrf-2 and iNOS pathways, respectively.

5.1 Introduction

The seed of industrial hemp, i.e. the non-drug cultivars of *Cannabis sativa*, stands out for its high protein (~25%) content (Callaway, 2004). The superior amino acid profile and high digestibility of hempseed proteins suggests their potential efficacy as a source of health-promoting peptides. In fact, different Authors have investigated the biological activity of peptides produced by hydrolyzing hempseed protein with different enzymes.

Due to the heterogeneous composition of the protein hydrolysates, it is likely that these materials may provide more than one biological activity (Lammi, Aiello, Boschini, & Arnoldi, 2019). This multifunctional behavior has been clearly highlighted for hempseed hydrolysates (Farinon, Molinari, Costantini, & Merendino, 2020). In fact,

hempseed peptides, obtained hydrolyzing the proteins with a combination of pepsin and pancreatin, possess both antioxidant and hypotensive activity either *in vitro* or *in vivo* (Girgih et al., 2014). The antioxidant and antihypertensive effects may be due to the presence of high levels of negatively charged amino acids for electron donation to reactive oxygen species and arginine for the production of nitric oxide (NO), a vasodilating agent, respectively. The hypotensive activity may depend also on the inhibition of angiotensin-converting enzyme (ACE) and renin (Girgih, He, & Aluko, 2014; Girgih et al., 2014). Other Authors have demonstrated, instead, that specific hempseed hydrolysate fractions are either antioxidant or neuroprotective (Rodriguez-Martin et al., 2019). Furthermore, hempseed protein hydrolysates obtained by different hydrolysis methods have *in vitro* neuroprotective activity (Malomo & Aluko, 2016) and *in vitro* and *in vivo* hypotensive activity (Malomo, Onuh, Girgih, & Aluko, 2015).

In addition, a recent investigation by our group has shown that a hydrolysate obtained digesting a total protein extract from hempseed with pepsin (HP) displays cholesterol-lowering activity through the inhibition of 3-hydroxy-3-methyl-glutaryl-coenzyme A reductase (HMGCoAR) (C Lammi, Bollati, Gelain, Arnoldi, & Pugliese, 2019; Zanoni, Aiello, Arnoldi, & Lammi, 2017). This inhibition leads to a positive low-density lipoprotein (LDL) receptor (LDLR) pathway modulation in human hepatic HepG2 cells (Zanoni et al., 2017). Finally, HP is also able to inhibit dipeptidyl peptidase-IV (DPP-IV), either *in vitro* on the human recombinant enzyme or in human intestinal Caco-2 cells, suggesting a potential anti-diabetic effect (Lammi et al., 2019).

Considering that there is currently a big interest for antioxidant peptides from dietary sources, the present study was aimed at fostering the multifunctional health promoting activities of hempseed peptides focusing the interest on the identification and characterization of bioavailable antioxidant peptides. More in details, the first objective of the work was the assessment of the antioxidant activity of the HP hydrolysate using the 1,1-diphenyl-2-picrylhydrazyl radical (DPPH) assay.

As the bioavailability is always a crucial feature, the second objective of the study was the identification of bioavailable peptides in the HP hydrolysate. In fact, we have

developed a strategy for identifying bioavailable and active peptides based on the use of differentiated Caco-2 cell: in practice, the differentiated Caco-2 monolayer is used as a “natural sieve of bioavailable species”. This permits to concentrate further research exclusively on absorbable peptides (Lammi et al., 2016).

The third objective of the work was the evaluation of the activity of absorbed peptides. To achieve this goal, the transported ones were synthesized and their direct antioxidant activity was tested using the most important antioxidant test [DPPH, oxygen radical absorbance capacity (ORAC), ferric reducing antioxidant power (FRAP), and 2,2-azino-bis-(3-ethylbenzothiazoline-6-sulfonic) acid (ABTS)]. The two most active peptides were further investigated in human hepatic HepG2 cells after the induction of oxidative stress using H₂O₂ for assessing their ability to reduce the level of reactive oxygen species (ROS), lipid peroxidation, and NO production. Finally, the effects of both peptides on the activation of nuclear factor erythroid 2-related factor 2 (Nrf-2) and inducible nitric oxide synthase (iNOS) pathway modulations were investigated in the same cells by performing western blotting experiments.

5.2 Material and Methods

5.2.1 Chemicals

All chemicals and reagents were of analytical grade. Dulbecco's modified Eagle's medium (DMEM), stable L-glutamine, fetal bovine serum (FBS), phosphate buffered saline (PBS), penicillin/streptomycin, chemiluminescent reagent, and 96-well plates were purchased from Euroclone (Milan, Italy). ROS and lipid peroxidation (MDA) assay kits, Griess reagent, bovine serum albumin (BSA), RIPA buffer, the anti-Nrf2 and anti-β-actin antibodies were from Sigma-Aldrich (St. Louis, MO, USA). The iNOS primary antibody came from Cell Signaling Technology (Danvers, MA, USA). The HepG2 cell line was bought from ATCC (HB-8065, ATCC from LGC Standards, Milan, Italy) and Caco-2 cells were obtained from INSERM (Paris, France). The synthetic peptides H1, H2, H3, H4, and H5 were synthesized by the company

GeneScript (Piscataway, NJ, USA) at >95% purity.

5.2.2 Preparation and analysis of the peptic hydrolysate from hempseed protein (HP)

Hempseeds (*C. sativa* cultivar Futura) were provided by the Institute of Agricultural Biology and Biotechnology, CNR (Milan, Italy). The isolation of hempseed proteins, their hydrolysis and peptidomic analysis was previously carried out applying methods already published (Zanoni et al., 2017). Briefly, 2 g of defatted hempseed flour were homogenized with 15 mL of 100 mM Tris-HCl/0.5 M NaCl buffer, pH 8.0. The extraction was performed in batch at 4 °C overnight under magnetic stirring. The solid residue was eliminated by centrifugation at 6800g for 30 min at 4 °C, and the supernatant was dialyzed against 100 mM Tris-HCl buffer, pH 8.0 for 36 h at 4 °C. The protein content was assessed according to the method of Bradford, using BSA as standard. The hydrolysis was performed on the total protein extract, changing the pH from 8 to 2 by adding 1 M HCl. The pepsin solution (4 mg/mL in NaCl 30 mM) was added in a ratio 1:50 enzyme/hempseed protein (w/w). The mixture was incubated for 16 h at 37 °C and then the enzyme inactivated changing the pH to 7.8 by adding 1 M NaOH. The sample was fractionated by ultrafiltration, using membranes with a 3-kDa molecular weight cutoff (MWCO; Millipore, U.S.A.). This permeate solution was used for investigating the biological activity. For determining its composition, it was acidified with 0.1% of formic acid, and then analyzed on a SL IT mass spectrometer interfaced with a HPLC Chip Cube source (Agilent Technologies, Palo Alto, CA, U.S.A.). Separation was carried out in gradient mode at a 300 nL/min flow. The LC solvent A was 95% water, 5% ACN, and 0.1% formic acid, and solvent B was 5% water, 95% ACN, and 0.1% formic acid. The nano pump gradient program was as follows: 5% solvent B (0 min), 80% solvent B (0–40 min), 95% solvent B (40–45 min), and back to 5% in 5 min. The drying gas temperature was 300 °C, and flow rate was 3 L/min (nitrogen). Data acquisition occurred in positive ionization mode. Capillary voltage was –1950 V, with an end plate offset of –500 V. Full scan mass spectra were acquired in the mass range from m/z 300 to 2000 Da. LC-MS/MS

analysis was performed in data dependent acquisition AutoMS(n) mode. The MS/MS data were analyzed by Spectrum Mill Proteomics Workbench (Rev B.04.00, Agilent Technologies, Palo Alto, CA, U.S.A.) consulting NCBI_ *Cannabis sativa* (531 sequences) protein sequences database. Two missed cleavages were allowed to pepsin; peptide mass tolerance was set to 1.2 Da and fragment mass tolerance to 0.9 Da. The threshold used for peptide identification score was ≥ 6 ; the scored peak intensity SPI% was $\geq 70\%$; and the autovalidation strategy either in peptide mode and in protein polishing was performed using an FDR cutoff of $\leq 1.2\%$.

5.2.3 Intestinal trans-epithelial transport of hempseed hydrolysate assessment

5.2.3.1 Caco-2 cell culture Caco-2 differentiation conditions

Human intestinal Caco-2 cells were cultured in DMEM high glucose with stable L-glutamine, supplemented with 10% FBS, 100 U/mL penicillin, 100 $\mu\text{g/mL}$ streptomycin (complete growth medium) with incubation at 37 °C under 5% CO₂ atmosphere, according to a published protocol (Lammi et al., 2016). For differentiation, Caco-2 cells were seeded on polycarbonate filters, 12 mm diameter, 0.4 μm pore diameter (Transwell, Corning Inc., Lowell, MA, US) at a 3.5×10^5 cells/cm² density in complete medium supplemented with 10% FBS in both apical (AP) and basolateral (BL) compartments for 2 d to allow the formation of a confluent cell monolayer. Starting from day three after seeding, cells were transferred to FBS-free medium in both compartments, supplemented with ITS (final concentration 10 mg/L insulin (I), 5.5 mg/L transferrin (T), 6.7 $\mu\text{g/L}$ sodium selenite (S) (GIBCO-Invitrogen, San Giuliano Milanese, Italy) only in the BL compartment, and allowed to differentiate for 18–21 days with regular medium changes three times weekly (Ferruzza, Rossi, Sambuy, & Scarino, 2013).

5.2.3.2 Evaluation of the cell monolayer integrity

The transepithelial electrical resistance (TEER) of differentiated Caco-2 cells was measured at 37 °C using the voltmeter apparatus Millicell (Millipore Co., Billerica, MA, USA), immediately before and at the end of the transport experiments. In

addition, at the end of transport experiments, cells were incubated from the AP side with 1 mM phenolred in PBS containing Ca ++ (0.9 mM) and Mg ++ (0.5 mM) for 1 h at 37 °C, to monitor the paracellular permeability of the cell monolayer. The BL solutions were then collected and NaOH (70 µL, 0.1 N) was added HI from Biotek (Winooski, VT, USA). Phenol-red passage was quantified using a standard phenol-red curve. Only filters showing TEER values and phenol red passages similar to untreated control cells were considered for peptide transport analysis.

5.2.3.3 Trans-epithelial transport experiments

Prior to experiments, the cell monolayer integrity and differentiation were checked by TEER measurement as described in detail above. Peptide trans-epithelial passage was assayed in differentiated Caco-2 cells in transport buffer solution (137 mM NaCl, 5.36 mM KCl, 1.26 mM CaCl₂, and 1.1 mM MgCl₂, 5.5 mM glucose) according to previously described conditions. In order to reproduce the pH conditions existing *in vivo* in the small intestinal mucosa, the AP solutions were maintained at pH 6.0 (buffered with 10 mM morpholinoethane sulfonic acid), and the BL solutions were maintained at pH 7.4 (buffered with 10 mM N-2-hydroxyethylpiperazine-N-4-butanesulfonic acid). Prior to transport experiments, cells were washed twice with 500 µL PBS containing Ca ++ and Mg ++. Peptide transportation by mature Caco-2 cells was assayed by loading the AP compartment with 1.0 mg/mL of HP hydrolysate in the AP transport solution (500 µL) and the BL compartment with the BL transport solution (700 µL). The plates were incubated at 37 °C and the BL solutions were collected at different time points (i.e., 15, 30, 60, 90, and 120 min) and replaced with fresh solutions pre-warmed at 37 °C. All BL and AP solutions collected at the end of the transport experiment were stored at –80 °C prior to analysis. Three independent transport experiments were performed, each in duplicate.

5.2.3.4 HPLC-Chip-MS/MS analysis

HPLC-Chip MS analysis of absorbed peptides was performed according to a previously published method (Lammi et al., 2016), as reported in Supplementary

material. The raw files obtained from the MS analyzer were processed by Spectrum Mill MS Proteomics Workbench (Rev B.04.00, Agilent). The extraction of MS/MS spectra was conducted accepting a minimum sequence length of 3 amino acids and merging scans with same precursor within a mass window of ± 0.4 m/z in a time frame of ± 5 s. Trypsin or pepsin were chosen as digestive enzymes; 2 missed cleavage were allowed. MS/MS search was conducted against the subset of *C. sativa* protein sequences (47576 entries) downloaded from UNIProtKB (<http://www.uniprot.org/>). The mass tolerance of parent and fragments of MS/MS data search was set at 1.0 Da for the precursor ions and 0.7 for fragment ions respectively. Threshold used for peptide identification score ≥ 8 ; Scored Peak Intensity SPI% $\geq 70\%$; Local False Discovery Rate $\leq 0.1\%$.

5.2.4 Antioxidant activity of hempseed peptides

5.2.4.1 1-Diphenyl-2-picrylhydrazyl radical (DPPH) assay

The DPPH assay was performed by a standard method with a slight modification. Briefly, 45 μ L of 0.0125 mM DPPH solution (dissolved in methanol) was added to 15 μ L of the HP hydrolysate and lysates of pretreated cells at the final concentrations of 0.50, 1.0, and 2.50 mg/mL, whereas the single peptides H2 and H3 were tested at the final concentrations of 10 up to 200 μ M. The reaction for scavenging the DPPH radicals was performed in the dark at room temperature and the absorbance was measured at 520 nm after 30 min incubation.

5.2.4.2 2,2'-Azino-bis (3-ethylbenzothiazoline-6-sulfonic) acid diammonium salt assay

The Trolox equivalent antioxidant capacity (TEAC) assay is based on the reduction of the 2,2'-azino-bis-(3-ethylbenzothiazoline-6-sulfonic) acid (ABTS) radical induced by antioxidants. The ABTS radical cation (ABTS⁺) was prepared by mixing a 7 mM ABTS solution (Sigma-Aldrich, Milan, Italy) with 2.45 mM potassium persulfate (1:1) and stored for 16 h at room temperature and in dark. To prepare the ABTS reagent,

the ABTS⁺ was diluted in 5 mM phosphate buffer (pH 7.4) to obtain a stable absorbance of 0.700 (\pm 0.02) at 730 nm. For the assay, 10 μ L of H2 and H3 peptides at the final concentrations of 10, 2, 50, 100, and 200 μ M were added to 140 μ L of diluted the ABTS⁺. The microplate was incubated for 30 min at 30 °C and the absorbance was read at 730 nm using a microplate reader Synergy H1 (Biotek). The TEAC values were calculated using a Trolox (Sigma-Aldrich, Milan, Italy) calibration curve (60–320 μ M).

5.2.4.3 FRAP assay

The FRAP assay evaluates the ability of a sample to reduce ferric ion (Fe³⁺) into ferrous ion (Fe²⁺). Thus, 10 μ L of H2 and H3 peptides at the final concentrations of 10, 25, 5, 100, and 200 μ M were mixed with 140 μ L of FRAP reagent. The FRAP reagent was prepared by mixing 1.3 mL of a 10 mM TPTZ (Sigma-Aldrich, Milan, Italy) solution in 40 mM HCl, 1.3 mL of 20 mM FeCl₃ \times 6 H₂O and 13 mL of 0.3 M acetate buffer (pH 3.6). The microplate was incubated for 30 min at 37 °C and the absorbance was read at 595 nm. The results were calculated by a Trolox (Sigma-Aldrich, Milan, Italy) standard curve obtained using different concentrations (3–400 μ M). Absorbances were recorded on a microplate reader Synergy H1 (Biotek).

5.2.4.4 ORAC assay

The ORAC assay is based on the scavenging of peroxy radicals generated by the azo 2,2'-azobis(2-methylpropionamidine) dihydrochloride (AAPH, Sigma-Aldrich, Milan, Italy). Briefly, 25 μ L of H2 and H3 peptides were added to 50 μ L sodium fluorescein (2.934 mg/L) at the final concentrations of 10, 25, 50, 100, and 200 μ M (Sigma-Aldrich, MO, USA) and incubated for 15 min at 37 °C. Then, 25 μ L of AAPH (60.84 mM) were added and the decay of fluorescein was measured at its maximum emission of 528/20 nm every 5 min for 120 min using a microplate reader Synergy H1 (Biotek). The area under the curve (AUC) was calculated for each sample subtracting the AUC of the blank. The results were calculated using a Trolox calibration curve (2–50 μ M).

5.2.5 Antioxidant activity of hempseed peptides on HepG2 cells

5.2.5.1 HepG2 cell culture conditions

Human hepatic HepG2 cells and intestinal Caco-2 cells were cultured in DMEM high glucose with stable L-glutamine, supplemented with 10% FBS, 100 U/mL penicillin, 100 µg/mL streptomycin (complete growth medium) with incubation at 37 °C under 5% CO₂ atmosphere.

5.2.5.2 3-(4,5-Dimethylthiazol-2-yl)-2,5-diphenyltetrazolium bromide (MTT) assay

A total of 3×10^4 HepG2 cells/well were seeded in 96-well plates and treated with peptides H2 and H3 (from 1 µM to 1 mM) or vehicle (H₂O) in complete growth media for 48 h at 37 °C under 5% CO₂ atmosphere. Subsequently, the solvent was aspirated and 100 µL/well of filtered 3-(4,5-dimethylthiazol-2-yl)-2,5-diphenyltetrazolium bromide (MTT) solution added. After 2 h of incubation at 37 °C under 5% CO₂ atmosphere, 0.5 mg/mL solution was aspirated and 100 µL/well of the lysis buffer (8 mM HCl + 0.5% NP-40 in DMSO) were added. After 10 min of slow shaking, the absorbance at 575 nm was read on the microplate reader Synergy H1 (Biotek).

5.2.5.3 Fluorometric intracellular ROS assay

For cells preparation, 3×10^4 HepG2 cells/well were seeded on a black 96-well plate overnight in growth medium. The day after, the medium was removed, 50 µL/well of Master Reaction Mix was added and the cells were incubated at 5% CO₂, 37 °C for 1 h in the dark. Then, the HP hydrolysate and peptides H2 and H3 were added to reach the final concentrations of 0.5 and 1.0 mg/mL (HP), 100.0 µM (H2) and 25.0 µM (H3), respectively, and incubated at 37 °C for 24 h. To induce ROS, cells were treated with H₂O₂ at a final concentration of 1.0 mM for 30 min at 37 °C in the dark and fluorescence signals (ex./em. 490/525 nm) were recorded using a microplate reader Synergy H1 (Biotek).

5.2.5.4 Lipid peroxidation (MDA) assay

HepG2 cells (2.5×10^5 cells/well) were seeded in a 24 well plate and, the following day, they were treated with H2 (100 μ M) and H3 (25.0 μ M) peptides for 24 h at 37 °C under 5% CO₂ atmosphere. The day after, cells were incubated with H₂O₂ 1 mM or vehicle (H₂O) for 1 h, then collected and homogenized in 150 μ L ice-cold MDA lysis buffer containing 3 μ L of butylated hydroxytoluene (BHT) (100 \times). Samples were centrifuged at 13,000 g for 10 min, then were filtered through a 0.2 μ m filter to remove insoluble material. To form the MDA-TBA adduct, 300 μ L of the TBA solution were added into each vial containing 100 μ L samples and incubated at 95 °C for 60 min, then cooled to RT for 10 min in an ice bath. For analysis, 100 μ L of each reaction mixture were pipetted into a clear 96 well plate and the absorbance were measured at 532 nm using the microplate reader Synergy H1 (Biotek). To normalize the data, total proteins for each sample were quantified by Bradford method.

5.2.5.5 Nitric oxide (NO) level evaluation on HepG2 cells

HepG2 cells (1.5×10^5 /well) were seeded on a 24-well plate. The next day, cells were treated with H2 and H3 peptides to reach the final concentrations of 100 μ M (H2) and 25 μ M (H3) and incubated at 37 °C under a 5% CO₂ atmosphere for 24 h. After incubation, cells were treated with H₂O₂ (1.0 mM) or vehicle (H₂O) for 1 h, then the cell culture media were collected and centrifuged at 13,000 g for 15 min to remove insoluble material. The NO determination was carried out by Griess test. Briefly, 1.0 g of Griess reagent powders were solved in 25.0 mL of distilled H₂O and 50 μ L of the solution were incubated with 50 μ L of the culture supernatants for 15 min at RT in the dark. The absorbance was measured at 540 nm using the microplate reader Synergy H1 (Biotek).

5.2.5.6 iNOS and Nrf-2 protein level evaluation by western blot analysis

A total of 1.5×10^5 HepG2 cells/well were seeded on 24-well plates and incubated at 37 °C under a 5% CO₂ atmosphere. The following day, cells were treated with 100

μM of H2, 25.0 μM of H3 peptides or vehicle (H_2O) in a complete growth medium for 24 h. The day after, cells were treated with H_2O_2 (1.0 mM) or vehicle (H_2O) for 1 h. After each treatment, cells were scraped in 30 μL ice-cold lysis buffer [RIPA buffer + inhibitor cocktail + 1:100 PMSF + 1:100Na-orthovanadate] and transferred in an ice-cold microcentrifuge tube. After centrifugation at 13,300 g for 15 min at 4 °C, the supernatant was recovered and transferred into a new ice-cold tube. Total proteins were quantified by the Bradford method and 50 μg of total proteins loaded on a precast 7.5% sodium dodecyl sulfate-polyacrylamide gel (SDS-PAGE) at 130 V for 45 min. Subsequently, the gel was pre-equilibrated with 0.04% SDS in H_2O for 15 min at RT and transferred to a nitrocellulose membrane (Mini nitrocellulose Transfer Packs, Bio-Rad) using a trans-Blot Turbo (Bio-Rad) at 1.3 A, 25 V for 7 min. On milk or BSA blocked membrane, target proteins were detected by primary antibodies as follows: anti-iNOS, anti-Nrf-2 and anti- β -actin. Secondary antibodies conjugated with HRP and a chemiluminescent reagent were used to visualize target proteins and their signal was quantified using the Image Lab Software (Bio-Rad). The internal control β -actin was used to normalize loading variations.

5.2.6 Statistical analysis

All the data sets were checked for normal distribution by D'Agostino and Pearson test. Since they are all normally distributed with p -values < 0.05 , we proceeded with statistical analyses by One-Way ANOVA followed by Tukey's post-hoc tests and using GraphPad Prism 9 (San Diego, CA, USA). Values were reported as means \pm standard deviation (s.d.); p -values < 0.05 were considered to be significant.

5.3 Results & discussion

5.3.1 Antioxidant activity of HP hydrolysate

To evaluate the radical scavenging activity of the HP hydrolysate, the DPPH assay was employed, since this test is widely applied to test the ability of natural compounds to act as free radical scavengers or hydrogen donors (Kedare & Singh,

2011). The hydrolysate was tested in the range from 0.5 to 2.5 mg/mL. The results (**Fig. 5.1A**) clearly suggest that this hydrolysate scavenges the DPPH radical with a dose–response trend. In detail, it reduces the DPPH radicals by $16.9 \pm 5.4\%$, $25.8 \pm 3.8\%$, and $50.7 \pm 7.8\%$, respectively, at 0.5, 1.0, and 2.5 mg/mL (**Fig. 5.1A**). Even though, the radical scavenging activity of food protein hydrolysates is influenced by many factors (such as the proteases used for the generation of the hydrolysates, the size and amino acid composition of the obtained peptides, and the DPPH assay conditions), our results suggest that HP hydrolysate is more active than other hempseed protein hydrolysate, obtained by co-digesting the proteins with pepsin and pancreatin, which are poor scavengers of DPPH, i.e. about 4% at 1 mg/mL (Girgih, Udenigwe, & Aluko, 2011). These different behaviors may be explained considering that the extensive protein hydrolysis obtained by the combination of pepsin and pancreatin probably impairs the antioxidant activity. Indeed, HP hydrolysate is 6.5-fold a more potent DPPH radicals scavenger than the hydrolysate obtained by co-digesting the hempseed proteins with pepsin and pancreatin. Moreover, HP hydrolysate is also a more active radical scavenger than a soybean protein hydrolysate obtained with the same enzyme (Lammi, Bollati, & Arnoldi, 2019).

In light with these pieces of evidence, the assessment of the ability of HP hydrolysate to scavenge the DPPH radicals was carried out also at cellular levels. More in details, HepG2 cells were treated with HP hydrolysate in the 0.5–2.5 mg/mL range of concentrations. After 24 h, cells were lysate and the DPPH assay was performed. In line with the previous results, our findings suggest that HP hydrolysate reduces the DPPH radical by $14.8 \pm 5.6\%$, $22.9 \pm 14.9\%$, and $56.6 \pm 8.4\%$, respectively, at 0.5, 1.0, and 2.5 mg/mL.

Based on these results, to evaluate whether the HP hydrolysate modulates the H₂O₂-induced ROS production, HepG2 cells were pretreated with it (0.5 and 1.0 mg/mL) overnight at 37 °C. The following day, the same cells were treated with 1 mM H₂O₂ for 30 min at 37 °C. Results (**Fig. 5.2**) clearly suggest that the treatment of HepG2 cells with H₂O₂ alone produces a significant augmentation of intracellular ROS levels by $153.3 \pm 5.6\%$ versus the control cells, which was attenuated by the pre-treatment

with the HP hydrolysate that reduced the H₂O₂-induced intracellular ROS by 14.1 ± 6.7% at 0.5 mg/mL. Interestingly, at 1 mg/mL, the HP hydrolysate reduces the ROS level by 72.1 ± 5.0% under basal conditions even in presence of H₂O₂ stimulation, confirming that it can act as a natural antioxidant. These results are in line with the effect of peptic soybean peptides in the modulation of intracellular ROS levels after the H₂O₂ stimulation of HepG2 cells (Lammi et al., 2019).

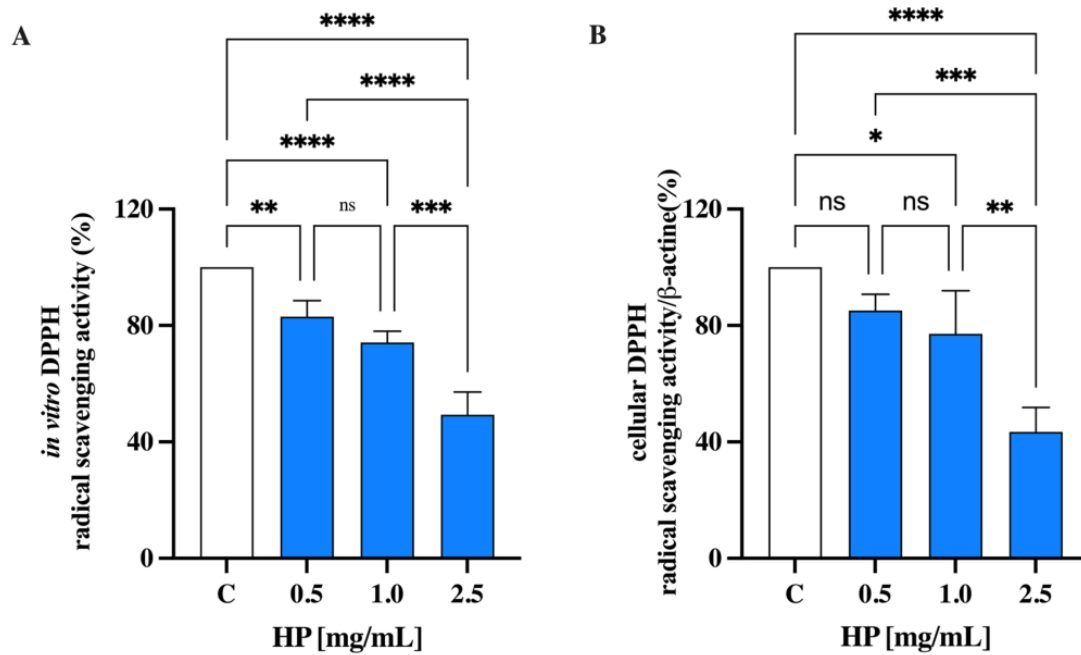


Figure 5.1 Chemical (A) and cellular (HepG2, B) DPPH radical scavenging activity of HP hydrolysate. The data points represent the averages ± s.d. of four independent experiments in duplicate. C: control sample. (*) $p < 0.05$, (**) $p < 0.01$, (***) $p < 0.001$, (****) $p < 0.0001$.

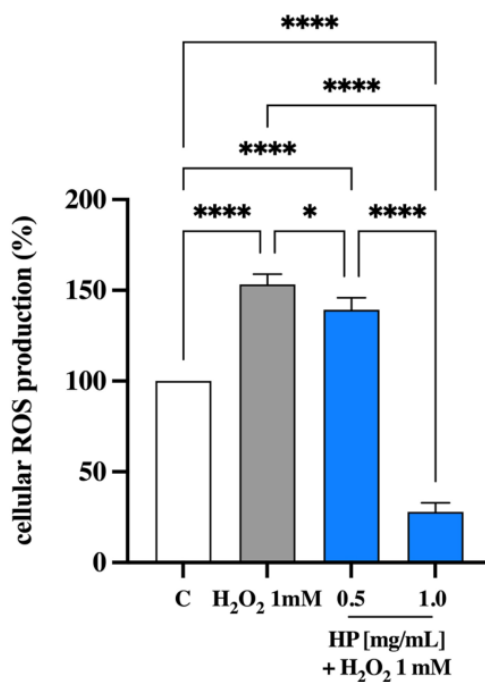


Figure 5.2 Effects of HP on the modulation of H₂O₂-induced ROS levels in HepG2 cells. HP reduce the H₂O₂ (1 mM)-induced ROS levels in HepG2 cells. Data represent the mean \pm s.d. of six independent experiments performed in triplicate. All data sets were analyzed by One-way ANOVA followed by Tukey's posthoc test. C: control sample. (*) $p < 0.05$, (****) $p < 0.0001$.

5.3.2 Trans-epithelial transport of HP hydrolysate using differentiated Caco-2 cells

Differentiated Caco-2 cells were incubated with the HP hydrolysate in the AP compartments at a 1 mg/mL concentration. After 4 h treatment, the AP and BL media were collected and submitted to HPLC-Chip-MS/MS analysis. For monitoring cell monolayer permeability and excluding non-specific peptide passage, TEER measurements were taken at the beginning and end of each experiment. Moreover, phenol-red passage across the monolayer was assayed at the experiment end (Ferruzza, Scarino, Gambling, Natella, & Sambuy, 2003). Both assays demonstrated that the incubation with the HP hydrolysate did not affect monolayer permeability (data not shown). Only filters showing TEER values and a phenol red passage similar to untreated control cells were considered for peptide transport analysis. The starting peptic peptide mixture and the AP and BL samples taken at the end of transport

experiments were analyzed by HPLC-Chip-MS/MS. **Fig. 5-S1** (Supplementary material) shows exemplary chromatographic profiles of AP and BL peptides, which were identified through MS/MS ion search, using the SpectrumMill search engine. **Table 5.1** shows the peptides identified in the starting hydrolysate as well as in the AP and/or BL samples. Notably, among the peptides present in the starting HP hydrolysate, only five peptides were able to cross the mature Caco-2 cells. Out of these five absorbed species, H1 belongs to Edestin 3 (A0A219D2X4), H2, H4, and H5 to Edestin1 (A0A090CXP7), whereas H3 belongs to Cytochrome c biogenesis protein CcsA (A0A0U2DTB8). H4 is the longest absorbed peptide with 12 amino acids residues within its sequence, whereas H3 and H5 are the shortest ones, accounting for 8 amino acid residues. Finally, H1 and H2 have 10 and 9 amino acid residue sequences, respectively. Moreover, H1 and H4 are absorbed by Caco-2 cells and are not degraded by the action of the peptidases, which are expressed at the AP side of the differentiated cells during incubation, whereas some other peptides, i.e. H2 and H5, are transported by Caco-2 cells but they are degraded during the 4 h of incubation by intestinal peptidase producing other shorter peptide fragments.

Working on a peptide mixture with a complex composition, it is not feasible to characterize the mechanism by which peptides are transported by intestinal cells, since more than one mechanism may occur at the same time during the trans-epithelial transport of the total hydrolysate.

Overall, food derived peptides may be transported across the intestinal brush-border membrane into the bloodstream via one or more of the following routes: (i) peptide transport 1 (PepT1)-mediated route, (ii) paracellular route via tight junctions, (iii) transcytosis route, and (iv) passive transcellular diffusion (Xu, Yan, Zhang, & Wu, 2019). Peptide size, charge, hydrophobicity, and degradation due to the action of peptidases are among the main factors influencing the absorption through one or more of these routes. In general, short peptides, such as dipeptides and tripeptides, are preferentially transported by PepT1, due to its high-capacity, low-affinity, and high expression in intestinal epithelium (Daniel, 2004), whereas highly hydrophobic peptides are transported by simple passive transcellular diffusion or by transcytosis

(Miguel et al., 2008). Based on these considerations, the hydrophobicity of all the transported peptides was calculated (see **Table 5.1**). The results suggest that these peptides may be preferentially transported by paracellular route and/or by transcytosis.

Table 5.1 LC-ESI-MS/MS based identification of peptic peptides from transport experiments.

Metabolite Sequence	Accession no^a	m/z^b (charge)	Observed^b [M + H]⁺ (Da)	Expected^b [M + H]⁺ (Da)	Peptide sequence^b	Short name	M	AP	BL	Hydrophobicity (Kcal*<i>mol</i>⁻¹)^d
Peptic hempseed peptides										
Edestin, 3	A0A219D2X4	545,28	1089,568	1089,568	₃₂₈ DVFSPQAGRL ₃₃₇	H1	+ ^e	+	+	+12.95
Edestin, 1	A0A090CXP7	586.93	986,541	986,541	₄₅₀ WVSPLAGRT ₅₅₈	H2	+	-	+	+8.41
Cytochrome c	A0A0U2DTB8	480,80	960,595	960,591	₂₉₃ IGFLIIWV ₃₀₀	H3	-	-	+	+0.18
biogenesis protein CcsA										
Edestin, 1	A0A090CXP7	645,81	1291,661	1291,664	₃₄₁ DVFTPQAGRIST ₃₅₂	H4	+	+	+	+13.58
Edestin, 1	A0A090CXP7	434,78	868,524	868,525	₄₆₁ IRALPEAV ₄₆₈	H5	+	-	+	+11.65

^aAccording to “UniProtKB” (<http://www.uniprot.org/>).

^bThe identification of protein parent was performed using SpectrumMill Workbench

^cM, starting peptide mixture of peptic peptides; AP, apical chamber samples; BL, basolateral chamber samples.

^dAccording to PepDraw (<http://pepdraw.com>).

^e+, detected.

5.3.3 Screening of the antioxidant activity of transported hempseed peptides

All peptides detected in the BL samples were synthesized and screened for their antioxidant activity at concentrations ranging from 10 to 200 μM using the ABTS, DPPH, ORAC, and FRAP assays (**Figs. 5.3 and 5-2S**). H2 and H3 resulted to be the best antioxidant peptides. H2 scavenged the ABTS radical by $147 \pm 7.9\%$, $164.2 \pm 1.1\%$, $174.1 \pm 0.4\%$, $178.8 \pm 0.9\%$, and $179.3 \pm 0.5\%$, whereas H3 by $142.7 \pm 10.3\%$, $146.1 \pm 8.1\%$, $149.6 \pm 5.6\%$, $153.1 \pm 2.5\%$, and $157.5 \pm 3.3\%$, respectively, at 10, 25, 50, 100, and 200 μM (**Fig. 5.3A, E**). H2 scavenged the DPPH radical by $24.8 \pm 0.3\%$, $33.4 \pm 4.2\%$ and $36.1 \pm 5.2\%$ (**Fig. 5.3B**), whereas H3 reduced the DPPH radical by $29.6 \pm 2.2\%$, $29.8 \pm 3.2\%$, $31.8 \pm 3\%$, $33.5 \pm 3.3\%$, and $33.6 \pm 0.6\%$, respectively, at 10, 25, 50, 100, and 200 μM (**Fig. 5.3F**).

In addition, in the ORAC test, H2 was able to scavenge the peroxy radicals generated by 2,2'-azobis(2-methylpropionamidine) dihydrochloride up to $489.4 \pm 56.9\%$, $614.8 \pm 13.3\%$, $678 \pm 52.4\%$, $679.5 \pm 55.6\%$, and $621.8 \pm 44.6\%$, whereas H3 by $148.9 \pm 12.1\%$, $181.8 \pm 12.5\%$, $207.5 \pm 13.7\%$, $331.3 \pm 14.5\%$, and $480.8 \pm 9.0\%$, respectively, at 10, 25, 50, 100, and 200 μM (**Fig. 5.3C and G**). Finally, H2 increased the FRAP by $143.1 \pm 28.2\%$, $144.5 \pm 32.5\%$, $212.6 \pm 31\%$, $298.1 \pm 58.7\%$, and $587.6 \pm 27.3\%$, whereas H3 by $207.5 \pm 23.5\%$, $299.3 \pm 42.8\%$, $355.8 \pm 19.3\%$, $519.5 \pm 13.7\%$, and $782 \pm 6.8\%$ at 10, 25, 50, 100, and 200 μM , respectively (**Fig. 5.3D and 5.3H**). By performing the same assays, H1, H4, and H5 did not show any significant antioxidant behavior (**Fig. 5-S2**).

Many physical–chemical factors may influence the ability of peptides to exert antioxidant activity. In fact, although certain aspects of the structure–function relationship of antioxidant peptides are still poorly understood (Harnedy, O’Keeffe, & FitzGerald, 2017), it has been suggested that chain length, amino acid type, amino acid composition, and amino acid sequence, the location of specific amino acids in a peptide chain may be critical issues for exerting the antioxidant property (Gallego, Mora, & Toldra, 2018). In this context, short peptides may be often potent antioxidants.

Literature indicates that, besides containing hydrophobic amino acids, such as Leu or Val, in their N-terminal regions, peptides containing nucleophilic sulfur-containing amino acid residues (Cys and Met), aromatic amino acid residues (Phe, Trp, and Tyr) and/or the imidazole ring-containing His are generally found to possess strong antioxidant properties (Nwachukwu & Aluko, 2018, 2019). Based on these considerations, H3 is the shortest peptide among those tested and it stands out for the presence of two aromatic amino acids (Trp and Phe) within its sequence, which certainly contribute to its antioxidant activity. In addition, since the repetitive di- or tri- amino acid residues within a peptide have been linked to enhanced antioxidant activity (Jin, Liu, Zheng, Wang, & He, 2016), the H3 antioxidant behavior may be linked to the repetitive II sequence.

The antioxidant activity of peptide H2 is linked to the presence of Trp residue located in the N-terminal portion of the peptide as well as to the presence of an Arg residue in the C-terminal. In particular, the Arg residue in C-terminal may be correlated with its high ABTS radical scavenging ability. This evidence is in line with the fact that the C-terminal Arg residue has been linked to high antioxidant activity of certain peptides, i.e. GLFGPR and GATGPQGPLGPR (Sae-Leaw et al., 2017).

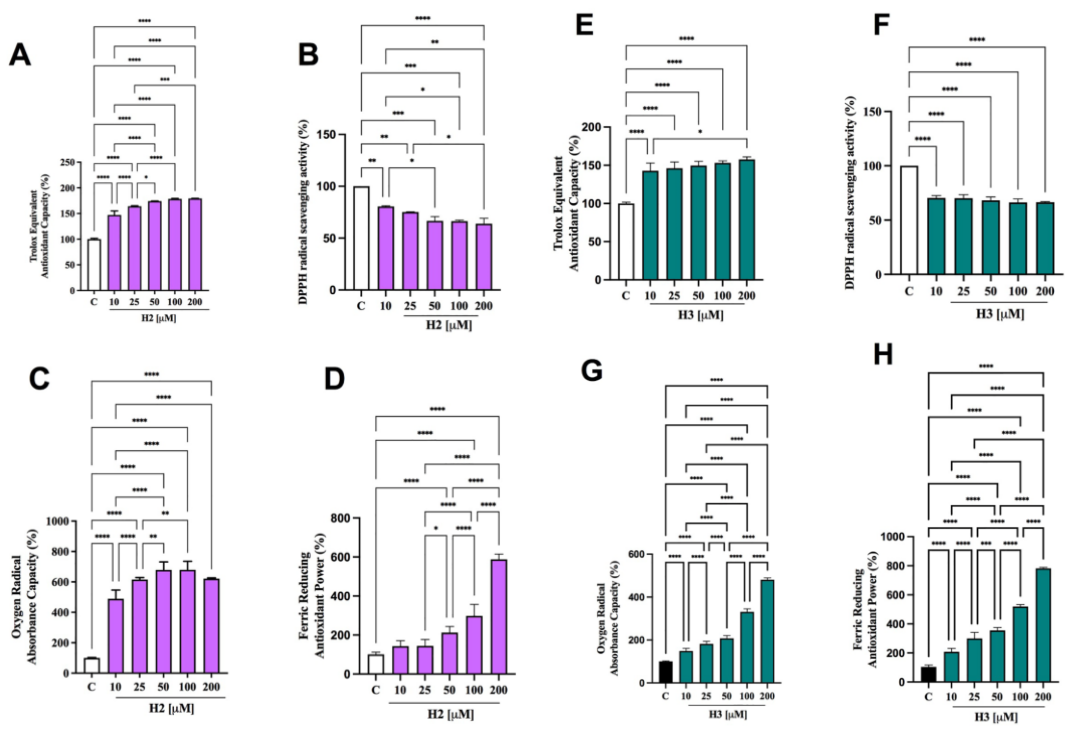


Figure 5.3 Antioxidant power evaluation of H2 and H3 peptides by 2,2-azino-bis-(3-ethylbenzothiazoline-6-sulfonic) acid (ABTS) (A, E), 2,2-diphenyl-1-picryl-hydrazyl (DPPH) (B, F), oxygen radical absorbance capacity (ORAC) (C, G) and ferric reducing antioxidant power (FRAP) (D, H) assays, respectively. The data points represent the averages \pm s.d. of four independent experiments performed in duplicate. All data sets were analyzed by One-way ANOVA followed by Tukey's post-hoc test. C: control sample. (*) $p < 0.5$; (**) $p < 0.01$; (***) $p < 0.001$; (****) $p < 0.0001$.

5.3.4 H2 and H3 decrease the H₂O₂-induced ROS and lipid peroxidation levels in hepatic HepG2 cells

Considering all the results obtained by the previous assays, only H2 and H3 were chosen for a deeper assessment of the antioxidant properties at cellular level, measuring their protective effects after induction of oxidative stress using H₂O₂ on human hepatic HepG2 cells. Before cellular evaluation, however, it was necessary to perform MTT experiments in order to exclude any potential cytotoxic effect. Results suggest that H2 is safe for the hepatic cells at all the doses in the range 1 nM - 1 mM, whereas for H3 the highest safe dose for HepG2 cell vitality is 25 μ M (**Fig. 5-S3**). In addition, any morphological variations of HepG2 cells treated w/o and with H₂O₂ (1 mM) for 1 h and cells pre-treated with both H2 (100 μ M) and H3 (25 μ M) peptides and then treated with H₂O₂ (1 mM) was observed by inverted microscopy (**Fig. 5-S4**). Based on the MTT results and on the antioxidant activity evaluation by chemical assays, it was decided to test the H2 and H3 effect on HepG2 cells at the fixed concentrations of 100 and 25 μ M, respectively. The concentration of H2 was selected based on its safety in the MTT assay, whereas that of H3 was the highest safe concentration even if it was not the most active in the antioxidant experiments performed employing ABTS, FRAP, ORAC, and DPPH assays, respectively.

Fig. 5.4A shows that the treatment of HepG2 cells with H₂O₂ alone produces a significant increase of intracellular ROS levels by $51.7 \pm 5.7\%$, which was attenuated by the pre-treatment with peptides H2 and H3: H2 reduced the ROS by $23.8 \pm 12.5\%$

at 100 μ M, whereas H3 by $23.2 \pm 12.8\%$ at 25 μ M. These findings indicate that both peptides H2 and H3 significantly protected the HepG2 cells from the H₂O₂-induced oxidative stress. Notably, H3 appeared to be 4-fold more effective than H2.

Other food peptides are antioxidant in cellular models. ADWGGPLPH, a wheat germ derived peptide, significantly reduces the intracellular ROS production deriving from hyperglycemia in vascular smooth muscle cells (F. Wang et al., 2020), peptides GPEGPMGLE, EGPFPGPEG, GFIGPTE, from collagen of red-lip croaker, decreases intracellular ROS levels in H₂O₂-treated HepG2 cells (Wang, Zhao, Zhao, Chi, & Wang, 2020), and peptides VEGNLQVLRPR, LAGNPHQQQN, HNLDTQTESDV, AGNDGFEYVTLK, QQRQQQGL, AELQVVDHLGQTV, EQEEEEESTGRMK, WSVWEQELED, from defatted walnut meal, decrease ROS production in H₂O₂-treated SHSY5Y cells (Sheng et al., 2019).

Lipids of cellular membranes are susceptible to oxidative attack, typically by ROS, resulting in a well-defined chain reaction with the generation of end products, such as malondialdehyde (MDA) and related compounds, known as TBA reactive substances (TBARS). Based on these considerations, the capacity of H2 and H3 to modulate the H₂O₂-induced lipid peroxidation in human hepatic HepG2 cells was assessed measuring the reaction of MDA precursor with the TBA reagent to form fluorometric ($\lambda_{\text{ex}} = 532/\lambda_{\text{em}} = 553 \text{ nm}$) product, proportional to the amount of TBARS (MDA equivalents) present. In agreement with the observed increase of ROS after the H₂O₂ treatment, a significant increase of the lipid peroxidation was observed up to $135.9 \pm 10.8\%$ at cellular level (**Fig. 5.4B**). In addition, the pre-treatment of HepG2 cells with both peptides determined a significant reduction of lipid peroxidation even under basal conditions. Fig. 4B clearly shows that H2 decreases the lipid peroxidation up to $99.5 \pm 14.6\%$ at 100 μ M, whereas H3 up to $91.9 \pm 13.3\%$ at 25 μ M (**Fig. 5.4B**). Since the lipid peroxidation is a validated marker of oxidative stress, these findings confirm the effective antioxidant property of hempseed peptides H2 and H3 and that H3 is 4-fold more active than H2 also in reducing intracellular MDA production. VNP and YGD, two peptides from fermented grain (Jiupei), are able to decrease the MDA levels in AAPH-treated HepG2 cells (Jiang et al., 2019). In addition, QDHCH, a

peptide from pine nut protein, reduced MDA content in H₂O₂-treated HepG2 cells (Liang, Zhang, & Lin, 2017). Finally, IYVVDLR, IYVFVR, VVFVDRL, VIYVVDLR are four soybean peptides, which modulate both MDA and ROS level in H₂O₂-treated Caco-2 cells (Zhang et al., 2019).

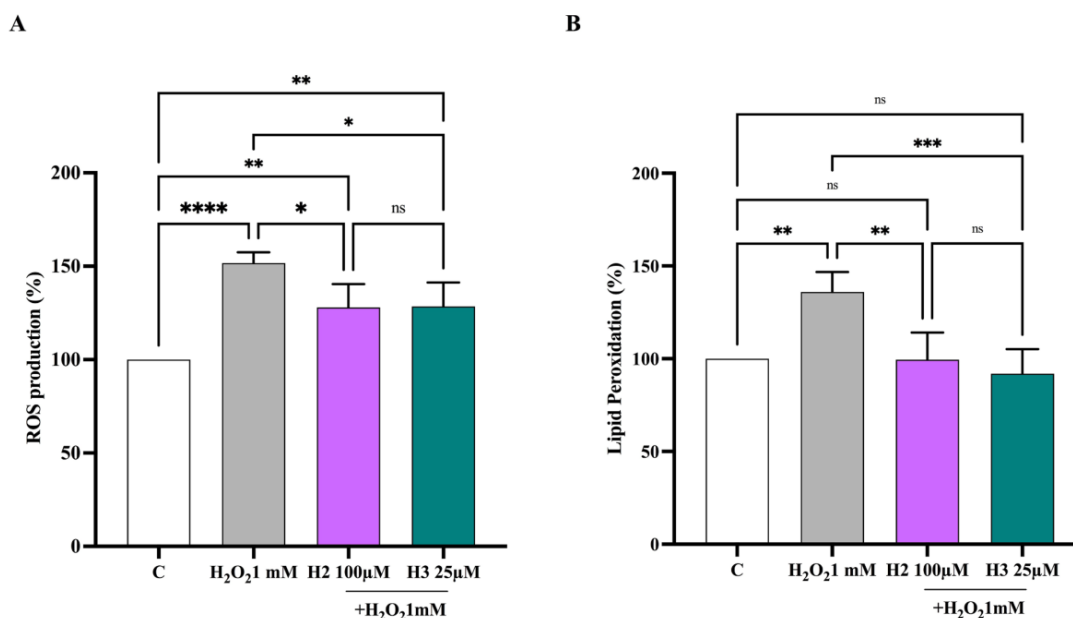


Figure 5.4 H2 and H3 peptides reduce the H₂O₂ (1 mM)-induced ROS levels in HepG2 cells (A). H2 and H3 peptides decrease the lipid peroxidation in the same cells after oxidative stress induction by H₂O₂ (B). Data represent the mean ± s.d. of six independent experiments performed in triplicate. All the data sets were analyzed by One-way ANOVA followed by Tukey’s post-hoc test. C: control sample; ns: not significant. (*) $p < 0.5$; (**) $p < 0.01$; (***) $p < 0.001$; (****) $p < 0.0001$.

5.3.5 H2 and H3 mediate antioxidant activity through the Nrf-2 pathway modulation

Nuclear factor erythroid 2-related factor 2 (Nrf-2)/antioxidant response elements (ARE) signaling plays a crucial role in the protection against oxidative stress and is responsible for the maintenance of homeostasis and redox balance in cells and tissue. Indeed, the Kelch-like ECH associated protein 1 (Keap1)-Nrf2 signaling pathway is considered one of the plausible antioxidant mechanisms of peptides *in vivo*. Nrf-2 regulates cellular responses against environmental stresses and is bound to Keap1 in

the cytoplasm under basal conditions. However, during oxidative stress conditions, Nrf-2 is released from Keap1 and translocated into the nucleus, where it binds to AREs and upregulates target genes, such as superoxide dismutase, catalase and glutathione, that are cellular antioxidant enzymes expected to protect cells from oxidative stress (Saha, Buttari, Panieri, Profumo, & Saso, 2020). To assess the effects of H2 and H3 on the Nrf-2-pathway, western blotting experiments were performed. Our findings indicated that after the treatment of HepG2 cells with H₂O₂ (1 mM), a significant decrease of Nrf-2 protein level by $25.3 \pm 10.8\%$ was observed versus control cells (**Fig. 5.5A-C**). The pretreatment with H2 and H3 produce antioxidant activity through the Nrf-2 pathway modulation in H₂O₂ treated HepG2 cells. In facts, H2 increased the Nrf-2 protein levels up to $126.1 \pm 19.7\%$ at 100 μ M (**Fig. 5.5A and 5.5C**), whereas H3 up to $115.4 \pm 12.7\%$ at 25 μ M (**Fig. 5.5 B, C**). Statistical analysis confirms that also in this case, H3 is 4-fold more active than H2, since any difference was observed between both peptides (**Fig. 5.5 C**). Moreover, it clearly appears that at 100 μ M H2 is able to increase the Nrf-2 protein level more than basal condition (C) even in the presence of H₂O₂ (**Fig. 5.5A and C**). Recently, Oryza Peptide-P60 (OP60), a commercial rice peptide, has been reported to increase intracellular glutathione levels and the evaluation of the mechanisms underlying the antioxidant potential of this peptide in HepG2 cells suggests that OP60 reduced the oxidant stress induced by H₂O₂ via the Nrf-2 signaling pathway (Moritani et al., 2020).

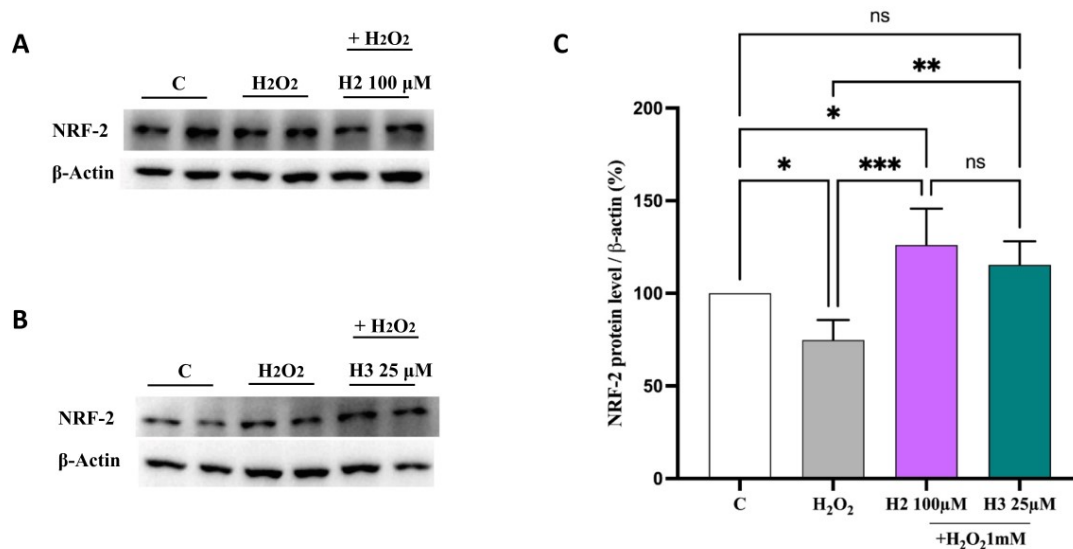


Figure 5.5 Effect of H2 (A, C) and H3 (B, C) peptides on the H₂O₂ (1 mM)-induced Nrf-2 levels in human hepatic HepG2 cells. The data points represent the averages ± s.d. of six independent experiments in duplicate. All data sets were analyzed by One-way ANOVA followed by Tukey's post-hoc test. C: control sample; ns: not significant; (*) $p < 0.5$, (**) $p < 0.01$, (***) $p < 0.001$.

5.3.6 H2 and H3 modulate the H₂O₂-induced NO level production via the iNOS protein modulation in HepG2 cells

Imbalanced ROS levels not only do impair the stability of intracellular macromolecules (such as DNA, proteins, and lipids) but also may react with NO leading to the production of peroxynitrite (ONOO⁻), which reduces the bioavailability of NO, which is a potent vasorelaxant signaling messenger in vascular system (Beckman, 1996; Shi et al., 2004). Increased oxidative stress and its downstream effects can lead to various conditions such as cardiovascular diseases (D'Oria et al., 2020).

Based on these considerations, the effects of both H2 and H3 on NO production were evaluated on human hepatic HepG2 cells after oxidative stress induction. Notably, H₂O₂ (1 mM) treatment induced an oxidative stress that led to an increase of intracellular NO levels up to $110 \pm 3.9\%$ (Fig. 5.6A). Pre-treatment with H2 and H3 reduced the H₂O₂-induced NO overproduction, reducing their values closer than the basal levels (Fig. 5.6A). In particular, H2 reduced the NO overproduction up to $96.2 \pm$

0.8%, whereas H3 up to $105.1 \pm 1.2\%$.

iNOS, is an enzyme expressed in different cell types (Soskić et al., 2011) and it is usually induced during inflammatory events (Habib & Ali, 2011). The generation of NO by iNOS is associated with the alteration of NO homeostasis, which is linked to many pathophysiological conditions. In this study, the effect of H2 and H3 on iNOS protein levels was assessed after oxidative stress induction by western blot experiments, in which the iNOS protein band at 130 kDa was detected and quantified (Fig. 5.6B-D). Results suggest that after H₂O₂ treatment (1 mM), the iNOS protein increased up to $147.8 \pm 18.6\%$ in HepG2 cells. In agreement with the modulation of NO production, pre-treatment of HepG2 cells with both peptides reduced the H₂O₂-induced iNOS protein, bringing their levels close to basal conditions. In particular, H2 reduced the iNOS levels up to $100.9 \pm 13.3\%$ at 100 μM (Fig. 5.6B, D), whereas H3 reduced up to $98.3 \pm 13.6\%$ at 25 μM (Fig. 5.6C, D).

Recent pieces of evidence suggest that many bioactive peptides from different food sources exert both antioxidants and anti-inflammatory activities through the modulation of NO levels via iNOS pathway regulation after oxidative stress induction (Zhu et al., 2020), suggesting a potential interplay of both antioxidant and anti-inflammatory activities exerted by these two peptides.

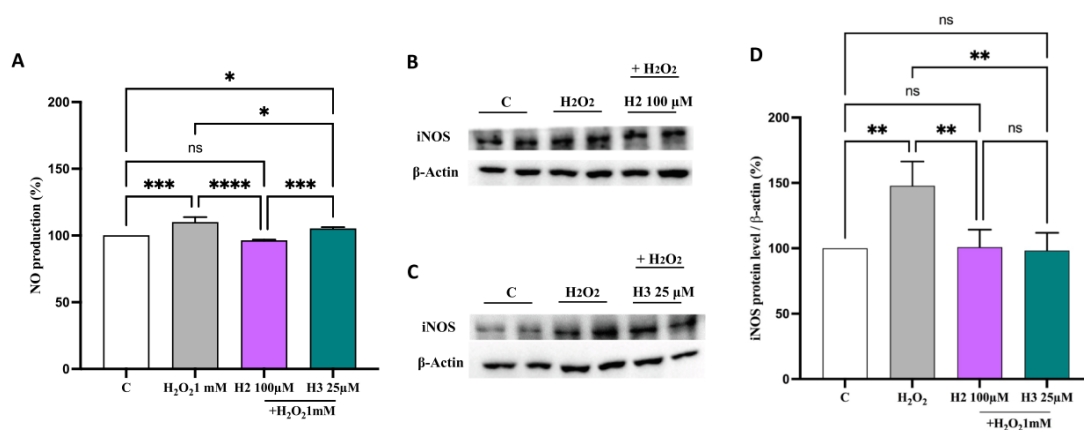


Figure 5.6 Effect of H2 and H3 peptides on the H₂O₂ (1 mM)-induced NO production (A) and inducible nitric oxide synthase (iNOS) protein levels (B–D) in human hepatic HepG2 cells. The data points represent the averages \pm s.d. of six independent experiments in duplicate. All data sets

were analyzed by One-way ANOVA followed by Tukey's post-hoc test. C: control sample; ns: not significant; (**) $p < 0.01$.

5.4 Conclusions

Antioxidant peptides are considered new useful tools for the prevention and treatment of multifactorial disease in which oxidative stress plays a relevant role. Whereas most published studies on antioxidant peptides restrain the evaluation to the application of chemical assays, here an integrated approach was applied that allowed the identification of two bioavailable hempseed peptides that are able to exert their antioxidant activity also in HepG2 cells where the oxidative stress had been induced by a H₂O₂ treatment (Fig. 5.7). Overall, our strategy focuses on the use of differentiated Caco-2 monolayer as a “natural sieve of bioavailable species”, which permits to identify few hempseeds absorbable peptides, whose antioxidant activity was investigated *in vitro* by using chemical and cell-based techniques. Indeed, this strategy permits to overcome the very crucial issue of bioavailability and the combination of *in vitro* biochemical and cellular assays represents a suitable approach for reducing the *in vivo* assays, which involve high costs and arise ethical issues for the excessive use of animals for routine research.

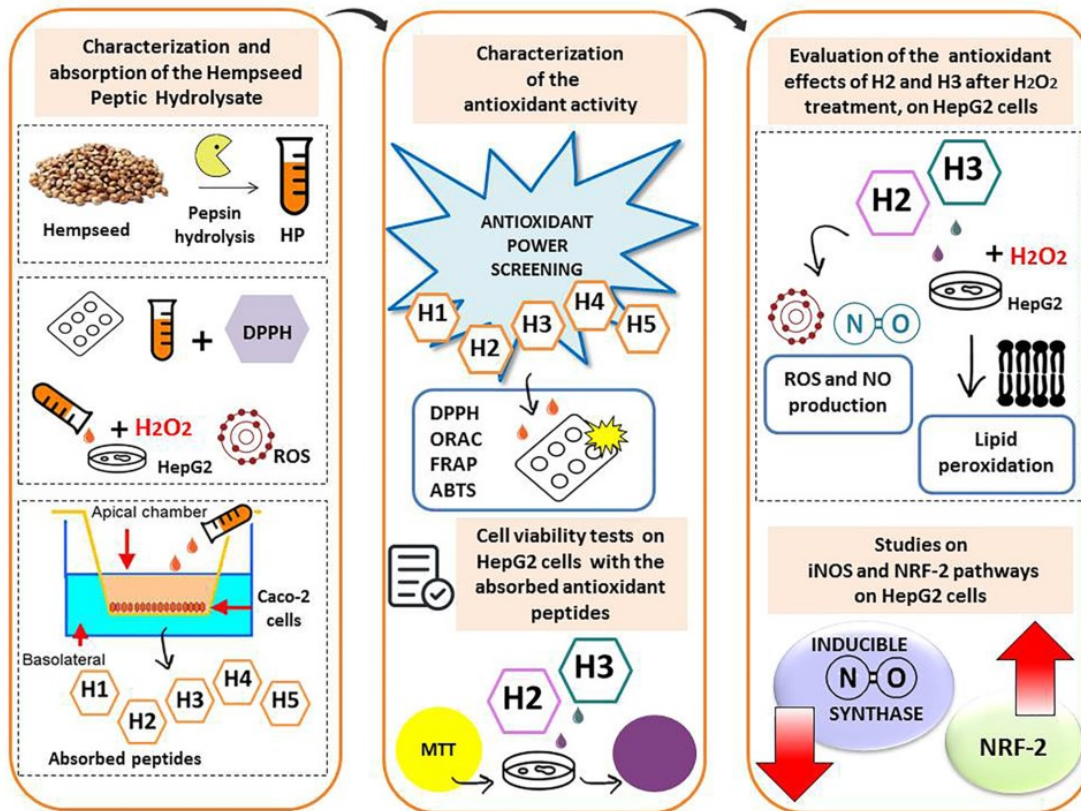


Figure 5.7 Flow chart which summarizes the strategy of the work.

5.5 Supporting information

HPLC-Chip-MS/MS analysis and data elaboration

The HP hydrolysate after the incubation on Caco-2 cells was collected from AP and BL chambers (500 μ L and 700 μ L, respectively), then both AP and BL samples were freeze-dried and residues were solubilized in HPLC water (100 μ L). Samples were purified by ultrafiltration, using membranes with a 3 kDa molecular weight cutoff (MWCO) (Millipore, USA). Filtered peptide mixtures were analyzed on a SL IT mass spectrometer interfaced with a HPLC-Chip Cube source (Agilent Technologies, Palo Alto, CA, USA). The peptides were enriched on 40 nL enrichment column (Zorbax 300SB-C18, 5 μ m pore size), and separated on a 43 mm \times 75 μ m analytical column (Zorbax 300SB-C18, 5 μ m pore size). The samples (5 μ L), acidified with formic acid, were loaded onto the enrichment column at a flow rate 3 μ L/min using isocratic 100% C solvent phase (99% water, 1% ACN and 0.1% formic acid). AP and BL peptides were eluted at the constant flow rate of 300 nL/min. The LC solvent A was 95% water, 5% ACN, 0.1% formic acid; solvent B was 5% water, 95% ACN, 0.1% formic acid. The nano-pump gradient program was as follows: 5% solvent B (0 min), 50% solvent B (0–50 min), 95% solvent B (50–60 min) and back to 5% in 10 min. The drying gas temperature was 300 $^{\circ}$ C, flow rate 3 L/min (nitrogen). Data were acquired in positive ionization mode, by applying a capillary voltage at -1950 V, and by acquiring the MS spectra in the mass range from m/z 300–2200, with target mass 700 m/z , average of 2 spectra, ICC target 30,000, and maximum accumulation time 150 ms. LC/MS analysis was performed in data dependent acquisition Auto MS(n) mode.

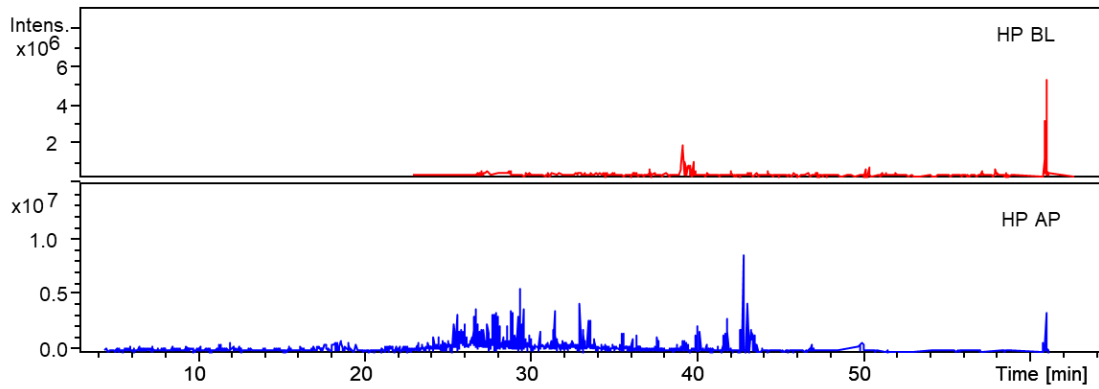


Figure 5-S1: HPLC-MS/MS analyses of the basolateral and apical solutions. Total Ion current chromatograms of the hempseed peptides identified in the basolateral (BL) and apical (AP) solutions.

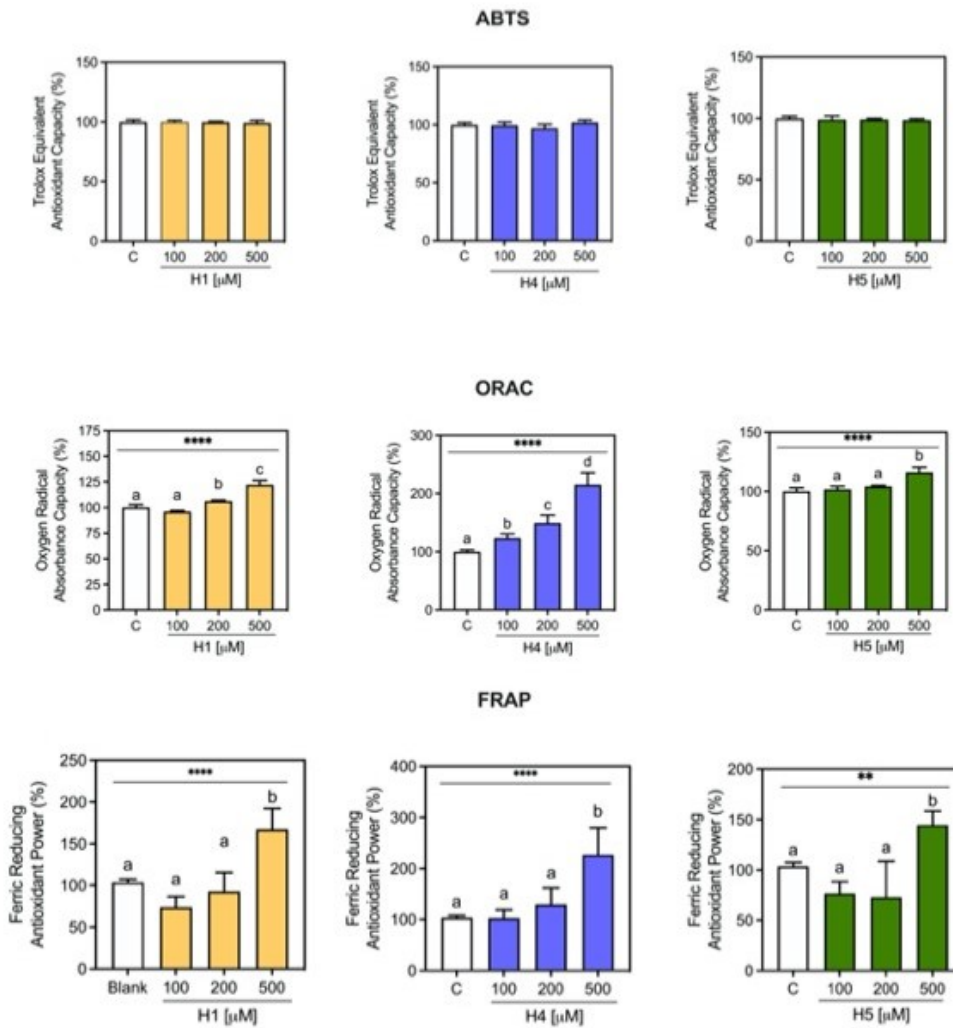


Figure 5-S2 Antioxidant scavenger activity of H1, H4, and H5 by ABTS, ORAC, and FRAP. Bars represent the mean \pm s.d. of three independent experiments performed in triplicate.

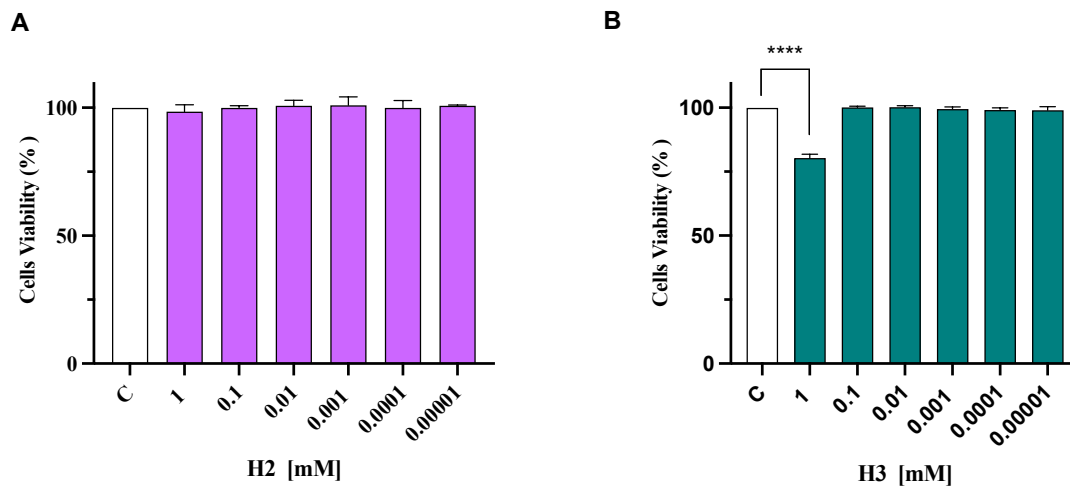


Figure 5-S3 Effect of H2 (A) and H3 (B) on the HepG2 cell viability evaluated by MTT experiments. Bars represent the mean \pm s.d. of three independent experiments performed in triplicate and stastically analysed by One-way Anova followed by Tukey's post-hoc test. (****, $p < 0.0001$).

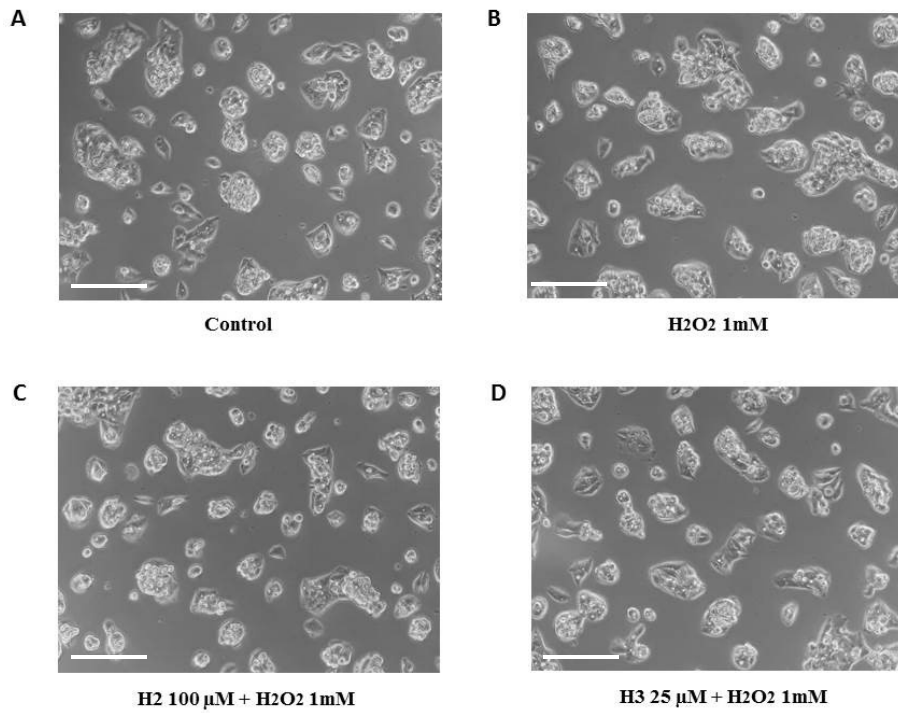


Figure 5-S4 Morphological investigation by inverted microscope (Zeiss, 10 ×) of HepG2 cells treated w/o (A) and with H₂O₂ (1mM) for 1 h (B) and pre-treated with both H₂ (100 μM, C) and H₃ (25 μM, D) for 24 h and then treated with H₂O₂ (1mM) for 1h.

5.6 Reference

- Beckman, J. S. (1996). Oxidative damage and tyrosine nitration from peroxynitrite. *Chemical Research in Toxicology*, 9(5), 836–844. <https://doi.org/10.1021/tx9501445>.
- Callaway, J. C. (2004). Hempseed as a nutritional resource: An overview. *Euphytica*, 140 (1–2), 65–72. <https://doi.org/10.1007/s10681-004-4811-6>.
- D’Oria, R., Schipani, R., Leonardini, A., Natalicchio, A., Perrini, S., Cignarelli, A., Giorgino, F. (2020). The role of oxidative stress in cardiac disease: from physiological response to injury factor. *Oxidative Medicine and Cellular Longevity*, 2020, 1–29. <https://doi.org/10.1155/2020/5732956>.
- Daniel, H. (2004). Molecular and integrative physiology of intestinal peptide transport. *Annual Review of Physiology*, 66(1), 361–384. <https://doi.org/10.1146/annurev.physiol.66.032102.144149>.
- Farinon, B., Molinari, R., Costantini, L., & Merendino, N. (2020). The seed of industrial hemp. *Nutrients*, 12(7). <https://doi.org/10.3390/nu12071935>.
- Ferruzza, S., Rossi, C., Sambuy, Y., & Scarino, M. L. (2013). Serum-reduced and serum-free media for differentiation of Caco-2 cells. *ALTEX*, 30(2), 159–168. <https://doi.org/10.14573/altex.2013.2.159>.
- Ferruzza, S., Scarino, M. L., Gambling, L., Natella, F., & Sambuy, Y. (2003). Biphasic effect of iron on human intestinal Caco-2 cells: Early effect on tight junction permeability with delayed onset of oxidative cytotoxic damage. *Cellular and Molecular Biology (Noisy-le-grand)*, 49(1), 89–99.
- Gallego, M., Mora, L., & Toldra, F. (2018). Characterisation of the antioxidant peptide AEEEYPDL and its quantification in Spanish dry-cured ham. *Food Chemistry*, 258, 8–15. <https://doi.org/10.1016/j.foodchem.2018.03.035>.
- Girgih, A. T., He, R., & Aluko, R. E. (2014). Kinetics and molecular docking studies of the inhibitions of angiotensin converting enzyme and renin activities by hemp seed (*Cannabis sativa* L.) peptides. *Journal of Agricultural and Food Chemistry*, 62(18), 4135–4144. <https://doi.org/10.1021/jf5002606>.
- Girgih, A. T., He, R., Malomo, S., Offengenden, M., Wu, J., & Aluko, R. E. (2014). Structural and functional characterization of hemp seed (*Cannabis sativa* L.) protein-derived antioxidant and

- antihypertensive peptides. *Journal of Functional Foods*, 6, 384–394. <https://doi.org/10.1016/j.jff.2013.11.005>.
- Girgih, A. T., Udenigwe, C. C., & Aluko, R. E. (2011). *In Vitro* Antioxidant Properties of Hemp Seed (*Cannabis sativa* L.) Protein Hydrolysate Fractions. *Journal of the American Oil Chemists Society*, 88(3), 381–389. <https://doi.org/10.1007/s11746-010-1686-7>.
- Habib, S., & Ali, A. (2011). Biochemistry of nitric oxide. *Indian Journal of Clinical Biochemistry*, 26(1), 3–17. <https://doi.org/10.1007/s12291-011-0108-4>.
- Harnedy, P. A., O’Keeffe, M. B., & FitzGerald, R. J. (2017). Fractionation and identification of antioxidant peptides from an enzymatically hydrolysed *Palmaria palmata* protein isolate. *Food Research International*, 100, 416–422. <https://doi.org/10.1016/j.foodres.2017.07.037>.
- Jiang, Y., Zhao, D., Sun, J., Luo, X., Li, H., Sun, X., & Zheng, F. (2019). Analysis of antioxidant effect of two tripeptides isolated from fermented grains (Jiupei) and the antioxidative interaction with 4-methylguaiacol, 4-ethylguaiacol, and vanillin. *Food Science & Nutrition*, 7(7), 2391–2403. <https://doi.org/10.1002/fsn3.2019.7.issue-710.1002/fsn3.1100>.
- Jin, D. X., Liu, X. L., Zheng, X. Q., Wang, X. J., & He, J. F. (2016). Preparation of antioxidative corn protein hydrolysates, purification and evaluation of three novel corn antioxidant peptides. *Food Chemistry*, 204, 427–436. <https://doi.org/10.1016/j.foodchem.2016.02.119>.
- Kedare, S. B., & Singh, R. P. (2011). Genesis and development of DPPH method of antioxidant assay. *Journal of Food Science and Technology*, 48(4), 412–422. <https://doi.org/10.1007/s13197-011-0251-1>.
- Lammi, C., Aiello, G., Boschin, G., & Arnoldi, A. (2019). Multifunctional peptides for the prevention of cardiovascular disease: A new concept in the area of bioactive food-derived peptides. *Journal of Functional Foods*, 55, 135–145. <https://doi.org/10.1016/j.jff.2019.02.016>.
- Lammi, C., Aiello, G., Vistoli, G., Zanoni, C., Arnoldi, A., Sambuy, Y., Ranaldi, G. (2016). A multidisciplinary investigation on the bioavailability and activity of peptides from lupin protein. *Journal of Functional Foods*, 24, 297–306. <https://doi.org/10.1016/j.jff.2016.04.017>.
- Lammi, C., Bollati, C., & Arnoldi, A. (2019). Antioxidant activity of soybean peptides on human hepatic HepG2 cells. *Journal of Food Bioactives*, 7(2019).
- Lammi, C., Bollati, C., Gelain, F., Arnoldi, A., & Pugliese, R. (2019). Enhancement of the stability and anti-DPPiV activity of hempseed hydrolysates through self-assembling peptide-based

hydrogels. *Frontiers in Chemistry*, 6.
<https://doi.org/10.3389/fchem.2018.00670>.
<https://doi.org/10.3389/fchem.2018.00670.s001>.

Liang, R., Zhang, Z. M., & Lin, S. Y. (2017). Effects of pulsed electric field on intracellular antioxidant activity and antioxidant enzyme regulating capacities of pine nut (*Pinus koraiensis*) peptide QDHCH in HepG2 cells. *Food Chemistry*, 237, 793–802.
<https://doi.org/10.1016/j.foodchem.2017.05.144>.

Malomo, S. A., & Aluko, R. E. (2016). *In vitro* acetylcholinesterase-inhibitory properties of enzymatic hemp seed protein hydrolysates. *Journal of the American Oil Chemists Society*, 93(3), 411–420. <https://doi.org/10.1007/s11746-015-2779-0>.

Malomo, S. A., Onuh, J. O., Girgih, A. T., & Aluko, R. E. (2015). Structural and antihypertensive properties of enzymatic hemp seed protein hydrolysates. *Nutrients*, 7(9), 7616–7632.
<https://doi.org/10.3390/nu7095358>.

Miguel, M., Davalos, A., Manso, M. A., de la Pena, G., Lasuncion, M. A., & Lopez-Fandino, R. (2008). Transepithelial transport across Caco-2 cell monolayers of antihypertensive egg-derived peptides. PepT1-mediated flux of Tyr-Pro-Ile. *Molecular Nutrition & Food Research*, 52(12), 1507–1513. <https://doi.org/10.1002/mnfr.200700503>.

Moritani, C., Kawakami, K., Shimoda, H., Hatanaka, T., Suzaki, E., & Tsuboi, S. (2020). Protective effects of rice peptide oryza peptide-P60 against oxidative injury through activation of Nrf2 signaling pathway *in vitro* and *in vivo*. *Acs Omega*, 5(22), 13096–13107.
<https://doi.org/10.1021/acsomega.0c01016>.

Nwachukwu, I. D., & Aluko, R. E. (2018). Antioxidant properties of flaxseed protein hydrolysates: influence of hydrolytic enzyme concentration and peptide size. *Journal of the American Oil Chemists Society*, 95(8), 1105–1118. <https://doi.org/10.1002/aocs.12042>.

Nwachukwu, I. D., & Aluko, R. E. (2019). Structural and functional properties of food protein-derived antioxidant peptides. *Journal of Food Biochemistry*, 43(1), e12761.
<https://doi.org/10.1111/jfbc.12761>.

Rodriguez-Martin, N. M., Toscano, R., Villanueva, A., Pedroche, J., Millan, F., Montserrat-de la Paz, S., & Millan-Linares, M. C. (2019). Neuroprotective protein hydrolysates from hemp (*Cannabis sativa* L.) seeds. *Food & Function*, 10(10), 6732–6739. <https://doi.org/10.1039/c9fo01904a>.

Sae-Leaw, T., Karnjanapratum, S., O’Callaghan, Y. C., O’Keeffe, M. B., FitzGerald, R. J., O’Brien, N.

- M., & Benjakul, S. (2017). Purification and identification of antioxidant peptides from gelatin hydrolysate of seabass skin. *Journal of Food Biochemistry*, 41 (3), e12350. <https://doi.org/10.1111/jfbc.2017.41.issue-310.1111/jfbc.12350>.
- Saha, S., Buttari, B., Panieri, E., Profumo, E., & Saso, L. (2020). An overview of Nrf2 signaling pathway and its role in inflammation. *Molecules*, 25(22), 5474. <https://doi.org/10.3390/molecules25225474>.
- Sheng, J., Yang, X., Chen, J., Peng, T., Yin, X., Liu, W., Yang, X. (2019). Antioxidative effects and mechanism study of bioactive peptides from defatted walnut (*Juglans regia* L.) meal hydrolysate. *Journal of Agricultural and Food Chemistry*, 67(12), 3305–3312. <https://doi.org/10.1021/acs.jafc.8b0572210.1021/acs.jafc.8b05722.s001>.
- Shi, J., Arunasalam, K., Yeung, D., Kakuda, Y., Mittal, G., & Jiang, Y. (2004). Saponins from edible legumes: Chemistry, processing, and health benefits. *Journal of medicinal food*, 7(1), 67–78.
- Soskić, S. S., Dobutović, B. D., Sudar, E. M., Obradović, M. M., Nikolić, D. M., Djordjević, J. D., ... Isenović, E. R. (2011). Regulation of inducible nitric oxide synthase (iNOS) and its potential role in insulin resistance, diabetes and heart failure. *Open Cardiovascular Medicine Journal*, 5, 153–163. <https://doi.org/10.2174/1874192401105010153>.
- Wang, F., Weng, Z., Lyu, Y.i., Bao, Y., Liu, J., Zhang, Y.u., ... Shen, X. (2020). Wheat germ-derived peptide ADWGGPLPH abolishes high glucose-induced oxidative stress via modulation of the PKC ζ /AMPK/NOX4 pathway. *Food & Function*, 11(8), 6843–6854. <https://doi.org/10.1039/D0FO01229G>.
- Wang, W. Y., Zhao, Y. Q., Zhao, G. X., Chi, C. F., & Wang, B. (2020). Antioxidant peptides from collagen hydrolysate of redlip croaker. *Mar Drugs*, 18(3). <https://doi.org/10.3390/md18030156>.
- Xu, Q., Yan, X., Zhang, Y., & Wu, J. (2019). Current understanding of transport and bioavailability of bioactive peptides derived from dairy proteins: A review. *International Journal of Food Science and Technology*, 54(6), 1930–1941. <https://doi.org/10.1111/ijfs.2019.54.issue-610.1111/ijfs.14055>.
- Zanoni, C., Aiello, G., Arnoldi, A., & Lammi, C. (2017). Hempseed peptides exert hypocholesterolemic effects with a statin-like mechanism. *Journal of Agricultural and Food Chemistry*, 65(40), 8829–8838. <https://doi.org/10.1021/acs.jafc.7b02742>.

- Zhang, Q., Tong, X., Li, Y., Wang, H., Wang, Z., Qi, B., Jiang, L. (2019). Purification and characterization of antioxidant peptides from alcalase-hydrolyzed soybean (*Glycine max* L.) hydrolysate and their cytoprotective effects in human intestinal caco-2 cells. *Journal of Agricultural and Food Chemistry*, 67(20), 5772–5781. <https://doi.org/10.1021/acs.jafc.9b01235>.
<https://doi.org/10.1021/acs.jafc.9b01235.s001>.
- Zhu, W., Ren, L., Zhang, L.i., Qiao, Q., Farooq, M. Z., & Xu, Q. (2020). The potential of food protein-derived bioactive peptides against chronic intestinal inflammation. *Mediators of Inflammation*, 2020, 1–15. <https://doi.org/10.1155/2020/6817156>.

CHAPTER 6

MANUSCRIPT 4

HEMPSEED (*CANNABIS SATIVA*) PEPTIDES WVSPLAGRT AND IGFLIIWV EXERT ANTI-INFLAMMATORY ACTIVITY IN THE LPS-STIMULATED HUMAN HEPATIC CELL LINE

Ivan Cruz-Chamorro¹, Guillermo Santos-Sánchez¹, Carlotta Bollati²,
Martina Bartolomei², **Jianqiang Li**², Anna Arnoldi², and Carmen
Lammi^{2*}

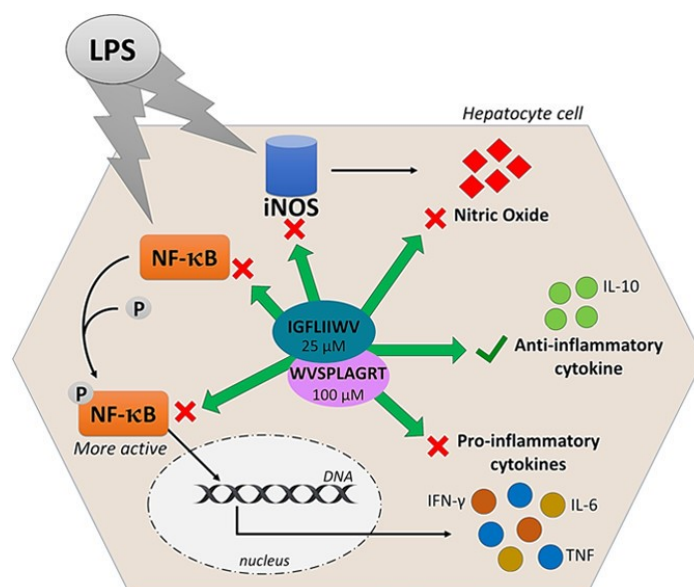
¹Department of Pharmaceutical Sciences, University of Milan, 20122 Milan, Italy

²Departamento de Bioquímica Médica y Biología Molecular e Inmunología,
Universidad de Sevilla, 41009 Seville, Spain

Author Contributions: Conceptualization, C.L.; methodology, I.C.-C., G.S.-S., C.B., M.B. and J.L.; investigation, I.C.-C., G.S.-S., C.B., M.B., J.L. and C.L.; data curation, C.L. and I.C.-C.; writing—original draft, I.C.-C., G.S.-S., C.B., M.B., J.L. and C.L.; writing—review & editing, C.L. and A.A.; supervision, C.L.; project administration, C.L.; funding acquisition, C.L., I.C.-C. and A.A.

6. Abstract

WVSPLAGRT (H2) and IGFLIIWV (H3) are two transepithelial transported intestinal peptides obtained from the hydrolysis of hempseed protein with pepsin, which exert antioxidant activity in HepG2 cells. Notably, both peptides reduce the H₂O₂-induced reactive oxygen species, lipid peroxidation, and nitric oxide (NO) production levels in HepG2 cells via the modulation of the nuclear factor erythroid 2-related factor 2 and the inducible nitric oxide synthase (iNOS) pathways, respectively. Due to the close link between inflammation and oxidative stress and with the objective of fostering the multifunctional behavior of bioactive peptides, in this study, the molecular characterization of the anti-inflammatory and immunomodulatory properties of H2 and H3 was carried out in HepG2 cells. In fact, both peptides were shown to modulate the production of pro (IFN- γ : $-33.0 \pm 6.7\%$ H2, $p = 0.011$; $-13.1 \pm 2.0\%$ H3, $p = <0.0001$; TNF: $-17.6 \pm 1.7\%$ H2, $p = 0.0004$; $-20.3 \pm 1.7\%$ H3, $p = <0.0001$; and IL-6: $-15.1 \pm 6.5\%$ H3, $p = 0.010$) and anti (IL-10: $+9.6 \pm 3.1\%$ H2, $p = 0.010$; $+26.0 \pm 2.3\%$ H3, $p = <0.0001$)-inflammatory cytokines and NO ($-9.0 \pm 0.7\%$ H2, $p = <0.0001$; $-7.2 \pm 1.8\%$ H3, $p = <0.0001$) through regulation of the NF- κ B and iNOS pathways, respectively, in HepG2 cells stimulated by lipopolysaccharides.



6.1 Introduction

Cannabis sativa L. is a plant belonging to the *Cannabis* genus that has been used for medicinal purposes for hundreds of years (Hartsel, Eades, Hickory, & Makriyannis, 2016; Thomas & ElSohly, 2016). Its species present different levels of Δ^9 -tetrahydrocannabinol, the main psychoactive component that causes cognitive effects and euphoria (Cascini & Boschi, 2017). The non-drug variety (also called “hemp”) is successfully used for industrial food industrial applications (i.e., nutritional supplements, fiber, and oil production) due to its quality nutritional composition (Frag & Kayser, 2017; Farinon, Molinari, Costantini, & Merendino, 2020). The hempseed is characterized by its high protein (20–25%) and oil content (more than 30%) as well as a complete profile of vitamins and minerals. Furthermore, its proteins (principally edestin and albumin) are easily digested and rich in essential amino acids, making hempseed an important source of bioactive peptides (Aiello, Lammi, Boschini, Zanoni, & Arnoldi, 2017; X.-S. Wang, Tang, Yang, & Gao, 2008). Indeed, extensive studies have been carried out in order to investigate the multifunctional bioactive properties of hempseed peptides (Farinon, Molinari, Costantini, & Merendino, 2020), demonstrating their antioxidant (Girgih, He, Malomo, Offengenden, Wu, & Aluko, 2014; Girgih, Udenigwe, & Aluko, 2011, 2013; Tang, Wang, & Yang, 2009; Teh, Bekhit, Carne, & Birch, 2016; X.-S. Wang, Tang, Chen, Yang, & Biotechnology, 2009), hypotensive (Malomo & Aluko, 2016; Orio, Boschini, Recca, Morelli, Ragona, Francescato, et al., 2017; Teh, Bekhit, Carne, & Birch, 2016), antiproliferative (Logarušić, Slivac, Radošević, Bagović, Redovniković, & Srček, 2019), anti-inflammatory (Rodriguez-Martin, Montserrat-de la Paz, Toscano, Grao-Cruces, Villanueva, Pedroche, et al., 2020; S. Wang, Luo, & Fan, 2019), and neuroprotective properties (Rodriguez-Martin, Toscano, Villanueva, Pedroche, Millan, Montserrat-de la Paz, et al., 2019). Recently, our group has shown that hempseed hydrolysates (HP) produced to digest total protein with pepsin have a hypocholesterolemic effect through the direct ability to reduce the activity of the 3-hydroxy-3-methylglutaryl-coenzyme A reductase enzyme (Lammi, Bollati, Gelain,

Arnoldi, & Pugliese, 2019; Zanoni, Aiello, Arnoldi, & Lammi, 2017), which in turn leads to the activation of the low-density lipoprotein (LDL) receptor with the following improvement in the hepatic cells' ability to absorb extracellular LDL (Zanoni, Aiello, Arnoldi, & Lammi, 2017). In addition, HP reduces the activity of the dipeptidyl peptidase-IV (DPP-IV) *in vitro* and in human intestinal Caco-2 cells, suggesting a potential anti-diabetic effect (Lammi, Bollati, Gelain, Arnoldi, & Pugliese, 2019). Recent experiments using intestinal trans-epithelial transport revealed that among the peptides contained within HP able to pass through the mature Caco-2 cell barrier, H2 (WVSPLAGRT) and H3 (IGFLIIWV) exert antioxidant activity in HepG2 cells. Specifically, we observed that H2 and H3 reduce the level of reactive oxygen species (ROS), lipid peroxidation, and nitric oxide (NO) production. Furthermore, H2 and H3 modulate the nuclear factor erythroid 2-related factor 2 (Nrf-2) and inducible nitric oxide synthase (iNOS) pathways in H₂O₂-stimulated HepG2 cells (Bollati, Cruz-Chamorro, Aiello, Li, Bartolomei, Santos-Sánchez, et al., 2022). In light of these observations and considering that there is a close link between inflammation and oxidative stress, the main objective of the present study was the evaluation of the anti-inflammatory effect of peptides H2 and H3 in HepG2 cells. Therefore, since the nuclear factor- κ B (NF- κ B) pathway is the main component implicated in the pro-inflammatory response (Liu, Zhang, Joo, & Sun, 2017), the effects of H2 and H3 on the NF- κ B and its more active phosphorylated form (p(Ser276)NF- κ B) protein levels in lipopolysaccharide (LPS)-stimulated HepG2 cells were characterized at a deeper level. Hence, the effect of both peptides on the modulation of the cellular pro (IFN- γ , TNF, and IL-6)- and anti (IL-10)-inflammatory cytokine production was evaluated. Finally, in parallel, the effects of H2 and H3 on the NO pathway, which plays a central role in inflammatory disorders (Zamora, Vodovotz, & Billiar, 2000), were investigated.

6.2 Material and methods

6.2.1 Chemicals and Reagents

All reagents and solvents were purchased from commercial sources and used without further purification. For further details, see the Supporting Information. The peptides were purchased from GenScript Biotech Corporation (Piscataway, NJ, USA). The purity of lyophilized peptides (>95%) was tested using a binary high-performance liquid chromatograph and an Agilent 6520 LCMS mass spectrometer (**Figure 6-S1**).

6.2.2 Cell Culture and Western Blot

A total of 1.5×10^5 HepG2 cells/well were seeded in 24-well plates and incubated at 37 °C under a 5% CO₂ atmosphere. The following day, the cells were stimulated with 1 µg/mL LPS or vehicle (H₂O) and treated with 100 µM H2 or 25 µM H3 peptides in a complete growth medium (10% fetal bovine serum, 100 U/mL penicillin, and 100 µg/mL streptomycin) for another 48 h. Finally, the supernatant was collected and stored at -20 °C for subsequent cytokine and NO quantification.

The cells were scraped in 40 µL of ice-cold lysis buffer (RIPA buffer + protease inhibitor cocktail (Roche, Base, Swiss) + 1:100 PMSF + 1:100 Na-orthovanadate + 1:1000 β-mercaptoethanol) and transferred to ice-cold microcentrifuge tubes. After centrifugation at 13,300 g for 15 min, the supernatants were recovered for Western Blot analysis. The total protein concentration was determined by Bradford's method. 50 µg of proteins was separated on a precast 7.5% sodium dodecyl sulfate-polyacrylamide gel in the presence of a reducing agent (β-mercaptoethanol), transferred to a nitrocellulose membrane (Mini nitrocellulose Transfer Packs, Biorad, Hercules, CA, USA), and stained with Ponceau red solution. Later, milk/BSA blocked membranes were incubated with primary antibodies against iNOS, NF-κB, phosphor(Ser276)-NF-κB (p(Ser276)NF-κB), and β-actin (more details in Supporting Information **Table 6-S1**). Membranes were incubated overnight at 4 °C and consequently with the horseradish peroxidase-conjugated secondary antibody. Finally, target proteins were detected with enhanced chemiluminescence (Euro-clone, Milan,

Italy), and densitometric analysis was performed using Image Lab Software (Biorad).

6.2.3 Cytokine Quantification

Cytokine quantification was performed using a human Quantikine ELISA kit (R&D Systems, Minneapolis, MN, USA) according to the manufacturer's instructions. Briefly, the supernatant was incubated in 96-well microplates coated with a monoclonal antibody for 2 h. After washing the wells, the human polyclonal antibody conjugated with horseradish peroxidase was added for another 2 h. The wells were washed, and then a substrate solution was added to obtain a color. The reaction was stopped by a stop solution (2 N sulfuric acid), and then the microplate was read to wavelength 450 nm and 540 nm with a Synergy H1 microplate reader (Biotek Instruments, Winooski, VT, USA).

6.2.4 Nitric Oxide Quantification

NO determination was quantified in the supernatants by the Griess test (Sigma-Aldrich, Milan, Italy) according to the manufacturer's instructions. Briefly, 50 μ L of the Griess reagent was incubated with 50 μ L of the culture supernatants for 15 min at room temperature in the dark. Absorbance at 540 nm was then measured using a Synergy H1 microplate reader (Biotek).

6.2.5 Statistical Analysis

The data were presented as the mean \pm the standard deviation (SD) of at least three independent experiments assayed for triplicate. All the data sets were checked for normal distribution by the D'Agostino and Pearson test. Since they are all normally distributed with *p*-values < 0.05, we proceeded with statistical analyses by one-way ANOVA, followed by Tukey's post-hoc tests and using GraphPad Prism 8 (San Diego, CA, USA).

6.3 Results

6.3.1 H2 and H3 Modulate the LPS-Activated NF- κ B Pathway in HepG2 Cells

To investigate the effects of H2 and H3 on the NF- κ B pathway, NF- κ B and p(Ser276)NF- κ B were quantified in LPS-stimulated HepG2 cells. As shown in **Figure 6.1**, the LPS stimulation confirmed the NF- κ B pathway activation, increasing the protein levels of NF- κ B (**Figure 6.1A–C**) and p(Ser276)NF- κ B (**Figure 6.1D–F**) in HepG2 cells up to $150.9 \pm 20.7\%$ ($p < 0.0001$) and $138.0 \pm 24.1\%$ ($p = 0.0008$), respectively. Treatment with H2 and H3 mitigated these effects. In detail, H2 (violet bars) significantly reduced the NF- κ B protein levels by $28.1 \pm 5.5\%$ ($p = 0.034$) at 100 μ M, with respect to LPS-stimulated cells (**Figure 6.1A,C**). Peptide H3 (aquamarine bar) showed a similar effect, reducing the NF- κ B levels by up to $44.3 \pm 11.2\%$ ($p = 0.002$) at 25 μ M (**Figure 6.1B,C**). In addition, both peptides were able to decrease the more active phosphorylated form of NF- κ B (**Figure 6.1D–F**). H2 was able to reduce the p(Ser276)NF- κ B levels by $34.1 \pm 8.5\%$ ($p = 0.013$) at 100 μ M (**Figure 6.1D,F**), while H3 decreased the levels by $57.2 \pm 13.0\%$ ($p = 0.0002$) at 25 μ M (**Figure 6.1E,F**). As shown in **Figure 6.2**, LPS treatment increased the p(Ser276)NF- κ B/NF- κ B ratio up to $137 \pm 37.7\%$ ($p = 0.039$), underlining more activation of NF- κ B, while both peptides were able to decrease this ratio, confirming that these peptides promoted less activation of this pathway. Specifically, H2 decreased the p(Ser276)NF- κ B/NF- κ B ratio by $42.9 \pm 14.0\%$ ($p = 0.046$) at 100 μ M, while H3 reduced this ratio by $54.7 \pm 0.7\%$ ($p = 0.014$) at 25 μ M (**Figure 6.2**).

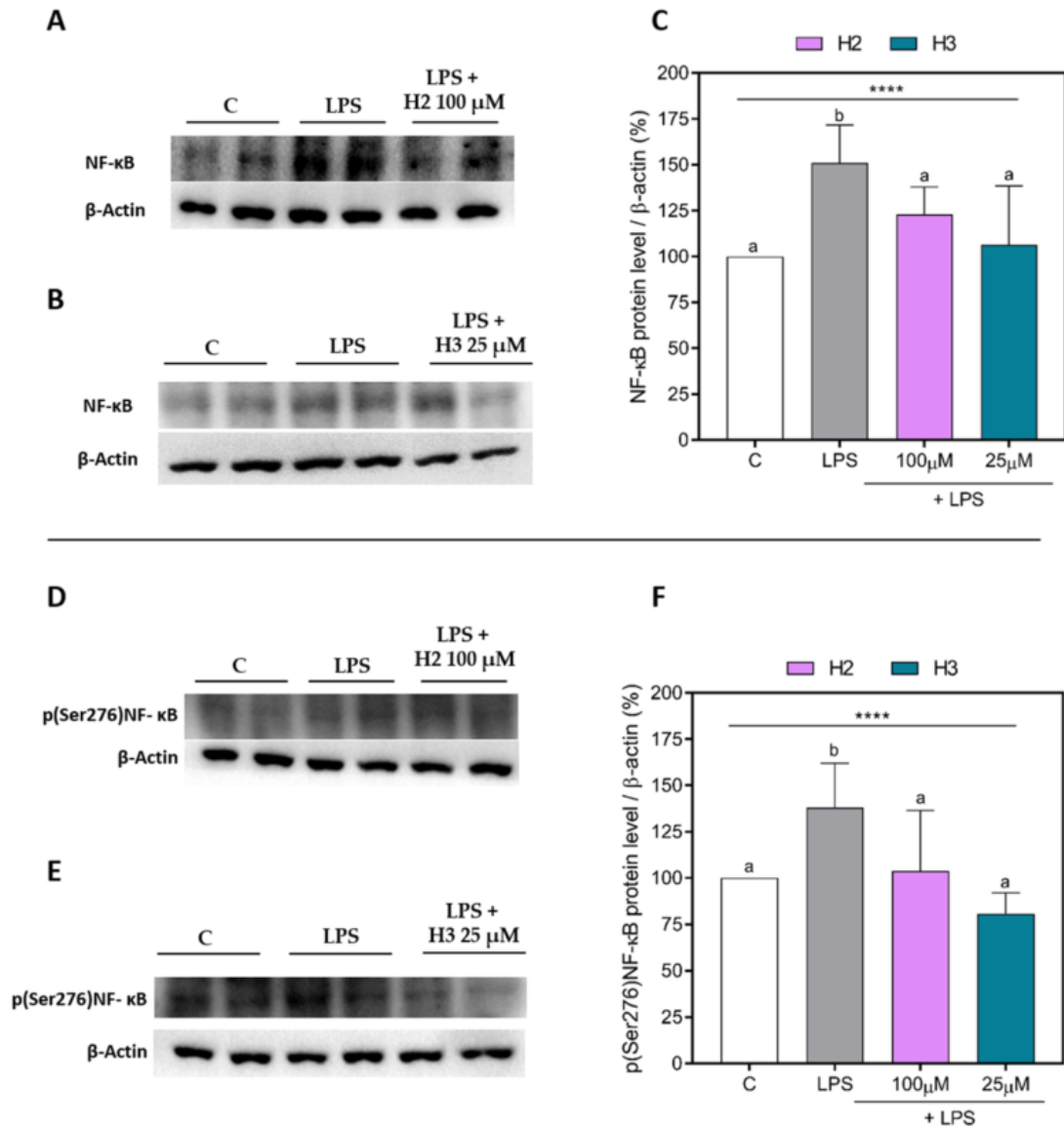


Figure 6.1 NF-κB and p(Ser276)NF-κB protein levels in LPS-stimulated HepG2 cells. Upper panel: representative Western Blots of NF-κB in H2 (A) and H3 (B) assays. Densitometric analyses of NF-κB (C). Bottom panel: representative Western Blots of p(Ser276)NF-κB in H2 (D) and H3 (E) assays. Densitometric analyses of p(Ser276)NF-κB (F). The data points represent the averages ± SD of three independent experiments in triplicate. All data sets were analyzed by one-way ANOVA, followed by Tukey's post-hoc test. Different letters indicate statistically significant differences. ****, $p \leq 0.0001$. C, unstimulated control group; LPS, lipopolysaccharide-stimulated cells; NF-κB, nuclear factor-κB; p(Ser276)NF-κB, phosphor(Ser276)-nuclear factor-κB.

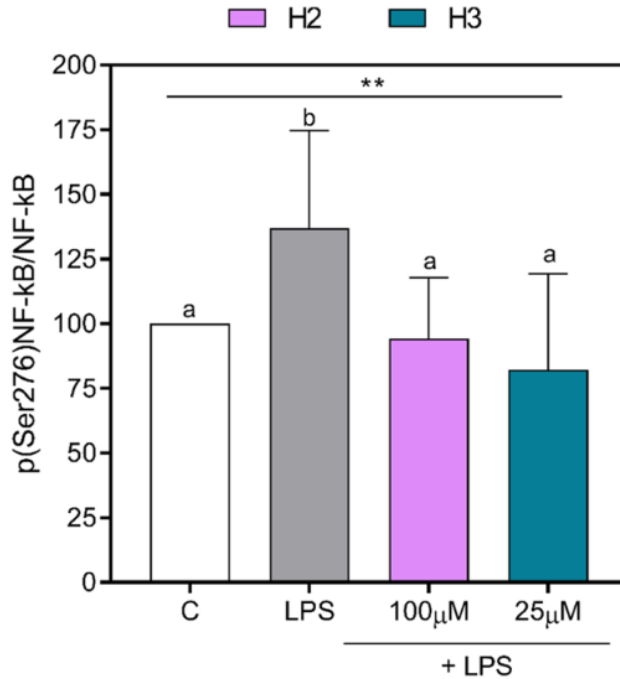


Figure 6.2 p(Ser276)NF-κB/NF-κB ratio. The histogram represents the averages \pm SD of the p(Ser276)NF-κB/NF-κB ratios of three independent experiments in triplicate. All data sets were analyzed by one-way ANOVA, followed by Tukey's post-hoc test. Different letters indicate statistically significant differences. **, $p \leq 0.01$. C, unstimulated control group; LPS, lipopolysaccharide-stimulated cells; NF-κB, nuclear factor-κB; p(Ser276)NF-κB, phosphor (Ser276)-nuclear factor-κB.

6.3.2 H2 and H3 Decrease the LPS-Induced Cytokine Production in Hepatic HepG2 Cells

To verify the possible immune effect of the two peptides, the influence of treatment with H2 (100 μ M) or H3 (25 μ M) on the production of pro-inflammatory (IFN- γ , TNF, IL-6) and anti-inflammatory (IL-10) cytokines was determined in LPS-stimulated HepG2 cell culture supernatants. As shown in **Figure 6.3**, the LPS stimulation increased the production of the pro-inflammatory cytokines (**Figure 6.3A–C, E–G**), without affecting the IL-10 production (**Figure 6.3D, H**), compared with LPS-unstimulated and untreated cells (control, C). Indeed, H2 successfully restored the normal concentrations of IFN- γ and TNF. In detail, H2 reduced by $33.0 \pm 6.7\%$ ($p = 0.011$) and $17.6 \pm 1.7\%$ ($p = 0.0004$) the LPS-induced IFN- γ and TNF production at

100 μM (**Figure 6.3A, B**), respectively. Despite this reduction, H2 was not able to alter the LPS-induced IL-6 production at the same concentration of 100 μM ($p = 0.581$) (**Figure 6.3C**). However, H2 increased the IL-10 production by $9.6 \pm 3.1\%$ at 100 μM ($p = 0.010$) compared to the LPS-stimulated cells (**Figure 6.3D**).

A similar scenario was also observed for the H3 peptide. In this case, anti-inflammatory effects were already observed at 25 μM (**Figure 6.3E–H**). In particular, H3 reduced IFN- γ and TNF production by $13.1 \pm 2.0\%$ ($p < 0.0001$) and $20.3 \pm 1.7\%$ ($p < 0.0001$), respectively, compared to LPS-stimulated cells (**Figure 6.3E, F**). In addition, unlike H2, H3 decreased IL-6 production by $15.1 \pm 6.5\%$ ($p = 0.010$) (**Figure 6.3G**), restoring the normal values as in LPS-unstimulated and untreated HepG2 cells (C). Surprisingly, H3 also increased the IL-10 production by $26.0 \pm 2.3\%$ ($p < 0.0001$) in comparison to the LPS-stimulated cells (**Figure 6.3H**).

Absolute values (mean \pm SD) of the cytokine production are reported in Supporting Information **Table 6-S2**.

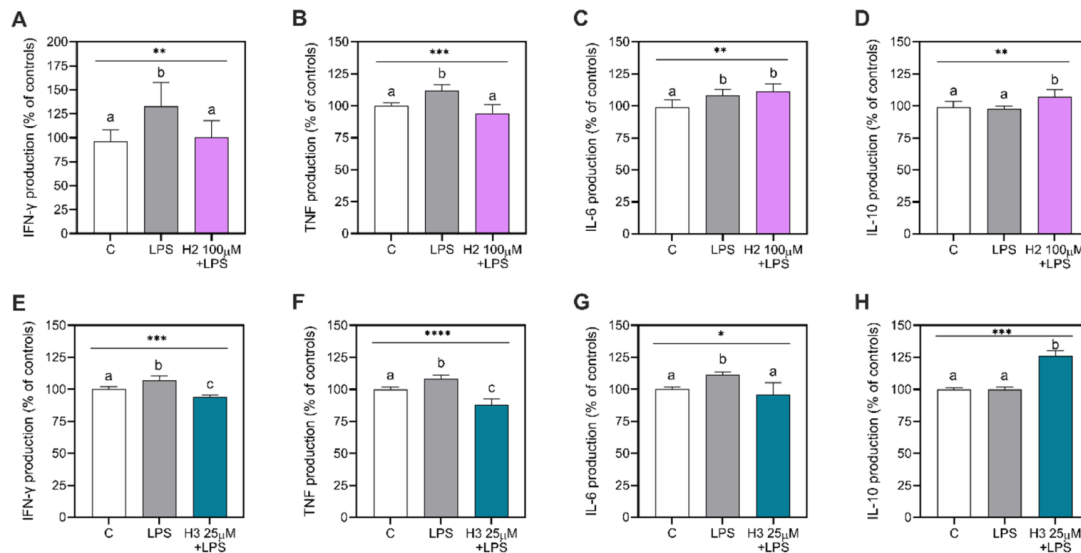


Figure 6.3 Cytokine production in HepG2 cells. Pro-inflammatory (A–C, E–G) and anti-inflammatory (D, H) cytokines. Data presented as mean \pm SD of three independent experiments performed in triplicate. All data sets were analyzed by one-way ANOVA, followed by Tukey’s post-hoc test. *, $p \leq 0.05$; **, $p \leq 0.01$; ***, $p \leq 0.001$; ****, $p \leq 0.0001$. Different letters indicate statistically significant differences. C, unstimulated control group; IFN- γ , interferon- γ ; IL,

interleukin; LPS, lipopolysaccharide-stimulated cells; TNF, tumor necrosis factor.

6.3.3 H2 and H3 Promote an Anti-inflammatory Microenvironment

In order to verify whether the peptides H2 and H3 were able to promote a more anti-inflammatory microenvironment, the anti- and pro-inflammatory cytokines' ratio was calculated. As shown in **Table 6.1**, H2 was able to increase the anti-inflammatory microenvironment (IL-10/IFN- γ : 100 μ M, $p = 0.002$; or IL-10/TNF: 100 μ M, $p = 0.0006$), skewing this ratio to a higher IL-10 content, in comparison with the LPS-stimulated cells. Also, in this case, when the ratio of IL-10 with IL-6 was calculated, a significant alteration in their proportion was observed (H2 100 μ M, $p = 0.336$).

In line with cytokine quantification, H3 showed an improvement in the proportion of IL-10 with respect to IFN- γ ($p \leq 0.0001$), TNF ($p \leq 0.0001$), and IL-6 ($p \leq 0.0001$) at 25 μ M, with respect to the LPS-stimulated cells' group.

Since the differences in the IL-10/IL6 ratio were not detected with H2 treatment, we decided to verify if there existed a correlation between the IL-10 and IL-6 production under the different experimental conditions; thus, Pearson correlation was performed. As shown in **Table 6.2**, the negative correlation between these two cytokines in the LPS-stimulated condition was lost. On the contrary, H2 treatment restored a negative correlation between the anti-inflammatory IL-10 and pro-inflammatory IL-6 cytokine, as in the unstimulated and untreated control group (C).

Table 6.1 Anti-/Pro-inflammatory Cytokines' Ratio^a.

	C	LPS	H2 [100 μM]
IL10/IFN-γ	1.05 ± 0.14 ^a	0.75 ± 0.15 ^b	1.10 ± 0.19 ^a
IL10/TNF	0.99 ± 0.07 ^a	0.88 ± 0.05 ^a	1.14 ± 0.11 ^b
IL10/IL-6	1.01 ± 0.10 ^a	0.90 ± 0.03 ^a	0.96 ± 0.07 ^a
	C	LPS	H3 [25 μM]
IL10/IFN-γ	1.00 ± 0.03 ^a	0.93 ± 0.05 ^a	1.34 ± 0.06 ^b
IL10/TNF	1.00 ± 0.02 ^a	0.92 ± 0.02 ^a	1.44 ± 0.12 ^b
IL10/IL-6	1.01 ± 0.10 ^a	0.90 ± 0.01 ^a	1.32 ± 0.13 ^b

^aRatios between anti-inflammatory (IL-10) and pro-inflammatory (IFN-γ, TNF, and IL-6) cytokines quantified in HepG2 cells stimulated or not with LPS and treated with H2 (100 μM) or H3 (25 μM). Data are presented as mean ± SD and were analyzed by one-way ANOVA, followed by Tukey's post-hoc test. Different letters indicate statistically significant differences ($p \leq 0.05$). C, unstimulated control group; IFN-γ, interferon-γ; IL, interleukin; LPS, lipopolysaccharide-stimulated cells; TNF, tumor necrosis factor.

Table 6.2 Pearson Correlation between IL-10 and IL-6 Production^a.

Pearson correlation	C	<i>p</i>-value	LPS	<i>p</i>-value	H2 [100 μM]	<i>p</i>-value
IL-10 vs IL-6	-0.9239	0.025	-0.4795	0.414	-0.9628	0.009

^aData represent the Pearson *r* value obtained by the correlation between IL-10 and IL-6 production under the different experimental conditions.

6.3.4 H2 and H3 Modulate the LPS-Activated iNOS Pathway in HepG2 Cells

As shown in Figure 4, LPS stimulation induced an inflammatory state in HepG2 cells, increasing the iNOS and NO levels' production up to $119.6 \pm 6.4\%$ ($p \leq 0.0001$) (Figure 6.4A–C) and $108.1 \pm 2.7\%$ ($p \leq 0.0001$) (Figure 6.4D), respectively. The treatment with H2 or H3 showed a significant reduction in iNOS and NO production, whose values were close to the baseline values. Specifically, H2 reduced the iNOS protein by $34.4 \pm 9.9\%$ ($p \leq 0.0001$) (Figure 6.4A, B) and NO production by $9.0 \pm 0.7\%$ ($p \leq 0.0001$) at 100 μM (Figure 6.4D). Furthermore, H3 was able to reduce the

iNOS protein by $25.3 \pm 4.4\%$ ($p \leq 0.0001$) (**Figure 6.4A, C**) and NO production by $7.2 \pm 1.8\%$ ($p \leq 0.0001$) $25 \mu\text{M}$ (**Figure 6.4D**).

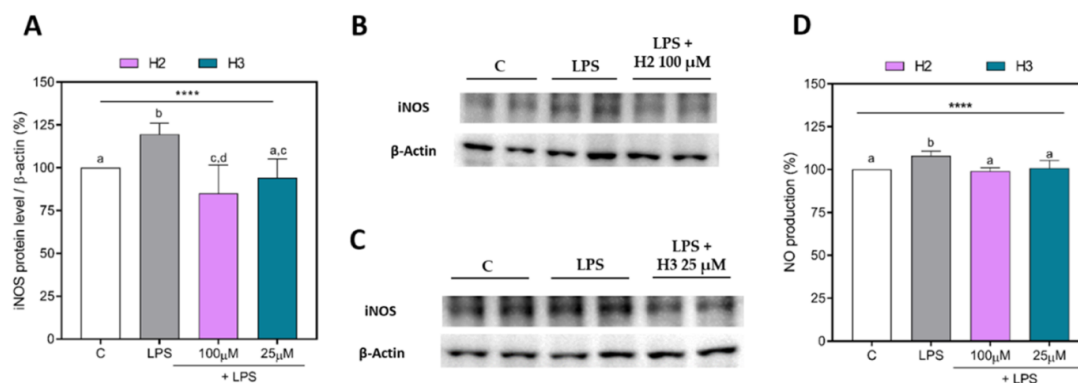


Figure 6.4 iNOS and NO production in HepG2 cells treated with H2 or H3. Densitometric analyses of iNOS protein levels (A); representative Western Blots of iNOS in H2 (B) and H3 (C) assays; NO production (D). The data points represent the averages \pm SD of three independent experiments in triplicate. All data sets were analyzed by one-way ANOVA, followed by Tukey's post-hoc test. Different letters indicate statistically significant differences. ****, $p < 0.0001$. C, unstimulated control group; iNOS, inducible nitric oxide synthase; LPS, lipopolysaccharide-stimulated cells; NO, nitric oxide.

6.4 Discussion

Recently, we demonstrated that peptides H2 and H3 exert antioxidant activity in HepG2 cells, modulating both the Nrf-2 and iNOS pathways, which led to the reduction of cellular H_2O_2 -induced ROS, NO, and lipid peroxidation levels (Bollati, et al., 2022). Since an increase in oxidative stress is always accompanied by an inflammatory process, it was interesting to study the immunomodulatory capacity of these two hempseed peptides in the same cellular system. Notably, HepG2 cells have been widely used as a model for characterizing the anti-inflammatory activity of many food-active compounds (Al-Bakheit & Abu-Qatouseh, 2020; Kanmani & Kim, 2018; Panahi, Pasalar, Zare, Rizzuto, & Meshkani, 2018; Wehmeier, Onstead-Haas, Wong, Mooradian, & Haas, 2016). To achieve this objective, we decided to perform tests

under the same conditions and study the same concentration of each peptide H2 (100 μ M) and H3 (25 μ M), which was previously demonstrated to be safe from a cytotoxic point of view and also effective for antioxidant activity (Bollati, et al., 2022). In particular, HepG2 cells were stimulated with LPS, a generic and commonly used pro-inflammatory stimulus. Therefore, the LPS stimulation activates the NF- κ B and iNOS pathways (Li, Yan, Brauner, & Tullus, 2002). NF- κ B is the main transcription factor involved in all pro-inflammatory processes of the mammalian organism, and it mediates the pro-inflammatory cytokine transcription, such as IFN- γ , TNF, and IL-6 (Liu, Zhang, Joo, & Sun, 2017). On the other hand, iNOS is involved in the immune response, producing NO, a free radical involved in the immune defense mechanism (Suschek, Schnorr, & Kolb-Bachofen, 2004).

In this work, we showed that hempseed hydrolysates can turn off pro-inflammatory signaling by modulating the NF- κ B and iNOS pathways' modulation. In fact, both H2 and H3 were able to decrease the NF- κ B protein as well as its more active form phospho(Ser276)NF- κ B. The p65 subunit of NF- κ B contains the transactivation domain, which is involved in the driving of transcription (Lecoq, Raiola, Chabot, Cyr, Arseneault, Legault, et al., 2017). There are several mechanisms involved in the modulation of the NF- κ B activity; therefore, the crosstalk with other signaling pathways allows one to act on the transactivating ability of NF- κ B. For example, the NF- κ B activity is favored by p38 mitogen-activated protein kinase, which phosphorylates the p65 subunit in the residue 276 serine (Baeza-Raja & Muñoz-Cánoves, 2004; Vermeulen, De Wilde, Van Damme, Vanden Berghe, & Haegeman, 2003). This phosphorylation allows interaction with other transcriptional co-activators, thus increasing the NF- κ B activity. Thus, the decrease of phospho-Ser276-p65 observed with H2 and H3 treatment demonstrated their NF- κ B activity inhibition capacity. In addition, both hydrolysates favored an anti-inflammatory microenvironment, skewing the ratio to the less active NF- κ B form. To confirm this NF- κ B inhibitory ability, the cytokine profile was studied. The results obtained showed that the NF- κ B pathway was inhibited since a decrease in pro-inflammatory cytokines was observed. Moreover, a major proportion of anti-inflammatory IL-10

cytokine was observed with respect to the pro-inflammatory cytokines. IL-10 exerts many anti-inflammatory functions, and it is the principal cytokine involved in finishing the inflammation processes, such as inhibiting the NF- κ B pathway, among others (Iyer & Cheng, 2012). Therefore, the increase in IL-10 production mediated by H2 and H3 is strongly related to the NF- κ B pathway inhibition.

Although H2 was not able to alter the LPS-induced IL-6 production and the IL-10/IL-6 ratio, a negative correlation was observed. In fact, LPS stimulation altered the correlation between IL-10 and IL-6, while H2 treatment re-establishes this negative correlation, demonstrating that a major IL-10 concentration corresponds to less IL-6 production. These effects can be explained by the negative modulation of the NF- κ B activity and then a less IL-6 production, although we did not observe significant differences by performing an ELISA assay.

Recently, hempseed hydrolysates obtained with Alcalase alone or in combination with Flavourzyme were shown to reduce the gene expression of TNF and IL-6, as well as increase IL-10 mRNA, in the LPS-stimulated BV2 microglia cell line (Rodriguez-Martin, et al., 2019). In addition, these same protein hydrolysates have been shown to reduce the production of inflammatory cytokines TNF, IL-6, and IL-1 β as well as increase the anti-inflammatory cytokine IL-10 in primary human monocytes (Rodriguez-Martin, et al., 2020). However, no specific peptides were singled out as being responsible for this biological effect. Recently, it was demonstrated that two egg tripeptides (IRW and IQW) from ovotransferrin are effective in the down-regulation of cytokine-induced inflammatory protein expression in vascular endothelium, at least partially through the modulation of the NF- κ B pathway (Huang, Chakrabarti, Majumder, Jiang, Davidge, & Wu, 2010; Majumder, Chakrabarti, Davidge, & Wu, 2013). These two peptides are shorter than both H2 and H3; however, comparing their sequences with H2 and H3, it is feasible to consider that the Trp and Ile presence may be positively correlated not only with the antioxidant but also with the anti-inflammatory effects, reinforcing the strong cross-linking between these two activities (Bollati, et al., 2022; Huang, Chakrabarti, Majumder, Jiang, Davidge, & Wu, 2010). Interestingly, the IRW and IQW beneficial effects require the presence of an

intact tripeptide as the corresponding dipeptides and constituent amino acids alone failed to replicate the anti-inflammatory functions, indicating a structure–function relationship between the tripeptide structure and blockade of inflammation. A very interesting feature of both H2 and H3 is that despite IRW and IQW, they are transported by intestinal cells and they are stable toward intestinal protease activity when they are within the hempseed hydrolysate (Bollati, et al., 2022).

Another interesting feature of our work is related to the ability evaluation of both H2 and H3 to modulate the iNOS pathway, which is known to be involved in immune response, producing NO, a free radical implicated in the immune defense mechanism (Suschek, Schnorr, & Kolb-Bachofen, 2004).

NO acts as a cytotoxic agent in pathological processes, specifically in inflammatory disorders (Silpak, Rintu, & Ena Ray, 2017). In this sense, numerous scientific articles have shown that NO production is elevated in chronic inflammatory diseases, such as diabetes (Soskić, Dobutović, Sudar, Obradović, Nikolić, Djordjevic, et al., 2011), atherosclerosis (Förstermann, Xia, & Li, 2017), or multiple sclerosis (Bagasra, Michaels, Zheng, Bobroski, Spitsin, Fu, et al., 1995). The iNOS protein is mainly responsible for the production of cellular NO (Zamora, Vodovotz, & Billiar, 2000); in fact, its inhibition may be a therapeutic target in inflammatory diseases (Lind, Hayes, Caprnda, Petrovic, Rodrigo, Kruzliak, et al., 2017). In our study, we observed that H2 and H3 peptides reduced NO and iNOS production in LPS-stimulated HepG2 cells. In addition, the reduction of NF- κ B by peptides is also confirmed by the observed results in the NO pathways. NF- κ B plays an important role in the regulation of iNOS production, inducing its expression (Jia, Liu, Zhang, Liu, & Qi, 2013), and, at the same time, it is well known that NO, in turn, can induce NF- κ B activation (Soskić, et al., 2011). Our findings suggest, together with those that we have previously observed, a potential interplay of both antioxidant and anti-inflammatory activities exerted by H2 and H3 peptides. Moreover, the present study confirms that H3 is fourfold more active than H2 not only as an antioxidant but also as an anti-inflammatory peptide. Taking together all the results and on the basis on our knowledge, this study is the first to observe the role of two specific peptides in the regulation of the NO pathway

in hepatic cells. In addition, although many food protein hydrolysates have demonstrated anti-inflammatory effects (Chakrabarti, Jahandideh, & Wu, 2014), our study is the pioneer in the identification of anti-inflammatory peptides that can be absorbed by the human intestinal barrier from the hempseed source (Bollati, et al., 2022).

In conclusion, all these findings demonstrate that H2 and H3 peptides possess great anti-inflammatory capacity in the HepG2 cells. Both antioxidant and anti-inflammatory effects in HepG2 cells point out the useful employment of H2 and H3 how possible strategies to prevent liver diseases, such as non-alcoholic steatohepatitis, characterized by inflammation and oxidative stress in the early stages of the disease (Buzzetti, Pinzani, & Tsochatzis, 2016), even though dedicated *in vivo* study is necessary to confirm this important feature.

6.5 Supporting information

Reagents

Dulbecco's modified Eagle's medium (DMEM), L-glutamine, fetal bovine serum (FBS), phosphate buffered saline (PBS), penicillin/streptomycin, chemiluminescent reagent, and 24 or 96-well plates were purchased from Euroclone (Milan, Italy). Bovine serum albumin (BSA), RIPA buffer was bought from Sigma-Aldrich (St. Louis, MO, USA). Phenylmethanesulfonyl fluoride (PMSF), Na-orthovanadate inhibitors were purchased from Santa Cruz Biotechnology Inc. (Santa Cruz, CA, USA). The inhibitor cocktail Complete Midi from Roche (Basel, Swiss). Mini protean TGX pre-cast gel 7.5%, and Mini nitrocellulose Transfer Packs were purchased from BioRad (Hercules, CA, USA).

Table 6-S1. Antibodies used in the Western Blot assays.

Name product	Dilution	Supplier
Anti-iNOS	1:1000	Cell Signaling Technology (D6B6S)
Anti-NF-kappaB, p65 subunit, active subunit, clone 12H11	1:1000	Sigma-Aldrich (MAB3026)
Anti-phospho-NF-kappaB p65 (pSer276)	1:1000	Sigma-Aldrich (SAB4504488)
Anti- β -actin	1:16000	Sigma-Aldrich (A5441)

Name of antibody, dilution used, and supplier. iNOS, inducible nitric oxide synthase; NF-kappaB, nuclear factor- κ B.

Figure 6-S1 Chromatogram and Mass Spectrum of H2 (A and C) and H3 (B and D)

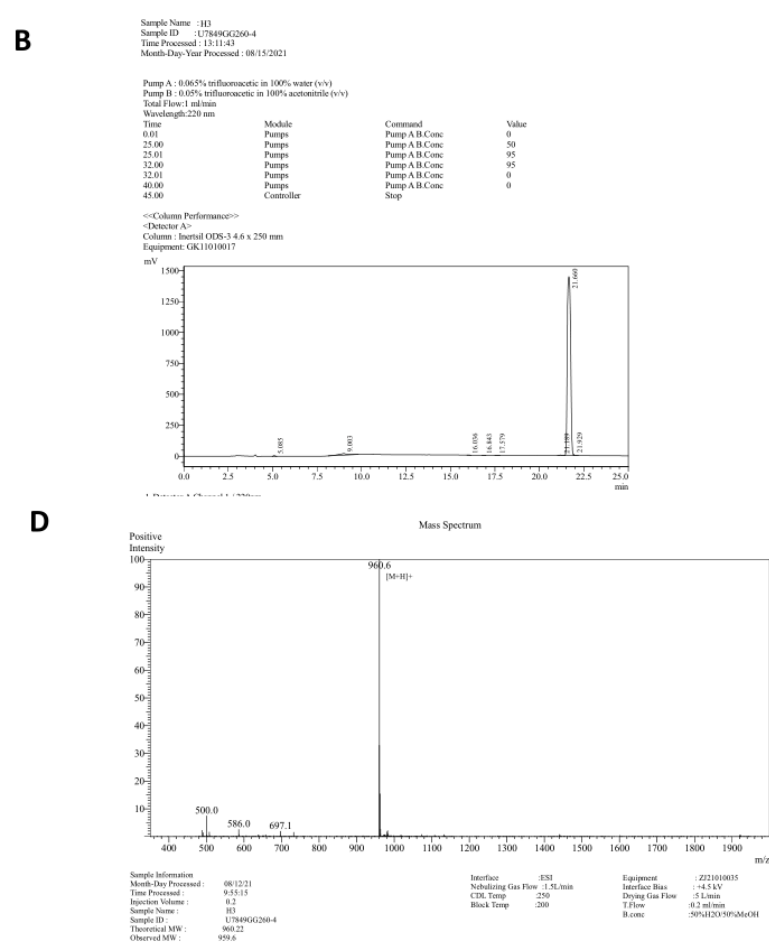
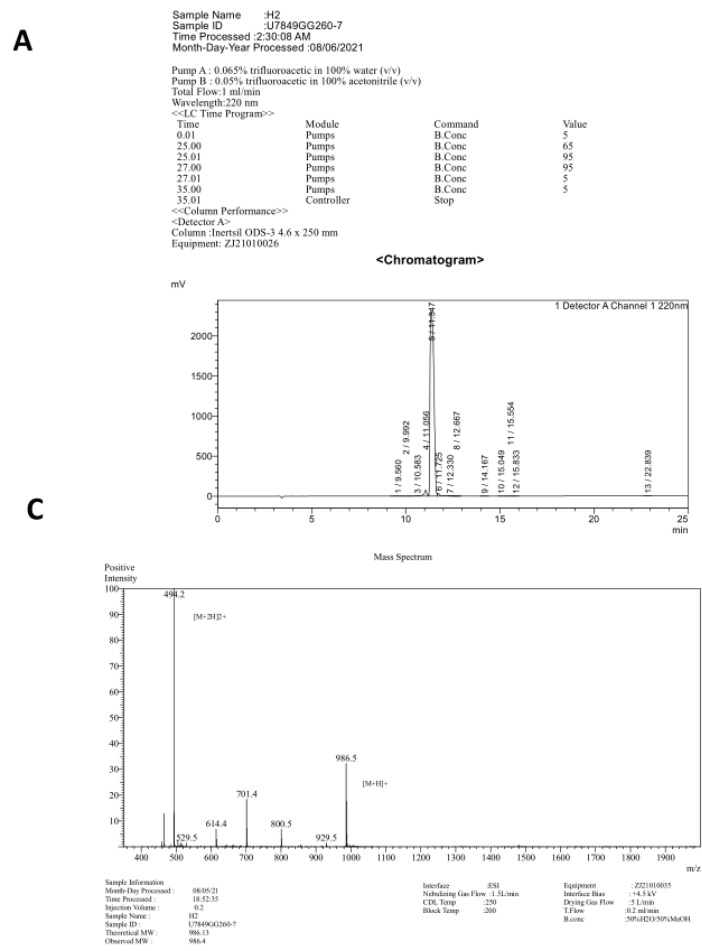


Table 6-S2 Absolute values of cytokine production.

Cytokine	C	LPS	H2 [100 μM]	C	LPS	H3 [25 μM]
IFN- γ (pg/mL)	25.50 \pm 5.04	34.12 \pm 5.94	26.00 \pm 1.41	28.28 \pm 1.28	30.35 \pm 0.35	26.50 \pm 0.58
TNF (pg/mL)	33.71 \pm 1.21	38.00 \pm 2.94	32.00 \pm 1.41	33.89 \pm 0.75	36.68 \pm 0.43	29.83 \pm 1.17
IL-6 (ng/mL)	1329 \pm 8.60	1448 \pm 1.23	1470 \pm 5.02	603.8 \pm 1.71	672.5 \pm 2.38	584.8 \pm 19.16
IL-10 (pg/mL)	21.68 \pm 0.22	20.98 \pm 1.32	23.25 \pm 0.13	48.90 \pm 0.36	49.74 \pm 1.43	61.88 \pm 0.17

Mean \pm standard deviation (SD) of the cytokines production. C, unstimulated control group; LPS, lipopolysaccharide-stimulated cells; H, hempseed peptide; IFN- γ , interferon- γ ; TNF, tumor necrosis factor; IL, interleukin.

6.6 References

- Aiello, G., Lammi, C., Boschin, G., Zanoni, C., & Arnoldi, A. (2017). Exploration of Potentially Bioactive Peptides Generated from the Enzymatic Hydrolysis of Hempseed Proteins. *Journal of Agricultural and Food Chemistry*, 65(47), 10174-10184.
- Al-Bakheit, A. a., & Abu-Qatouseh, L. (2020). Sulforaphane from broccoli attenuates inflammatory hepcidin by reducing IL-6 secretion in human HepG2 cells. *Journal of Functional Foods*, 75, 104210.
- Baeza-Raja, B., & Muñoz-Cánoves, P. (2004). p38 MAPK-induced Nuclear Factor- κ B Activity Is Required for Skeletal Muscle Differentiation: Role of Interleukin-6. *Molecular Biology of the Cell*, 15(4), 2013-2026.
- Bagasra, O., Michaels, F. H., Zheng, Y. M., Bobroski, L. E., Spitsin, S. V., Fu, Z. F., Tawadros, R., & Koprowski, H. (1995). Activation of the inducible form of nitric oxide synthase in the brains of patients with multiple sclerosis. *Proceedings of the National Academy of Sciences*, 92(26), 12041-12045.
- Bollati, C., Cruz-Chamorro, I., Aiello, G., Li, J., Bartolomei, M., Santos-Sánchez, G., Ranaldi, G., Ferruzza, S., Sambuy, Y., Arnoldi, A., & Lammi, C. (2022). Investigation of the intestinal trans-epithelial transport and antioxidant activity of two hempseed peptides WVSPLAGRT (H2) and IGFLIIWV (H3). *Food Research International*, 152, 110720.
- Buzzetti, E., Pinzani, M., & Tsochatzis, E. A. (2016). The multiple-hit pathogenesis of non-alcoholic fatty liver disease (NAFLD). *Metabolism*, 65(8), 1038-1048.
- Cascini, F., & Boschi, I. (2017). Chapter e1 - Tetrahydrocannabinol Concentration and Genetic Characterization of Cannabis. In V. R. Preedy (Ed.), *Handbook of Cannabis and Related Pathologies*, (pp. e1-e10). San Diego: Academic Press.
- Chakrabarti, S., Jahandideh, F., & Wu, J. (2014). Food-Derived Bioactive Peptides on Inflammation and Oxidative Stress. *BioMed Research International*, 2014, 608979.
- Farag, S., & Kayser, O. (2017). Chapter 1 - The Cannabis Plant: Botanical Aspects. In V. R. Preedy (Ed.), *Handbook of Cannabis and Related Pathologies*, (pp. 3-12). San Diego: Academic Press.

- Farinon, B., Molinari, R., Costantini, L., & Merendino, N. (2020). The Seed of Industrial Hemp (*Cannabis sativa* L.): Nutritional Quality and Potential Functionality for Human Health and Nutrition. In *Nutrients*, vol. 12).
- Förstermann, U., Xia, N., & Li, H. (2017). Roles of Vascular Oxidative Stress and Nitric Oxide in the Pathogenesis of Atherosclerosis. *Circulation Research*, 120(4), 713-735.
- Girgih, A. T., He, R., Malomo, S., Offengenden, M., Wu, J., & Aluko, R. E. (2014). Structural and functional characterization of hemp seed (*Cannabis sativa* L.) protein-derived antioxidant and antihypertensive peptides. *Journal of Functional Foods*, 6, 384-394.
- Girgih, A. T., Udenigwe, C. C., & Aluko, R. E. (2011). *In Vitro* Antioxidant Properties of Hemp Seed (*Cannabis sativa* L.) Protein Hydrolysate Fractions. *Journal of the American Oil Chemists' Society*, 88(3), 381-389.
- Girgih, A. T., Udenigwe, C. C., & Aluko, R. E. (2013). Reverse-phase HPLC Separation of Hemp Seed (*Cannabis sativa* L.) Protein Hydrolysate Produced Peptide Fractions with Enhanced Antioxidant Capacity. *Plant Foods for Human Nutrition*, 68(1), 39-46.
- Hartsel, J. A., Eades, J., Hickory, B., & Makriyannis, A. (2016). Chapter 53 - *Cannabis sativa* and Hemp. In R. C. Gupta (Ed.), *Nutraceuticals*, (pp. 735-754). Boston: Academic Press.
- Huang, W., Chakrabarti, S., Majumder, K., Jiang, Y., Davidge, S. T., & Wu, J. (2010). Egg-Derived Peptide IRW Inhibits TNF- α -Induced Inflammatory Response and Oxidative Stress in Endothelial Cells. *Journal of Agricultural and Food Chemistry*, 58(20), 10840-10846.
- Iyer, S. S., & Cheng, G. J. C. R. i. I. (2012). Role of interleukin 10 transcriptional regulation in inflammation and autoimmune disease. 32(1).
- Jia, J., Liu, Y., Zhang, X., Liu, X., & Qi, J. (2013). Regulation of iNOS Expression by NF- κ B in Human Lens Epithelial Cells Treated With High Levels of Glucose. *Investigative Ophthalmology & Visual Science*, 54(7), 5070-5077.
- Kanmani, P., & Kim, H. J. F. i. i. (2018). Protective effects of lactic acid bacteria against TLR4 induced inflammatory response in hepatoma HepG2 cells through modulation of toll-like receptor negative regulators of mitogen-activated protein kinase and NF- κ B signaling. 9, 1537.
- Lammi, C., Bollati, C., Gelain, F., Arnoldi, A., & Pugliese, R. J. F. i. C. (2019). Enhancement of the stability and anti-DPPiV activity of hempseed hydrolysates through self-assembling peptide-based hydrogels. 6, 670.

- Lecoq, L., Raiola, L., Chabot, P. R., Cyr, N., Arseneault, G., Legault, P., & Omichinski, J. G. (2017). Structural characterization of interactions between transactivation domain 1 of the p65 subunit of NF- κ B and transcription regulatory factors. *Nucleic Acids Research*, *45*(9), 5564-5576.
- Li, Y.-H., Yan, Z.-Q., Brauner, A., & Tullus, K. (2002). Activation of macrophage nuclear factor- κ B and induction of inducible nitric oxide synthase by LPS. *Respiratory Research*, *3*(1), 16.
- Lind, M., Hayes, A., Caprnda, M., Petrovic, D., Rodrigo, L., Kruzliak, P., & Zulli, A. (2017). Inducible nitric oxide synthase: Good or bad? *Biomedicine & Pharmacotherapy*, *93*, 370-375.
- Liu, T., Zhang, L., Joo, D., & Sun, S.-C. (2017). NF- κ B signaling in inflammation. *Signal Transduction and Targeted Therapy*, *2*(1), 17023.
- Logarušić, M., Slivac, I., Radošević, K., Bagović, M., Redovniković, I. R., & Srček, V. G. (2019). Hempseed protein hydrolysates' effects on the proliferation and induced oxidative stress in normal and cancer cell lines. *Molecular Biology Reports*, *46*(6), 6079-6085.
- Majumder, K., Chakrabarti, S., Davidge, S. T., & Wu, J. (2013). Structure and Activity Study of Egg Protein Ovotransferrin Derived Peptides (IRW and IQW) on Endothelial Inflammatory Response and Oxidative Stress. *Journal of Agricultural and Food Chemistry*, *61*(9), 2120-2129.
- Malomo, S. A., & Aluko, R. E. (2016). *In Vitro* Acetylcholinesterase-Inhibitory Properties of Enzymatic Hemp Seed Protein Hydrolysates. *Journal of the American Oil Chemists' Society*, *93*(3), 411-420.
- Orio, L. P., Boschin, G., Recca, T., Morelli, C. F., Ragona, L., Francescato, P., Arnoldi, A., & Speranza, G. (2017). New ACE-Inhibitory Peptides from Hemp Seed (*Cannabis sativa* L.) Proteins. *Journal of Agricultural and Food Chemistry*, *65*(48), 10482-10488.
- Panahi, G., Pasalar, P., Zare, M., Rizzuto, R., & Meshkani, R. (2018). High glucose induces inflammatory responses in HepG2 cells via the oxidative stress-mediated activation of NF- κ B, and MAPK pathways in HepG2 cells. *Archives of Physiology and Biochemistry*, *124*(5), 468-474.
- Rodriguez-Martin, N. M., Montserrat-de la Paz, S., Toscano, R., Grao-Cruces, E., Villanueva, A., Pedroche, J., Millan, F., & Millan-Linares, M. C. (2020). Hemp (*Cannabis sativa* L.) Protein Hydrolysates Promote Anti-Inflammatory Response in Primary Human Monocytes. In *Biomolecules*, vol. 10).

- Rodriguez-Martin, N. M., Toscano, R., Villanueva, A., Pedroche, J., Millan, F., Montserrat-de la Paz, S., & Millan-Linares, M. C. (2019). Neuroprotective protein hydrolysates from hemp (*Cannabis sativa* L.) seeds. *Food & Function*, *10*(10), 6732-6739.
- Silpak, B., Rintu, D., & Ena Ray, B. (2017). Role of free radicals in human inflammatory diseases. *AIMS Biophysics*, *4*(4), 596-614.
- Soskić, S. S., Dobutović, B. D., Sudar, E. M., Obradović, M. M., Nikolić, D. M., Djordjevic, J. D., Radak, D. J., Mikhailidis, D. P., & Isenović, E. R. J. T. o. c. m. j. (2011). Regulation of inducible nitric oxide synthase (iNOS) and its potential role in insulin resistance, diabetes and heart failure. *5*(1).
- Suschek, V. C., Schnorr, O., & Kolb-Bachofen, V. (2004). The Role of iNOS in Chronic Inflammatory Processes *In Vivo*: Is it Damage-Promoting, Protective, or Active at all? *Current Molecular Medicine*, *4*(7), 763-775.
- Tang, C.-H., Wang, X.-S., & Yang, X.-Q. (2009). Enzymatic hydrolysis of hemp (*Cannabis sativa* L.) protein isolate by various proteases and antioxidant properties of the resulting hydrolysates. *Food Chemistry*, *114*(4), 1484-1490.
- Teh, S.-S., Bekhit, A. E.-D. A., Carne, A., & Birch, J. (2016). Antioxidant and ACE-inhibitory activities of hemp (*Cannabis sativa* L.) protein hydrolysates produced by the proteases AFP, HT, Pro-G, actinidin and zingibain. *Food Chemistry*, *203*, 199-206.
- Thomas, B. F., & ElSohly, M. A. (2016). Chapter 1 - The Botany of *Cannabis sativa* L. In B. F. Thomas & M. A. ElSohly (Eds.), *The Analytical Chemistry of Cannabis*, (pp. 1-26): Elsevier.
- Vermeulen, L., De Wilde, G., Van Damme, P., Vanden Berghe, W., & Haegeman, G. (2003). Transcriptional activation of the NF- κ B p65 subunit by mitogen- and stress-activated protein kinase-1 (MSK1). *The EMBO Journal*, *22*(6), 1313-1324.
- Wang, S., Luo, Q., & Fan, P. (2019). Cannabisin F from Hemp (*Cannabis sativa*) Seed Suppresses Lipopolysaccharide-Induced Inflammatory Responses in BV2 Microglia as SIRT1 Modulator. In *International Journal of Molecular Sciences*, vol. 20).
- Wang, X.-S., Tang, C.-H., Chen, L., Yang, X.-Q. J. F. T., & Biotechnology. (2009). Characterization and antioxidant properties of hemp protein hydrolysates obtained with Neutrase®. *47*(4), 428-434.

- Wang, X.-S., Tang, C.-H., Yang, X.-Q., & Gao, W.-R. (2008). Characterization, amino acid composition and *in vitro* digestibility of hemp (*Cannabis sativa* L.) proteins. *Food Chemistry*, *107*(1), 11-18.
- Wehmeier, K., Onstead-Haas, L. M., Wong, N. C. W., Mooradian, A. D., & Haas, M. J. (2016). Pro-inflammatory signaling by 24,25-dihydroxyvitamin D3 in HepG2 cells. *Journal of Molecular Endocrinology*, *57*(2), 87-96.
- Zamora, R., Vodovotz, Y., & Billiar, T. R. (2000). Inducible Nitric Oxide Synthase and Inflammatory Diseases. *Molecular Medicine*, *6*(5), 347-373.
- Zanoni, C., Aiello, G., Arnoldi, A., & Lammi, C. (2017). Hempseed Peptides Exert Hypocholesterolemic Effects with a Statin-Like Mechanism. *Journal of Agricultural and Food Chemistry*, *65*(40), 8829-8838.

CHAPTER 7

MANUSCRIPT 5

HEMPSEED (*CANNABIS SATIVA*) PEPTIDE H3 (IGFLIIWV) EXERTS CHOLESTEROL-LOWERING EFFECTS IN HUMAN HEPATIC CELL LINE

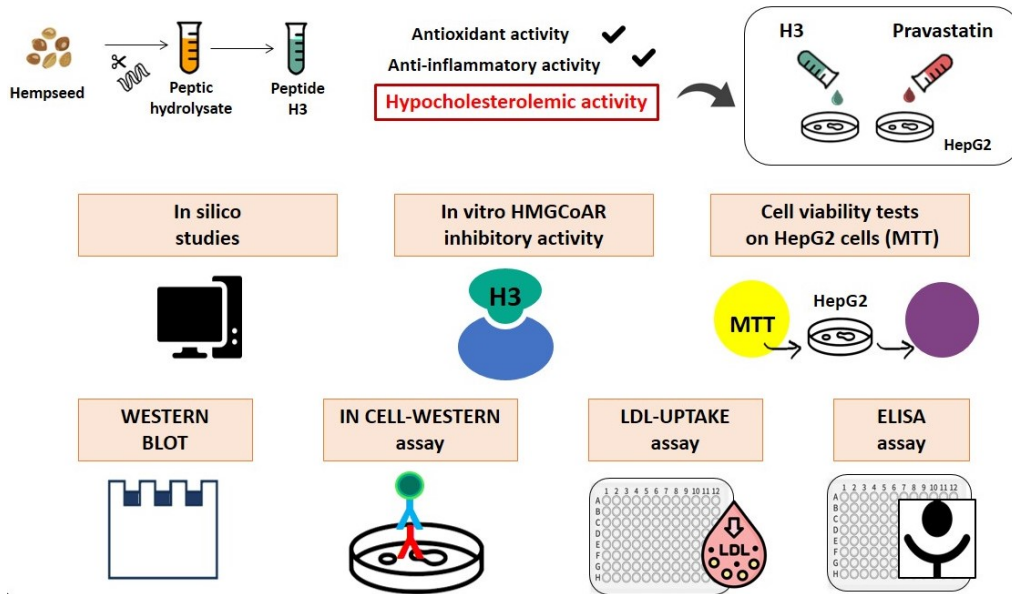
Jianqiang Li, Carlotta Bollati, Martina Bartolomei, Angelica Mazzolari,
Anna Arnoldi, Giulio Vistoli and Carmen Lammi*

Department of Pharmaceutical Sciences, University of Milan, 20122 Milan, Italy

Author Contributions: Conceptualization, C.L.; methodology, J.L., C.B. and M.B.; investigation, J.L., C.B., M.B. and C.L.; data curation, C.L., A.M. and G.V.; writing—original draft, J.L. and C.L.; writing—review & editing, C.L., G.V. and A.A.; supervision, C.L.; project administration, C.L.; funding acquisition, C.L. and A.A.

7. Abstract

Hempseed (*Cannabis sativa*) protein is an important source of bioactive peptides. H3 (IGFLIIWV), a transepithelial transported intestinal peptide obtained from the hydrolysis of hempseed protein with pepsin, carries out antioxidant and anti-inflammatory activities in HepG2 cells. In this study, the main aim was to assess its hypocholesterolemic effects at a cellular level and the mechanisms behind this health-promoting activity. The results showed that peptide H3 inhibited the 3-hydroxy-3-methylglutaryl co-enzyme A reductase (HMGCoAR) activity *in vitro* in a dose-dependent manner with an IC_{50} value of 59 μ M. Furthermore, the activation of the sterol regulatory element binding proteins (SREBP)-2 transcription factor, followed by the increase of low-density lipoprotein (LDL) receptor (LDLR) protein levels, was observed in human hepatic HepG2 cells treated with peptide H3 at 25 μ M. Meanwhile, peptide H3 regulated the intracellular HMGCoAR activity through the increase of its phosphorylation by the activation of AMP-activated protein kinase (AMPK)-pathways. Consequently, the augmentation of the LDLR localized on the cellular membranes led to the improved ability of HepG2 cells to uptake extracellular LDL with a positive effect on cholesterol levels. Unlike the complete hempseed hydrolysate (HP), peptide H3 can reduce the proprotein convertase subtilisin/kexin 9 (PCSK9) protein levels and its secretion in the extracellular environment via the decrease of hepatic nuclear factor (HNF) -1 α . Considering all these evidences, H3 may represent a new bioactive peptide to be used for the development of dietary supplements and/or peptidomimetics for cardiovascular disease (CVD) prevention.



7.1 Introduction

Low-density lipoprotein (LDL) receptor (LDLR) is a cell membrane glycoprotein that functions in the binding and internalizing of circulating cholesterol-containing lipoprotein particles to maintain cholesterol homeostasis in lipoprotein and lipid metabolism (Go & Mani, 2012). Defects in LDLR function or expression trigger an elevated LDL cholesterol and result in cardiovascular disease (CVD), one of the largest causes of mortality worldwide (Mattiuzzi, Sanchis-Gomar, & Lippi, 2020). The LDLR expression is not only modulated by intracellular cholesterol content, but also regulated by a transcription factor, named sterol-responsive element binding protein-2 (SREBP-2), which plays a pivotal role in LDLR mRNA expression (Goldstein & Brown, 1990). As another SREBP-2 gene target, 3-hydroxy-3-methylglutaryl coenzyme A reductase (HMGCoAR) is a key factor in intracellular cholesterol biosynthesis. HMGCoAR is the rate-controlling enzyme in the mevalonate pathway and is also regulated by the AMP-activated protein kinase (AMPK) pathway (Hardie, 2014). In more detail, there are three isoforms of sterol regulatory element binding proteins (SREBPs), including SREBP-1a, -1c, and -2, each having different roles in lipid synthesis. Particularly, SREBP-2 is specific to cholesterol synthesis and is responsible for the LDLR and HMGCoAR transcription. Upon sterol deficiency, the complex of SREBP-2 and SREBP cleavage-activating protein (SCAP) membrane experiences a successive two-step cleavage process in the golgi to liberate the amino-

terminal portion of SREBP-2. Subsequently, this portion of SREBP-2 enters the nucleus, followed by the activation of the transcription of LDLR and HMGCoAR by binding to sterol regulatory elements (SREs) (Brown & Goldstein, 1997; Shimano, 2001). The increase of LDLR determines an enhanced clearance of plasmatic LDL-cholesterol with an improvement of dyslipidemia (Xiao, Dash, Morgantini, Hegele, & Lewis, 2016).

In addition, proprotein convertase subtilisin/kexin type 9 (PCSK9) is the major regulator of the LDL, which subsequently affects its ability to efficiently remove LDL-cholesterol from circulation. Briefly, PCSK9 binds to LDLR and causes their destruction within lysosomes, whereas its inhibition results in the recycling of LDLR, leading to the internalization of more LDL-cholesterol and a reduction in the blood levels of LDL. Recently, some papers have shown that specific peptides deriving from food and/or plant proteins are efficiently able to lower LDL and are also safe (Cho, Juillerat, & Lee, 2007), a fact that has attracted the attention of more and more researchers.

Industrial hemp, the non-drug variety of *Cannabis sativa*, has been used for food and fiber for centuries (Leonard, Zhang, Ying, & Fang, 2020; Wang & Xiong, 2019). Recently, hempseed protein has become an important source of bioactive peptides, because of its high nutritive potential and purported health benefits. Briefly, whole hempseeds contain 20% to 25% protein [the main components being globulin (60% to 80%) and albumin] that exerts a positive effect in the regulation of organ function and human metabolism (Aiello, Lammi, Boschini, Zanoni, & Arnoldi, 2017; Wang & Xiong, 2019). This fact has stimulated a great interest especially for research on multifunctional bioactive peptides.

In some of our preceding publications (Aiello, Lammi, Boschini, Zanoni, & Arnoldi, 2017; Zanoni, Aiello, Arnoldi, & Lammi, 2017a), hydrolysates derived from hempseed have been shown to provide a hypocholesterolemic effect by dropping the activity of HMGCoAR, which in turn leads to the activation of the LDLR, followed by the improvement of the hepatic cells' ability to absorb extracellular LDL. Although an increase of the PCSK9 protein levels was detected, the hempseed hydrolysate (HP) showed a hypocholesterolemic effect similar to that of statins. Considering that proteins are hydrolyzed during digestion, the activity may be attributed to specific peptides encrypted in the protein sequences that are released by digestion and absorbed at an intestinal level (Hartmann & Meisel, 2007). Indeed,

further experiments on the intestinal trans-epithelial transport revealed that some peptides in the HP were able to pass through the mature Caco-2 cell barrier. Particularly, H3 (IGFLIIWV) is one of these peptides that provides an antioxidant activity in HepG2 cells by modulating the Nrf-2 and iNOS pathways (Wenshuang Sun, Meng, Wang, Yuan, Qian, Chen, et al., 2017), leading to the decrease of cellular H₂O₂-induced ROS, NO, and lipid peroxidation levels (Bollati, Cruz-Chamorro, Aiello, Li, Bartolomei, Santos-Sánchez, et al., 2022). Considering the link between inflammation and oxidative stress, the evaluation of the anti-inflammatory effect of H3 was also carried out in HepG2 cells. As expected, H3 modulates the production of pro-inflammatory cytokines (IFN- γ , TNF and IL-6), anti-inflammatory cytokines (IL-10), and NO through the regulation of the NF- κ B and iNOS pathways (Sarkar, Saha, Gamre, Bhattacharjee, Hariharan, Ganguly, et al., 2008), exerting an effective anti-inflammatory capacity (Cruz-Chamorro, Santos-Sánchez, Bollati, Bartolomei, Li, Arnoldi, et al., 2022).

In light of these observations, a deeper mechanistic investigation was undertaken with the following objectives: (1) to assess the inhibitory activity of peptide H3 on HMGCoAR *in vitro* and *in silico*; (2) to figure out how peptide H3 may modulate the activity of the key targets involved in cholesterol metabolism, i.e., LDLR, SREBP-2, HMGCoAR, p-AMPK (Thr 172), HNF-1 α , and PCSK9; and (3) to evaluate the capacity of HepG2 cells treated with peptide H3 to absorb extracellular LDL cholesterol.

7.2 Material and methods

7.2.1 Chemicals

Dulbecco's modified Eagle's medium (DMEM), stable L-glutamine, fetal bovine serum (FBS), phosphate buffered saline (PBS), penicillin/streptomycin, chemiluminescent reagent, and 96-well plates were purchased from Euroclone (Milan, Italy). The HMGCoAR assay kit, bovine serum albumin (BSA), Janus Green B, formaldehyde, HCl and H₂SO₄ were from Sigma-Aldrich (St. Louis, MO, USA). The antibody against LDLR and the 3,3',5,5'-tetramethylbenzidine (TMB) substrate were bought from Thermo Fisher Scientific (Waltham, MA, USA). The Quantikine ELISA kit was bought from R&D Systems (Minneapolis, MN, USA). The LDL-DyLightTM

550 was from Cayman Chemical (Ann Arbor, MI, USA). The CircuLex PCSK9 *in vitro* binding Assay Kit was from CircuLex (CycLex Co., Nagano, Japan). The peptides H3 was synthesized by the company GeneScript (Piscataway, NJ, USA) at > 95% purity. The antibody against HMGCoAR was bought from Abcam (Cambridge, UK). Phenylmethanesulfonyl fluoride (PMSF), Na-orthovanadate inhibitors, and the antibodies against rabbit Ig-horseradish peroxidase (HRP), mouse Ig-HRP, and SREBP-2 (which recognizes epitope located in a region between 833–1141 and bands at about 132 kDa) were purchased from Santa Cruz Biotechnology Inc. (Santa Cruz, CA, USA). The inhibitor cocktail Complete Midi was from Roche (Basel, Switzerland). Mini protean TGX pre-cast gel 7.5% and Mini nitrocellulose Transfer Packs were purchased from BioRad (Hercules, CA, USA).

7.2.2 HepG2 Cell Culture Conditions and Treatment

The HepG2 cell line was bought from ATCC (HB-8065, ATCC from LGC Standards, Milan, Italy) and was cultured in DMEM high glucose with stable L-glutamine, supplemented with 10% FBS, 100 U/mL penicillin, 100 µg/mL streptomycin (complete growth medium) with incubation at 37 °C under 5% CO₂ atmosphere.

7.2.3 HMGCoAR Activity Assay

The experiments were carried out following the manufacturer instructions and optimized protocol (Zanoni, Aiello, Arnoldi, & Lammi, 2017b). The assay buffer, NADPH, substrate solution, and HMGCoAR were provided in the HMGCoAR Assay Kit (Sigma Aldrich SRL, Milan, Italy). The experiments were carried out following the manufacturer instructions at 37 °C. In particular, each reaction (200 µL) was prepared adding the reagents in the following order: 1 × assay buffer, a 10–1000 µM doses of H3 or vehicle (C), the NADPH (4 µL), the substrate solution (12 µL), and finally the HMGCoAR (catalytic domain) (2 µL). Subsequently, the samples were mixed and the absorbance at 340 nm read by the microplate reader Synergy H1 (Winooski, VT, USA) at time 0 and 10 min. The HMGCoAR-dependent oxidation of NADPH and the inhibition properties of peptides were measured by absorbance

reduction, which is directly proportional to enzyme activity.

7.2.4 MTT Assay

A total of 3×10^4 HepG2 cells/well were seeded in 96-well plates and treated with 0.00001, 0.0001, 0.001, 0.01, 0.1 and 1.0 mM of peptide H3, respectively, or vehicle (H₂O) in complete growth media for at 37 °C under 5% CO₂ atmosphere for 48 h. Subsequently, the treatment solvent was aspirated, and 100 µL/well of 3-(4,5 dimethylthiazol-2-yl)-2,5-diphenyltetrazolium bromide (MTT) filtered solution was added. After 2 h of incubation at 37 °C under 5% CO₂ atmosphere, the 0.5 mg/mL solution was aspirated, and 100 µL/well of the lysis buffer (8 mM HCl + 0.5% NP-40 in DMSO) was added. After 5 min of slow shaking, the absorbance at 575 nm was read on the Synergy H1 fluorescence plate reader (Biotek, Bad Friedrichshall, Germany).

7.2.5 In-Cell Western (ICW) Assay

For the experiments, a total of 3×10^4 HepG2 cells/well were seeded in 96-well plates. The following day, cells were washed with PBS and then starved overnight (O/N) in DMEM without FBS and antibiotics. After starvation, HepG2 cells were treated with peptide H3 (25.0 µM) and vehicle (H₂O) for 24 h at 37 °C under 5% CO₂ atmosphere. Subsequently, they were fixed in 4% paraformaldehyde for 20 min at room temperature (RT). Cells were washed 5 times with 100 µL of PBS/well (each wash was for 5 min at RT) and the endogenous peroxides activity quenched adding 3% H₂O₂ for 20 min at RT. Non-specific sites were blocked with 100 µL/well of 5% bovine serum albumin (BSA, Sigma) in PBS for 1.5 h at RT. LDLR primary antibody solution (1:3000 in 5% BSA in PBS, 25 µL/well) was incubated overnight (O/N) at + 4 °C. Subsequently, the primary antibody solution was discarded and each sample was washed 5 times with 100 µL/well of PBS. Goat anti-rabbit Ig-HRP secondary antibody solution (Santa Cruz) (1:6000 in 5% BSA in PBS, 50 µL/well), was added and incubated 1 h at RT. The secondary antibody solution was washed 5 times with 100 µL/well of PBS. Freshly prepared TMB substrate (Pierce, 100 µL/well) was

added and the plate was incubated at RT until desired color was developed. The reaction was stopped with 2 M H₂SO₄ and then the absorbance at 450 nm was measured using the microplate reader Synergy H1 (Winooski, VT, USA). After the read, cells were stained by adding 1 X Janus Green stain, incubating for 5 min at RT. The dye was removed and the sample washed 5 times with water. Afterward 100 µL 0.5 M HCl for well were added and incubated for 10 min. After 10 min shaking, the OD at 595 nm was measured using the microplate reader Synergy H1 (Winooski, VT, USA).

7.2.6 Fluorescent LDL Uptake

HepG2 cells (3×10^4 /well) were seeded in 96-well plates and kept in complete growth medium for 2 days before treatment. The third day, cells were washed with PBS and then starved overnight (O/N) in DMEM without FBS and antibiotics. After starvation, they were treated with peptide H3 (25.0 µM), and vehicle (H₂O) for 24 h with at 37 °C under 5% CO₂ atmosphere. At the end of the treatment, the culture medium was replaced with 50 µL/well LDL-DyLight™ 550 working solution (Cayman Chemical Company, Ann Arbor, MI, USA) prepared in DMEM without FBS and antibiotics. The cells were additionally incubated for 2 h at 37 °C and then the culture medium was aspirated and replaced with PBS (100 µL/well). The degree of LDL uptake was measured using the Synergy H1 fluorescent plate reader (Winooski, VT, USA) (excitation and emission wavelengths 540 and 570 nm, respectively). Fluorescent LDL-uptake was finally assessed following optimized protocol (Zanoni, Aiello, Arnoldi, & Lammi, 2017b).

7.2.7 Western Blot Analysis

Immunoblotting experiments were performed using optimized protocol (Zanoni, Aiello, Arnoldi, & Lammi, 2017b). A total of 1.5×10^5 HepG2 cells/well (24-well plate) were treated with 25.0 µM of H3 for 24 h. After each treatment, the supernatants were collected and stored at -20 °C; cells were scraped in 40 µL ice-cold lysis buffer (RIPA buffer + inhibitor cocktail + 1:100 PMSF + 1:100 Na-

orthovanadate + 1:1000 β -mercaptoethanol) and transferred in ice-cold microcentrifuge tubes. After centrifugation at 13,300 g for 15 min at 4 °C, the supernatants were recovered and transferred into new ice-cold tubes. Total proteins were quantified by the Bradford's method and 50 μ g of total proteins loaded on a pre-cast 7.5% Sodium Dodecyl Sulfate-Polyacrylamide (SDS-PAGE) gel at 130 V for 45 min. Subsequently, the gel was pre-equilibrated in H₂O for 5 min at room temperature (RT) and transferred to a nitrocellulose membrane (Mini nitrocellulose Transfer Packs,) using a Trans-Blot Turbo at 1.3 A, 25 V for 7 min. Target proteins, on milk or BSA blocked membrane, were detected by primary antibodies as follows: anti-SREBP-2, anti-LDLR, anti-HMGCoAR, anti-PCSK9, anti HNF-1 α , anti-p-HMGCoAR (Ser 872), anti-p-AMPK (Thr 172) and anti- β -actin. Secondary antibodies conjugated with HRP and a chemiluminescent reagent were used to visualize target proteins and their signal was quantified using the Image Lab Software (Biorad, Hercules, CA, USA). The internal control β -actin was used to normalize loading variations.

7.2.8 Quantification through ELISA of PCSK9 Secreted by HepG2 Cells

The supernatants collected from treated HepG2 cells (25.0 μ M of H3) were centrifuged at 600 \times g for 10 min at 4 °C and ELISA assay performed using protocol already optimized (Zanoni, Aiello, Arnoldi, & Lammi, 2017b). They were recovered and diluted to the ratio 1:10 with DMEM in a new ice-cold tube. PCSK9 was quantified by ELISA (R&D System, Minneapolis, MN, USA). Briefly, the experiments were carried out at 37 °C, following the manufacturer's instructions. Before starting the assay, human PCSK9 standard curve (20.0, 10.0, 5.0, 2.5, 1.25, and 0.625 ng/mL) was prepared by serial dilutions from a 40 ng/mL stock. 100 μ L of the Assay Diluent RD1-9 (provided into the kit) were placed in each well, before adding the standards and the samples (50 μ L) and incubating the ELISA plate for 2 h at RT. Subsequently, wells were washed 4 times with the wash buffer, and 200 μ L of human PCSK9-conjugate (HRP-labelled anti-PCSK9) was added to each well for 2 h at RT. Following aspiration, wells was washed 4 times with the kit wash buffer. After

the last wash, 200 μ L of substrate solution were added to the wells and allowed to incubate for 30 min at RT. The reaction was stopped with 50 μ L of the stop solution (2 M sulfuric acid) and the absorbance at 450 nm was measured using Synergy H1 microplate (Winooski, VT, USA).

7.2.9 Computational Methods

Docking simulations were performed by using the already-published computational procedure (Lammi, Sgrignani, Roda, Arnoldi, & Grazioso, 2019). Briefly, the H3 peptide was built by using the VEGA program and its conformational profile was explored by quenched MonteCarlo analysis (Pedretti, Mazzolari, Gervasoni, Fumagalli, & Vistoli, 2021). The minimized peptide was then docked within the previously prepared HMGC_oAR structure. Docking simulations were carried out using PLANTS and the 10 generated poses ranked by the ChemPLP scoring function with the speed equal to 1 (Korb, Stützle, & Exner, 2009). The so-obtained complexes were finally minimized and rescored, as implemented in ReScore+ (Vistoli, Mazzolari, Testa, & Pedretti, 2017).

7.2.10 Statistical Analysis

All the data sets were checked for normal distribution by the D'Agostino and Pearson test. Since they are all normally distributed with p -values < 0.05 , we proceeded with statistical analyses by t-test and One-Way ANOVA followed by the Dunnett's and Tukey's post-hoc tests and using Graphpad Prism 9 (San Diego, CA, USA). Values were reported as means \pm S.D.; p -values < 0.05 were considered to be significant.

7.3 Results

7.3.1 Peptide H3 Drops HMGC_oAR Activity *In Vitro*

HMGC_oAR is the known target of statins, the main drugs used for the therapy of hypercholesterolemia (Brown & Goldstein, 1997; Istvan & Deisenhofer, 2001). Since the HP is able to drop the catalytic activity of HMGC_oAR, we decided to evaluate the inhibitory ability of peptide H3 *in vitro* using the purified catalytic domain of

HMGC_oAR, testing concentrations ranging from 10 to 1000 μ M. As shown in **Figure 7.1A**, the catalytic activity of HMGC_oAR was inhibited by peptide H3 in a dose-dependent manner with an IC₅₀ value of 59 μ M. Pravastatin, which was used as positive control, instead inhibits enzyme activity with an IC₅₀ equal to 0.55 μ M. This value agrees with the IC₅₀ of 0.47 μ M reported in the literature (Mosley, Kalinowski, Schafer, & Tanaka, 1989). Pravastatin is, thus, at least 100-fold more potent than H3 (**Figure 7.1A**).

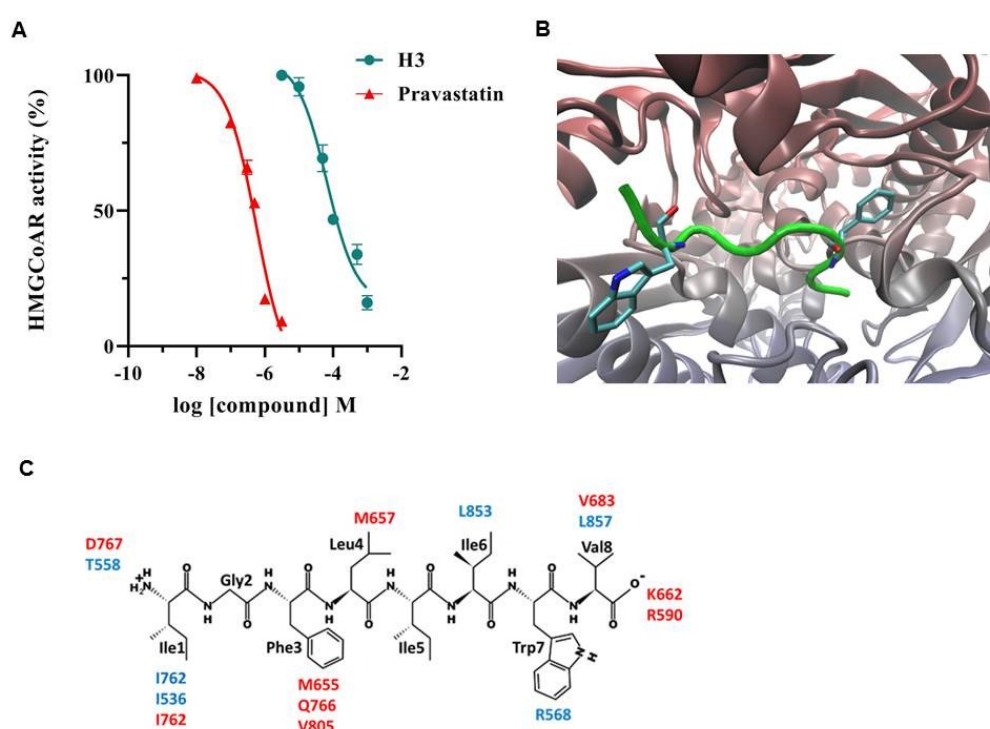


Figure 7.1 *In vitro* inhibition and *in silico* analysis of the peptide H3 interaction with HMGC_oAR. In (A), points indicate the effects of H3 and pravastatin on the HMGC_oAR activity. The data points represent the averages \pm S.D. of three independent experiments in triplicate. (B) shows the putative pose of H3 (in green) within the binding cavity of HMGC_oAR, which is placed at the interface between the two monomers (drawn in blue and red). (C) details the key interactions stabilized by each residue of H3 (the residue labels are colored according to the monomer).

To obtain further insight in the interaction of peptide H3 and HMGC_oAR, a docking study was undertaken. **Figure 7.1B** reports the computed putative complex between

H3 and HMGC_oAR, revealing that peptide H3 is conveniently accommodated at the interface between the two monomers, with which it stabilizes a diverse pattern of interactions. **Figure 7.1B** also indicates that Phe-3 is nicely inserted within a narrow sub-pocket, mostly lined by hydrophobic residues. Similarly, Trp-7 approaches the L α 1 helix of the other monomer, where it stabilizes a clear charge-transfer interaction with Arg-568. Although both charged termini are involved (as expected) in key ion-pairs, **Figure 7.1C** emphasizes the remarkable role played by the hydrophobic contacts in the H3 binding. In detail, almost all the central residues are engaged in hydrophobic interactions involving both alkyl side chains and methionine residues, which can also elicit π -sulphur interactions with aromatic residues (i.e., Phe-5). A comparison with the key interactions stabilizing the resolved complex of HMGC_oAR with statins (Zuckerandl & Pauling, 1965) reveals an interesting agreement with those observed for the H3 peptide, which concern both the basic residues bridging the ligand's carboxylate (K662 and R590) and the hydrophobic side chains which also approach the apolar moieties of the statins (V683, L853, L857).

7.3.2 Peptide H3 Effects on the Cell Vitality of HepG2

MTT experiments were performed to exclude any potential effect of peptide H3 on HepG2 cellular vitality. Because HepG2 cells are a slow growing cell line with an average doubling time of around 2 days, they were incubated for 48 h with different concentrations of peptide H3 before MTT assay. After a 48 h treatment, no effect on HepG2 viability was observed up to 100 μ M versus the control cells (C). Instead, a reduced cell viability equal to $19.63 \pm 0.59\%$ was detected after the treatment with 1 mM H3 (**Figure 7-S1**). These results are in line with previous evidences (Bollati, et al., 2022; Cruz-Chamorro, et al., 2022). Based on these results, the following experiments, aimed at investigating the molecular and functional effects of peptide H3, were assessed at 25.0 μ M, a dose which is 40-fold less concentrated than the lowest dose (1 mM) affecting cell viability.

7.3.3 Peptide H3 Modulates the LDLR Pathway

For assessing the ability of peptide H3 to modulate the LDLR pathway, immunoblotting experiments were performed on HepG2 cell lysates obtained after their treatment with peptide H3 at 25.0 μM . In parallel, HepG2 cells were also treated with pravastatin (1.0 μM) as the reference compound. The results suggest that the LDLR pathway was effectively activated after 24 h treatment (**Figure 7.2**). In more detail, peptide H3 induced an up-regulation of the total protein level of the mature SREBP-2 transcription factor (65 KDa) by $118.3\% \pm 7.00\%$ versus the untreated cells ($p < 0.05$, **Figure 7.2A**). In addition, H3 increased the mature nuclear SREBP-2 protein levels (65 KDa) up to $147.0 \pm 13.8\%$ ($p < 0.001$, **Figure 7.2B**). In agreement with these data, an improvement of the nuclear/total mature SREBP-2 (65 KDa) ratio up to $147.1 \pm 10.4\%$ was detected in the HepG2 cells treated with the peptide compared to the untreated cells ($p < 0.01$, **Figure 7.2C**). In parallel, the precursor form of SREBP-2 (125 KDa) was also detected in the cytosolic fraction of HepG2 cells, and the ratio of mature (65 KDa)/precursor (125 KDa) SREBP-2 protein levels was calculated (**Figure 7-S2A,B**). The results indicate that peptide H3 improved the precursor SREBP-2 (125 KDa) protein up to $157.5 \pm 10.9\%$ ($p < 0.05$) and the mature (65 KDa)/precursor (125 KDa) SREBP-2 protein level ratio up to $122.1 \pm 1.2\%$ ($p < 0.01$) versus the untreated cells (**Figure 7-S2A,B**), confirming the improvement of mature SREBP-2 protein levels in the nuclear fraction, which, consequently, led to an increment of total LDLR proteins up to $150.2 \pm 17.02\%$ versus the control ($p < 0.001$, **Figure 7-2D**). Under the same conditions, pravastatin (1.0 μM) improved the protein levels of total mature SREBP-2 (65 KDa) and nuclear mature SREBP-2 (65 KDa) targets by $134.9 \pm 17.3\%$ ($p < 0.001$, **Figure 7.2A**) and $152.3 \pm 8.2\%$ ($p < 0.0001$, **Figure 7.2B**), respectively, versus the untreated cells. The ratio between the nuclear mature SREBP-2 (65 KDa) and total mature SREBP-2 (65 KDa) was increased up to $153.2 \pm 19.5\%$ ($p < 0.01$, **Figure 7.2C**). In addition, pravastatin increased the precursor SREBP-2 (125 KDa) protein levels in the cytoplasmic fraction up to $140.8 \pm 9.0\%$ ($p < 0.05$) leading to an augmentation of the mature (65 KDa)/precursor (125

KDa) SREBP-2 protein level ratio up to $122.4 \pm 2.6\%$ ($p < 0.01$) (**Figure 7-S2A, B**). In agreement with the improved mature SREBP-2 levels in the nuclear fraction of HepG2 cells, pravastatin ($1.0 \mu\text{M}$) increased the LDLR up to $140.8 \pm 15.35\%$ ($p < 0.001$, **Figure 7.2D**) versus the control cells.

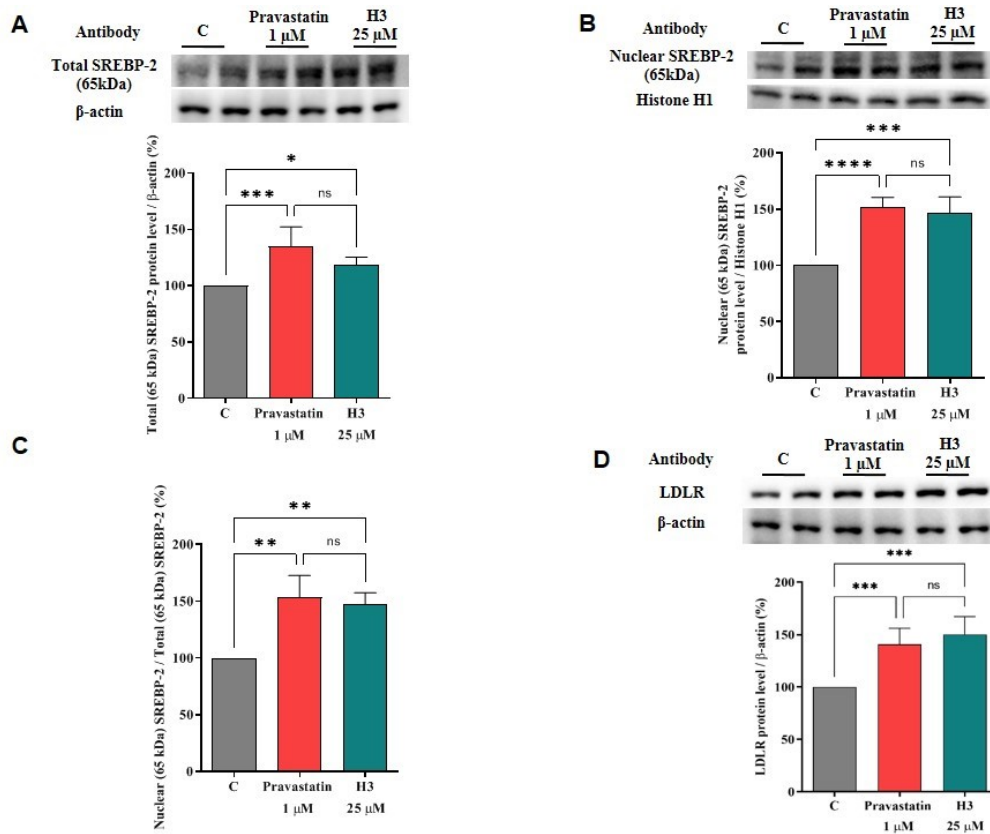


Figure 7.2 Effect of peptide H3 on LDLR pathway. HepG2 cells were treated with peptide H3 ($25.0 \mu\text{M}$) or pravastatin ($1.0 \mu\text{M}$). Mature SREBP-2 (65 KDa) on total lysate, mature SREBP-2 (65 KDa) on nuclear fraction of HepG2 cells, LDLR, β -actin, and histone H1 immunoblotting signals were detected using specific anti-SREBP-2, anti-LDLR, anti- β -actin, and anti-histone H1 primary antibodies, respectively. The total (A) and nuclear (B) SREBP-2 (65 KDa) signals, as well as the LDLR (D) signals, were quantified by ImageJ Software and normalized with β -actin or with histone H1 signals. Panel (C) indicates the nuclear/total SREBP-2 (65 KDa) ratio. Bars represent the averages of three independent experiments \pm S.D., each performed in duplicate. ns: not significant, (*) $p < 0.05$, (**) $p < 0.01$, (***) $p < 0.001$, and (****) $p < 0.0001$ vs. control: C.

7.3.4 Peptide H3 Modulates Intracellular HMGCoAR Protein Levels

Because of the augmentation of the SREBP-2 transcription factor followed by an improvement of the LDLR protein levels, an increase of the HMGCoAR protein levels was also observed after 24 h treatment with peptide H3. The HMGCoAR protein levels were improved by $129.9 \pm 9.16\%$ ($p < 0.001$, **Figure 7.3A**) versus the control, while pravastatin (1.0 μM) increased the enzyme protein by $129.3 \pm 9.33\%$ ($p < 0.01$, **Figure 7.3A**). The literature evidences suggest that statins induce the activation of the AMPK-pathway through the augmentation of its phosphorylation on threonine 172 in different cellular systems (Athyros, Boutari, Stavropoulos, Anagnostis, Imprialos, Doumas, et al., 2018; Dehnavi, Kiani, Sadeghi, Biregani, Banach, Atkin, et al., 2021; Izumi, Shiota, Kusakabe, Hikita, Nakao, Nakamura, et al., 2009), which in turn produces an inhibition of HMGCoAR activity through its phosphorylation on Ser872 residue (Viollet, Foretz, Guigas, Horman, Dentin, Bertrand, et al., 2006), which is the phosphorylation site of AMPK. In light of this observation, and with the aim of comparing the hypocholesterolemic behavior of H3 with statin, further immunoblotting experiments were designed to investigate the effect of the treatment with peptide H3 and pravastatin on AMPK activation and HMGCoAR inactivation (AMPK substrate). Notably, the augmentation of phosphorylation levels of HMGCoAR (serine872, AMPK phosphorylation site) were detected up to $171.2 \pm 25.71\%$ versus the control ($p < 0.001$, **Figure 7.3B**) upon cellular treatment with H3. This result is in line with the increase of AMPK phosphorylation (threonine 172) up to $138.5 \pm 14.04\%$ versus the control ($p < 0.001$, **Figure 7.3C**). In line with the literature evidences, as a reference compound, pravastatin (1.0 μM) was able to increase the AMPK phosphorylation (threonine 172) up to ated ones. In fact, the peptide H3 and pravastatin increased it up to $127.6 \pm 10.21\%$ ($p < 0.01$, **Figure 3D**) and $121.3 \pm 2.17\%$ ($p < 0.05$, **Figure 7.3D**), respectively.

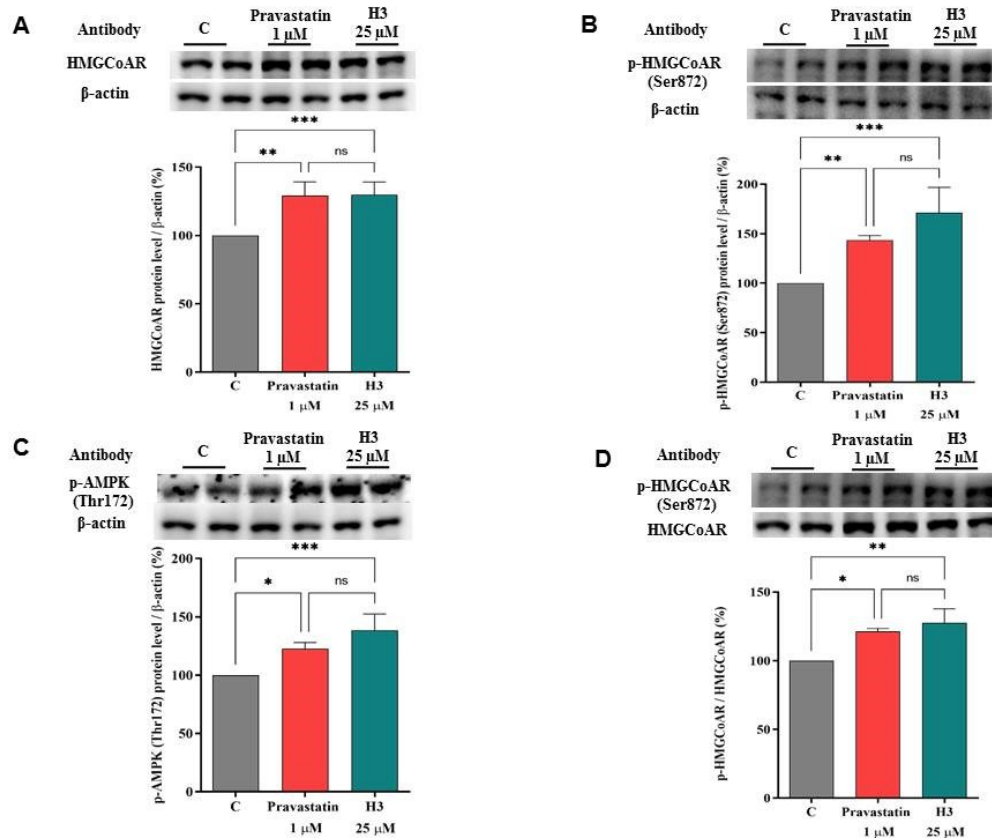


Figure 7.3 Peptide H3 and pravastatin increased HMGCAR protein levels (A). Peptide H3 and pravastatin improved the inactive phosphorylated HMGCAR (p-HMGCAR) protein levels (B) due to the activation of AMPK through the augmentation of its phosphorylation on Thr172 residue (C). The ratio between p-HMGCAR and total HMGCAR was calculated after treatment with peptide H3 versus the C sample (D). Bars represent the averages of three independent experiments \pm S.D., each performed in duplicate. ns: not significant, (*) $p < 0.05$, (**) $p < 0.01$, (***) $p < 0.001$.

The p-HMGCAR/total HMGCAR ratio of the H3-treated, pravastatin-treated, and untreated cells were also calculated. The ratio of treated cells was higher than that of untreated ones. In fact, the peptide H3 and pravastatin increased it up to $127.6 \pm 10.21\%$ ($p < 0.01$, **Figure 7.3D**) and $121.3 \pm 2.17\%$ ($p < 0.05$, **Figure 7.3D**), respectively.

7.3.5 Peptide H3 Increases the Expression of LDLR Localized on Cellular Membranes and Modulates LDL-uptake in the HepG2 Cell Environment

The capacity of peptide H3 to modulate the LDLR protein levels on the hepatocyte cellular surface was investigated using an ICW assay, i.e., a quantitative colorimetric cell-based assay (Lammi, Zanoni, & Arnoldi, 2015b). An improvement of the LDLR protein levels specifically localized on the cellular membrane of hepatocytes was observed up to $176.9 \pm 11.31\%$ ($p < 0.0001$, **Figure 7.4A**). As reference compound, pravastatin (1.0 μM) also increased the LDLR protein levels by $127.3 \pm 14.31\%$ ($p < 0.0001$, **Figure 7.4A**). From a functional point of view, the augmentation of the membrane LDLR protein levels led to the improved ability of HepG2 cells to absorb LDL from the extracellular environment by $191.1 \pm 30.30\%$ after the treatment with peptide H3 at the same concentration of 25.0 μM ($p < 0.0001$, **Figure 7.4B**). In the same conditions, pravastatin (1.0 μM) improved the capacity of HepG2 cells to absorb extracellular LDL by $226.9 \pm 11.05\%$ ($p < 0.0001$, **Figure 7.4B**). The statin increases the LDL uptake more efficiently than the peptide, whereas H3 is more efficient in increasing the LDLR levels. This apparent contradictory fact may be explained by considering that the LDL-uptake assay and ICW display different sensitivities. Indeed, the former (LDL-uptake) works in fluorescence, which is a more sensitive assay than the latter (ICW), which is a colorimetric test. However, these results indicate that the hypocholesterolemic behavior of peptide H3 is similar to that of pravastatin.

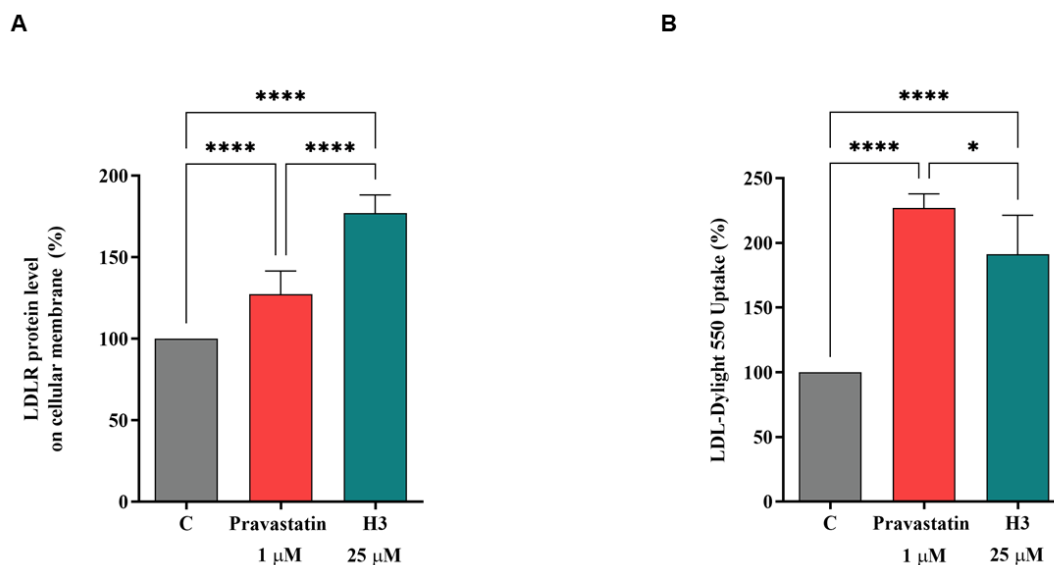


Figure 7.4 HepG2 cells were treated with peptide H3 (25.0 μM) or pravastatin (1.0 μM) for 24 h. (A) The percentage of LDLR protein up-regulation was measured by ICW. (B) The specific fluorescent LDL-uptake signals were analyzed by Synergy H1 (Biotek). The data points represent the averages ± S.D. of three experiments in triplicate. (*) $p < 0.05$, (****) $p < 0.0001$ vs. control: C.

7.3.6 Effect of Peptide H3 on the Modulation of PCSK9 Protein and Release Levels

Previous studies have evidenced a similar hypocholesterolemic effect of hempseed hydrolysates (HP) to statins, leading to the increase of the PCSK9 protein levels (Zanoni, Aiello, Arnoldi, & Lammi, 2017a). To assess if peptide H3 can perform a satisfactory modulation on the hepatic intracellular PCSK9 protein and release levels or maintain the same ability of HP for PCSK9, dedicated experiments were conducted. Hence, HepG2 cells were treated with peptide H3 at 25.0 μM to investigate the modulation on PCSK9 and its transcription factor HNF-1α. Surprisingly, the results clearly indicate that peptide H3 caused a $10.85 \pm 6.12\%$ reduction of intracellular PCSK9 protein levels versus the control ($p < 0.01$, **Figure 7.5A**), playing an opposite effect on PCSK9 compared with HP. As expected, this finding agrees with the ability of peptide H3 to reduce the HNF-1α transcription factor levels by $19.40 \pm 5.18\%$

compared to the untreated cells ($p < 0.0001$, **Figure 7.5B**). In contrast, after treatment with pravastatin (1.0 μM), the direct activation of HNF-1 α was up to $116.9 \pm 3.21\%$ ($p < 0.0001$, **Figure 7.5B**), resulting in the increase of PCSK9 protein levels up to $118.8 \pm 6.11\%$ ($p < 0.0001$, **Figure 7.5A**).

In light of these results, the effect of peptide H3 on the regulation of the mature PCSK9 release was evaluated by ELISA assay. In agreement with the molecular results, peptide H3 could decrease the secretion of the mature PCSK9 by $16.58 \pm 4.64\%$ versus control ($p < 0.001$, **Figure 7.5C**), while pravastatin (1.0 μM) improved the release of PCSK9 up to $119.6 \pm 1.18\%$ ($p < 0.001$, **Figure 7.5C**).

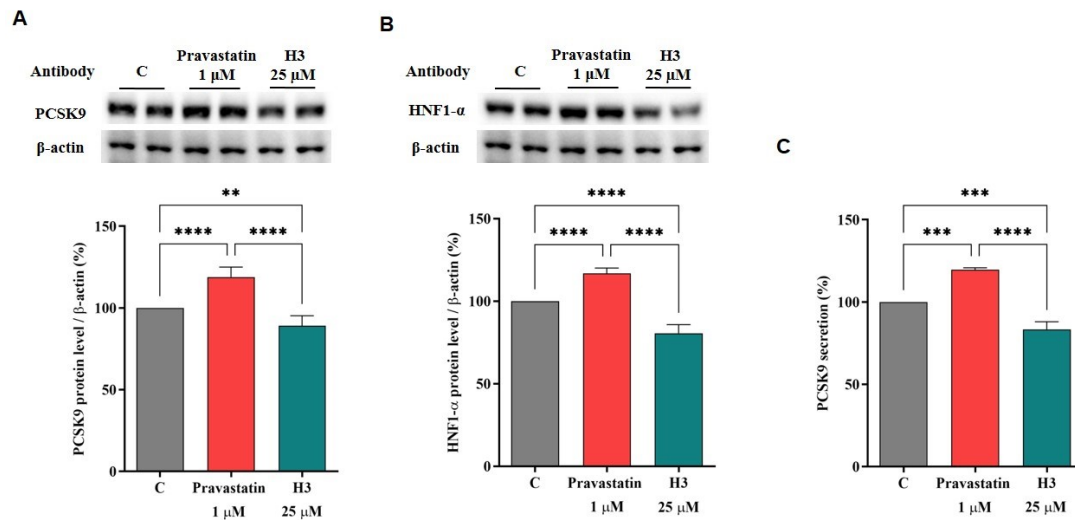


Figure 7.5 After 24 h treatment with peptide H3 (25.0 μM) or pravastatin (1.0 μM), effects on the PCSK9 protein levels (A), effects on the HNF-1 α protein levels (B), and effects on mature PCSK9 release (C). The Panel signals were quantified by ImageJ Software and normalized with β -actin signals. Data points represent the averages \pm S.D. of three experiments in duplicate. (**) $p < 0.001$, (***) $p < 0.001$, and (****) $p < 0.0001$ vs. control: C.

7.4 Discussion

CVD is a multifactorial pathology in which oxidative and inflammatory status as well as hypercholesterolemia are among the main risk factors (Bays, Taub, Epstein,

Michos, Ferraro, Bailey, et al., 2021). Peptide H3 is a multifunctional octapeptide, obtained from the hydrolysis of hempseed proteins using pepsin (Bollati, et al., 2022), that is transported intact by differentiated Caco-2 and is able to exert both antioxidant and anti-inflammatory activity in HepG2 cells (Bollati, et al., 2022; Cruz-Chamorro, et al., 2022). These results prompted us to better investigate its multifunctional behavior. To achieve this goal, a deeper study was carried out for characterizing the potential effect of peptide H3 on cholesterol metabolism. Peptide H3 reduces the *in vitro* HMGCoAR activity with a dose-response trend and an IC₅₀ value of 59 μM (**Figure 7.1**). Its activity is similar to peptide LTFPGSAED (from lupin protein hydrolysis with pepsin) and peptide VGVL (from amaranth protein hydrolysis with pepsin), displaying IC₅₀ values equal to 68.4 and 50 μM, respectively (Soares, Mendonça, De Castro, Menezes, & Arêas, 2015). On the contrary, peptide H3 is about 2.5-fold more potent than LILPKHSDAD (from lupin protein hydrolysis with pepsin) (Zanoni, Aiello, Arnoldi, & Lammi, 2017b). In addition, in contrast to other soybean peptides such as IAVPTGVA, IAVPGEVA, and LPYP (from soybean glycinin hydrolysis with pepsin), and YVVNPDNDEN and YVVNPDNNEN (from soybean β-conglycinin) which are less effective inhibitors of HMGCoAR (IC₅₀ values equal to 247, 222, 300 μM (Lammi, Zanoni, & Arnoldi, 2015a) and 150, and 200 μM (Lammi, Zanoni, Arnoldi, & Vistoli, 2015), respectively) peptide H3 exerts a more potent inhibitory activity of this enzyme (up to five-fold higher).

From a computational point of view, the docking results emphasize that a convenient HMGCoAR binding can be pursued by properly combining polar and hydrophobic interactions. This result is in agreement with the resolved HMGCoAR structures in complex with statins, and emphasizes that peptides which are too polar have to pay the unfavorable price of desolvation energy, regardless of their interacting capacity. In light of these evidences, the effect of peptide H3 on cholesterol metabolism was analyzed using human hepatic HepG2 cells, the major cell involved in plasma LDL cholesterol clearance due to its ability to express the highest number of active LDLR on its surface (Zhang, Lagace, Garuti, Zhao, McDonald, Horton, et al., 2007). Indeed, HepG2 cells are globally considered a reliable model for investigating the cholesterol-

lowering effects of bioactive agents from different sources (Donato, Tolosa, & Gómez-Lechón, 2015; Ho & Pal, 2005; Lammi, Zanoni, Calabresi, & Arnoldi, 2016; Lammi, Zanoni, Ferruzza, Ranaldi, Sambuy, & Arnoldi, 2016; Shin, Park, Sung, Chung, & Hwang, 2016).

Preliminary MTT experiments were carried out to exclude any potential dose impacting on cell viability. In line with previous evidences (Bollati, et al., 2022; Cruz-Chamorro, et al., 2022), the results confirmed that H3 is safe for HepG2 cells up to 100 μ M (**Figure 7-S1**). Based on these results, HepG2 cells were treated with 25 μ M of peptide H3. Similarly to pravastatin (1 μ M, the positive control), by inhibiting HMGCoAR activity, peptide H3 modulates the intracellular cholesterol pathway, leading to an increase of the LDLR and HMGCoAR protein levels through the modulation of SREBP-2 (**Figure 7.2**, **Figure 7.3** and **Figure 7-S2**). Notably, HMGCoAR is a highly regulated enzyme (Goldstein & Brown, 1990): it can be regulated long-term by the control of its synthesis and its degradation or short-term through phosphorylation or dephosphorylation (Pallottini, Martini, Pascolini, Cavallini, Gori, Bergamini, et al., 2005). In particular, its regulation is achieved through phosphorylation of Ser872 by AMPK, which decreases the enzyme activity (Ching, Davies, & Hardie, 1996).

The literature reports that some natural compounds such as policosanols are able to increase the phosphorylation of AMPK with the direct inhibition of HMGCoAR (Oliaro-Bosso, Calcio Gaudino, Mantegna, Giraud, Meda, Viola, et al., 2009). Furthermore, it is also known that statins are able to activate AMPK (Wei Sun, Lee, Zhu, Gu, Wang, Zhu, et al., 2006) with the consequence of a synergistic inhibition of HMGCoAR activity, its direct target (Viollet, et al., 2006). In agreement with these evidences, our results provide a clear indication that, similarly to statins (Athys, et al., 2018; Dehnavi, et al., 2021; Izumi, et al., 2009), peptide H3 increases the phosphorylation level of AMPK at the Thr172 residue of the catalytic subunit, which in turn produces an inhibition of HMGCoAR activity through its phosphorylation on the Ser872 residue (Viollet, et al., 2006), which is the phosphorylation site of AMPK (**Figure 7.3**). In line with these findings, an improvement of the p-

HMGC_oAR/HMGC_oAR protein ratio with the consequence of a diminished enzyme activity was observed, in agreement with the literature (Levy, Ouadda, Spahis, Sane, Garofalo, Grenier, et al., 2013) (**Figure 7.3**). Other plant peptides share the same mechanism of HMGC_oAR inhibition, in particular IAVPGEVA, IAVPTGVA, and LPYP, deriving from soybean protein (Lammi, Zanoni, Ferruzza, Ranaldi, Sambuy, & Arnoldi, 2016), and LTFPGSAED and LILPHKSDAD from lupin proteins (Zanoni, Aiello, Arnoldi, & Lammi, 2017b). In addition, it was demonstrated that this hempseed peptide increases the LDLR localized on HepG2 cell surfaces, leading from a functional point of view to the improved ability of these cells to clear extracellular LDL with a final cholesterol-lowering consequence (**Figure 7.4**). The cholesterol-lowering behavior of peptide H3 is similar to that of pravastatin; however, a different effect was observed on the PCSK9 protein levels. Interestingly, both PCSK9 and LDLR are co-regulated by SREBP-2 transcription factor (Dubuc, Chamberland, Wassef, Davignon, Seidah, Bernier, et al., 2004; Maxwell, Fisher, & Breslow, 2005). However, since the HNF-1 α binding site is unique to the PCSK9 promoter, and is not present in the LDLR promoter, the modulation of the PCSK9 transcription through HNF-1 α does not affect the LDLR pathway. Thus, the co-regulation of PCSK9 from LDLR and other SREBP target genes is disconnected by the HNF-1 α binding site (Dong, Li, Singh, Cao, & Liu, 2015; Maxwell, Fisher, & Breslow, 2005). In this context, it is known that statins increase the protein levels of PCSK9, which quench any effective LDL clearance by promoting LDLR degradation (Chaudhary, Garg, Shah, & Sumner, 2017), thereby counteracting the therapeutic effects of these drugs (Dubuc, et al., 2004).

Indeed, our results confirm that pravastatin improves the mature PCSK9 protein levels through HNF-1 α enhancement; on the contrary, peptide H3 reduces both HNF-1 α and PCSK9 levels. In line with these results, it was observed that only peptide H3 reduces the PCSK9 release in extracellular environments, whereas pravastatin was ineffective. This result contributes to explaining the better ability of peptide H3 to raise the level of the LDLR population localized on the surface of HepG2 cells than pravastatin. Indeed, the effect of peptide H3 on the PCSK9 protein and release levels is similar to

lupin hydrolysate (Lammi, Zanoni, Calabresi, & Arnoldi, 2016; Lammi, Zanoni, Ferruzza, Ranaldi, Sambuy, & Arnoldi, 2016) but different from the behavior of the hempseed hydrolysates (Zanoni, Aiello, Arnoldi, & Lammi, 2017a). Indeed, only lupin hydrolysate is able to modulate the HMGCoAR activity and PCSK9 protein and release levels, whereas hempseed seems to exert the cholesterol lowering activity targeting HMGCoAR activity similarly to statin, without producing an effect on PCSK9 secretion and protein levels (Zanoni, Aiello, Arnoldi, & Lammi, 2017a).

7.5 Conclusins

In this study, peptide H3 obtained from the hydrolysis of hempseed protein was shown to exert cholesterol-lowering effects, displaying a multifunctional activity which is better compared with hempseed hydrolysates (HP), especially in the modulation of PCSK9 protein and release levels. Since there is a lack of studies showing how peptide H3 affects PCSK9, relevant experiments will be carried out in the future to elucidate the specific mechanism. Indeed, it may be feasibly concluded that peptide H3 might be exploited in the future for the development of new dietary supplements and/or used as a scaffold for the synthesis of new peptidomimetics for the prevention of CVD and/or metabolic syndrome. In this context, it will be imperative to carry out *in vivo* experiments on suitable animal models to confirm H3 pleiotropic activity and to establish the right amount of peptides that should be consumed in the human diet or in supplements to achieve its health-promoting activity.

7.6 Supporting information

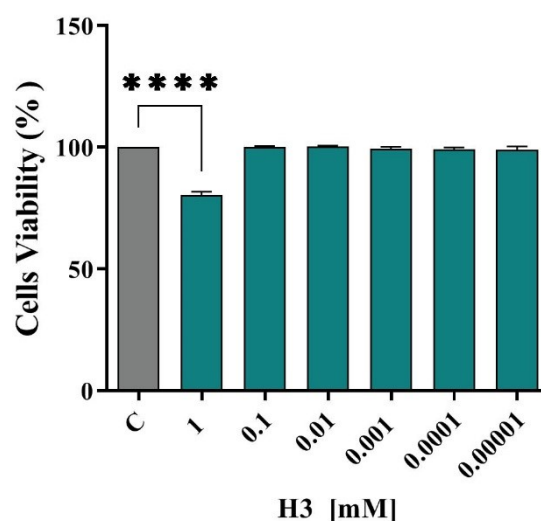


Figure 7-S1. Effect of H3 on HepG2 cell viability. The bar graphs indicating the results of cell viability assay of HepG2 cells after peptide H3 (0.00001 – 1 mM) treatment for 48 h. The data points represent the averages \pm S.D. of three experiments in triplicate. (****) $p < 0.0001$ vs control (C).

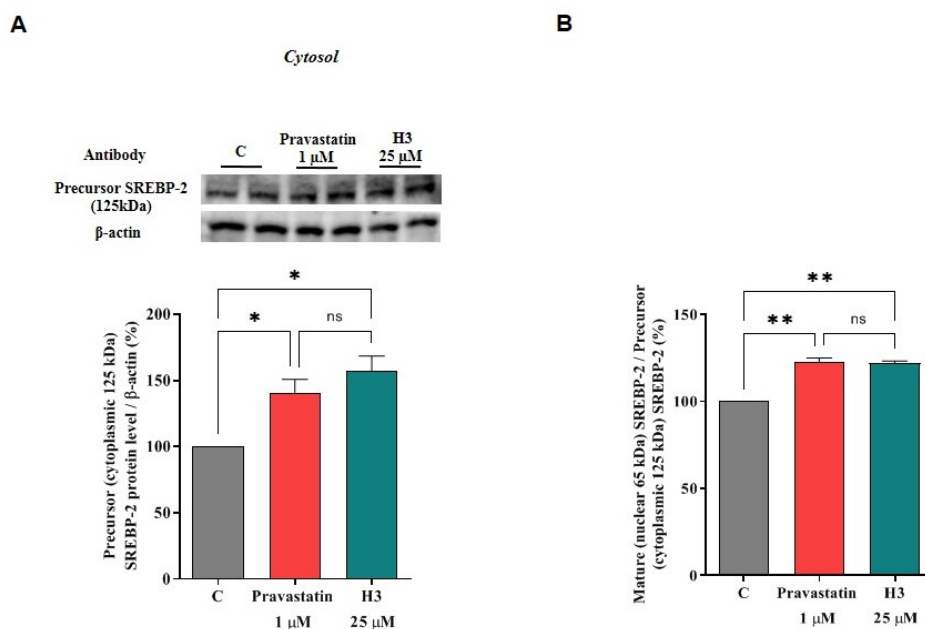


Figure 7-S2. Effect of peptide H3 and pravastatin on the modulation of precursor SREBP-2 levels in cytoplasmatic fraction (A) and mature (nuclear 65 KDa)/precursor (125 KDa) SREBP-2 ratio (B). C: control; (* $p < 0.05$), (** $p < 0.01$)

7.7 References

- Aiello, G., Lammi, C., Boschin, G., Zanoni, C., & Arnoldi, A. (2017). Exploration of Potentially Bioactive Peptides Generated from the Enzymatic Hydrolysis of Hempseed Proteins. *Journal of Agricultural and Food Chemistry*, 65(47), 10174-10184.
- Athyros, V. G., Boutari, C., Stavropoulos, K., Anagnostis, P., Imprialos, K. P., Doulas, M., & Karagiannis, A. J. C. V. P. (2018). Statins: an under-appreciated asset for the prevention and the treatment of NAFLD or NASH and the related cardiovascular risk. *16(3)*, 246-253.
- Bays, H. E., Taub, P. R., Epstein, E., Michos, E. D., Ferraro, R. A., Bailey, A. L., Kelli, H. M., Ferdinand, K. C., Echols, M. R., Weintraub, H., Bostrom, J., Johnson, H. M., Hoppe, K. K., Shapiro, M. D., German, C. A., Virani, S. S., Hussain, A., Ballantyne, C. M., Agha, A. M., & Toth, P. P. (2021). Ten things to know about ten cardiovascular disease risk factors. *American Journal of Preventive Cardiology*, 5, 100149.
- Bollati, C., Cruz-Chamorro, I., Aiello, G., Li, J., Bartolomei, M., Santos-Sánchez, G., Ranaldi, G., Ferruzza, S., Sambuy, Y., Arnoldi, A., & Lammi, C. (2022). Investigation of the intestinal trans-epithelial transport and antioxidant activity of two hempseed peptides WVSPLAGRT (H2) and IGFLIIWV (H3). *Food Research International*, 152, 110720.
- Brown, M. S., & Goldstein, J. L. J. C. (1997). The SREBP pathway: regulation of cholesterol metabolism by proteolysis of a membrane-bound transcription factor. *89(3)*, 331-340.
- Chaudhary, R., Garg, J., Shah, N., & Sumner, A. (2017). PCSK9 inhibitors: A new era of lipid lowering therapy. *World journal of cardiology*, 9(2), 76-91.
- Ching, Y. P., Davies, S. P., & Hardie, D. G. (1996). Analysis of the Specificity of the AMP-Activated Protein Kinase by Site-Directed Mutagenesis of Bacterially Expressed 3-hydroxy 3-methylglutaryl-CoA Reductase, Using a Single Primer Variant of the Unique-site-elimination Method. *European Journal of Biochemistry*, 237(3), 800-808.
- Cho, S.-J., Juillerat, M. A., & Lee, C.-H. (2007). Cholesterol Lowering Mechanism of Soybean Protein Hydrolysate. *Journal of Agricultural and Food Chemistry*, 55(26), 10599-10604.
- Cruz-Chamorro, I., Santos-Sánchez, G., Bollati, C., Bartolomei, M., Li, J., Arnoldi, A., & Lammi, C. (2022). Hempseed (*Cannabis sativa*) Peptides WVSPLAGRT and IGFLIIWV Exert Anti-

- inflammatory Activity in the LPS-Stimulated Human Hepatic Cell Line. *Journal of Agricultural and Food Chemistry*, 70(2), 577-583.
- Dehnavi, S., Kiani, A., Sadeghi, M., Biregani, A. F., Banach, M., Atkin, S. L., Jamialahmadi, T., & Sahebkar, A. (2021). Targeting AMPK by Statins: A Potential Therapeutic Approach. *Drugs*, 81(8), 923-933.
- Donato, M. T., Tolosa, L., & Gómez-Lechón, M. J. (2015). Culture and Functional Characterization of Human Hepatoma HepG2 Cells. In M. Vinken & V. Rogiers (Eds.), *Protocols in In Vitro Hepatocyte Research*, (pp. 77-93). New York, NY: Springer New York.
- Dong, B., Li, H., Singh, A. B., Cao, A., & Liu, J. J. J. o. B. C. (2015). Inhibition of PCSK9 transcription by berberine involves down-regulation of hepatic HNF1 α protein expression through the ubiquitin-proteasome degradation pathway. *290(7)*, 4047-4058.
- Dubuc, G., Chamberland, A., Wassef, H., Davignon, J., Seidah, N. G., Bernier, L., & Prat, A. (2004). Statins Upregulate PCSK9, the Gene Encoding the Proprotein Convertase Neural Apoptosis-Regulated Convertase-1 Implicated in Familial Hypercholesterolemia. *Arteriosclerosis, Thrombosis, and Vascular Biology*, 24(8), 1454-1459.
- Go, G. W., & Mani, A. (2012). Low-density lipoprotein receptor (LDLR) family orchestrates cholesterol homeostasis. *The Yale journal of biology and medicine*, 85(1), 19-28.
- Goldstein, J. L., & Brown, M. S. (1990). Regulation of the mevalonate pathway. *Nature*, 343(6257), 425-430.
- Hardie, D. G. (2014). AMPK—Sensing Energy while Talking to Other Signaling Pathways. *Cell Metabolism*, 20(6), 939-952.
- Hartmann, R., & Meisel, H. (2007). Food-derived peptides with biological activity: from research to food applications. *Current Opinion in Biotechnology*, 18(2), 163-169.
- Ho, S. S., & Pal, S. (2005). Margarine phytosterols decrease the secretion of atherogenic lipoproteins from HepG2 liver and Caco2 intestinal cells. *Atherosclerosis*, 182(1), 29-36.
- Istvan, E. S., & Deisenhofer, J. (2001). Structural Mechanism for Statin Inhibition of HMG-CoA Reductase. *Science*, 292(5519), 1160-1164.
- Izumi, Y., Shiota, M., Kusakabe, H., Hikita, Y., Nakao, T., Nakamura, Y., Muro, T., Miura, K., Yoshiyama, M., & Iwao, H. (2009). Pravastatin accelerates ischemia-induced angiogenesis through AMP-activated protein kinase. *Hypertension Research*, 32(8), 675-679.

- Korb, O., Stützel, T., & Exner, T. E. (2009). Empirical Scoring Functions for Advanced Protein–Ligand Docking with PLANTS. *Journal of Chemical Information and Modeling*, 49(1), 84-96.
- Lammi, C., Sgrignani, J., Roda, G., Arnoldi, A., & Grazioso, G. (2019). Inhibition of PCSK9D374Y/LDLR Protein–Protein Interaction by Computationally Designed T9 Lupin Peptide. *ACS Medicinal Chemistry Letters*, 10(4), 425-430.
- Lammi, C., Zanoni, C., & Arnoldi, A. (2015a). IAVPGEVA, IAVPTGVA, and LPYP, three peptides from soy glycinin, modulate cholesterol metabolism in HepG2 cells through the activation of the LDLR-SREBP2 pathway. *Journal of Functional Foods*, 14, 469-478.
- Lammi, C., Zanoni, C., & Arnoldi, A. (2015b). A simple and high-throughput in-cell Western assay using HepG2 cell line for investigating the potential hypocholesterolemic effects of food components and nutraceuticals. *Food Chemistry*, 169, 59-64.
- Lammi, C., Zanoni, C., Arnoldi, A., & Vistoli, G. (2015). Two Peptides from Soy β -Conglycinin Induce a Hypocholesterolemic Effect in HepG2 Cells by a Statin-Like Mechanism: Comparative *in Vitro* and *in Silico* Modeling Studies. *Journal of Agricultural and Food Chemistry*, 63(36), 7945-7951.
- Lammi, C., Zanoni, C., Calabresi, L., & Arnoldi, A. (2016). Lupin protein exerts cholesterol-lowering effects targeting PCSK9: From clinical evidences to elucidation of the *in vitro* molecular mechanism using HepG2 cells. *Journal of Functional Foods*, 23, 230-240.
- Lammi, C., Zanoni, C., Ferruzza, S., Ranaldi, G., Sambuy, Y., & Arnoldi, A. (2016). Hypocholesterolaemic Activity of Lupin Peptides: Investigation on the Crosstalk between Human Enterocytes and Hepatocytes Using a Co-Culture System Including Caco-2 and HepG2 Cells. *8*(7), 437.
- Leonard, W., Zhang, P., Ying, D., & Fang, Z. (2020). Hempseed in food industry: Nutritional value, health benefits, and industrial applications. *19*(1), 282-308.
- Levy, E., Ouadda, A. B. D., Spahis, S., Sane, A. T., Garofalo, C., Grenier, É., Emonnot, L., Yara, S., Couture, P., Beaulieu, J.-F., Ménard, D., Seidah, N. G., & Elchebly, M. (2013). PCSK9 plays a significant role in cholesterol homeostasis and lipid transport in intestinal epithelial cells. *Atherosclerosis*, 227(2), 297-306.

- MattiuZZi, C., Sanchis-Gomar, F., & Lippi, G. (2020). Worldwide burden of LDL cholesterol: Implications in cardiovascular disease. *Nutrition, Metabolism and Cardiovascular Diseases*, *30*(2), 241-244.
- Maxwell, K. N., Fisher, E. A., & Breslow, J. L. (2005). Overexpression of PCSK9 accelerates the degradation of the LDLR in a post-endoplasmic reticulum compartment. *102*(6), 2069-2074.
- Mosley, S. T., Kalinowski, S. S., Schafer, B. L., & Tanaka, R. D. J. J. o. L. R. (1989). Tissue-selective acute effects of inhibitors of 3-hydroxy-3-methylglutaryl coenzyme A reductase on cholesterol biosynthesis in lens. *30*(9), 1411-1420.
- Oliaro-Bosso, S., Calcio Gaudino, E., Mantegna, S., Giraudo, E., Meda, C., Viola, F., & Cravotto, G. (2009). Regulation of HMGCoA Reductase Activity by Policosanol and Octacosadienol, a New Synthetic Analogue of Octacosanol. *Lipids*, *44*(10), 907.
- Pallottini, V., Martini, C., Pascolini, A., Cavallini, G., Gori, Z., Bergamini, E., Incerpi, S., & Trentalance, A. (2005). 3-Hydroxy-3-methylglutaryl coenzyme A reductase deregulation and age-related hypercholesterolemia: A new role for ROS. *Mechanisms of Ageing and Development*, *126*(8), 845-851.
- Pedretti, A., Mazzolari, A., Gervasoni, S., Fumagalli, L., & Vistoli, G. (2021). The VEGA suite of programs: an versatile platform for cheminformatics and drug design projects. *Bioinformatics*, *37*(8), 1174-1175.
- Sarkar, D., Saha, P., Gamre, S., Bhattacharjee, S., Hariharan, C., Ganguly, S., Sen, R., Mandal, G., Chattopadhyay, S., Majumdar, S., & Chatterjee, M. (2008). Anti-inflammatory effect of allylpyrocatechol in LPS-induced macrophages is mediated by suppression of iNOS and COX-2 via the NF- κ B pathway. *International Immunopharmacology*, *8*(9), 1264-1271.
- Shimano, H. (2001). Sterol regulatory element-binding proteins (SREBPs): transcriptional regulators of lipid synthetic genes. *Progress in Lipid Research*, *40*(6), 439-452.
- Shin, E. J., Park, J. H., Sung, M. J., Chung, M.-Y., & Hwang, J.-T. (2016). Citrus junos Tanaka peel ameliorates hepatic lipid accumulation in HepG2 cells and in mice fed a high-cholesterol diet. *BMC Complementary and Alternative Medicine*, *16*(1), 499.
- Soares, R. A. M., Mendonça, S., De Castro, L. Í. A., Menezes, A. C. C. C., & Arêas, J. A. G. (2015). Major Peptides from Amaranth (*Amaranthus cruentus*) Protein Inhibit HMG-CoA Reductase Activity. *16*(2), 4150-4160.

- Sun, W., Lee, T.-S., Zhu, M., Gu, C., Wang, Y., Zhu, Y., & Shyy, J. Y.-J. (2006). Statins Activate AMP-Activated Protein Kinase *In Vitro* and *In Vivo*. *114*(24), 2655-2662.
- Sun, W., Meng, J., Wang, Z., Yuan, T., Qian, H., Chen, W., Tong, J., Xie, Y., Zhang, Y., Zhao, J., & Bao, N. (2017). Proanthocyanidins Attenuation of H₂O₂-Induced Oxidative Damage in Tendon-Derived Stem Cells via Upregulating Nrf-2 Signaling Pathway. *BioMed Research International*, 2017, 7529104.
- Viollet, B., Foretz, M., Guigas, B., Horman, S., Dentin, R., Bertrand, L., Hue, L., & Andreelli, F. (2006). Activation of AMP-activated protein kinase in the liver: a new strategy for the management of metabolic hepatic disorders. *The Journal of Physiology*, 574(1), 41-53.
- Vistoli, G., Mazzolari, A., Testa, B., & Pedretti, A. (2017). Binding Space Concept: A New Approach To Enhance the Reliability of Docking Scores and Its Application to Predicting Butyrylcholinesterase Hydrolytic Activity. *Journal of Chemical Information and Modeling*, 57(7), 1691-1702.
- Wang, Q., & Xiong, Y. L. (2019). Processing, Nutrition, and Functionality of Hempseed Protein: A Review. *18*(4), 936-952.
- Xiao, C., Dash, S., Morgantini, C., Hegele, R. A., & Lewis, G. F. (2016). Pharmacological Targeting of the Atherogenic Dyslipidemia Complex: The Next Frontier in CVD Prevention Beyond Lowering LDL Cholesterol. *Diabetes*, 65(7), 1767-1778.
- Zanoni, C., Aiello, G., Arnoldi, A., & Lammi, C. (2017a). Hempseed Peptides Exert Hypocholesterolemic Effects with a Statin-Like Mechanism. *Journal of Agricultural and Food Chemistry*, 65(40), 8829-8838.
- Zanoni, C., Aiello, G., Arnoldi, A., & Lammi, C. (2017b). Investigations on the hypocholesterolaemic activity of LILPKHSDAD and LTFPGSAED, two peptides from lupin β -conglutin: Focus on LDLR and PCSK9 pathways. *Journal of Functional Foods*, 32, 1-8.
- Zhang, D.-W., Lagace, T. A., Garuti, R., Zhao, Z., McDonald, M., Horton, J. D., Cohen, J. C., & Hobbs, H. H. J. J. o. B. C. (2007). Binding of proprotein convertase subtilisin/kexin type 9 to epidermal growth factor-like repeat A of low density lipoprotein receptor decreases receptor recycling and increases degradation. *282*(25), 18602-18612.
- Zuckerkindl, E., & Pauling, L. (1965). Evolutionary Divergence and Convergence in Proteins. In V. Bryson & H. J. Vogel (Eds.), *Evolving Genes and Proteins*, (pp. 97-166): Academic Press.

Part III.
Concluding Remarks

GENERAL CONCLUSIONS AND PERSPECTIVES

The present thesis provides a comprehensive evaluation of the *in vitro* hypocholesterolemic activity of plant derived peptides targeting HMGCoAR and PCSK9.

In the present study, the peptides derived from lupin (*Lupinus albus*) and hempseed (*Cannabis sativa*) generally presented significant cholesterol-lowering activity. In detail, peptides derived from lupin showed PCSK9 inhibitory activity. Among these, the most active peptide, known as P5 (LILPHKSDAD), reduced the protein-protein interaction between PCSK9 and LDLR with an IC_{50} equals to 1.6 μ M and showed a dual hypocholesterolemic activity, since it shows complementary inhibition of the HMGCoAR. Moreover, P5 was successfully transported by differentiated human intestinal Caco-2 cells through transcytosis, and, during transport, it was partially metabolized in a breakdown fragment (LPKHSDAD, P5-met), which retained the biological activity of the parent peptide. Based on these observations, P5 analogs, including P5-Best (LYLPKHSDRD), P5-H6A (LILPKASDAD) and P5-S7A (LILPKHADAD), were computationally designed to target both PCSK9 and HMGCoAR, displaying an improved and dual hypocholesterolemic activity evaluated by biochemical assays (Table 1).

Table 1. Effect of lupin (*Lupinus albus*) peptides on the modulation of targets protein levels in HepG2 cells.

Peptides (50 μ M)	Protein levels (%)				
	SREBP-2	HMGCoAR	LDLR	HNF-1 α	PCSK9
P5	124.7 \pm 9.57	117.3 \pm 9.06	133.4 \pm 15.57	89.5 \pm 1.79	69.2 \pm 8.04
P5-Met	130.4 \pm 16.42	117.9 \pm 12.13	150.4 \pm 29.21	89.2 \pm 3.57	71.0 \pm 8.16
P5-Best	118.6 \pm 17.76	86.5 \pm 22.8	148.4 \pm 23.37	99.17 \pm 15.45	78.3 \pm 11.80
P5-H6A	115.5 \pm 10.11	94.1 \pm 12.19	143.5 \pm 24.00	89.7 \pm 2.37	71.8 \pm 17.50
P5-S7A	96.9 \pm 16.12	71.5 \pm 15.53	126.5 \pm 13.61	81.38 \pm 7.66	74.2 \pm 17.94

HepG2 cells were treated with lupin peptides, respectively. The percentage of targets protein levels were measured by western blot versus with untreated cells. The data points represent the means \pm s.d. of three experiments in triplicate.

In addition, hydrolysates derived from hempseed were shown to have a hypocholesterolaemia effect by dropping the activity of the HMGCoAR, showing a similar cholesterol-lowering activity of statins. Since proteins are hydrolysed during digestion, the activity may be attributed to specific peptides encrypted in the protein sequences that are released by digestion and absorbed at an intestinal level. Hence, further experiments using intestinal trans-epithelial transport revealed that among the peptides contained within hempseed hydrolysates are able to pass through the mature Caco-2 cell barrier. Particularly, peptide H3 (IGFLIIWV) possess antioxidant activity in HepG2 cells by modulating the Nrf-2 and iNOS pathways, leading to the decrease of cellular H₂O₂-induced ROS, NO, and lipid peroxidation levels. Meanwhile, since there is a link between inflammation and oxidative stress, the evaluation of the anti-inflammatory effect of peptide H3 in HepG2 cells was carried out. As expected, peptide H3 was shown to modulate the production of pro (IFN- γ , TNF and IL-6)- and anti (IL-10)-inflammatory cytokines and NO through regulation of the NF- κ B and iNOS pathways, exerting an anti-inflammatory capacity in the HepG2 cells. Furthermore, a deeper mechanistic investigation of peptide H3 was also performed in HepG2 cells. Peptide H3 can modulate the activity of the key targets involved in

cholesterol metabolism, i.e., LDLR, SREBP-2, HMGCoAR, p-AMPK (Thr 172), HNF-1 α , and PCSK9, and improve the capacity of HepG2 cells treated with peptide H3 to absorb extracellular LDL cholesterol (**Figure 1**).

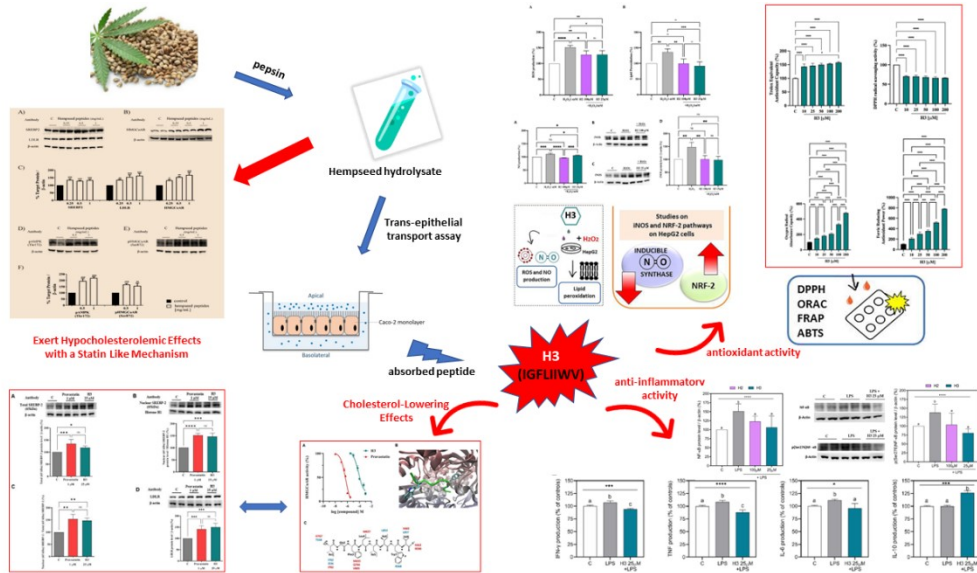


Figure 1. The flowchart summarizes the investigation strategy for hempseed (*Cannabis sativa*) peptides.

In conclusion, the investigation of bioactive peptides holds significant promise in developing novel molecular entities with hypocholesterolemic activity. This study provides valuable insights into the potential of lupin peptides (P5 and its derivatives) and hempseed peptide (H3) as peptide-based inhibitors targeting PCSK9 and HMGCoAR, making them viable candidates for hypocholesterolemic interventions. However, it is important to acknowledge that in cases where the condition's severity leads to significant pathology, food- or food-supplement-based interventions may not be effective. Additionally, it is crucial to recognize that the current evidence is primarily derived from *in vitro* studies, highlighting the need for further research to validate these findings in animal models and human clinical trials. Conducting rigorous clinical trials in the future will provide a more comprehensive understanding of the efficacy and safety of bioactive peptides, ultimately enhancing cholesterol

management strategies and improving overall health outcomes.

In summary, this study underscores the promise of investigating bioactive peptides for hypocholesterolemic interventions. Nevertheless, it is imperative to conduct additional research to validate these findings and consider the limitations of food- or food-supplement-based approaches in cases involving severe pathology. By addressing these knowledge gaps, we can advance our understanding of bioactive peptides, optimize cholesterol management strategies, and ultimately improve overall health outcomes.

Appendix

In addition to the main research focused on lupin and hempseed bioactive peptides, another project is dedicated to evaluating the multifunctional angiotensin-converting enzyme (ACE) and dipeptidyl-dipeptidases (DPP)-IV inhibitory effect of protein hydrolysates generated from soybean protein, pea protein, and casein, respectively. ACE and DPP-IV are important enzymes involved in regulating blood pressure and blood glucose levels, respectively. Inhibition of these enzymes has been shown to be a potential strategy for the management of hypertension and diabetes.

This project employed mass spectrometry techniques to identify the compositions of peptides derived from soybean protein hydrolysate, pea protein hydrolysate and casein hydrolysate, respectively. Then, their potential hypotensive and anti-diabetic activities were evaluated by initially measuring the ability of these hydrolysates to inhibit, *in vitro* ACE and DPP-IV activity and, afterward, by carrying out experiments using Caco-2 cells that express both enzymes on their membrane surfaces.

Project I

INTEGRATED EVALUATION OF THE MULTIFUNCTIONAL DPP-IV AND ACE INHIBITORY EFFECT OF SOYBEAN AND PEA PROTEIN HYDROLYSATES

Carlotta Bollati¹, Ruoxian Xu¹, Giovanna Boschini¹, Martina Bartolomei¹,
Fabrizio Rivardo², **Jianqiang Li**¹, Anna Arnoldi¹ and Carmen Lammi^{1*}

¹Department of Pharmaceutical Sciences, University of Milan, 20122 Milan, Italy

²A. Costantino & C. Spa, Via Francesco Romana 11, 10083 Torino, Italy

Author Contributions: Conceptualization, C.L.; methodology, C.L., C.B., R.X., G.B., M.B., F.R. and J.L.; writing—original draft, C.L. and C.B.; writing—review & editing, C.L. and A.A.; supervision, C.L.

I. Abstract

Nowadays, notwithstanding their nutritional and technological properties, food bioactive peptides from plant sources garner increasing attention for their ability to impart more than one beneficial effect on human health. Legumes, which stand out thanks to their high protein content, represent valuable sources of bioactive peptides. In this context, this study focused on the characterization of the potential pleotropic activity of two commercially available soybean (SH) and pea (PH) protein hydrolysates, respectively. Since the biological activity of a specific protein hydrolysate is strictly correlated with its chemical composition, the first aim of the study was to identify the compositions of the SH and PH peptides. Peptidomic analysis revealed that most of the identified peptides within both mixtures belong to storage proteins. Interestingly, according to the BIOPEP-UWM database, all the peptides contain more than one active motive with known inhibitory angiotensin converting enzyme (ACE) and dipeptidyl-dipeptidases (DPP)-IV sequences. Indeed, the results indicated that both SH and PH inhibit DPP-IV and ACE activity with a dose-response trend and IC_{50} values equal to 1.15 ± 0.004 and 1.33 ± 0.004 mg/mL, and 0.33 ± 0.01 and 0.61 ± 0.05 mg/mL, respectively. In addition, both hydrolysates reduced the activity of DPP-IV and ACE enzymes which are expressed on the surface of human intestinal Caco-2 cells. These findings clearly support that notion that SH and PH may represent new ingredients with anti-diabetic and hypotensive effects for the development of innovative multifunctional foods and/or nutraceuticals for the prevention of metabolic syndrome.

I-1 Introduction

Food bioactive peptides are short protein fragments (2–20 amino acid residues in length) that, in addition to their known nutritional value, are able to modulate physiological pathways, thereby exerting a positive impact on human health (Lammi, Aiello, Boschini, & Arnoldi, 2019). Hence, both animal and plant foods or by-products with high protein content represent valuable sources of functional bioactive peptides,

which can be produced either by enzymatic hydrolysis (using proteolytic enzymes from either plants or microbes), hydrolysis with digestive enzymes (simulated gastrointestinal digestion), or by fermentation. Some studies also used a combination of these methods to produce peptides with a biological activity (Akbarian, Khani, Eghbalpour, & Uversky, 2022). Legumes, pseudocereals, and hempseed are among the plant foods which can be considered good sources of bioactive peptides (Aguchem, Okagu, Okagu, Ndefo, & Udenigwe, 2022; Cruz-Chamorro, Santos-Sánchez, Bollati, Bartolomei, Li, Arnoldi, et al., 2022; Fukui, Tachibana, Wanezaki, Tsuzaki, Takamatsu, Yamamoto, et al., 2002; Udenigwe & Aluko, 2012).

In this panorama, legumes, which stand out thanks to their high protein content, are a cheap, sustainable, and a healthy source of nutrition. Notably, soybeans (*Glycine max*) are on average composed of ~35–40% protein (Arnoldi, Zanoni, Lammi, & Boschini, 2015). Clinical studies have linked the consumption of soy-based food with a reduced risk of developing a number of chronic diseases, such as obesity, hypercholesterolemia, and insulin-resistance/type II diabetes. As for the active substance in soy foods, protein plays a role in cardiovascular disease prevention (Fukui, et al., 2002; Liu, Ho, Chen, Ho, To, Tomlinson, et al., 2014), and some cholesterol-lowering and anti-diabetic peptides have already been singled out in glycinin and β -conglycinin sequences, respectively (Lammi, Zanoni, & Arnoldi, 2015).

In addition to soybean, pea (*Pisum sativum* L.) represents one of the major legumes in the world and it is composed of ~26% protein (Arnoldi, Zanoni, Lammi, & Boschini, 2015). Thanks to its excellent yields, availability, and its low production costs, pea is most widely used as a source of commercial proteins for different purpose (Sun & Arntfield, 2011). Many studies have highlighted the health benefits associated with the consumption of pea protein. In particular, pea protein and its hydrolysates exert antioxidant, antihypertensive, and hypocholesterolemic activities (Aluko, Girgih, He, Malomo, Li, Offengenden, et al., 2015; Ge, Sun, Corke, Gul, Gan, & Fang, 2020; H. Li & Aluko, 2010; H. Li, Prairie, Udenigwe, Adebisi, Tappia, Aukema, et al., 2011). In general, most previous studies in this area have focused on the consumption of pea

and soybean proteins, but the health-promoting activity does not lie in the protein but in the peptides, which are encrypted within the protein and released upon digestion/hydrolysis. Hence, with a more mature perception of the phenomenon, owing to the presence of numerous bioactive peptides, these protein hydrolysates may provide more than one biological activity, therefore eliciting multiple health benefits (Bollati, Cruz-Chamorro, Aiello, Li, Bartolomei, Santos-Sánchez, et al., 2022; Lammi, Aiello, Dellafiora, Bollati, Boschini, Ranaldi, et al., 2020; Lammi, Arnoldi, & Aiello, 2019; Lammi, Zanoni, Ferruzza, Ranaldi, Sambuy, & Arnoldi, 2016). For this reason, the production of hydrolysates with multifunctional behavior represents a valid strategy in the development of new generations of functional foods and nutraceuticals (Chakrabarti, Guha, & Majumder, 2018).

Indeed, this study focused on the deep characterization of the potential pleiotropic health-promoting behavior of two commercially available soybean (SH) and pea (PH) protein hydrolysates, respectively. Both SH and PH are obtained by industrial processes, beginning with the selection of soybean and pea protein sources (isolated proteins or enriched protein flours) in combination with a hydrolysis process which is able to deliver an optimized performance in terms of structure and, thanks to the resulting taste being almost neutral, allows for a nutritional contribution to food and beverage formulations. SH and PH are then filtered and concentrated before spray drying to obtain a purified product for different food applications.

In addition to, and in part thanks to, their nutritional and technological properties (as a smoothing and whipping agent), SH and PH are successfully used in every formulation to replace nutritional content of animal origin, and they may also be exploited as new valuable and pleiotropic ingredients for making innovative multifunctional foods and/or nutraceuticals.

Thus, since the biological activity of a specific protein hydrolysate is strictly correlated with its chemical composition, the first aim of this study was to identify the compositions of SH and PH peptides by peptidomic analysis. Then, their potential hypotensive and anti-diabetic activities were evaluated by initially measuring the

ability of both hydrolysates to inhibit, *in vitro*, angiotensin converting enzyme (ACE) and dipeptidyl-dipeptidases (DPP)-IV activity and, afterwards, by carrying out experiments using Caco-2 cells that express both enzymes on their membrane surfaces.

I-2 Material and methods

I-2.1 Chemicals

Dulbecco's modified Eagle's medium (DMEM), L-glutamine, fetal bovine serum (FBS), phosphate buffered saline (PBS), penicillin/streptomycin and 96-well plates were purchased from Euroclone (Milan, Italy). Sitagliptin, Gly-Pro-amido-4-methylcoumarin hydrobromide (Gly-Pro-AMC) and ACE from porcine kidney were from Sigma-Aldrich (St. Louis, MO, USA). ACE1 Activity Assay Kit come from Biovision (Milpitas Blvd., Milpitas, CA, USA). Caco-2 cells were obtained from INSERM (Paris, France).

SH and PH sample descriptions: A. Costantino S.R.L. (Italy), supplies the soybean and pea hydrolysates as spray dried samples (Soy Peptone FM batch 221/00351, 100 g; Pea Protein Hydrolysate GT Plus batch 221F0001, 100 g) directly from the production process. See Supplementary Material for the technical data sheet of both samples.

I-2.2 SH and PH Ultrafiltration

Before proceeding to the assessment of biological activity, SH and PH were passed through ultrafiltration (UF) membranes with a 3 kDa cut-off, using a Millipore UF system (Millipore, Bedford, MA, USA). The recovered peptides solution was lyophilized and store -80 °C until use.

I-2.3 Mass Spectrometry Analysis (HPLC Chip ESI-MS/MS)

Samples were dissolved with 50 µL of a solution of 99% water and 1% ACN containing 0.1% formic acid. 2 µL of each sample were injected in a nano-chromatographic system, HPLC-Chip (Agilent Palo Alto, CA, USA). The analysis

was conducted on a SLIT mass spectrometer. LC-MS/MS analysis were performed in data-dependent acquisition AutoMS(n)mode. To increase the number of identified peptides, three replicates (LC-MS/MS runs) were run. Spectrum Mill Proteomics Workbench (Rev B.04.00, Agilent), consulting database downloaded from the Uniprot was used for the automated peptide identification from tandem mass spectra. The mass tolerance was set at 1.0 Da and 0.8 Da for MS1 and MS2, respectively.

I-2.4 Biochemical Investigation of DPP-IV and ACE Inhibitory Activity of SH and PH Peptides

I-2.4.1 *In Vitro* DPP-IV Activity Assay

The experiments were carried out in triplicate in a half volume 96 well solid plate (white). Each reaction (50 μ L) was prepared adding the reagents in the following order in a microcentrifuge tube: 1 X assay buffer [20 mM Tris-HCl, pH 8.0, containing 100 mM NaCl, and 1 mM EDTA] (30 μ L), SH and PH at final concentration range of 0.01-2.0 mg/mL (10 μ L) or Sitagliptin 1mM (10 μ L) or vehicle (10 μ L) and finally the DPP IV enzyme (10 μ L). Subsequently, the samples were mixed and 50 μ L of each reaction were transferred in each well of the plate. The reactions were started by adding 50 μ L of substrate solution to each well and incubated at 37 °C for 30 minutes. Fluorescence signals were measured using the Synergy H1 fluorescent plate reader from Biotek (excitation and emission wavelengths 360 and 465 nm, respectively).

I-2.4.2 *In Vitro* Measurement of ACE Inhibitory Activity

ACE inhibitory activity was tested by measuring with HPLC the formation of hippuric acid (HA) from hippuryl-histidyl-leucine (HHL), used as mimic substrate for ACE I. Tests were performed in 100 mM Tris-HCOOH, 300 mM NaCl pH 8.3 buffer, and using ACE from porcine kidney (Sigma-Aldrich, Milan, Italy). SH and PH hydrolysates were tested at 0.08, 0.17, 0.35, 0.7 and 1.0 mg/mL. All experimental details of samples preparation and analyses conditions have been published elsewhere (Boschin, Scigliuolo, Resta, & Arnoldi, 2014a, 2014b).

I-2.5 Cellular Measurement of SH and PH Inhibitory Effect of DPP-IV and ACE Activities

I-2.5.1 Cell Culture Conditions

Caco-2 cells were routinely sub-cultured at 50% density and maintained at 37 °C in a 90% air/10% CO₂ atmosphere in DMEM containing 25 mM of glucose, 3.7 g/L of NaHCO₃, 4 mM of stable L-glutamine, 1% nonessential amino acids, 100 U/L of penicillin, and 100 µg/L of streptomycin (complete medium), supplemented with 10% heat-inactivated fetal bovine serum.

I-2.5.2 Evaluation of Caco-2 Cell Viability by MTT Experiments

A total of 3×10^4 Caco-2 cells/well were seeded in 96-well plates and, the day after, they were treated with 1.0, 2.5 and 5 mg/mL of SH and PH hydrolysates or vehicle (H₂O) in complete growth media for 48 h at 37 °C under 5% CO₂ atmosphere. Subsequently, the treatment solvent was aspirated and 100 µL/well of 3-(4,5-dimethylthiazol-2-yl)-2,5-diphenyltetrazolium bromide (MTT) filtered solution added. After 2 h of incubation at 37 °C under 5% CO₂ atmosphere, 0.5 mg/mL solution was aspirated and 100 µL/well of the lysis buffer (8 mM HCl + 0.5% NP-40 in DMSO) added. After 10 min of slow shaking, the absorbance at 575 nm was read on the Synergy H1 fluorescence plate reader (Biotek, Bad Friedrichshall, Germany).

I-2.5.3 Evaluation of the inhibitory effect of SH and PH on cellular DPP-IV activity

For the experiments, Caco-2 cells were seeded on black 96-well plates with clear bottoms at a density of 5×10^4 cells/well. After one day, cells were treated with 1.0, 2.5 and 5.0 mg/mL of SH and PH for 1, 3 and 6 h; at the end of the incubation, cells were washed once with 100 µL of PBS, then, 50 µL of Gly-Pro-AMC substrate at concentrations of 25 µM in PBS were added and the fluorescence signals (excitation/emission wavelengths 350/450 nm) in each well were measured using a Synergy H1 (BioTek Instruments, Winooski, VT, USA) every 1 min, for up to 10 min.

I-2.5.4 Evaluation of the inhibitory effect of SH and PH on cellular ACE1 activity

Caco-2 cells were seeded on 96-well plates at a density of 5×10^4 cells/well for 24 h. The following day, cells were treated with SH and PH (from 0.1 to 5.0 mg/mL) or vehicle in growth medium for 6 h at 37 °C, then cells were scraped in 30 μ L of ice-cold ACE1 lysis buffer and transferred in an ice-cold microcentrifuge tube. After centrifugation at 13 300g for 15 min at 4 °C, the supernatant was recovered and transferred into a new ice-cold tube. Total proteins were quantified by Bradford method, and 2 μ g of total proteins (the equivalent of 2 μ L) were added to 18 μ L of ACE1 lysis buffer in each well in a black 96-well plates with clear bottoms. For the background control, 20 μ L of ACE1 lysis buffer were added to 20 μ L of ACE1 assay buffer. Subsequently, 20 μ L of 4% of ACE1 substrate (prepared in assay buffer) was added in each well except the background one and the fluorescence (Ex/Em 330/430 nm) was measured in a kinetic mode for 10 min at 37°C.

I-2.6 Statistical Analysis

Statistical analyses were carried out by one-way ANOVA (Graphpad Prism 9, GraphPad Software, La Jolla, CA, USA) followed by Dunnett or Tukey's multiple comparison test. For each assay at least four independent experiments were performed, and each experiment were performed in triplicate. Values were expressed as means \pm SD; *p*-values < 0.05 were considered to be significant.

I-3 Results

I-3.1 Peptidomic Characterization of SH and PH

The compositions of the peptides of SH and PH hydrolysates were analyzed by HPLC-ESI-MS/MS. **Figure I-1** reports the total ion current (TIC) of the MS/MS of eluted peptides, while **Table I-1** shows the peptide molecular weight distribution of each sample, and the overall peptides, which were identified, are reported in **Table I-S1**.

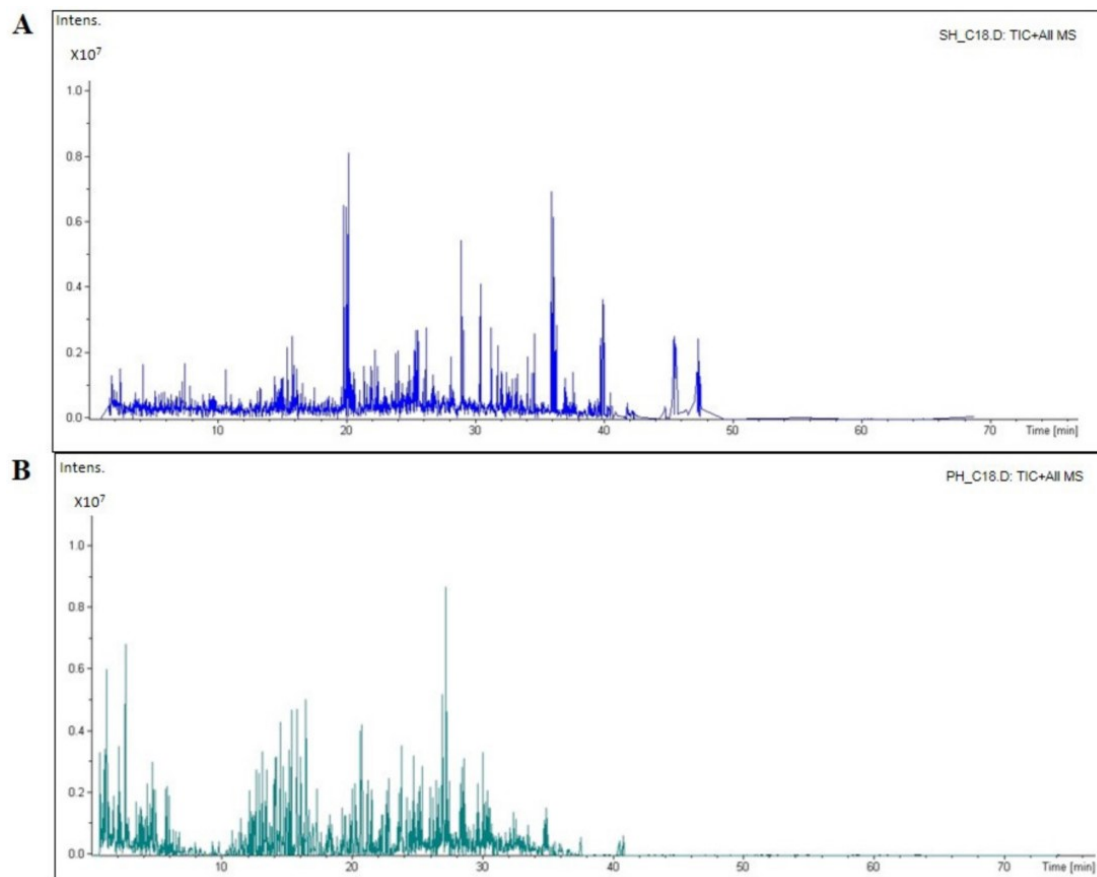


Figure I-1 The total ion chromatogram (TIC) of the soybean (SH, (A)) and pea (PH, (B)) hydrolysates, respectively. The mass spectrometer ran for 70 min. Most of the SH sample peptides were eluted between 20 and 40 min, while the PH peptides were mostly eluted in 30–40 min.

Table I-1. Molecular weight distribution of SH and PH peptides.

Hydrolysate	MW > 3 kDa (%)	MW < 3 kDa (%)
SH	53.6	46.4
PH	57.15	42.85

Table I-2 lists the identified peptides from the most abundant proteins. Among these, six and nine peptides were identified in the SH and PH samples, respectively. The length of those peptides ranged from 9 to 25 amino acids with a molecular weight in the range 1055 –2422.3 KDa, and in both samples, most of the identified peptides belong to storage proteins. Indeed, 50% of the identified soybean peptides belong to Glycinin G1, whereas in the case of the pea derived peptides, 55% and 33% belong to the Vicilin and Legumin A2 proteins, respectively. Interestingly, according to

BIOPEP-UWM database (<https://biochemia.uwm.edu.pl/biopep-uwm/>, accessed on 20 May 2022), all the peptides contain more than one active motive with both known inhibitory ACE and DPP-IV sequences.

Table I-2. SH and PH peptides from the most abundant protein, with ACE and DPP-IV inhibitory activity.

Hydrolysate	Protein name	Peptide sequence	Spectrum Intensity	ACE inhibitor sequence ^a	DPP-IV inhibitor sequence ^a
SH	Ankyrin repeat domain-containing protein 52	IRSWIVQVMS	5.11E+07	IVQ, VQV, VM	WI, IR, QV, SW, VM, VQ
	Glycinin G1	VSIIDTNSLENQLDQ	4.56E+07	PR	SL, DQ, II, NQ, QL, SI, TN, VS
		IIDTNSLENQLDQMPR	2.07E+07		MP, SL, DQ, II, NQ, QL TN
	Hydrolase_4 domain-containing protein DNA-directed RNA polymerase (Fragment)	ANSLLNALPEEVIQ	1.75E+07	EV, LN, ALP, LP	LP, LL, AL, SL, EV, IQ, LN, NA, VI
		AAEGGGFSDPAPAPPRL AIPEV	1.45E+07	PR, AIP, IP, AP, LA, AA, GF, GG, AI, EG, PAP, EV, PP	PP, LA, AP PA, IP, AA AE, DP, EG EV, GF, GG, RL
		FDIYRVMRPGEPPTMDS AEAMFNA	1.48E+07	IY, MF, GEP, RP, GE, EA, PG, PT, PP, VM	PP, RP, EP, AE, FN, GE, MF, MR, NA, PG, PT, TM, VM, YR
PH	Vicilin 47k	EITPEKNQQQLQDLDFVN	2.26E+07	IF, EI, LQ EK, TP	TP, EK, EI NQ, QD, QL, QQ, VN
		NQQQLQDLDFVN	2.80E+07	IF, LQ	NQ, QD, QL, QQ, VN
		KNQQQLQDLDFVN	7.09E+07	IF, LQ	NQ, QD, QL, QQ VN
	Vicilin	ITPEKNPQLQDLDFVN	1.58E+07	IF, LQ, PQ, EK, TP	TP, NP, EK, PQ, QD, QL, VN
		KNPQLQDLDFVN	5.13E+07	IF, LQ, PQ	NP, PQ, QD, QL, VN
	AsmA family protein	GGLSFDRKAAKTASGG LTLSKADA	2.73E+07	AA, GL, DA, GG, SG, SF, KA, TLS, DR	KA, TA, TT, GL, AA, AD, AS, DR, GG, KT, LT, RK, SF, SK, TL
		Legumin A2	LFGQAGLDPLPVDVGA NGRL	1.80E+07	PLP, RL, LF, PL, VG, GA, GL, AG, GR, FG, GQ, NG, LP
	ALEPDNRIE		1.53E+07	IE, ALEP	EP, AL, DN, NR, RI
	SVINNPLPLDVVA		4.96E+07	PL, LPL, LP	VA, LP, VV, LPL, PL, IN, NL, NN, SV, VI

^aAccording to the BIOPEP-UWM database; <https://biochemia.uwm.edu.pl/biopep-uwm/> accessed on 20 May 2022.

I-3.2 SH and PH Peptides: Biochemical Investigation of DPP-IV and ACE Inhibitory Activities

I-3.2.1 SH and PH Inhibit *In Vitro* DPP-IV Activity

In order to assess the ability of SH and PH to modulate DPP-IV activity, preliminary *in vitro* experiments were performed using the purified recombinant DPP-IV enzyme. **Figure I-2A** shows that SH drops *in vitro* DPP-IV activity by $10.18 \pm 7.0\%$, $40.0 \pm 1.6\%$, $58.22 \pm 2.57\%$, and $82.48 \pm 1.41\%$ at 0.1, 0.5, 1.0, and 2.5 mg/mL respectively. **Figure I-2B** indicates that PH decreases DPP-IV activity *in vitro* by $0.11 \pm 0.21\%$, $31.0 \pm 3.9\%$, $52.05 \pm 2.31\%$, and $79.1 \pm 1.04\%$ at 0.1, 0.5, 1.0, and 2.5 mg/mL, respectively. Both SH and PH inhibit the enzyme with a dose-response trend and calculated IC_{50} values equal to 1.15 ± 0.004 and 1.33 ± 0.004 , respectively.

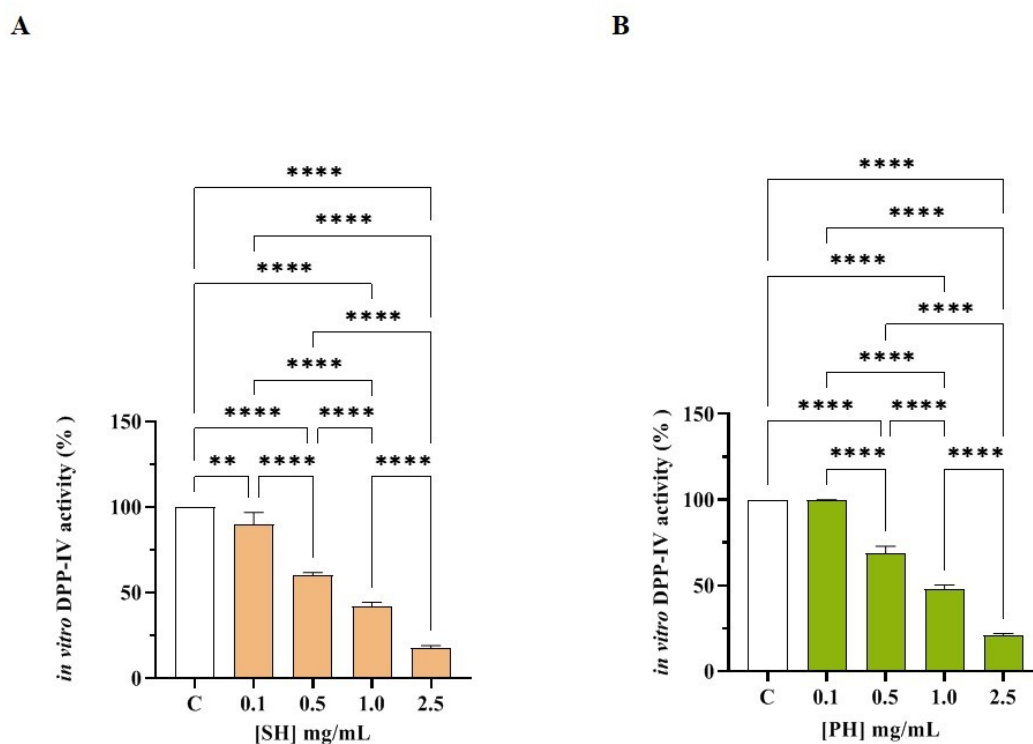


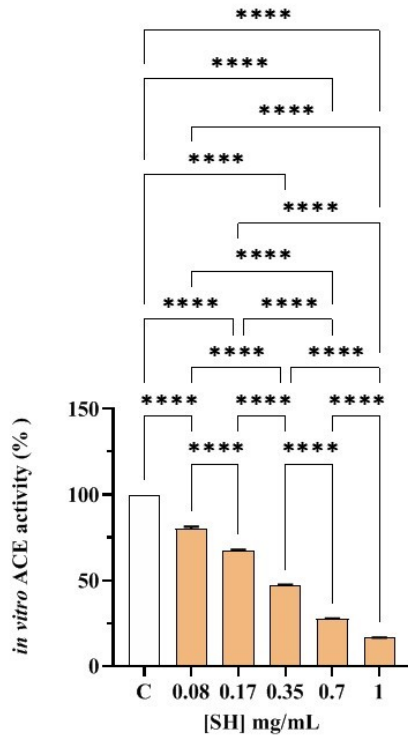
Figure I-2. Evaluation of the *in vitro* inhibitory effects of SH (A) and PH (B) hydrolysates on human recombinant DPP-IV. Bars represent the average \pm SD of three independent experiments in duplicates. **** $p < 0.0001$, ** $p < 0.01$, versus control (C) sample (activity), non-significant (ns) is not shown.

In parallel, the *in vitro* DPP-IV activity inhibition of both hydrolysates was confirmed by the experiments conducted on the low molecular weight fractions (<3 kDa) of SH (F3) and PH (F3), as reported in Figure S1. Notably, SH (F3) inhibits DPP-IV activity *in vitro* by $12.7 \pm 4.9\%$, $23.9 \pm 4.56\%$, $41.9 \pm 2.56\%$, $57.3 \pm 2.3\%$, and $79.5 \pm 2.5\%$ at 0.01, 0.1, 0.5, 1.0, and 2.0 mg/mL, respectively (**Figure I-S1A**), and PH (F3) reduced the enzymatic activity by $8.5 \pm 2.01\%$, $15.1 \pm 4.21\%$, $41.6 \pm 3.4\%$, $56.8 \pm 4.4\%$, and $79.1 \pm 1.70\%$ at the same concentrations (**Figure I-S1B**). Indeed, both SH (F3) and PH (F3) decreased DPP-IV activity with a dose-response trend and IC₅₀ values equal to 0.82 ± 0.01 and 1.0 ± 0.01 mg/mL, respectively. Comparing the IC₅₀ values obtained by analyzing the total SH and PH hydrolysates with the those obtained by testing the <3 kDa fractions of SH and PH, it is evident that the short peptides which are contained within SH and PH hydrolysates, respectively, are those responsible of DPP-IV inhibitory activity.

I-3.2.2 SH and PH Peptides Inhibit *In Vitro* ACE Activity

Both SH and PH efficiently inhibited ACE activity with a dose-response trend and calculated IC 50 values that were 0.33 ± 0.01 and 0.61 ± 0.05 mg/mL, respectively (**Figure I-3A, B**). More specifically, SH inhibited ACE activity by $19.88 \pm 1.21\%$, $32.74 \pm 0.57\%$, $53.01 \pm 0.43\%$, $72.35 \pm 0.16\%$, and $83.38 \pm 0.06\%$ at 0.08, 0.17, 0.35, 0.7, and 1.0 mg/mL, respectively (**Figure I-3A**), whereas PH reduced ACE activity by $3.55 \pm 0.07\%$, $12.92 \pm 0.11\%$, $35.40 \pm 0.01\%$, $53.51 \pm 0.11\%$, and $62.23 \pm 0.15\%$ at the same concentrations (**Figure I-3B**).

A



B

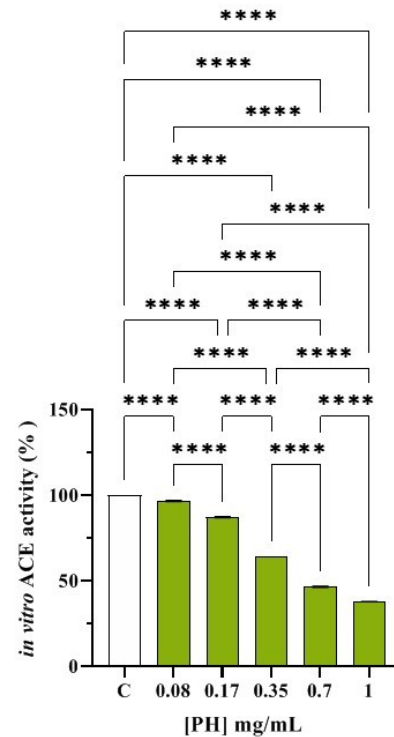


Figure I-3. Assessment of the *in vitro* ACE-inhibitory effects of SH (A) and PH (B) hydrolysates. Bars represent the sd of three independent experiments in duplicate. **** $p < 0.0001$ versus control sample (C).

In parallel, the *in vitro* ACE activity inhibition of both hydrolysates was confirmed by the experiments conducted on the low molecular weight fractions (< 3 kDa) of both SH (F3) and PH (F3), as shown in **Figure I-S2**. In particular, SH (F3) inhibits ACE activity *in vitro* by $9.15 \pm 0.07\%$, $24.62 \pm 0.13\%$, $48.39 \pm 0.02\%$, $63.29 \pm 0.02\%$, and $74.09 \pm 0.08\%$ at 0.08, 0.17, 0.35, 0.7, and 1.0 mg/mL, respectively (**Figure I-S2A**), whereas PH (F3) reduced the enzymatic activity by $17.21 \pm 0.10\%$, $26.74 \pm 0.25\%$, $44.26 \pm 0.02\%$, $63.96 \pm 0.01\%$, and $74.64 \pm 0.08\%$ at the same concentrations (**Figure I-S2B**). Indeed, both SH (F3) and PH (F3) reduced the ACE activity with a dose-response trend and IC_{50} values equal to 0.40 ± 0.01 and 0.43 ± 0.01 mg/mL, respectively, clearly suggesting that the short peptides which are contained within SH and PH hydrolysates are those responsible for ACE inhibitory activity.

Finally, **Table I-3** summarizes the comparison of IC_{50} values of both samples against

DPP-IV and ACE.

Table I-3. IC₅₀ values obtained testing SH, PH and their corresponding low molecular fractions (<3 kDa) against DPP-IV and ACE targets.

	IC ₅₀ (mg/mL) DPP-IV	IC ₅₀ (mg/mL) ACE
SH	1.15 ± 0.004	0.33 ± 0.01
PH	1.33 ± 0.004	0.61 ± 0.05
SH <3 kDa (F3)	0.82 ± 0.01	0.40 ± 0.01
PH <3 kDa (F3)	1.0 ± 0.003	0.43 ± 0.01

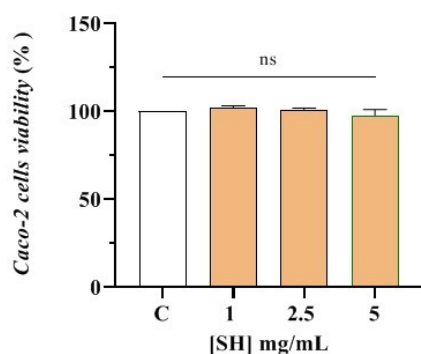
Interestingly, whereas P5-met was abundant and was produced in both conditions, P5-frag was detected only when P5 was tested in combination with P3 and P7 and, based on the spectral intensity, was a minor metabolite. This suggests that the transformation of P5-frag into P5-met may be such a fast process that only the concomitant presence of very easily cleavable peptides (like P7) permitted its detection, by protecting it from degradation. However, we cannot exclude those other smaller fragments, such as tripeptides and dipeptides, were also generated in these conditions, since they are intrinsically difficult to detect.

I-3.3 Cellular Assessment of DPP-IV and ACE Inhibition by SH and PH Peptides

I-3.3.1 Effect of SH and PH Peptides on Caco-2 Cell Viability

The MTT assay was used for assessing the safe range of concentrations of the SH and PH hydrolysates on Caco-2 cells. After a 48 h treatment, any effect on the Caco-2 cell viability was observed in the range of 1.0–5.0 mg/mL versus untreated cells (C) (**Figure I-4**).

A



B

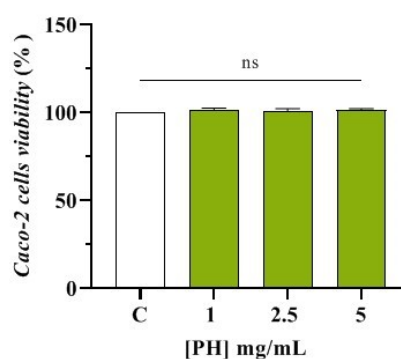


Figure I-4. MTT assay. Effect of SH (A) and PH (B) hydrolysates on Caco-2 cells viability. Data represent the averages \pm S.D. of four independent experiments performed in triplicate.

The ability of SH and PH to inhibit DPP-IV was then investigated in cell-based conditions using Caco-2 cells, which express high levels of this protease on their membranes. Briefly, these cells were treated with SH and PH (1.0- 5.0 mg/mL) and their DPP-IV inhibitory effects were assessed in a kinetic mode after 1, 3, and 6 h (**Figure I-S3A, C**). **Figure I-S3A** shows that, after 1 h, SH inhibited cellular DPP-IV activity by $25.07 \pm 8.07\%$, $36.91 \pm 2.37\%$, and 40.32 ± 2.46 at 1.0, 2.5, and 5 mg/mL, respectively, and by $25.07 \pm 6.78\%$, $42.46 \pm 6.49\%$, and $48.69 \pm 7.29\%$ at the same concentrations after 3 h. The maximum reductions in DPP-IV activity were observed at 6 h (**Figure I-S3A and Figure I-5A**), where SH inhibited cellular DPP-IV activity by $37.9 \pm 10.0\%$, $56.6 \pm 3.6\%$, and $59.4 \pm 2.4\%$ at 1.0, 2.5, and 5 mg/mL, respectively, versus untreated cells, following a dose-response trend, confirming the *in vitro* results. As indicated in **Figure I-S3C**, after 1 h, the PH sample inhibited cellular DPP-IV activity by $19.9 \pm 8.2\%$, $40.9 \pm 3.6\%$, and $47.4 \pm 3.3\%$ at 1.0, 2.5, and 5 mg/mL, respectively, and by $22.6 \pm 5.4\%$, $47.9 \pm 2.79\%$, and $53.6 \pm 2.3\%$ at the same concentrations after 3 h (**Figure I-S3C**). The maximum inhibition of DPP-IV activity was observed after 6 h (**Figure I-S3C, Figure I-5B**), where PH inhibited cellular DPP-IV activity by $27.9 \pm 5.3\%$, $52.8 \pm 2.2\%$, and $60.7 \pm 1.6\%$ at 1.0, 2.5 and 5

mg/mL, respectively, versus untreated cells, supporting the *in vitro* results.

In parallel, the *in situ* DPP-IV activity inhibition of both hydrolysates was confirmed by the experiments carried out on the low molecular weight fractions (< 3 kDa) of both SH (F3) and PH (F3), as shown in **Figure I-S3B, D**. In particular, **Figure I-S3B** shows that, after 1 h, SH (F3) inhibited cellular DPP-IV activity by $10.4 \pm 8.3\%$, $37.2 \pm 4.1\%$, and $42.3 \pm 3.10\%$ at 1.0, 2.5, and 5 mg/mL, respectively, and by $13.62 \pm 6.88\%$, $43.1 \pm 5.91\%$, and $47.9 \pm 4.4\%$ at the same concentrations after 3 h. The highest decreases in DPP-IV activity were observed at 6 h (**Figure I-S3B**), where SH (F3) inhibited cellular DPP-IV activity by $17.7 \pm 4.9\%$, $54 \pm 1.6\%$, and $61.5 \pm 3.9\%$ at 1.0, 2.5, and 5 mg/mL, respectively, versus untreated cells, in a dose-dependent manner, supporting the *in vitro* results.

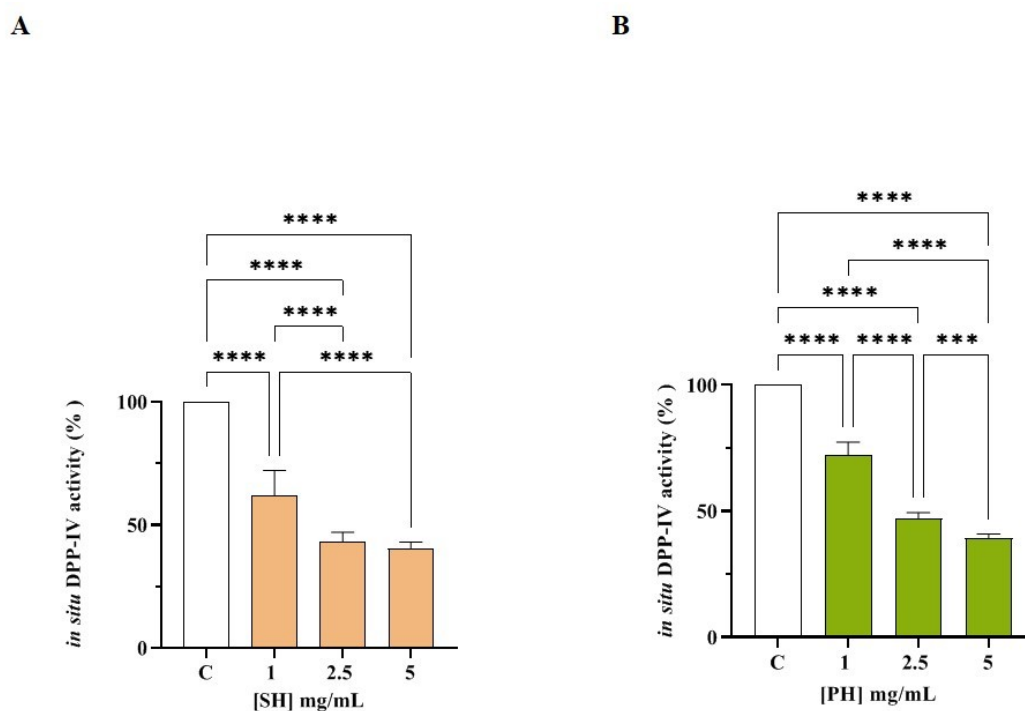


Figure I-5 Effect of SH (A) and PH (B) on the cellular DPP-IV activity. The data points represent the averages \pm S.D. of four independent experiments performed in triplicate. All data sets were analyzed by one-way ANOVA followed by Tukey's post-hoc test; C: control sample (H₂O), **** $p < 0.0001$, *** $p < 0.001$, non-significant (ns) is not shown.

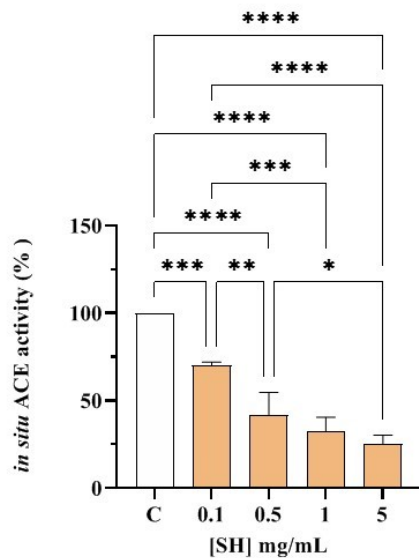
Similarly, as shown in **Figure I-S3D**, PH (F3) inhibited cellular DPP-IV activity by

6.8 ± 6.5%, 31.6 ± 5.5%, and 45.5 ± 4.9% at 1.0, 2.5, and 5 mg/mL, respectively, after 1 h, and by 7.25 ± 4.03%, 48.67 ± 2.42%, and 54.11 ± 3.09% at the same concentrations after 3 h. The highest inhibition of DPP-IV activity was observed at 6 h (**Figure I-S3D**), where PH (F3) inhibited cellular enzymatic activity by 14.4 ± 3.9%, 60.2 ± 1.5%, and 61.8 ± 2.7% at 1.0, 2.5, and 5 mg/mL, respectively, versus untreated cells, confirming the *in vitro* results.

I-3.3 SH and PH Inhibit ACE Activity Expressed on Human Intestinal Caco-2 Cells

Human intestinal Caco-2 cells were treated with SH and PH (1.0–5.0 mg/mL) for 6 h. The ACE activity was measured in the presence of a fluorescent substrate using cell lysates. The results indicated that both hydrolysates reduced cellular ACE activity with a dose-response trend. In more detail, SH reduced the enzyme activity by 29.9 ± 1.8%, 57.9 ± 12.6%, 67.5 ± 8.1%, and 74.6 ± 4.9% at 0.1, 0.5, 1.0, and 5.0 mg/mL, respectively (**Figure I-6A**), whereas PH hydrolysate reduced it by 39.6 ± 14.6%, 52.2 ± 10.6%, 64.7 ± 5.2, and 82.3 ± 4.2%, respectively, at the same concentrations (**Figure I-6B**). In parallel, the cellular ACE activity inhibition of both hydrolysates was confirmed by the experiments performed on the low molecular fractions (3 kDa) of both SH and PH (**Figure I-S4**). Notably, SH (F3) inhibited cellular ACE activity by 10.1 ± 4.5%, 47.6 ± 2.7%, 61.0 ± 7.5%, and 76.2 ± 2.3% at 0.1, 0.5, 1.0, and 5.0 mg/mL, respectively (**Figure I-S4A**), whereas PH (F3) reduced the cellular enzymatic activity by 32.0 ± 13.7%, 42.7 ± 11.3%, 60.5 ± 13.5%, and 69.5 ± 11.3% at the same concentrations (**Figure I-S4B**).

A



B

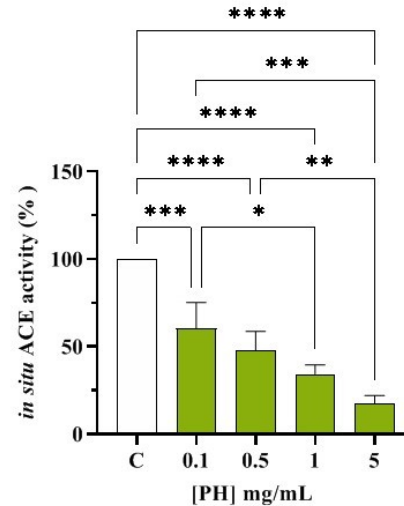


Figure I-6 ACE inhibitory effects of SH (A) and PH (B) hydrolysates in cell-based conditions. Bars represent the SD of three independent experiments in triplicate. **** $p < 0.0001$, *** $p < 0.001$, ** $p < 0.01$, * $p < 0.05$ versus control sample (C), non-significant (ns) is not shown.

I-4 Discussion

In recent decades, many studies have clearly demonstrated the ability of food protein hydrolysates to modulate ACE or DPP-IV activity (Daskaya-Dikmen, Yucetepe, Karbancioglu-Guler, Daskaya, & Ozcelik, 2017; Lammi, Zaroni, Arnoldi, & Vistoli, 2016; Nongonierma & FitzGerald, 2019). In particular, hydrophobic medium-length and/or shorter peptides from different food sources are considered to be mostly responsible for the inhibition of both enzymes (Daskaya-Dikmen, Yucetepe, Karbancioglu-Guler, Daskaya, & Ozcelik, 2017; Nongonierma & FitzGerald, 2019). In this panorama, the main limitation of most of previous studies lies in the fact that the characterization of the DPP-IV or ACE inhibitory property of food hydrolysates was performed by analyzing each bioactivity without taking into account that the same hydrolysate may be endowed with both activities. In addition, most works available in the literature rely exclusively on *in vitro* tests for assessing the biological

activity: this is particularly true in the case of the inhibition of DPP-IV and ACE activity. In light of these observations, a standout feature of this study is that the multifunctional DPP-IV and ACE inhibitory activities of two commercially available soybean (SH) and pea (PH) protein hydrolysates were evaluated together using *in vitro* tests which were implemented by cellular assays that permitted deeper insights into the mechanism of action and, contextually, a consideration of other relevant issues, such as metabolism (this is particularly true when Caco-2 cells were employed).

Overall, the present study demonstrates that SH and PH are effective at reducing DPP-IV and ACE activity in both cell-free and cell-based conditions. More specifically, as indicated in the **Table I-3**, when comparing the calculated IC₅₀ values, it is clear that SH and PH display the same ability to reduce DPP-IV activity, with SH being about 2-fold more potent than PH in terms of ACE inhibition (***, $p < 0.001$). In addition, the results indicated that SH and PH are 3- and 2-fold more potent as ACE than DPP-IV inhibitors, respectively (****, $p < 0.0001$). Moreover, comparing the IC₅₀ values of each total hydrolysate with those corresponding to each low molecular weight fraction (<3 kDa) (**Table I-3**), it is clear that the medium-length and shorter peptides, which are abundant in each total hydrolysate (**Table I-1**), are responsible for the biological activities, even though, in the case of SH and SH (F3), the same IC₅₀ values were observed against ACE enzyme. Interestingly, **Table I-2** indicates that all the most abundant peptides identified within both SH and PH contained at least one motive with DPP-IV and ACE inhibitory activity that has already been demonstrated, explaining why these hydrolysates are active on two different targets, such as ACE and DPP-IV.

As reported in the **Table I-3**, in the case of PH, the low molecular weight fractions (<3 kDa) are about 0.8- and 1,5-fold more potent than total PH as DPP-IV and ACE inhibitors, respectively (****, $p < 0.0001$). This result might be explained considering that the bioactivity of total hydrolysate depends strictly on its total composition, including the inactive and active species and possible synergistic or antagonist effects (Aiello, Lammi, Boschini, Zanoni, & Arnoldi, 2017; Zanoni, Aiello, Arnoldi, &

Lammi, 2017). Therefore, it is reasonable to conclude that longer peptides of PH (57.2%) may affect the activity exerted by the medium-length and shorter ones (42.8%) when present in PH hydrolysate. A similar trend was observed for SH. In fact, the SH (F3) is more active than the total hydrolysate against DPP-IV (***, $p < 0.001$), whereas a similar IC_{50} value against the ACE target was calculated (**Table I-3**).

Recently, it was demonstrated that soybean hydrolysates obtained using pepsin and trypsin reduced *in vitro* DPP-IV activity by 16.3% and 31.4%, and by 15.3% and 11.0%, respectively, at 1.0 and 2.5 mg/mL (Lammi, Arnoldi, & Aiello, 2019). Other recent studies demonstrated that the protein hydrolysates from germinated and non-germinated soybean, obtained after simulated gastrointestinal digestion, show a modest ability to inhibit the DPP-IV (González-Montoya, Hernández-Ledesma, Mora-Escobedo, & Martínez-Villaluenga, 2018; Nongonierma & FitzGerald, 2015). In addition, soybean hydrolysates obtained using Corolase L10, Promod 144 MG, or Protamex reduced the enzyme, with IC_{50} values of 2.5, 0.86, and 0.96 mg/mL, respectively (Nongonierma & FitzGerald, 2015). Indeed, SH is more active than hydrolysates obtained using pepsin, trypsin, and Corolase, whereas its activity is very similar to those of peptide mixtures obtained using both Promod and Protamex.

Pea proteins digested with Corolase L10 and Promod 144 MG inhibited DPP-IV activity with IC_{50} values higher than 2.5 mg/mL, whereas the pea hydrolysate obtained using Protamex dropped the enzyme activity with an IC_{50} value of 0.96 mg/mL (Nongonierma & FitzGerald, 2015). In this case, PH displays a DPP-IV activity totally in line with those of hydrolysates obtained using Protamex, whereas it is more active than the peptide mixtures obtained using Corolase and Promod.

Soybean proteins extracted with microwave-assisted technology and hydrolysate using Alcalase inhibited the ACE enzyme, and peptides belonging to the low molecular weight fraction were responsible for the biological activities. Moreover, it was also demonstrated that pea proteins digested using a thermolysin-generated peptide mixture exerted ACE inhibitory properties in a spontaneous hypertensive rat (SHR) model and in a clinical study (Aluko, et al., 2015; H. Li, et al., 2011).

Interestingly, among the peptides belonging to the low molecular weight fraction (<3

kDa) of pea hydrolysate, peptide LTFPG was isolated, whose hypotensive activity has been demonstrated both *in vitro* and *in vivo* in the SHR model (Aluko, et al., 2015). Notably, LTFPG is a conserved active peptide that has also been identified and characterized in a lupin sample (Lammi, et al., 2020).

DPP-IV and ACE are important membrane peptidases which are physiological expressed by many tissues, i.e., intestine (Howell, Kenny, & Turner, 1992; Mentlein, 2004). Indeed, human intestinal Caco-2 cells represent a reliable model which has been already developed and validated for the study of peptides with DPP-IV or ACE inhibitory properties (Lammi, Bollati, Gelain, Arnoldi, & Pugliese, 2019; Lammi, Boschin, Bollati, Arnoldi, Galaverna, & Dellafiora, 2021; Y. Li, Aiello, Fassi, Boschin, Bartolomei, Bollati, et al., 2021). In this study, it was clearly demonstrated that both SH and PH maintain their ability to reduce the activity of both DPP-IV and ACE on Caco-2 cells, even though both hydrolysates are active at a concentration ranging between 0.1 and 5 mg/mL, indicating that SH and PH are less active in cell-based than in cell-free conditions, respectively. Similar results have been previously obtained on peptic and tryptic hydrolysates of spirulina and chlorella proteins, respectively (Aiello, Li, Boschin, Bollati, Arnoldi, & Lammi, 2019; Y. Li, Aiello, Bollati, Bartolomei, Arnoldi, & Lammi, 2020; Y. Li, et al., 2021). Also, in those cases, it was observed that all the tested hydrolysates were more active in cell-free than in cell-based assays, respectively. The reduced activity in the cellular assays may be explained considering the metabolic ability of Caco-2 cells (Y. Li, et al., 2021). Indeed, the intestinal brush border expresses many active proteases and peptidases that might actively hydrolyze food peptides modulating their bioactivity through the production of new breakdown fragments. Therefore, the intestine plays an important role not only in the process of valuable nutrient absorption, but also in actively modulating the physico-chemical and biological profiles of food protein hydrolysates. All these biochemical and cellular results represent an important starting point for future investigations of SH and PH through *in vivo* and clinical studies on suitable animal models and human volunteers in order to obtain a “proof of concept” with respect to their multifunctional and pleotropic behavior.

I-5 Conclusions

In conclusion, our results indicate that SH and PH are multifunctional hydrolysates endowed with both anti-diabetic and hypotensive activity. It is doubtless that they are among the most potent DPP-IV and ACE inhibitor hydrolysates reported in the literature, suggesting that they may be successfully used as new valuable ingredients for the development of innovative functional foods and or dietary supplements for the prevention of cardiovascular disease and metabolic syndrome. Therefore, future *in vivo* and clinical studies need to be undertaken for their benefits to be better exploited in the nutraceutical sector.

I-6 Supporting information

Table I-S1: LC-MS/MS based identification of SH and PH peptides.

Hydrolysate	Protein name	Peptide sequence	Spectrum Intensity	
SH	Uncharacterized protein	(W)FNIVGQWAVTT(S)	5,19E+07	
	Ankyrin repeat domain-containing protein 52	(A)IRSWIVQVMS(Q)	5,11E+07	
	Uncharacterized protein	(I)GKQASIIEDPRPGQGN(L)	2,34E+07	
	Uncharacterized protein	(A)GMPVHSVEDLPGAPFGDA(G)	2,57E+07	
	Glycinin G1	(A)VSIIDTNSLENQLDQ(M)	4,56E+07	
		(S)IIDTNSLENQLDQMPR(R)	2,07E+07	
		(G)ANSLLNALPEEVIQ(H)	2,25E+07	
	Hydrolase_4 domain-containing protein	(A)AAEGGGFSDPAPAPRLAIPV(P)	1,45E+07	
	DNA-directed RNA polymerase (Fragment)	(L)FDIYRVMRPGEPPTMDSAEAMFNA(L)	1,48E+07	
	Heterokaryon incompatibility protein	(L)GGLVQPIQMSKSARADGGDVSAQLANLDS(A)	1,64E+07	
	Uncharacterized protein	(Q)HGLGLEVIELGNCMVDFYLSR(S)	4,81E+07	
	Phosphatidylinositol-specific phospholipase C	(H)DNDIATALSNLGIFTFSEQ(F)	1,15E+07	
	Uncharacterized protein	(P)LQRIGVGLVFSILAMVSAALI(E)	2,57E+07	
	Uncharacterized protein	(K)HKYVVPIPIAMATGESG(E)	5,83E+07	
	C-x8-C-x5-C-x3-H type zinc finger protein	(N)TAVDRTLADFGRGFGRG(Q)	2,12E+07	
	PRONE domain-containing protein	(S)PQVPKSGLS(D)	1,34E+07	
	PH domain-containing protein	(P)PSISSQSRASSDSSSK(E)	9,54E+06	
	GMC_OxRdtase_N domain-containing protein	(N)AGFYSRADADFFARS(G)	2,08E+07	
	PH	Vicilin	(E)ITPEKNPQLQDLDFVN(S)	3,14E+07
			(E)KNPQLQDLDFVN(S)	5,96E+07
Vicilin 47k		(F)EITPEKNQQLQDLDFVN(S)	2,26E+07	
		(E)KNQQLQDLDFVN(S)	7,09E+07	
		(K)NQQQLQDLDFVN(S)	4,01E+07	
Legumin A2		(N)ALEPDNRIE(S)	1,53E+07	
		(S)SVINNPLDVVA(A)	4,96E+07	
Mannonate dehydratase		(T)GATNIVSSLHQVPIGRAWT(E)	3,28E+07	
LysR family transcriptional regulator		(K)HLFILGGLGWGGLPASVVKDDL(A)	1,04E+08	
Aldehyde dehydrogenase		(T)GATAQWAAINCGLGADILREAA(A)	1,70E+07	

Leucine-rich repeat receptor-like protein	(F)GIDLSNNLLHGEIPRGLFGLAGLE(Y)	3,11E+07
AsmA family protein	(S)GGLSFDRKAAKTTASGGLTLSKADA(G)	2,73E+07
	(I)LFGQAGLDPLPVDVANGRL(T)	1,80E+07
TP-binding protein	(L)DRMFCGIIDRDGGAPGTDRIF(P)	3,23E+07
Putative aromatic aminotransferase protein	(A)TFIQAAVPRIIT(Q)	3,03E+07
Argonaute 2	(Q)WPCLQVGNPQRPNYLPMEVCKIVEG(Q)	2,95E+07
ABC transporter substrate-binding protein	(G)WAGAAFGFEESPELKALVDAGKLPVVE(K)	6,51E+07
ABC transporter substrate-binding protein	(S)GGGTWEAAQKKAFFDPFTRDTGIKV(L)	5,85E+07
Mannonate dehydratase	(I)RGGKLSFMETFPDEGDMDMVRS(V)	5,80E+07
LysR family transcriptional regulator	(K)HLFILGGLGWGGLPASVVKDDL(A)	2,92E+07
Clink	(F)SQLPEELKEKIMNEHLKEI(K)	2,79E+07
Peptidoglycan-associated protein	(K)KPPNSAGDLGLGTGAGGAATPGSAQDFTVNV(G)	6,60E+07
Sporulation protein	(P)ITPAPQQVAASPRPAPVFA(P)	1,82E+07
Dioxygenase RAMOSUS5	(P)KPVPAPAPIPTTDVVIPGRILQPVQPF I(D)	1,36E+07
Putative DNA modification/repair radical SAM protein	(L)NIELPTDSGITRF(A)	2,14E+07
Hydantoinase/oxoprolinase family protein	(Y)EGDVLVSTSIGGCNQISDVISKPIQLAK(S)	3,06E+07
Aspartate/tyrosine/aromatic aminotransferase	(F)IDLAYQGLGDGLEQDAAPARM(V)	1,59E+07
DNA replication licensing factor MCM3	(G)THLRGDINMMMVGDPVSAKS(Q)	2,79E+07
L-threonine 3-dehydrogenase	(V)PMVVGHEFSGEIAEIGSAVTRY(H)	4,36E+06

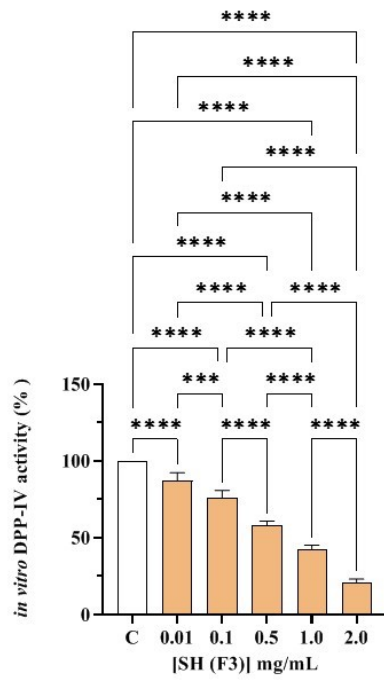
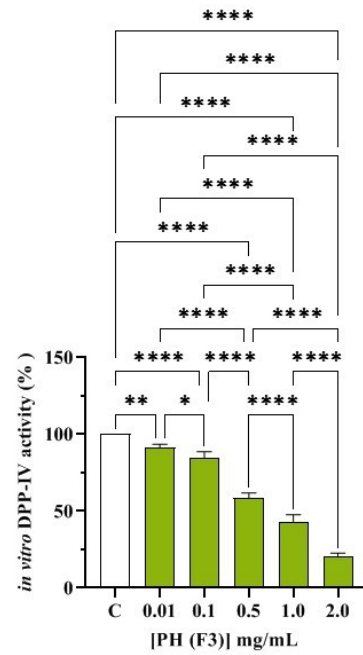
A**B**

Figure I-S1: Evaluation of the *in vitro* inhibitory effects of SH (F3) (A) and PH (F3) (B) hydrolysates on human recombinant DPP-IV. Bars represent the average \pm s.d. of three independent experiments in duplicates. **** $p < 0.0001$, *** $p < 0.001$, ** $p < 0.01$, * $p < 0.05$ versus control (C) sample (Activity).

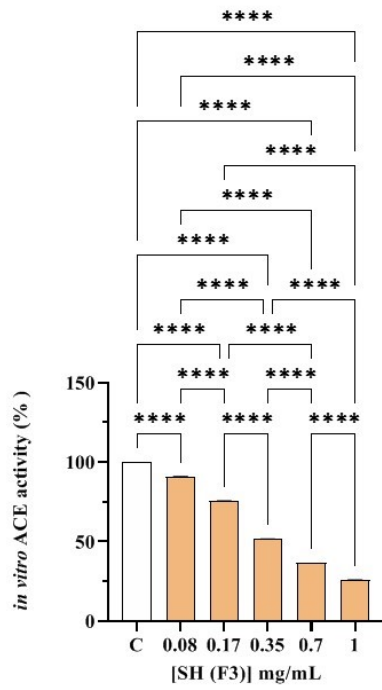
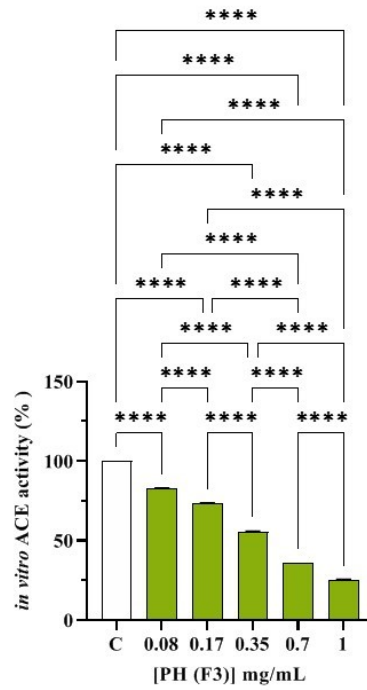
A**B**

Figure I-S2: Evaluation of the *in vitro* inhibitory effects of SH (F3) (A) and PH (F3) (B) hydrolysates on ACE. Bars represent the means \pm sd of three independent experiments in duplicate. **** $p < 0.0001$ versus Control sample (C).

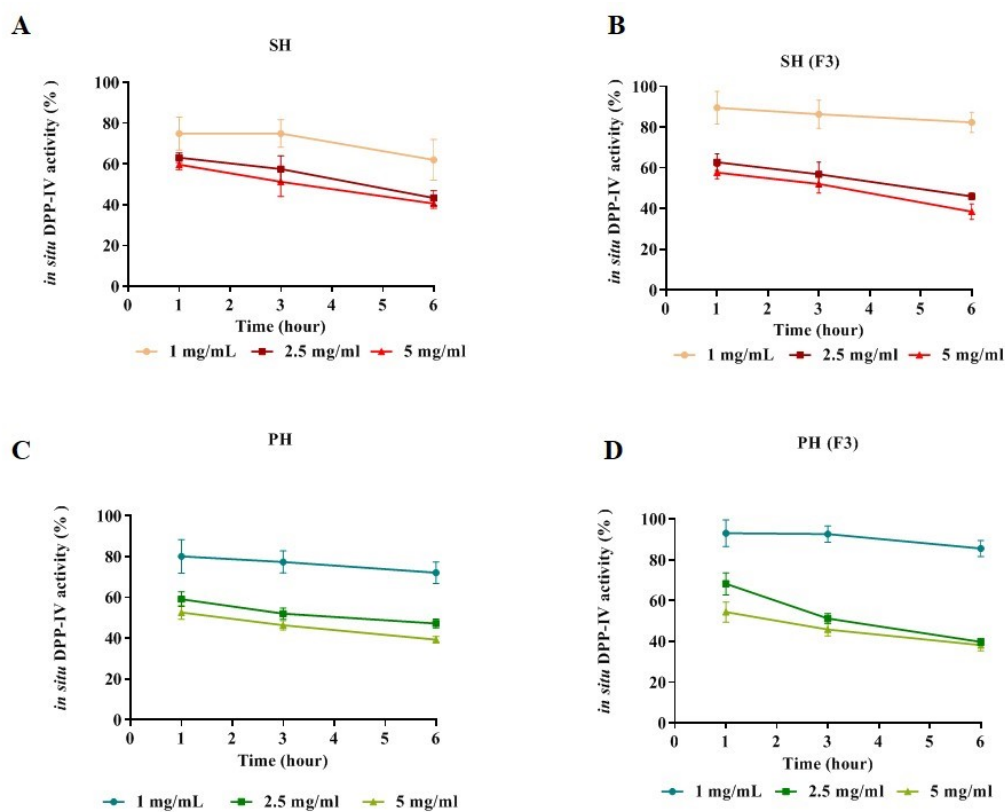


Figure I-S3: The kinetics of the inhibition of cellular DPP-IV activity after incubating Caco-2 cells with the SH (A), SH (F3) (B), PH (C) and PH (F3) (D) hydrolysates for 1, 3 and 6 hours at different concentrations. The data are represented as the means \pm s.d. of four independent experiments, performed in triplicate.

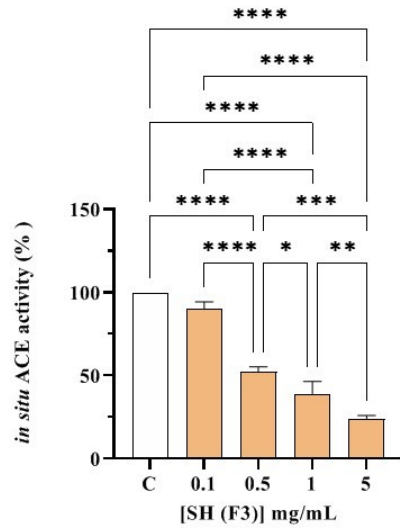
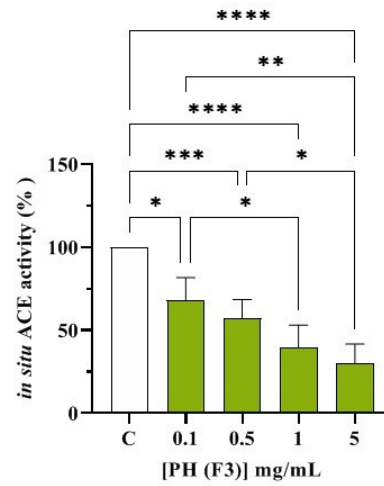
A**B**

Figure I-S4: Evaluation of the inhibitory effects of SH (F3) (A) and PH (F3) (B) hydrolysates on ACE expressed on Caco-2 cells membranes. Bars represent the SD of three independent experiments in triplicate. **** $p < 0.0001$, *** $p < 0.001$, ** $p < 0.01$, * $p < 0.05$ versus Control sample (C), non-significant (ns) is not shown.

I-7 References

- Aguchem, R. N., Okagu, I. U., Okagu, O. D., Ndefo, J. C., & Udenigwe, C. C. (2022). A review on the techno-functional, biological, and health-promoting properties of hempseed-derived proteins and peptides. *Journal of Food Biochemistry*, *46*(7), e14127.
- Aiello, G., Lammi, C., Boschin, G., Zanoni, C., & Arnoldi, A. (2017). Exploration of Potentially Bioactive Peptides Generated from the Enzymatic Hydrolysis of Hempseed Proteins. *Journal of Agricultural and Food Chemistry*, *65*(47), 10174-10184.
- Aiello, G., Li, Y., Boschin, G., Bollati, C., Arnoldi, A., & Lammi, C. (2019). Chemical and biological characterization of spirulina protein hydrolysates: Focus on ACE and DPP-IV activities modulation. *Journal of Functional Foods*, *63*, 103592.
- Akbarian, M., Khani, A., Eghbalpour, S., & Uversky, V. N. (2022). Bioactive Peptides: Synthesis, Sources, Applications, and Proposed Mechanisms of Action. In *International Journal of Molecular Sciences*, vol. 23).
- Aluko, R. E., Girgih, A. T., He, R., Malomo, S., Li, H., Offengenden, M., & Wu, J. (2015). Structural and functional characterization of yellow field pea seed (*Pisum sativum* L.) protein-derived antihypertensive peptides. *Food Research International*, *77*, 10-16.
- Arnoldi, A., Zanoni, C., Lammi, C., & Boschin, G. (2015). The Role of Grain Legumes in the Prevention of Hypercholesterolemia and Hypertension. *Critical Reviews in Plant Sciences*, *34*(1-3), 144-168.
- Bollati, C., Cruz-Chamorro, I., Aiello, G., Li, J., Bartolomei, M., Santos-Sánchez, G., Ranaldi, G., Ferruzza, S., Sambuy, Y., Arnoldi, A., & Lammi, C. (2022). Investigation of the intestinal trans-epithelial transport and antioxidant activity of two hempseed peptides WVSPLAGRT (H2) and IGFLIIWV (H3). *Food Research International*, *152*, 110720.
- Boschin, G., Scigliuolo, G. M., Resta, D., & Arnoldi, A. (2014a). ACE-inhibitory activity of enzymatic protein hydrolysates from lupin and other legumes. *Food Chemistry*, *145*, 34-40.
- Boschin, G., Scigliuolo, G. M., Resta, D., & Arnoldi, A. (2014b). Optimization of the Enzymatic Hydrolysis of Lupin (*Lupinus*) Proteins for Producing ACE-Inhibitory Peptides. *Journal of Agricultural and Food Chemistry*, *62*(8), 1846-1851.

- Chakrabarti, S., Guha, S., & Majumder, K. (2018). Food-Derived Bioactive Peptides in Human Health: Challenges and Opportunities. In *Nutrients*, vol. 10).
- Cruz-Chamorro, I., Santos-Sánchez, G., Bollati, C., Bartolomei, M., Li, J., Arnoldi, A., & Lammi, C. (2022). Hempseed (*Cannabis sativa*) Peptides WVSPLAGRT and IGFLIIWV Exert Anti-inflammatory Activity in the LPS-Stimulated Human Hepatic Cell Line. *Journal of Agricultural and Food Chemistry*, 70(2), 577-583.
- Daskaya-Dikmen, C., Yucetepe, A., Karbancioglu-Guler, F., Daskaya, H., & Ozcelik, B. (2017). Angiotensin-I-Converting Enzyme (ACE)-Inhibitory Peptides from Plants. In *Nutrients*, vol. 9).
- Fukui, K., Tachibana, N., Wanezaki, S., Tsuzaki, S., Takamatsu, K., Yamamoto, T., Hashimoto, Y., & Shimoda, T. (2002). Isoflavone-Free Soy Protein Prepared by Column Chromatography Reduces Plasma Cholesterol in Rats. *Journal of Agricultural and Food Chemistry*, 50(20), 5717-5721.
- Ge, J., Sun, C.-X., Corke, H., Gul, K., Gan, R.-Y., & Fang, Y. (2020). The health benefits, functional properties, modifications, and applications of pea (*Pisum sativum* L.) protein: Current status, challenges, and perspectives. *Comprehensive Reviews in Food Science and Food Safety*, 19(4), 1835-1876.
- González-Montoya, M., Hernández-Ledesma, B., Mora-Escobedo, R., & Martínez-Villaluenga, C. (2018). Bioactive Peptides from Germinated Soybean with Anti-Diabetic Potential by Inhibition of Dipeptidyl Peptidase-IV, α -Amylase, and α -Glucosidase Enzymes. In *International Journal of Molecular Sciences*, vol. 19).
- Howell, S., Kenny, A. J., & Turner, A. J. (1992). A survey of membrane peptidases in two human colonic cell lines, Caco-2 and HT-29. *Biochemical Journal*, 284(2), 595-601.
- Lammi, C., Aiello, G., Boschin, G., & Arnoldi, A. (2019). Multifunctional peptides for the prevention of cardiovascular disease: A new concept in the area of bioactive food-derived peptides. *Journal of Functional Foods*, 55, 135-145.
- Lammi, C., Aiello, G., Dellafiora, L., Bollati, C., Boschin, G., Ranaldi, G., Ferruzza, S., Sambuy, Y., Galaverna, G., & Arnoldi, A. (2020). Assessment of the Multifunctional Behavior of Lupin Peptide P7 and Its Metabolite Using an Integrated Strategy. *Journal of Agricultural and Food Chemistry*, 68(46), 13179-13188.

- Lammi, C., Arnoldi, A., & Aiello, G. (2019). Soybean Peptides Exert Multifunctional Bioactivity Modulating 3-Hydroxy-3-Methylglutaryl-CoA Reductase and Dipeptidyl Peptidase-IV Targets *in Vitro*. *Journal of Agricultural and Food Chemistry*, 67(17), 4824-4830.
- Lammi, C., Bollati, C., Gelain, F., Arnoldi, A., & Pugliese, R. J. F. i. C. (2019). Enhancement of the stability and anti-DPPiV activity of hempseed hydrolysates through self-assembling peptide-based hydrogels. 6, 670.
- Lammi, C., Boschin, G., Bollati, C., Arnoldi, A., Galaverna, G., & Dellafiora, L. (2021). A heuristic, computer-driven and top-down approach to identify novel bioactive peptides: A proof-of-principle on angiotensin I converting enzyme inhibitory peptides. *Food Research International*, 150, 110753.
- Lammi, C., Zanoni, C., & Arnoldi, A. (2015). Three Peptides from Soy Glycinin Modulate Glucose Metabolism in Human Hepatic HepG2 Cells. In *International Journal of Molecular Sciences*, vol. 16 (pp. 27362-27370).
- Lammi, C., Zanoni, C., Arnoldi, A., & Vistoli, G. (2016). Peptides Derived from Soy and Lupin Protein as Dipeptidyl-Peptidase IV Inhibitors: *In Vitro* Biochemical Screening and *in Silico* Molecular Modeling Study. *Journal of Agricultural and Food Chemistry*, 64(51), 9601-9606.
- Lammi, C., Zanoni, C., Ferruzza, S., Ranaldi, G., Sambuy, Y., & Arnoldi, A. (2016). Hypocholesterolaemic Activity of Lupin Peptides: Investigation on the Crosstalk between Human Enterocytes and Hepatocytes Using a Co-Culture System Including Caco-2 and HepG2 Cells. In *Nutrients*, vol. 8).
- Li, H., & Aluko, R. E. (2010). Identification and Inhibitory Properties of Multifunctional Peptides from Pea Protein Hydrolysate. *Journal of Agricultural and Food Chemistry*, 58(21), 11471-11476.
- Li, H., Prairie, N., Udenigwe, C. C., Adebisi, A. P., Tappia, P. S., Aukema, H. M., Jones, P. J. H., & Aluko, R. E. (2011). Blood Pressure Lowering Effect of a Pea Protein Hydrolysate in Hypertensive Rats and Humans. *Journal of Agricultural and Food Chemistry*, 59(18), 9854-9860.
- Li, Y., Aiello, G., Bollati, C., Bartolomei, M., Arnoldi, A., & Lammi, C. (2020). Phycobiliproteins from *Arthrospira Platensis* (Spirulina): A New Source of Peptides with Dipeptidyl Peptidase-IV Inhibitory Activity. In *Nutrients*, vol. 12).

- Li, Y., Aiello, G., Fassi, E. M., Boschini, G., Bartolomei, M., Bollati, C., Roda, G., Arnoldi, A., Grazioso, G., & Lammi, C. (2021). Investigation of *Chlorella pyrenoidosa* Protein as a Source of Novel Angiotensin I-Converting Enzyme (ACE) and Dipeptidyl Peptidase-IV (DPP-IV) Inhibitory Peptides. In *Nutrients*, vol. 13).
- Liu, Z.-m., Ho, S. C., Chen, Y.-m., Ho, S., To, K., Tomlinson, B., & Woo, J. (2014). Whole soy, but not purified daidzein, had a favorable effect on improvement of cardiovascular risks: A 6-month randomized, double-blind, and placebo-controlled trial in equol-producing postmenopausal women. *Molecular Nutrition & Food Research*, 58(4), 709-717.
- Mentlein, R. (2004). Cell-Surface Peptidases**Dedicated to Professor Dr. Eberhard Heymann on the occasion of his 65th birthday. In *International Review of Cytology*, vol. 235 (pp. 165-213): Academic Press.
- Nongonierma, A. B., & FitzGerald, R. J. (2015). Investigation of the Potential of Hemp, Pea, Rice and Soy Protein Hydrolysates as a Source of Dipeptidyl Peptidase IV (DPP-IV) Inhibitory Peptides. *Food Digestion: Research and Current Opinion*, 6(1), 19-29.
- Nongonierma, A. B., & FitzGerald, R. J. (2019). Features of dipeptidyl peptidase IV (DPP-IV) inhibitory peptides from dietary proteins. *Journal of Food Biochemistry*, 43(1), e12451.
- Sun, X. D., & Arntfield, S. D. (2011). Gelation properties of salt-extracted pea protein isolate catalyzed by microbial transglutaminase cross-linking. *Food Hydrocolloids*, 25(1), 25-31.
- Udenigwe, C. C., & Aluko, R. E. (2012). Food Protein-Derived Bioactive Peptides: Production, Processing, and Potential Health Benefits. *Journal of Food Science*, 77(1), R11-R24.
- Zanoni, C., Aiello, G., Arnoldi, A., & Lammi, C. (2017). Hempseed Peptides Exert Hypocholesterolemic Effects with a Statin-Like Mechanism. *Journal of Agricultural and Food Chemistry*, 65(40), 8829-8838.

Project II

EVALUATION OF THE MULTIFUNCTIONAL DIPEPTIDYL-PEPTIDASE IV AND ANGIOTENSIN CONVERTING ENZYME INHIBITORY PROPERTIES OF A CASEIN HYDROLYSATE USING CELL-FREE AND CELL-BASED ASSAYS

Jianqiang Li¹, Carlotta Bollati¹, Gilda Aiello², Martina Bartolomei¹,
Fabrizio Rivardo³, Giovanna Boschin¹, Anna Arnoldi¹, Carmen Lammi^{1*}

¹**Department of Pharmaceutical Sciences, University of Milan, Via Mangiagalli
25, 20133 Milan, Italy.**

²**Department of Human Science and Quality of Life Promotion, Telematic
University San Raffaele, 00166 Rome, Italy.**

³**A. Costantino & C. Spa, Via Francesco Romana 11-15 - 10083 Favria (TO) –
Italy.**

Author Contributions: Conceptualization, C.L.; methodology, C.L., J.L., C.B., G.A.,
M.B., G.B. and FR.; writing—original draft, C.L. and J.L.; writing—review & editing,
C.L. and A.A.; supervision, C.L.

II. Abstract

The objective of the study was the evaluation of the potential pleiotropic effect of a commercial casein hydrolysate (CH). After an analysis of the composition, the BIOPEP-UWM database suggested that these peptides contained numerous sequences with potential inhibitory activities on angiotensin converting enzyme (ACE) and dipeptidyl-peptidase IV (DPP-IV). The anti-diabetic and anti-hypertensive effects of these peptides were thus assessed using either cell-free or cell-based assays. In the cell-free system, CH displayed inhibitory properties against DPP-IV (IC_{50} value equal to 0.38 ± 0.01 mg/mL) and ACE (IC_{50} value equal to 0.39 ± 0.01 mg/mL). Further, CH reduced the DPP-IV and ACE activities expressed by human intestinal Caco-2 cells by $61.10 \pm 1.70\%$ and $76.90 \pm 4.47\%$, respectively, versus untreated cells, after 6 h of treatment at the concentration of 5 mg/mL. This first demonstration of the multifunctional behavior of this material suggests that it may become an anti-diabetic and/or anti-hypertensive ingredient to be included in the formulation of different functional food or nutraceuticals.

II-1 Introduction

Type II diabetes is a chronic disease, which affects millions of people worldwide: the inadequate secretion of insulin by β -cells and/or insulin resistance in tissues are its main characteristics (1). Dipeptidyl-peptidase IV (DPP-IV) is known for its inactivation of two intestinal hormones, including glucagon-like peptide-1 (GLP-1) and glucose-dependent insulinotropic polypeptide (GIP), which possess potent insulin-secretory activity, and consequently lower prandial plasma glucose (Eizirik et al., 2020). Due to the short half-life (< 2 min) of the degradation of GLP-1 and GIP by DPP-IV, the inhibition of DPP-IV is an attractive therapeutic strategy to maintain the insulinotropic activity of GLP-1 and GIP, resulting in an improved homeostasis of glucose in type II diabetes (Holst & Deacon, 1998). Interestingly, a number of studies indicate that most people with diabetes will eventually develop hypertension and other blood circulation complications, especially showing a close association between

Type II diabetes and hypertension (de Boer et al., 2017; Schutta, 2007). There are many factors associated with the development of hypertension, one of them is related to the conversion of angiotensin I, an active decapeptide, into angiotensin II, a potent vasoconstrictor octapeptide, by the angiotensin-converting enzyme (ACE) system. Meanwhile, the inactivation of bradykinin, which shows a significant vasodilator activity, is caused by ACE. Therefore, inhibition of ACE is considered an effective treatment for lowering blood pressure in hypertensive subjects (Bernstein et al., 2018). Inhibitors of DPP-IV and/or ACE are regularly applied in therapy to lower morbidity and mortality of patients with type II diabetes and/ or hypertension. Synthetic inhibitors of DPP-IV and/or ACE are the first-line option for the treatment of these events (Juillerat-Jeanneret, 2014), however, inevitable and evitable side effects of them, such as coughing, skin rashes, taste disturbances, angioedema, hyperkalaemia (ACE inhibitors) (Kostis et al., 2018; Sica, 2005), and nasopharyngitis, headache, diarrhea, joint pain, urinary tract infection (DPP-IV inhibitors) (Gallwitz, 2019; Kshirsagar et al., 2011), highlight the importance of developing new natural, innovative side-effect free compounds to prevent and/or alleviate diabetes and hypertension. Over the past few decades, many evidences have underlined that protein hydrolysates obtained from both plant (soybean, pea, rice bran, lupin, wheat, and many others) and/or animal (milk, egg yolk, beef, pork, chicken, sardine, salmon, and many others) foods may be useful for the prevention of these pathologies and several food derived peptides with potent DPP-IV-inhibitory and/or ACE-inhibitory activities have been successfully identified and characterized (Bollati et al., 2022; Guang & Phillips, 2009; Lee & Hur, 2017; Liu et al., 2019; Murray & FitzGerald, 2007; Zambrowicz et al., 2015). These peptides are encrypted within the protein sequences and are released by the hydrolysis (Bhandari et al., 2020). They may be obtained with digestive enzymes (i.e., pepsin and trypsin), mimicking the action of *in vivo* gastrointestinal digestion, or produced using plant (i.e., Bromelin) or microbial (i.e., Alcalase® and Flavourzyme®) food grade enzymes, as well as during some food manufacture processes, such fermentation (Hernández-Ledesma et al., 2011; Maestri et al., 2016).

It has been clearly demonstrated (Samtiya et al., 2022) that milk protein derived peptides possess different biological properties, including antimicrobial (Singh et al., 2023), antioxidant (Perpetuo et al., 2003), anti-inflammatory (Brück et al., 2003), antithrombotic, hypocholesterolemic (Nagaoka et al., 2001) and anti-hypertensive (Perpetuo et al., 2003) activities useful for cardiovascular risk prevention. Moreover, they are active in preventing nervous system and bone diseases (Bu et al., 2021; Mohanty et al., 2016). Most of these bioactive peptides are generated from the degradation of casein, which makes up around 80% of the protein in cow milk and it is composed by α -, β - and κ -caseins (Goulding et al., 2020).

In light with these considerations, this study had the goal of assessing the pleiotropic health-promoting effects of a commercial casein hydrolysate (CH), obtained by an industrial process. Since casein is an excellent source of biologically active peptides, it was hypothesized that this industrial product may possess a dual biological behavior, including DPP-IV-inhibitory and/or ACE-inhibitory activity. The first objective of the study was the characterization of the chemical composition of CH for identifying sequences that may be responsible for its biological activity. The second aim was the evaluation of the potential anti-diabetic and hypotensive effects of CH by measuring its inhibitory activities toward both DPP-IV and ACE. This was achieved by using either cell-free tests or cell assays based on human intestinal Caco-2 cells. Finally, the same experimental procedures were employed to evaluate the activities of the fraction with a molecular weight lower than 3 kDa [CH (F3)].

II-2 Material and methods

II-2.1 Chemicals

Dulbecco's modified Eagle's medium (DMEM), L-glutamine, fetal bovine serum (FBS), phosphate buffered saline (PBS), penicillin/streptomycin and 96-well plates were purchased from Euroclone (Milan, Italy). Sitagliptin, Gly-Pro-amido-4-methylcoumarin hydrobromide (Gly-Pro-AMC) and ACE from porcine kidney were from Sigma-Aldrich (St. Louis, MO, USA). ACE1 Activity Assay Kits come from

Biovision (Milpitas Blvd., Milpitas, CA, USA). Caco-2 cells were obtained from INSERM (Paris, France). Casein hydrolysates (CH), which is spray dried samples from the production process, was supplied by A. Costantino S.R.L. (Italy). (Casein hydrolysate sport/health batch 218F0004, 100 g).

II-2.2 Ultrafiltration of CH

Before proceeding to the assessment of biological activity, CH was passed through ultrafiltration (UF) membranes with a 3 kDa cut-off, using a Millipore UF system (Millipore, Bedford, MA, USA). The recovered peptides solution was lyophilized (lyophilizer LIO5P, Cinquepascal S.r.l., Milan, Italy) and store -80 °C until use.

II-2.3 Analysis of mass spectrometry

Samples were dissolved with 50 µL of a solution of 99% water and 1% ACN containing 0.1% formic acid. All samples have been analyzed at UNITECH OMICs (University of Milano, Italy) using: Dionex Ultimate 3000 nano-LC system (Sunnyvale CA, USA) connected to Orbitrap Fusion™ Tribrid™ Mass Spectrometer (Thermo Scientific, Bremen, Germany) equipped with nanoelectrospray ion source. Peptide mixtures were pre-concentrated onto an Acclaim PepMap 100 – 100 µm × 2 cm C18 (Thermo Scientific) and separated on EASY-Spray column ES900, 25 cm × 75 µm ID packed with Thermo Scientific Acclaim PepMap RSLC C18, 3 µm, 100 Å using mobile phase A (0.1 % formic acid in water) and mobile phase B (0.1% formic acid in acetonitrile 20/80, v/v) at a flow rate of 0.300 µL/min. The following gradient profile was used: 0.00 min, 4 % B; 3.00 min, 4 % B; 103.00 min, 28 % B; 113.00 min, 95 % B; 120.00 min, 4 % B; 126.00 min, 95 % B; 135.00 min, 4% B; 138 min, 95% B; 144.00 min, 4% B. The temperature was set to 35 °C and the sample were injected in triplicates. MS spectra were collected over an m/z range of 375 – 1500 Da at 120,000 resolutions (m/z 200), operating in the data-dependent mode, cycle time of 3 sec between masters scans. HCD was performed with collision energy set at 35 eV. Polarity: positive. MS data were analyzed by Proteome Discoverer 2.5 by using *Bos taurus* (sp_incl_isoforms TaxID=9913_and_subtaxonomies) (v2022-12-14) senza

without any specific enzymatic cut. Carbamidomethylation of cysteine was defined as fixed modification, while oxidation of methionine and acetylation at the protein N-terminus were specified as variable modifications.

II-2.4 Characterization of the inhibitory effects of CH on DPP-IV and ACE through biochemical assays

II-2.4.1 *In vitro* assessment of DPP-IV-inhibitory activity

The *in vitro* assessment of DPP-IV-inhibitory activity was performed following the manufacturer instructions (DPP-IV inhibitor screening assay kit–Cayman Chemical) and previously reported methods (Aiello et al., 2019; Lammi et al., 2019). The experiments were carried out in triplicate in a half volume 96 well solid plate (white). Each reaction (50 μ L) was prepared adding the reagents in the following order in a microcentrifuge tube: 1 X assay buffer [20 mM Tris-HCl, pH 8.0, containing 100 mM NaCl, and 1 mM EDTA] (30 μ L), CH at final concentration range of 0.01-2.0 mg/mL (10 μ L) or vehicle (10 μ L) and finally the DPP-IV enzyme (10 μ L). Subsequently, the samples were mixed and 50 μ L of each reaction were transferred in each well of the plate. The reactions were started by adding 50 μ L of substrate solution to each well and incubated at 37 °C for 30 minutes. Fluorescence signals were measured using the Synergy H1 fluorescent plate reader from Biotek (excitation and emission wavelengths 360 and 465 nm, respectively).

II-2.4.2 *In vitro* assessment of ACE-inhibitory activity

The ACE-inhibitory activity of the CH was evaluated following previously reported methods (Boschin et al., 2014a; Boschin et al., 2014b) and tested by measuring with HPLC the formation of hippuric acid (HA) from hippuryl-histidyl-leucine (HHL), used as mimic substrate for ACE. Tests were performed in 100 mM Tris-HCOOH, 300 mM NaCl pH 8.3 buffer, and using ACE from porcine kidney (Sigma-Aldrich, Milan, Italy). CH hydrolysate was tested at 0.08, 0.17, 0.35, 0.7 and 1.0 mg/mL.

II-2.5 Assessment of the inhibitory effects of CH on DPP-IV and ACE activities using cellular assays

II-2.5.1 Culture of Caco-2 cells

Caco-2 cells were routinely sub-cultured at 50% density and maintained at 37 °C in 5% CO₂ atmosphere in Dulbecco's modified Eagle's medium (DMEM) containing 25 mM of glucose, 3.7 g/L of NaHCO₃, 4 mM of stable L-glutamine, 1% nonessential amino acids, 100 U/L of penicillin, and 100 µg/L of streptomycin (complete medium), supplemented with 10% heat-inactivated fetal bovine serum (FBS), as reported elsewhere (Lammi et al., 2016). The cells were used for no more than 20 passages.

II-2.5.2 MTT Assay

A total of 3×10^4 Caco-2 cells/well were seeded in 96-well plates and, the day after, they were treated with 1.0, 2.5 and 5 mg/mL of CH or CH (F3) or vehicle (H₂O) in complete growth media for 48 h at 37 °C under 5% CO₂ atmosphere. Subsequently, the treatment solvent was aspirated and 100 µL/well of 3-(4,5-dimethylthiazol-2-yl)-2,5-diphenyltetrazolium bromide (MTT) filtered solution added. After 2 h of incubation at 37 °C under 5% CO₂ atmosphere, 0.5 mg/mL solution was aspirated and 100 µL/well of the lysis buffer (8 mM HCl + 0.5% NP-40 in DMSO) added. After 10 min of slow shaking, the absorbance at 575 nm was read on the Synergy H1 fluorescence plate reader (Biotek, Bad Friedrichshall, Germany).

II-2.5.3 Assessment of the inhibitory activity of CH on cellular DPP-IV activity

Caco-2 cells were seeded on black 96-well plates with clear bottoms at a density of 3×10^4 cells/well. After one day, cells were treated with 1.0, 2.5 and 5.0 mg/mL of CH or CH (F3) for 1, 3 and 6 h; at the end of the incubation, cells were washed once with 100 µL of PBS, then, 50 µL of Gly-Pro-AMC substrate at concentrations of 25 µM in PBS were added and the fluorescence signals (excitation/emission wavelengths 350/450 nm) in each well were measured using a Synergy H1 (BioTek Instruments, Winooski, VT, USA) every 1 min, for up to 10 min.

II-2.5.4 Assessment of the inhibitory activity of CH on cellular ACE1 activity

The inhibitory activity of CH on cellular ACE1 activity was evaluated following a previously reported method (Lammi et al., 2020). Caco-2 cells were seeded on 96-well plates at a density of 3×10^4 cells/well for 24 h. The following day, cells were treated with CH or CH (F3) (0.1 - 5.0 mg/mL) or vehicle in growth medium for 6 h at 37 °C, then cells were scraped in 30 μ L of ice-cold ACE1 lysis buffer and transferred in an ice-cold eppendorf tube. After centrifugation at 13300 g for 15 min at 4 °C, the supernatant was recovered and transferred into a new ice-cold tube. Total proteins were quantified by Bradford method, and 2 μ g of total proteins (the equivalent of 2 μ L) were added to 18 μ L of ACE1 lysis buffer in each well in a black 96-well plates with clear bottoms. For the background control, 20 μ L of ACE1 lysis buffer were added to 20 μ L of ACE1 assay buffer. Subsequently, 20 μ L of 4% of ACE1 substrate (prepared in assay buffer) was added in each well except the background one and the fluorescence (Ex/Em 330/430 nm) was measured in a kinetic mode for 10 min at 37 °C.

II-2.6 Statistical analysis

The statistical analysis was conducted through one-way ANOVA (GraphPad Prism 9.1, GraphPad Software, La Jolla, CA, USA), and Tukey's multiple comparison test was used for post-hoc analysis. The assays were performed independently at least four times, and each experiment was conducted in triplicate. The data were expressed as mean \pm standard deviation (s.d.), and statistical significance was set at $p < 0.05$.

II-3 Results

II-3.1 Peptidomic characterization of CH

The peptide composition of CH was analyzed by using HPLC-ESI-MS/MS. **Figure II-1** displays the total ion current (TIC) of the MS/MS of eluted peptides. The percentage of peptides with MW > 3 kDa was 37.95%, whereas the percentage of

peptides with MW < 3 kDa was 62.05%. In addition, CH was ultra-filtered using a 3 kDa cutoff obtaining the low molecular peptide fraction, named CH (F3), which was investigated in parallel with total CH sample.

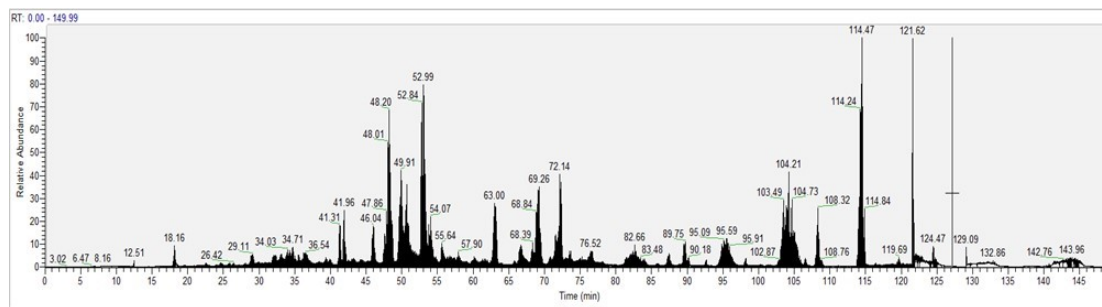


Figure II-1. The total ion chromatogram (TIC) of CH.

As shown in **Table II-1**, 37 identified peptides belong to caseins: in particular, 18 belong to α -S1-casein, whereas 19 belong to β -casein. The lengths of those peptides range from 6 to 18 amino acids, whereas their isoelectric points (pI) and hydrophobicity range from 2.87 to 11.13 (pH) and from +4.41 to +23.87 ($\text{kcal} \times \text{mol}^{-1}$), respectively. Additionally, as reported by the BIOPEP-UWM database (accessed on 16 Feb 2023), all peptides contain one or more motives including known sequences of either ACE or DPP-IV inhibitors.

Table II-1. Identified peptides belonging to caseins, with inhibitory activity against both ACE and DPP-IV.

Protein Name	Peptide Sequence	Modifications	Theo. MH+ [Da]	Isoelectric point (pI)	Hydrophobicity (Kcal* mol^{-1}) ^a	ACE Inhibitor Sequence ^b	DPP-IV Inhibitor Sequence ^b
α-S1-casein [OS=Bos taurus]	DIPNPIGSE		941,45745	2.87	+15.67	IP, IG, GS	IP, NP, PI, PN
	DIPNPIGSEN		1055,50038	2.89	+16.52	IP, IG, GS	IP, NP, PI, PN
	DIPNPIGSENSEK		1399,66996	3.73	+23.41	IP, IG, GS, EK	IP, NP, EK, PI, PN
	EDVPSEER		831,38429	3.72	+20.75	VP, ER	VP, PS
	IPNPIGSE		826,43051	3.09	+12.03	IP, IG, GS	IP, NP, PI, PN
	IPNPIGSENSEK		1284,64302	4.08	+19.77	IP, IG, GS, EK	IP, NP, EK, PI, PN
	IPNPIGSENSEKTTMP	1xOxidation [M15]	1730,82654	4.08	+19.74	IP, IG, GS, EK	MP, IP, NP, EK, KT, PI, PN, TM, TT
	KEDVPSEER		1122,54258	4.33	+22.84	RY, VP, KE, KEDVPSE, ER	VP, KE, PS
	KEPMIGVN	1xOxidation [M4]	903,46043	6.53	+14.22	IG, GV, KE	EP, GV, KE, MI, PM, VN
	LEQILR		771,47231	6.84	+10.49	IL, LR	IL, QI
	SDIPNPIGSE		1028,48948	2.87	+16.13	IP, IG, GS	IP, NP, PI, PN
	SDIPNPIGSEN		1142,53241	2.89	+16.98	IP, IG, GS	IP, NP, PI, PN
	SDIPNPIGSENS		1229,56444	2.92	+17.44	IP, IG, GS	IP, NP, PI, PN
	SDIPNPIGSENSE		1358,60703	2.79	+21.07	IP, IG, GS	IP, NP, PI, PN
	SDIPNPIGSENSEK		1486,70199	3.73	+23.87	IP, IG, GS, EK	IP, NP, EK, PI, PN
	SDIPNPIGSENSEKTT		1688,79735	3.73	+24.37	IP, IG, GS, EK	IP, NP, EK, KT, PI, PN, TT
	SDIPNPIGSENSEKTTMP	1xOxidation [M17]	1932,88551	3.73	+23.84	IP, IG, GS, EK	MP, IP, NP, EK, KT, PI, PN, TM, TT
	VPNSAEER	1xPhospho [S4]	981,40372	4.08	+18.46	VP, ER	VP, AE, PN

β-casein [OS=Bos taurus]	EMPFPKYP	1xOxidation [M2]	1024,48083	6.67	+11.66	FP, EMPFPK, YP, KY, PFP	MP, FP, YP, KY, PF, PK, MPF
	EMPFPKYPVEP	1xOxidation [M2]	1349,64460	4.08	+14.97	FP, EMPFPK, YP, KY, VE, PFP	MP, FP, YP, EP, KY, PF, PK, PV, VE, MPF
	EPVLGPVRGPPF		1264,70483	6.72	+12.32	FP, LGP, GP, GPV, LG, VR, RG, LGPVRGPPF, VRGP, PFP	GP, FP, EP, VLGP, VR, PF, PV, RG, VL, GPV, GPF
	FPKYPVE		879,46108	6.61	+11.73	FP, YP, KY, VE	FP, YP, KY, PK, PV, VE
	FPKYPVEP		976,51384	6.61	+11.87	FP, YP, KY, VE	FP, YP, EP, KY, PK, PV, VE
	GPVRGPPF		826,45700	11.13	+10.26	FP, GP, GPV, VR, RG, VRGP, PFP	GP, FP, VR, PF, PV, RG, GPV, GPF
	GPVRGPPFII		1052,62513	11.13	+8.02	FP, GP, GPV, VR, GPVRGPPFII, RG, VRGP, PFP	GP, FP, VR, II, PF, PI, PV, RG, GPV, GPF
	GPVRGPPFIIIV		1151,69354	11.03	+7.56	FP, GP, GPV, VRGP, PFP, VR, GPF, RGPF, GPVRGPPFII, FPIIV, RG, VRGP, PFP	GP, FP, VR, II, PF, PI, PV, RG, GPV, GPF
	IPPLTQTPVVVP		1260,75620	5.23	+5.98	IPP, PL, IP, VP, TQ, PP, TP, PPL, IPPLTQTPV	PP, VP, VV, IP, TP, PL, PPL, IPPLTQTPV, LT, PV, QT, TQ
	IPPLTQTPVVVPP		1357,80896	5.23	+6.12	IPP, VPP, PL, IP, VP, TQ, PP, VVPP, TP, PPL, IPPLTQTPV	PP, VP, VV, IP, TP, PL, PPL, IPPLTQTPV, LT, PV, QT, TQ
	IPPLTQTPVVVPPF		1504,87738	5.46	+4.41	IPP, VPP, PL, IP, VP, TQ, PP, VVPP, TP, LTQTPVVVPPF, VVVPPF, PPL,	PP, VP, VV, IP, TP, PL, PPL, IPPLTQTPV, LT, PF, PV, QT, TQ

MPFPKYPVE	1xOxidation [M1]	1123,54924	6.60	+11.20	IPPLTQTPV FP, YP, KY, VE, PFP	MP, FP, YP, KY, PF, PK, PV, VE, MPF
MPFPKYPVEP		1204,60709	6.60	+11.34	FP, YP, KY, VE, PFP	MP, FP, YP, EP, KY, PF, PK, PV, VE, MPF
MPFPKYPVEP	1xOxidation [M1]	1220,60201	6.60	+11.34	FP, YP, KY, VE, PFP	MP, FP, YP, EP, KY, PF, PK, PV, VE, MPF
NIPPLTQTPVVVPP		1471,85189	5.09	+6.97	IPP, VPP, NIPPLTQTPV, PL, IP, VP, TQ, PP, VVPP, TP, PPL, IPPLTQTPV	PP, VP, VV, IP, TP, PL, PPL, IPPLTQTPV, LT, PV, QT, TQ
PLTQTPVVVPP		1147,67214	5.25	+7.10	VPP, PL, VP, TQ, PP, VVPP, TP	PP, VP, VV, TP, PL, LT, PV, QT, TQ
QEPVLPVVRGPPF		1392,76341	6.57	+13.09	FP, LGP, GP, GPV, LG, VR, RG, QEPVLPVVRGPPF, LGPVVRGPPF, VRGP, PFP	GP, FP, EP, VLGP, VR, PF, PV, QE, RG, VL, GPV, GPF
VLGPVVRGPPF		1038,60948	11.11	+8.55	FP, LGP, GP, GPV, LG, VR, RG, LGPVVRGPPF, VRGP, PFP	GP, FP, VLGP, VR, PF, PV, RG, VL, GPV, GPF
YQEPVLPVVRGPPF		1555,82674	6.58	+12.38	FP, LGP, GP, GPV, LG, VR, RG, YQEPVL, QEPVLPVVRGPPF, LGPVVRGPPF, VRGP, PFP	GP, FP, EP, VLGP, VR, PF, PV, QE, RG, VL, YQ, GPV, GPF

^aAccording to PepDraw (<http://pepdraw.com>).

^bAccording to the BIOPEP-UWM database; <https://biochemia.uwm.edu.pl/biopep-uwm/> accessed on 16 Feb 2023.

II-3.2 Biochemical study of the DPP-IV and ACE inhibitory activities of CH

II-3.2.1 The inhibition of *in vitro* DPP-IV activity by CH and CH (F3)

The assessment of CH ability to regulate the DPP-IV activity was carried out using the purified recombinant DPP-IV enzyme. Results clearly demonstrated that CH decreased the DPP-IV activity *in vitro* with a dose–response trend in the concentration range of 0.1, 0.5, 1.0, and 2.5 mg/mL, displaying an IC_{50} value of 0.38 ± 0.01 mg/mL (**Figure II-2A**). To investigate if the medium and short/sized peptides are responsible of the bioactivity of CH sample, the experiments were carried out on the low molecular weight fraction (<3 kDa), named CH (F3), in the same experimental conditions (**Figure II-2B**). This low molecular weight fraction dropped the DPP-IV activity *in vitro* too, showing a dose–response trend and an IC_{50} value of 0.31 ± 0.05 mg/mL (**Figure II-2B**).

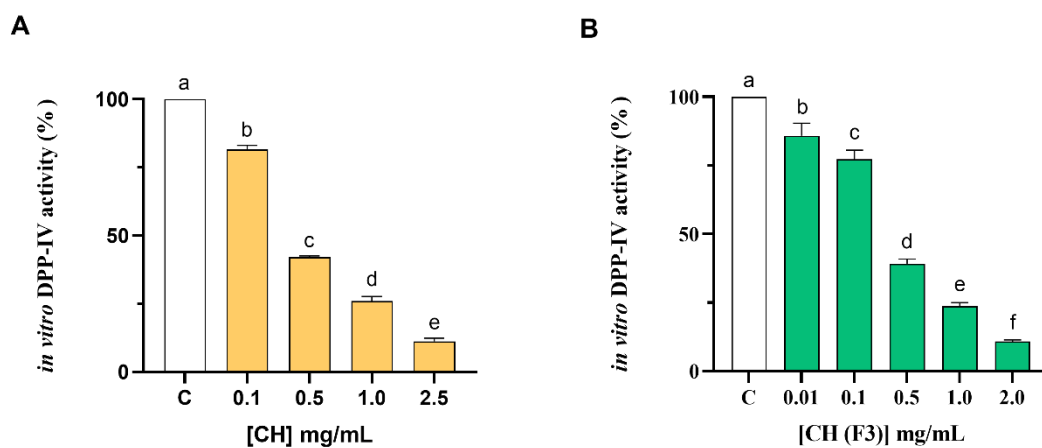


Figure II-2. Examining the *in vitro* inhibitory properties of CH (A) and CH (F3) (B) against human recombinant dipeptidyl peptidase-IV (DPP-IV), obtained using cell-free assay. The bars show the mean \pm s.d. of three independent experiments carried out in duplicate. Different lowercase letters indicate a significant difference ($p < 0.05$) between different concentrations. C (H₂O): control cells.

A comparison of the IC₅₀ value of the total CH hydrolysate with that of CH (F3) suggests that short-sized peptides are mainly responsible for the DPP-IV inhibitory activity (**Table II-2**).

Table II-2. IC₅₀ values obtained testing CH and its fractions (molecular weight: < 3 kDa) against *in vitro* DPP-IV and ACE.

Hydrolysate	IC ₅₀ (mg/mL)	IC ₅₀ (mg/mL)
	DPP-IV	ACE
CH	0.38 ± 0.01	0.39 ± 0.01
CH < 3 kDa (F3)	0.31 ± 0.05	0.24 ± 0.01

II-3.2.2 Effect of CH and CH (F3) on *in vitro* ACE activity

The inhibitory effects of CH on the *in vitro* ACE activity were tested at 0.08–1.0 mg/mL concentration range. As shown in **Figure II-3A**, CH efficiently inhibited the *in vitro* ACE activity with a dose–response trend and a calculated IC₅₀ value of 0.39 ± 0.01 mg/mL, whereas CH (F3) displayed an IC₅₀ value of 0.24 ± 0.01 mg/mL (**Figure II-3B**). Interestingly, the inhibitory activities of CH (F3) were slightly higher than that of CH at the same concentrations, indicating that short peptides are probably responsible for the *in vitro* ACE inhibitory activity.

Finally, **Table II-2** summarizes a comparison of the *in vitro* IC₅₀ values of CH and CH (F3) against DPP-IV and ACE.

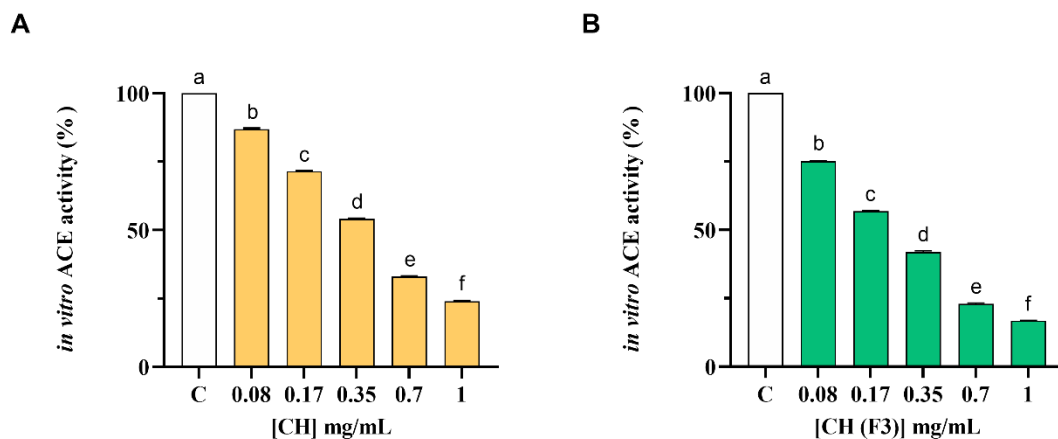


Figure II-3. The inhibitory effects of CH (A) and CH (F3) (B) on angiotensin converting enzyme (ACE) were evaluated *in vitro*, using cell-free assay. The bars representing the mean \pm s.d. of three independent experiments performed in duplicate. Different lowercase letters indicate a significant difference ($p < 0.05$) between different concentrations. C (H₂O): control cells.

II-3.3 The examination of DPP-IV and ACE inhibition by CH and CH (F3) at the cellular level

II-3.3.1 CH and CH (F3) inhibit DPP-IV activity expressed by Caco-2 cells

No effects of CH and CH (F3) on human intestinal Caco-2 cells viability was observed by performing MTT after 48-h treatment within the concentration range of 1.0–5.0 mg/mL compared with control cells (C) (**Figure II-4**), suggesting that both samples are safe in the range of doses tested.

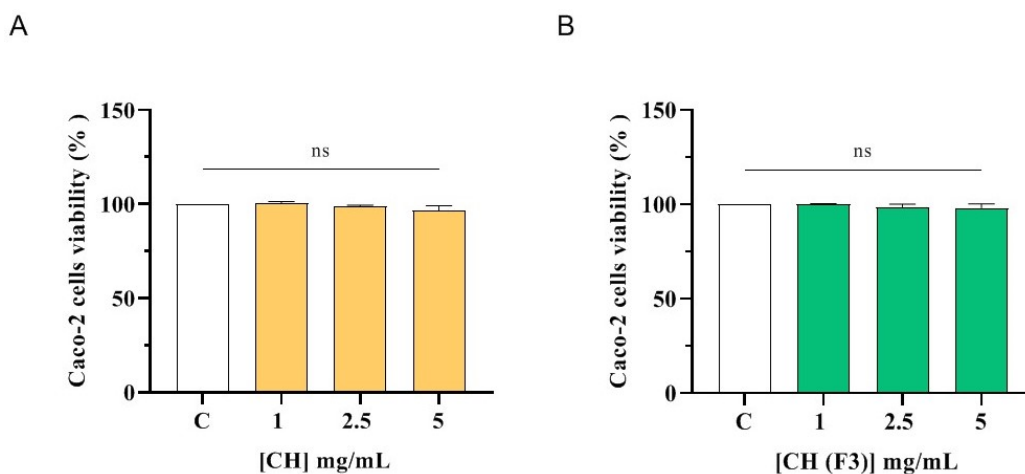


Figure II-4: Effect of CH (A) and CH (F3) (B) on the Caco-2 cells viability. Data represents the mean \pm s.d. of four independent experiments carried out in duplicate. ns: no significance, C: control cells (H₂O).

The CH inhibitory effect of DPP-IV expressed on Caco-2 cellular membranes was then investigated. In detail, the inhibitory effect of CH and CH (F3) on cellular DPP-IV activity was measured in a kinetic mode after 1, 3, and 6 h of incubation with CH or CH (F3) in the range of concentrations 1.0–5.0 mg/mL. As shown in **Figure II-5A**, CH dropped the cellular DPP-IV activity by $28.20 \pm 7.11\%$, $45.11 \pm 5.38\%$, and $47.04 \pm 8.73\%$ at 1.0, 2.5 and 5 mg/mL, respectively (after 1 h), and by $23.46 \pm 5.79\%$, $41.73 \pm 2.88\%$ and $51.68 \pm 4.71\%$ at the same concentrations (after 3 h). However, the maximal inhibition of cellular DPP-IV activity was observed after 6 h (**Figure II-5A, B**), when CH inhibited the cellular enzyme activity by $29.23 \pm 9.98\%$, $57.26 \pm 2.69\%$, and $61.10 \pm 1.70\%$ at 1.0, 2.5 and 5 mg/mL, respectively, compared with untreated cells, displaying a dose–response trend and confirming the *in vitro* results.

In parallel, the evaluation of CH (F3) inhibitory activity of cellular DPP-IV was carried. Notably, CH (F3) reduced the cellular DPP-IV activity by $23.55 \pm 4.31\%$, $43.82 \pm 3.98\%$, and $55.35 \pm 2.55\%$ at 1.0, 2.5 and 5 mg/mL (1 h), respectively, and by $11.63 \pm 7.27\%$, $43.50 \pm 3.59\%$, and $54.07 \pm 1.87\%$ at 3 h (**Figure II-5C**). In line with CH, the best inhibition of cellular DPP-IV activity by CH (F3) was detected at 6 h (**Figure II-5C, D**), when it dropped the cellular activity by $11.54 \pm 5.39\%$, $51.22 \pm$

8.74%, and $60.53 \pm 6.68\%$ at 1.0, 2.5, and 5 mg/mL, respectively, versus untreated cells.

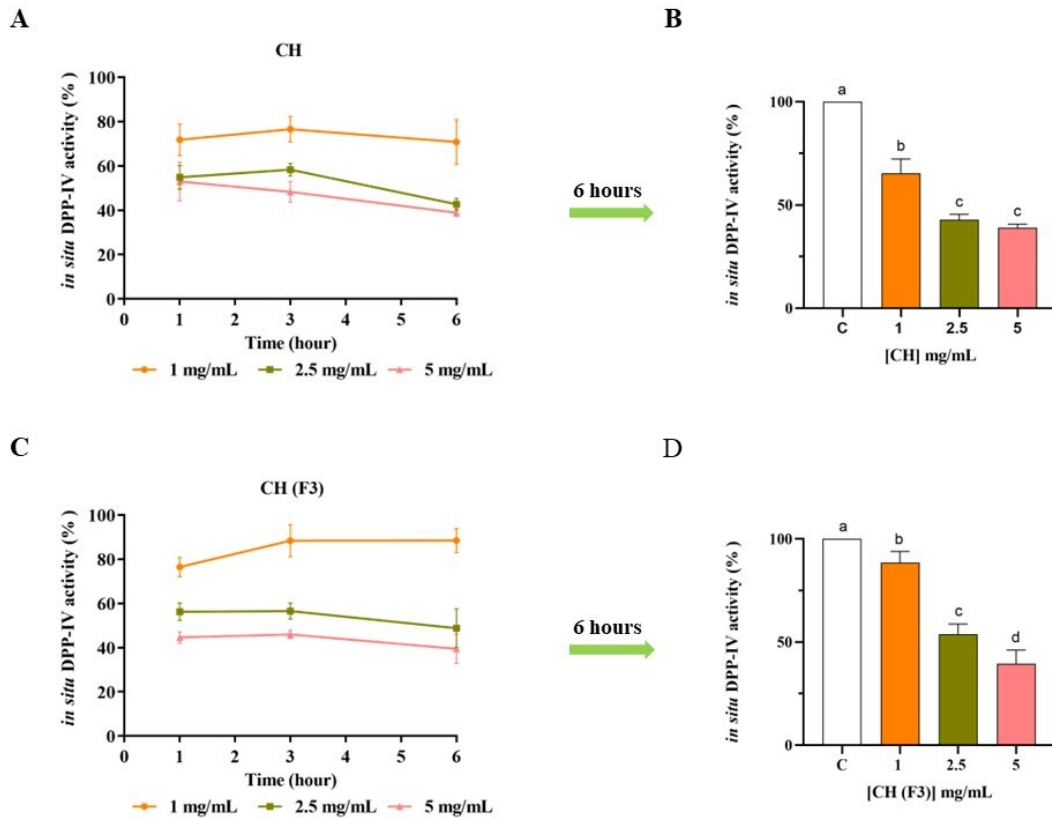


Figure II-5: The effect of CH (A, B) and CH (F3) (C, D) on cellular dipeptidyl peptidase-IV (DPP-IV) activity was determined, and the mean \pm s.d. of four independent experiments performed in triplicate are displayed as data points. Different lowercase letters indicate a significant difference ($p < 0.05$) between different concentrations. ns: no significance; C (H₂O): control cells.

II-3.3.2 CH and CH (F3) inhibit ACE activity expressed by Caco-2 cells

The CH inhibitory effect on the ACE expressed on the membranes of Caco-2 cells was evaluated treating cells with CH at 1.0–5.0 mg/mL for 6 h. Results indicated that CH inhibited the cellular ACE activity with a dose–response manner, reducing the enzyme activity by $25.04 \pm 0.49\%$, $52.36 \pm 3.53\%$, $56.10 \pm 3.78\%$, and $76.90 \pm 4.47\%$, respectively, at 0.1, 0.5, 1.0 and 5.0 mg/mL (**Figure II-6A**). Meanwhile, CH (F3) is able to decrease the cellular ACE activity by $31.42 \pm 11.19\%$, $50.75 \pm 8.75\%$, $63.63 \pm$

6.08%, and $81.39 \pm 5.05\%$ at 0.1, 0.5, 1.0, and 5.0 mg/mL after 6 h, respectively (Figure II-6B).

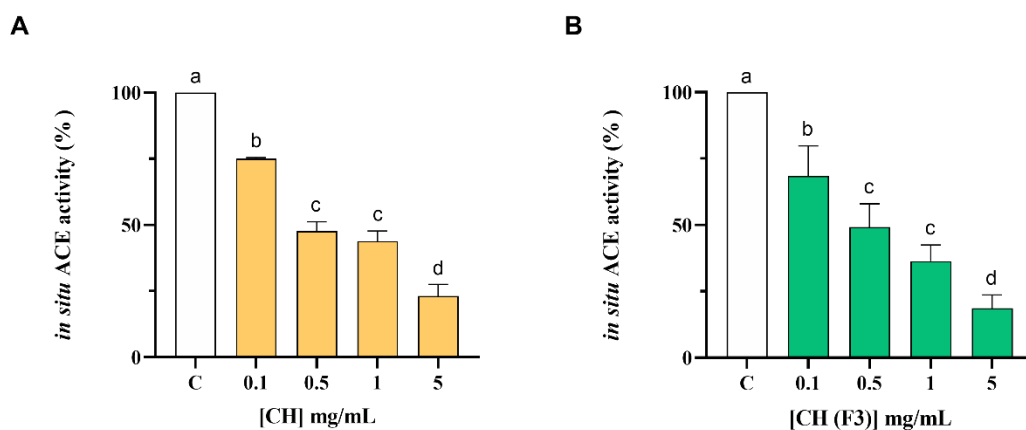


Figure II-6: Evaluation of the inhibitory effect of CH (A) and CH (F3) (B) on angiotensin converting enzyme (ACE) expressed on Caco-2 cells membranes. Bars represent the mean \pm s.d. of three independent experiments in triplicate. Different lowercase letters indicate a significant difference ($p < 0.05$) between different concentrations. ns: no significance; C (H₂O): control cells.

II-4. Discussion

Undoubtedly, casein is among the most studied sources of bioactive peptides with health promoting activities. Indeed, several literatures evidences report that casein acts as a precursor of a diversity of bioactive peptides with anti-hypertensive, immunological, antioxidant, antithrombotic and anti-diabetic effects (Aguilar-Toalá et al., 2017; Elfahri et al., 2014; Nongonierma et al., 2017). In this context, the ACE-inhibitory activity was the most investigated, and numerous ACE-inhibitory peptides have been identified, for instance, VPP (Nakamura et al., 1995), IPP (Manso & López-Fandiño, 2003), NMAINPSKENLCSTFCK (Tu et al., 2018), RYPSYG and DERF (Jiang et al., 2010). In addition, also DPP-IV-inhibitory peptides have also been identified from casein and characterized, such as LPQNIPPL (Uenishi et al., 2012) and VPYPQ (Zheng et al., 2019). In this panorama, the main limitation of most previous studies on casein hydrolysate consists on the fact that the characterization of

DPP-IV or ACE inhibitory activities has been carried out independently without taking into account that the same hydrolysate may be endowed with a multifunctional behavior exerting, therefore, both activities. Moreover, great part of published papers is based exclusively on cell-free assays (i.e., pure enzyme inhibition), whereas a main peculiarity of the present study is that the *in vitro* tests were implemented and substantiated by cellular assays that permitted either to get a deeper insight in the mechanism of action or to contextually consider other relevant issues, such as metabolism (this is particularly true while employing Caco-2 cells).

Overall, our findings suggested that CH is able to modulate the DPP-IV and ACE activities both in cell-free and cell-based conditions. More in details, CH displayed potent inhibitory properties against DPP-IV (IC_{50} value of 0.38 ± 0.01 mg/mL) and ACE (IC_{50} value of 0.39 ± 0.01 mg/mL) in cell-free condition, respectively.

Furthermore, a comparison of the IC_{50} values of complete hydrolysate with those of the low molecular weight fraction (<3 kDa) (**Table II-2**), showed that medium and short-sized peptides, which account for about two thirds of the hydrolysate (62.05%), are mainly responsible of the observed biological activities.

Literature suggests that a camel total casein hydrolysate is less efficient than CH in reducing the ACE activity being its effect not observed up to 0.6 mg/mL. Whereas, the <3 kDa fraction of the same material displays an IC_{50} equal to 91 ± 20 μ g/mL (Rahimi et al., 2016). In addition, the IC_{50} values of a thermolysin casein hydrolysate was 45–83 μ g/mL (Otte et al., 2007). As regards the DPP-IV inhibitory activity, previous evidences suggest that casein hydrolysates showed IC_{50} values in the range 0.88–1.1 mg/mL (Nongonierma & FitzGerald, 2013), suggesting that CH is slightly more active. In addition, as reported by Zhang et al., using different proteases, casein proteins released peptides that determined the 50% of DPP-IV inhibition at 1.25 μ g/mL, clearly suggesting that CH is more active (Zhang et al., 2016). Notably, recent evidences suggest that both soybean hydrolysate and pea hydrolysate inhibit DPP-IV and ACE activity with a dose–response trend and IC_{50} values equal to 1.15 ± 0.004 and 1.33 ± 0.004 mg/mL, and 0.33 ± 0.01 and 0.61 ± 0.05 mg/mL, respectively (Bollati et al., 2022).

In principle, the bioactivity of a food derived hydrolysate depends strictly on its total composition, including inactive and active species and possible synergistic or antagonist effects (Aiello et al., 2017; Zanoni et al., 2017). In light with this observation, **Table II-1** reveals that all the major identified peptides derived from CH included at least one motif with established DPP-IV and ACE inhibitory activity, which clarifies the reason why this peptide mixture is effective against both targets. Being the composition of casein hydrolysate naturally heterogeneous, it is feasible to consider that some peptides may be active against one of the two targets, but we cannot exclude that some specific peptides may be contemporary endowed by the dual ability to target both ACE and DPP-IV. In addition, some peptides with post-translational modifications were also identified. Notably, it was observed that peptide VPNSAEER displays a phosphorylation on serine residue in position 4, whereas 6 different peptides (IPNPIGSENSEKTTMP, KEPMIGVN, SDIPNPIGSENSEKTTMP, EMPFPKYP, EMPFPKYPVEP, and MPFPKYPVEP) contain within their sequences oxidized methionine residue.

These results are in line with a previous work which focused on two commercially available soybean (SH) and pea (PH) protein hydrolysates (Bollati et al., 2022). In particular, as regards the ACE inhibitory activity, CH displayed comparable IC₅₀ values with those obtained of both SH and PH, whereas as regards DPP-IV activity, CH hydrolysates is about 3.5-fold more potent than both SH and PH (Bollati et al., 2022).

DPP-IV and ACE are vital membrane peptidases expressed physiologically by many tissues, such as the intestine (Howell et al., 1992; Mentlein, 2004). As a matter of fact, human intestinal Caco-2 cells offer a dependable model that has already been established and confirmed for the investigation of peptides possessing DPP-IV or ACE inhibitory characteristics (Lammi et al., 2019; Lammi et al., 2021; Li et al., 2021). Our findings indicated that CH maintains its ability to modulate the activity of both DPP-IV and ACE on Caco-2 cells, even though both hydrolysates are active in the range of concentration between 0.1 and 5 mg/mL as a function of the time (**Figure II-5A, C**). In particular, CH inhibits both enzymes activity by $61.10 \pm 1.70\%$ and

76.90 ± 4.47% at the concentration of 5 mg/mL after 6 h of treatment (**Figure II-5, 6**), versus untreated cells, respectively, indicating that CH is less active in cell-based than in cell-free conditions. Similar results have been previously obtained on SH, PH, and peptic and tryptic hydrolysates of *Arthrospira platensis* (*Spirulina*) and *Chlorella pyrenoidosa* proteins, respectively (Aiello et al., 2019; Bollati et al., 2022; Lammi et al., 2021; Li et al., 2020; Li et al., 2021). Also in these cases, the tested hydrolysates showed greater activity in cell-free assays than in cell-based assays. More in details, PH and SH inhibited the cellular DPP-IV activity by 53.6 ± 2.3% and 48.69 ± 7.29%, respectively, and the cellular ACE activity by 82.3 ± 4.2% and 74.6 ± 4.9%, respectively, at 5 mg/mL after 3 h (Bollati et al., 2022). In addition, *C. pyrenoidosa* hydrolysates obtained using pepsin (CP) and trypsin (CT) inhibited the cellular ACE activity by 61.5 ± 7.7% and 69.9 ± 0.8%, respectively, at 5 mg/mL. When tested at the same concentration, they reduced the cellular DPP-IV activity by 38.4 and 42.5%, respectively (Li et al., 2021).

This discrepancy in efficacy may be explained by the metabolic capabilities of Caco-2 cells, which express active proteases and peptidases that can actively metabolize peptides and impact their bioactivity (Li et al., 2021). Thus, the intestine performs a dynamic function, not only in the process of vital nutrient absorption but also in actively modulating the physicochemical and biological profiles of food protein hydrolysates. Moreover, the peptides composition of CH here investigated results in line with a recent research dealing with the identification of novel casein-derived bioactive peptides and their potential (ACE)-inhibitory, antioxidant, and DPP-IV inhibitory activity when casein were fermented with *Lactobacillus helveticus* (Fan et al., 2019). Some of the identified peptides, i.e., DIPNPIGSE, EDVPSE, FPKYPVE are common to those generated by the fermentation.

II-5 Conclusions

For the first time, we have characterized the multifunctional behavior of a commercial casein hydrolysate, demonstrating its dual inhibitory properties on DPP-IV and ACE, using both cell-free and cell-based assays. Indeed, the active intestinal peptidases,

which are expressed on cellular membrane, modulate peptide profile without impair their pleotropic activity. Hence, our findings constitute a significant foundation for future investigation of CH by *in vivo* and clinical studies for confirming its multifunctional and pleotropic behavior. With its ability to confer both hypotensive and antidiabetic benefits, CH may be a highly promising ingredient for use in the development of functional foods and dietary supplements aimed at preventing cardiovascular disease and metabolic syndrome.

II-6 References

- Aguilar-Toalá, J.E., Santiago-López, L., Peres, C.M., Peres, C., Garcia, H.S., Vallejo-Cordoba, B., González-Córdova, A.F., Hernández-Mendoza, A. 2017. Assessment of multifunctional activity of bioactive peptides derived from fermented milk by specific *Lactobacillus plantarum* strains. *Journal of Dairy Science*, 100(1), 65-75.
- Aiello, G., Lammi, C., Boschin, G., Zandoni, C., Arnoldi, A. 2017. Exploration of Potentially Bioactive Peptides Generated from the Enzymatic Hydrolysis of Hempseed Proteins. *Journal of Agricultural and Food Chemistry*, 65(47), 10174-10184.
- Aiello, G., Li, Y., Boschin, G., Bollati, C., Arnoldi, A., Lammi, C. 2019. Chemical and biological characterization of spirulina protein hydrolysates: Focus on ACE and DPP-IV activities modulation. *Journal of Functional Foods*, 63, 103592.
- Bernstein, K.E., Khan, Z., Giani, J.F., Cao, D.-Y., Bernstein, E.A., Shen, X.Z. 2018. Angiotensin-converting enzyme in innate and adaptive immunity. *Nature Reviews Nephrology*, 14(5), 325-336.
- Bhandari, D., Rafiq, S., Gat, Y., Gat, P., Waghmare, R., Kumar, V. 2020. A Review on Bioactive Peptides: Physiological Functions, Bioavailability and Safety. *International Journal of Peptide Research and Therapeutics*, 26(1), 139-150.
- Bollati, C., Xu, R., Boschin, G., Bartolomei, M., Rivardo, F., Li, J., Arnoldi, A., Lammi, C. 2022. Integrated Evaluation of the Multifunctional DPP-IV and ACE Inhibitory Effect of Soybean and Pea Protein Hydrolysates. in: *Nutrients*, Vol. 14.
- Boschin, G., Scigliuolo, G.M., Resta, D., Arnoldi, A. 2014a. ACE-inhibitory activity of enzymatic protein hydrolysates from lupin and other legumes. *Food Chemistry*, 145, 34-40.
- Boschin, G., Scigliuolo, G.M., Resta, D., Arnoldi, A. 2014b. Optimization of the Enzymatic Hydrolysis of Lupin (*Lupinus*) Proteins for Producing ACE-Inhibitory Peptides. *Journal of Agricultural and Food Chemistry*, 62(8), 1846-1851.
- Brück, W.M., Graverholt, G., Gibson, G.R. 2003. A two-stage continuous culture system to study the effect of supplemental α -lactalbumin and glycomacropeptide on mixed cultures of human gut bacteria challenged with enteropathogenic *Escherichia coli* and *Salmonella* serotype Typhimurium. *Journal of Applied Microbiology*, 95(1), 44-53.

- Bu, T., Zheng, J., Liu, L., Li, S., Wu, J. 2021. Milk proteins and their derived peptides on bone health: Biological functions, mechanisms, and prospects. *Comprehensive Reviews in Food Science and Food Safety*, 20(2), 2234-2262.
- de Boer, I.H., Bangalore, S., Benetos, A., Davis, A.M., Michos, E.D., Muntner, P., Rossing, P., Zoungas, S., Bakris, G. 2017. Diabetes and Hypertension: A Position Statement by the American Diabetes Association. *Diabetes Care*, 40(9), 1273-1284.
- Eizirik, D.L., Pasquali, L., Cnop, M. 2020. Pancreatic β -cells in type 1 and type 2 diabetes mellitus: different pathways to failure. *Nature Reviews Endocrinology*, 16(7), 349-362.
- Elfahri, K.R., Donkor, O.N., Vasiljevic, T. 2014. Potential of novel *Lactobacillus helveticus* strains and their cell wall bound proteases to release physiologically active peptides from milk proteins. *International Dairy Journal*, 38(1), 37-46.
- Fan, M., Guo, T., Li, W., Chen, J., Li, F., Wang, C., Shi, Y., Li, D.X.-a., Zhang, S. 2019. Isolation and identification of novel casein-derived bioactive peptides and potential functions in fermented casein with *Lactobacillus helveticus*. *Food Science and Human Wellness*, 8(2), 156-176.
- Gallwitz, B. 2019. Clinical Use of DPP-4 Inhibitors. 10.
- Goulding, D.A., Fox, P.F., O'Mahony, J.A. 2020. Chapter 2 - Milk proteins: An overview. in: *Milk Proteins (Third Edition)*, (Eds.) M. Boland, H. Singh, Academic Press, pp. 21-98.
- Guang, C., Phillips, R.D. 2009. Plant Food-Derived Angiotensin I Converting Enzyme Inhibitory Peptides. *Journal of Agricultural and Food Chemistry*, 57(12), 5113-5120.
- Hernández-Ledesma, B., del Mar Contreras, M., Recio, I. 2011. Antihypertensive peptides: Production, bioavailability and incorporation into foods. *Advances in Colloid and Interface Science*, 165(1), 23-35.
- Holst, J.J., Deacon, C.F. 1998. Inhibition of the activity of dipeptidyl-peptidase IV as a treatment for type 2 diabetes. *Diabetes*, 47(11), 1663-1670.
- Howell, S., Kenny, A.J., Turner, A.J. 1992. A survey of membrane peptidases in two human colonic cell lines, Caco-2 and HT-29. *Biochemical Journal*, 284(2), 595-601.
- Jiang, Z., Tian, B., Brodkorb, A., Huo, G. 2010. Production, analysis and *in vivo* evaluation of novel angiotensin-I-converting enzyme inhibitory peptides from bovine casein. *Food Chemistry*, 123(3), 779-786.

- Juillerat-Jeanneret, L. 2014. Dipeptidyl Peptidase IV and Its Inhibitors: Therapeutics for Type 2 Diabetes and What Else? *Journal of Medicinal Chemistry*, 57(6), 2197-2212.
- Kostis, W.J., Shetty, M., Chowdhury, Y.S., Kostis, J.B. 2018. ACE Inhibitor-Induced Angioedema: a Review. *Current Hypertension Reports*, 20(7), 55.
- Kshirsagar, A.D., Aggarwal, A.S., Harle, U.N., Deshpande, A.D. 2011. DPP IV inhibitors: Successes, failures and future prospects. *Diabetes & Metabolic Syndrome: Clinical Research & Reviews*, 5(2), 105-112.
- Lammi, C., Aiello, G., Dellafiora, L., Bollati, C., Boschin, G., Ranaldi, G., Ferruzza, S., Sambuy, Y., Galaverna, G., Arnoldi, A. 2020. Assessment of the Multifunctional Behavior of Lupin Peptide P7 and Its Metabolite Using an Integrated Strategy. *Journal of Agricultural and Food Chemistry*, 68(46), 13179-13188.
- Lammi, C., Bollati, C., Gelain, F., Arnoldi, A., Pugliese, R.J.F.i.C. 2019. Enhancement of the stability and anti-DPP-IV activity of hempseed hydrolysates through self-assembling peptide-based hydrogels. 6, 670.
- Lammi, C., Boschin, G., Bollati, C., Arnoldi, A., Galaverna, G., Dellafiora, L. 2021. A heuristic, computer-driven and top-down approach to identify novel bioactive peptides: A proof-of-principle on angiotensin I converting enzyme inhibitory peptides. *Food Research International*, 150, 110753.
- Lammi, C., Zanoni, C., Ferruzza, S., Ranaldi, G., Sambuy, Y., Arnoldi, A. 2016. Hypocholesterolaemic Activity of Lupin Peptides: Investigation on the Crosstalk between Human Enterocytes and Hepatocytes Using a Co-Culture System Including Caco-2 and HepG2 Cells. in: *Nutrients*, Vol. 8.
- Lee, S.Y., Hur, S.J. 2017. Antihypertensive peptides from animal products, marine organisms, and plants. *Food Chemistry*, 228, 506-517.
- Li, Y., Aiello, G., Bollati, C., Bartolomei, M., Arnoldi, A., Lammi, C. 2020. Phycobiliproteins from *Arthrospira Platensis* (Spirulina): A New Source of Peptides with Dipeptidyl Peptidase-IV Inhibitory Activity. in: *Nutrients*, Vol. 12.
- Li, Y., Aiello, G., Fassi, E.M., Boschin, G., Bartolomei, M., Bollati, C., Roda, G., Arnoldi, A., Grazioso, G., Lammi, C. 2021. Investigation of *Chlorella pyrenoidosa* Protein as a Source of

- Novel Angiotensin I-Converting Enzyme (ACE) and Dipeptidyl Peptidase-IV (DPP-IV) Inhibitory Peptides. in: *Nutrients*, Vol. 13.
- Liu, R., Cheng, J., Wu, H. 2019. Discovery of Food-Derived Dipeptidyl Peptidase IV Inhibitory Peptides: A Review. in: *International Journal of Molecular Sciences*, Vol. 20.
- Maestri, E., Marmioli, M., Marmioli, N. 2016. Bioactive peptides in plant-derived foodstuffs. *Journal of Proteomics*, 147, 140-155.
- Manso, M.A., López-Fandiño, R. 2003. Angiotensin I Converting Enzyme–Inhibitory Activity of Bovine, Ovine, and Caprine κ -Casein Macropeptides and Their Tryptic Hydrolysates. *Journal of Food Protection*, 66(9), 1686-1692.
- Mentlein, R. 2004. Cell-surface peptidases. *Int Rev Cytol*, 235, 165-213.
- Mohanty, D.P., Mohapatra, S., Misra, S., Sahu, P.S. 2016. Milk derived bioactive peptides and their impact on human health – A review. *Saudi Journal of Biological Sciences*, 23(5), 577-583.
- Murray, A.B., FitzGerald, J.R. 2007. Angiotensin Converting Enzyme Inhibitory Peptides Derived from Food Proteins: Biochemistry, Bioactivity and Production. *Current Pharmaceutical Design*, 13(8), 773-791.
- Nagaoka, S., Futamura, Y., Miwa, K., Awano, T., Yamauchi, K., Kanamaru, Y., Tadashi, K., Kuwata, T. 2001. Identification of Novel Hypocholesterolemic Peptides Derived from Bovine Milk β -Lactoglobulin. *Biochemical and Biophysical Research Communications*, 281(1), 11-17.
- Nakamura, Y., Yamamoto, N., Sakai, K., Okubo, A., Yamazaki, S., Takano, T. 1995. Purification and Characterization of Angiotensin I-Converting Enzyme Inhibitors from Sour Milk. *Journal of Dairy Science*, 78(4), 777-783.
- Nongonierma, A.B., FitzGerald, R.J. 2013. Dipeptidyl peptidase IV inhibitory and antioxidative properties of milk protein-derived dipeptides and hydrolysates. *Peptides*, 39, 157-163.
- Nongonierma, A.B., Paoletta, S., Mudgil, P., Maqsood, S., FitzGerald, R.J. 2017. Dipeptidyl peptidase IV (DPP-IV) inhibitory properties of camel milk protein hydrolysates generated with trypsin. *Journal of Functional Foods*, 34, 49-58.
- Otte, J., Shalaby, S.M., Zakora, M., Pripp, A.H., El-Shabrawy, S.A. 2007. Angiotensin-converting enzyme inhibitory activity of milk protein hydrolysates: Effect of substrate, enzyme and time of hydrolysis. *International Dairy Journal*, 17(5), 488-503.

- Perpetuo, E.A., Juliano, L., Lebrun, I. 2003. Biochemical and Pharmacological Aspects of Two Bradykinin-Potentiating Peptides Obtained from Tryptic Hydrolysis of Casein. *Journal of Protein Chemistry*, 22(7), 601-606.
- Rahimi, M., Ghaffari, S.M., Salami, M., Mousavy, S.J., Niasari-Naslaji, A., Jahanbani, R., Yousefinejad, S., Khalesi, M., Moosavi-Movahedi, A.A. 2016. ACE- inhibitory and radical scavenging activities of bioactive peptides obtained from camel milk casein hydrolysis with proteinase K. *Dairy Science & Technology*, 96(4), 489-499.
- Samtiya, M., Samtiya, S., Badgajar, P.C., Puniya, A.K., Dhewa, T., Aluko, R.E. 2022. Health-Promoting and Therapeutic Attributes of Milk-Derived Bioactive Peptides. in: *Nutrients*, Vol. 14.
- Schutta, M.H. 2007. Diabetes and Hypertension: Epidemiology of the Relationship and Pathophysiology of Factors Associated With These Comorbid Conditions. 2(2), 124-130.
- Sica, D.A. 2005. Angiotensin-Converting Enzyme Inhibitors' Side Effects—Physiologic and Non-Physiologic Considerations. 7(s8), 17-23.
- Singh, A., Duche, R.T., Wandhare, A.G., Sian, J.K., Singh, B.P., Sihag, M.K., Singh, K.S., Sangwan, V., Talan, S., Panwar, H. 2023. Milk-Derived Antimicrobial Peptides: Overview, Applications, and Future Perspectives. *Probiotics and Antimicrobial Proteins*, 15(1), 44-62.
- Tu, M., Wang, C., Chen, C., Zhang, R., Liu, H., Lu, W., Jiang, L., Du, M. 2018. Identification of a novel ACE-inhibitory peptide from casein and evaluation of the inhibitory mechanisms. *Food Chemistry*, 256, 98-104.
- Uenishi, H., Kabuki, T., Seto, Y., Serizawa, A., Nakajima, H. 2012. Isolation and identification of casein-derived dipeptidyl-peptidase 4 (DPP-4)-inhibitory peptide LPQNIPPL from gouda-type cheese and its effect on plasma glucose in rats. *International Dairy Journal*, 22(1), 24-30.
- Zambrowicz, A., Pokora, M., Setner, B., Dąbrowska, A., Szoltyś, M., Babij, K., Szewczuk, Z., Trziszka, T., Lubec, G., Chrzanowska, J. 2015. Multifunctional peptides derived from an egg yolk protein hydrolysate: isolation and characterization. *Amino Acids*, 47(2), 369-380.
- Zanoni, C., Aiello, G., Arnoldi, A., Lammi, C. 2017. Hempseed Peptides Exert Hypocholesterolemic Effects with a Statin-Like Mechanism. *Journal of Agricultural and Food Chemistry*, 65(40), 8829-8838.

- Zhang, Y., Chen, R., Zuo, F., Ma, H., Zhang, Y., Chen, S. 2016. Comparison of dipeptidyl peptidase IV-inhibitory activity of peptides from bovine and caprine milk casein by *in silico* and *in vitro* analyses. *International Dairy Journal*, 53, 37-44.
- Zheng, L., Xu, Q., Lin, L., Zeng, X.-A., Sun, B., Zhao, M. 2019. *In Vitro* Metabolic Stability of a Casein-Derived Dipeptidyl Peptidase-IV (DPP-IV) Inhibitory Peptide VPYPQ and Its Controlled Release from Casein by Enzymatic Hydrolysis. *Journal of Agricultural and Food Chemistry*, 67(38), 10604-10613.

SCIENTIFIC PUBLICATIONS & COMMUNICATIONS

Published Articles

1. **Li J**, Bollati C, Bartolomei M, Mazzolari A, Arnoldi A, Vistoli G, Lammi C: Hempseed (*Cannabis sativa*) Peptide H3 (IGFLIIWV) Exerts Cholesterol-Lowering Effects in Human Hepatic Cell Line. In: *Nutrients*. vol. 14; 2022.
2. **Li J**, Bollati C, Aiello G, Bartolomei M, Rivardo F, Boschini G, Arnoldi A, Lammi C: Evaluation of the multifunctional dipeptidyl-peptidase IV and angiotensin converting enzyme inhibitory properties of a casein hydrolysate using cell-free and cell-based assays. *Frontiers in nutrition* 2023, 10.
3. Tombling BJ, Lammi C, Lawrence N, **Li J**, Arnoldi A, Craik DJ, Wang CK: Engineered EGF-A Peptides with Improved Affinity for Proprotein Convertase Subtilisin/Kexin Type 9 (PCSK9). *ACS Chemical Biology* 2021, 16(2):429-439.
4. Lammi C, Aiello G, Bollati C, **Li J**, Bartolomei M, Ranaldi G, Ferruzza S, Fassi EM, Grazioso G, Sambuy Y *et al*: Trans-Epithelial Transport, Metabolism, and Biological Activity Assessment of the Multi-Target Lupin Peptide LILPKHSDAD (P5) and Its Metabolite LPKHSDAD (P5-Met). In: *Nutrients*. vol. 13; 2021.
5. Cruz-Chamorro I, Santos-Sánchez G, Bollati C, Bartolomei M, **Li J**, Arnoldi A, Lammi C: Hempseed (*Cannabis sativa*) Peptides WVSPLAGRT and IGFLIIWV Exert Anti-inflammatory Activity in the LPS-Stimulated Human Hepatic Cell Line. *Journal of Agricultural and Food Chemistry* 2022, 70(2):577-583.
6. Lammi C, Fassi EMA, **Li J**, Bartolomei M, Benigno G, Roda G, Arnoldi A, Grazioso G: Computational Design and Biological Evaluation of Analogs of Lupin Peptide P5 Endowed with Dual PCSK9/HMG-CoAR Inhibiting Activity. In: *Pharmaceutics*. vol. 14; 2022.
7. Bollati C, Xu R, Boschini G, Bartolomei M, Rivardo F, **Li J**, Arnoldi A, Lammi C: Integrated Evaluation of the Multifunctional DPP-IV and ACE Inhibitory Effect of Soybean and Pea Protein Hydrolysates. In: *Nutrients*. vol. 14; 2022.

8. Bollati C, Cruz-Chamorro I, Aiello G, **Li J**, Bartolomei M, Santos-Sánchez G, Ranaldi G, Ferruzza S, Sambuy Y, Arnoldi A *et al*: Investigation of the intestinal trans-epithelial transport and antioxidant activity of two hempseed peptides WVSPLAGRT (H2) and IGFLIIWV (H3). *Food Research International* 2022, 152:110720.
9. Bartolomei M, Capriotti AL, Li Y, Bollati C, **Li J**, Cerrato A, Cecchi L, Pugliese R, Bellumori M, Mulinacci N *et al*: Exploitation of Olive (*Olea europaea* L.) Seed Proteins as Upgraded Source of Bioactive Peptides with Multifunctional Properties: Focus on Antioxidant and Dipeptidyl-Dipeptidase—IV Inhibitory Activities, and Glucagon-like Peptide 1 Improved Modulation. In: *Antioxidants*. vol. 11; 2022.
10. Bartolomei M, Bollati C, **Li J**, Arnoldi A, Lammi C: Assessment of the Cholesterol-Lowering Effect of MOMAST®: Biochemical and Cellular Studies. In: *Nutrients*. vol. 14; 2022.
11. Aiello G, Xu R, Pugliese R, Bartolomei M, **Li J**, Bollati C, Rueller L, Robert J, Arnoldi A, Lammi C: Quality Assessment of the Protein Ingredients Recovered by Ultrasound-Assisted Extraction from the Press Cakes of Coconut and Almond Beverage Preparation. In: *Foods*. vol. 11; 2022.
12. Cerrato A, Lammi C, Laura Capriotti A, Bollati C, Cavaliere C, Maria Montone C, Bartolomei M, Boschin G, **Li J**, Piovesana S *et al*: Isolation and functional characterization of hemp seed protein-derived short- and medium-chain peptide mixtures with multifunctional properties for metabolic syndrome prevention. *Food Research International* 2023, 163:112219.
13. Bollati C, Marzorati S, Cecchi L, Bartolomei M, **Li J**, Bellumori M, d'Adduzio L, Verotta L, Piazza L, Arnoldi A *et al*: Valorization of the Antioxidant Effect of Mantua PGI Pear By-Product Extracts: Preparation, Analysis and Biological Investigation. In: *Antioxidants*. vol. 12; 2023.
14. Bartolomei M, Crotova J, Bollati C, Kvangarsnes K, d'Adduzio L, **Li J**, Boschin G, Lammi C: Rainbow Trout (*Oncorhynchus mykiss*) as Source of

Multifunctional Peptides with Antioxidant, ACE and DPP-IV Inhibitory Activities. In: *Nutrients*. vol. 15; 2023.

15. Lammi C, Fassi EMA, Manenti M, Brambilla M, Conti M, **Li J**, Roda G, Camera M, Silvani A, Grazioso G: Computational Design, Synthesis, and Biological Evaluation of Diimidazole Analogues Endowed with Dual PCSK9/HMG-CoAR-Inhibiting Activity. *Journal of Medicinal Chemistry* 2023.
16. Bollati C, Di Profio E, Bartolomei M, **Li J**, d'Adduzio L, Fanzaga M, Tosi M, Burlina A, Zuccotti G, Verduci E, Lammi C: Investigation of the antioxidant and anti-inflammatory activity of slow-release amino acids in human intestinal Caco-2 cells. *Food Science and Human Wellness* 2023.
17. Cruz-Chamorro I, Santos-Sánchez G, Ponce-España E, Bollati C, d'Adduzio L, Bartolomei M, **Li J**, Carrillo-Vico A, Lammi C: MOMAST®; Reduces the Plasmatic Lipid Profile and Oxidative Stress and Regulates Cholesterol Metabolism in a Hypercholesterolemic Mouse Model: The Proof of Concept of a Sustainable and Innovative Antioxidant and Hypocholesterolemic Ingredient. In: *Antioxidants*. vol. 12; 2023.

Submitted Manuscripts

Carmen Lammi, Carlotta Bollati, Laura Fiori, **Jianqiang Li**, Melissa Fanzaga, Lorenza d'Adduzio, Martina Tosi, Alberto Burlina, Gianvincenzo Zuccotti, Elvira Verduci. Glycomacropeptide (GMP) rescued the oxidative and inflammatory activity of free L-AAs in human Caco-2 cells: new insights that support GMP as a valid and health-promoting product for the dietary management of phenylketonuria (PKU) patients. *Food Research International*, 2023.

Abstract in Conference Proceedings

Li J., Lammi C., Arnoldi A. Screening and identification of new food derived peptides with multi-target cholesterol-lowering activity. 1st edition of Autumn School in Food Chemistry. Pavia, 17-18th October 2022.